INVESTIGATING FERRIC ION PRODUCTION AND CONSUMPTION TRENDS IN A SIMULATED E-WASTE BIOLEACHING ENVIRONMENT FOR MAXIMUM METAL DISSOLUTION EFFICIENCY

By Research Candidate:

MARK KINOTI GITUMA

Student No: GTMMAR001

Supervisor:

Prof. S.T.L. Harrison

Thesis submitted in accomplishment of the requirements of the

Master of Science in Engineering degree,

Centre for Bioprocess Engineering Research,

Department of Chemical Engineering,

University of Cape Town

February 2015

University of Cape Town

The copyright of this thesis vests in the author. No quotation from it or information derived from it is to be published without full acknowledgement of the source. The thesis is to be used for private study or non-commercial research purposes only.

Published by the University of Cape Town (UCT) in terms of the non-exclusive license granted to UCT by the author.

University of Cape Town

Plagiarism Declaration

1. I know that plagiarism is wrong. Plagiarism is to use another's work and pretend that it is one's own.
2. I have used the Harvard convention for citation and referencing. Each contribution to, and quotation in, this thesis from the work(s) of other people has been attributed, and has been cited and referenced.
3. This thesis is my own work.
4. I have not allowed, and will not allow, anyone to copy my work with the intention of passing it off as his or her own work.

"I know the meaning of plagiarism and declare that all the work in the document, save for that which is properly acknowledged, is my own. This thesis/dissertation has been submitted to the Turnitin module (or equivalent similarity and originality checking software) and I confirm that my supervisor has seen my report and any concerns revealed by such have been resolved with my supervisor."

Name: Mark Kinoti Gituma

Signature: Signed by candidate

Signature removed

Date: 26-October-2016

Acknowledgements

- I would like to acknowledge my supervisor, **Professor Sue Harrison** for her guidance and support for the duration of this study.
- I would like to thank **Lesley Mostert** for your help in writing and editing the thesis and urging me to finish strong.
- To **Athanasios Kotsiopoulos** for your help in giving my thesis substance and guiding me through the modelling and simulation section.
- I would like to acknowledge members from my department such as **Elaine Govender**, **Liabo Motleleng**, **Latifa Mrisho, Rory Ravells**, **Alex Opitz** and **Sarah Jones** also my house mates **Chido Warambwa**, **Nathan Floor** and **Benjamin Hugo** for spurring me to keep at it.
- To my mother **Rosemary Gituma** for being a strong woman and always encouraging me to aim higher.
- And highest of all I would like to acknowledge **God**, without whose help I would never have made it this far.

Abstract

Electrical and electronic equipment has become an integral part of life in the modern world. When disposed of, it is termed Waste Electrical and Electronic Equipment (WEEE) and is one of the fastest growing waste streams in the world. Disposing the WEEE has associated risks as they contain a high amount of toxic metals (e.g. lead) which can leach into the soil, they place a high load on the land and they contain valuable metals making their recovery beneficial.

Printed circuit boards (PCBs) are an essential part of WEEE. Although WEEE forms a small part of the waste stream (3 %), it contains a high concentration of metals. As such, PCBs form the focus of this study. Base metals, especially copper, hamper the recovery of gold and PGMs by cyanidation. Further the copper grades of WEEE exceed those of many low grade ores exploited. Hence copper recovery from PCBs has garnered considerable focus. Bioleaching using the ferric ion and ferrous ion regeneration cycle is applied to the recovery of metals from metal sulphides in virgin ores and there is growing interest in its application to WEEE. The two sub-processes in the ferric regeneration cycle are ferric ion production through microbial oxidation of ferrous ion for growth and metabolic activity; and ferric ion consumption through the reduction of metals leading to metal dissolution.

The ferric ion consumption and production rates depend on each other and other factors. The metal dissolution through ferric iron reduction is a function of ferric iron concentration, affected by how fast ferric iron is produced through microbial oxidation. Ferric iron production is a function of both the ferrous iron and ferric iron concentrations and so depends on how fast the ferrous ion substrate is produced through the dissolution of metals which consumes ferric ion in the process. Ferric ion production is also affected by the microbial population and microbial specific rates of oxidation of ferrous ion. Ferric ion consumption is also dependent on the metal dissolution rate which is affected by mass transfer limitations and the type of metal for dissolution. These are two competing sub-processes where the dissolution efficiency of metals is limited by the slower process.

The first objective of this study is to compare the ferric ion production and consumption trends to determine the limiting sub-process. If the ferric ion consumption rate is significantly greater than the ferric ion production rate, the energy intensive fine crushing of PCBs may not be required and enhancement of the ferric ion production process will be a key focus. If the ferric ion consumption rate is significantly slower than the ferric ion production rate, methods to optimize the ferric ion consumption rate are required.

A second objective of this study was to investigate the system variables that would increase the performance of the slow step. This was done by modelling the system and performing a sensitivity analysis of the different variables affecting the system in a simulation.

Due to the complex interactions involved, ideal conditions have been suggested for this early stage study. These include using metal powder instead of PCBs to reduce mass transfer limitations. In order to identify the metals of focus, dissolution of PCBs was conducted in a solution of ferric sulphate. The major metals leached were then investigated further. To identify the ferric ion consumption and production trends in the presence of microorganisms, two main experiments were conducted. In the first, copper metal powder was added at varying initial masses to a microbial culture of bioleaching bacteria grown on ferrous sulphate solution and ferric production and consumption trends followed during microbial growth. The second experiment consisted of serial addition of 0.2 g and 0.4 copper powder to 100 ml ferric sulphate at peak initial microbial population. The experiment allowed comparison of the ferric ion consumption and production rates when both processes were at peak rates. In the third experiment, the ferric ion chemical leaching of copper, tin and zinc were carried out to determine the metal dissolution rate constants.

From the experiments, it was found that copper, tin, lead and zinc were leached with the highest concentrations from a sample of PCBs (20 – 45 mg of each metal per g PCB Sample A and 6 – 120 mg of each metal per g PCB Sample B) Due to its inherent toxicity, lead was not investigated in this study. From the experiment where copper addition was conducted during inoculation, it was found that the time for maximum ferric ion concentration to be reached was proportional to the initial mass of copper: the higher the initial mass the longer the time for maximum ferric ion concentration to be reached. When investigating the addition of base copper metal to a solution containing ferric sulphate at peak microbial population, it was found that the initial ferric ion consumption rate was 39 times faster than the ferric ion production rate. On greater additions of copper, the ferric ion production rate increased which was attributed to an increasing microbial population from (7.36×10^7 cells at Addition 1 to 6.29×10^8 at Addition 6 in the 0.4 g copper addition). This reduced the ratio of ferric ion consumption to production from 39 to 13. It was found that copper and tin dissolution could be described by the chemical controlled shrinking particle model by $X = 1 - (1 - 0.00436.C_{Fe^{3+}}^{0.56}.t)^3$ and $X = 1 - (1 - 0.000593.C_{Fe^{3+}}^{0.269}.t)^3$ respectively. However the dissolution of zinc could not be modelled by the chemical controlled shrinking particle model, but could be modelled by the logarithmic model by $X = 1 - e^{-0.00751t^{0.5}}$. The correlation between experimental and calculated data for copper, tin and zinc was 0.95, 0.91 and 0.93 respectively.

In order to conduct the sensitivity analysis, a model was developed of a two stage process in which the ferric ion production and consumption processes were separated into two reactors (biooxidation and chemical). The microbial ferric ion production process took place in the biooxidation reactor and the ferric ion consumption process associated with leaching of the metals took place in the chemical reactor. Decoupling the two processes into separate reactors allowed for the investigation of system parameters through a sensitivity analysis. The sensitivity analysis was conducted by changing the initial volume of the biooxidation reactor, the initial microbial population, varying the initial metal mass in the chemical reactor and changing the initial ferric and ferrous ratio. A simulation was also conducted where a mixture of metals was leached in the same reactor. From the simulation it was found increasing the volume hence residence time of the biooxidation reactor and the microbial population increased the dissolution efficiency of the simulated metal. This is because increasing the residence time resulted in greater production of ferric ion. However increasing the microorganism population meant more cells were available for microbial oxidation which increased the ferric ion production rate.

As ideal conditions were considered in the experiments and simulation, the results found would not be directly applicable to an industrial process. However, they form a guideline on the system parameters on which to focus when investigating leaching of metals from PCB and the larger WEEE stream, thereby informing the assessment of potential of this route for implementation and providing insight into design and operating conditions. It is anticipated that the bioleaching of PCBs and other WEEE may make significant contribution to both the remediation of these wastes and may provide an efficient approach to the beneficiation of “urban ores”, a new label put forward for WEEE.

Contents

Plagiarism Declaration i
Acknowledgements ii
Abstract iii
Glossary xiv
Nomenclature xv
1 .. Introduction 1
1.1 Background of e-waste recovery 1
1.2 Recycling Technologies for e-waste recovery 1
1.2.1 Pyrometallurgy Technology for the Recovery of Metals from E-waste 1
1.2.2 Electromechanical Separation Technology for the Recovery of Metals from E-waste 2
1.2.3 Hydrometallurgy for the Recovery of Metals from E-waste 2
1.2.4 Bioleaching Technology for the Recovery of Metals from E-waste 2
1.3 Problem statement 3
1.4 Research Objectives 3
1.5 Scope and Limitation 4
1.6 Thesis Outline 5
2 Literature Review 6
2.1 Background of Printed Circuit Boards (PCBs) 6
2.1.1 Properties of Printed Circuit Boards 7
2.1.2 Production of Printed Circuit Boards 7
2.1.3 Metal Composition in Printed Circuit Boards 8
2.1.4 Recovery of Metals from Printed Circuit Boards 9
2.2 Bioleaching Technology for Base Metal Extraction 11
2.2.1 Overview of Bioleaching of Sulphide Minerals 12
2.2.2 Bioleaching Mechanisms for Metal Sulphide Leaching 12
2.2.3 Use of Bioleaching in Extraction Metals from Mineral Sulphide Ores 14
2.3 Application of Bioleaching for the Treatment of Printed Circuit Boards 15
2.3.1 Mechanisms of Metal Recovery from Printed Circuit Boards 15
2.3.2 Industrial applications of Metal Extraction from PCS using Bioleaching Technology 16
2.3.3 The Role of Microorganisms in PCB bioleaching 17

2.3.4 Inhibition of Microorganisms by High Zero-Valence Metal and Metal Ion Concentrations 18
2.3.5 Influence of Initial Iron Concentration on the Leaching Efficiency of Metals from PCBs 20
2.3.6 Effect of Particle Size on Metal Recovery from PCBs 24
2.3.7 Impact of Microorganism Concentration on the Leaching Rate of Metals from PCBs 24
2.4 Kinetics of Metal Recovery from Printed Circuit Boards by Bioleaching 25
2.4.1 Kinetics of the Reactions in the Bioleaching Process 26
2.5 Overview of Literature and Research Approach 30
2.5.1 Motivation for Study from Literature Review 30
2.5.2 Objectives of Study 31
2.5.3 Hypothesis 32
2.5.4 Key Questions 32
3 Materials and Method 34
3.1 Microorganisms used for the Bioleaching Experiments 34
3.1.1 Maintenance Growth Media for the Microorganisms 34
3.1.2 Microorganism Cell Count 35
3.2 Analytical Techniques 36
3.2.1 Iron Determination 36
3.2.2 Monitoring of pH 37
3.2.3 Monitoring of Redox 37
3.2.4 Metal Ion Analysis 37
3.3 Chemicals and Solutions Used 37
3.3.1 Hydrochloric Acid 37
3.3.2 Ferric Sulphate Solution 38
3.4 Experimental Equipment and Set-up 38
3.4.1 Magnetic Stirrer Mode of Operation 38
3.4.2 Shake Flasks Experiments 39
3.5 Experimental Plan 40
3.5.1 Printed Circuit Board Characterization Experiments 40
3.5.2 Chemical Leach of Select Metal Powders 40

3.5.3 Bacteria Batch Leaching Experiments to Understand Ferric Ion Trends during Microorganism Growth 41
3.5.4 Bioleaching with Fed Batch Copper Addition at Peak Microbial oxidation 42
4 Understanding the Kinetics of Metal Dissolution 45
4.1 Characterisation of Printed Circuit Boards 45
4.2 Chemical Leach Experiments 47
4.2.1 Kinetics for Chemical Leaching of Copper 47
4.2.2 Kinetics for Chemical Leaching of Tin 51
4.2.3 Kinetics for Chemical Leaching of Zinc 55
4.3 Batch Bioleaching Experiments 61
4.3.1 Ferric ion Production in the presence of Microorganisms 62
4.3.2 Reaction Mechanisms involved in the Leaching of Copper in the presence of Microorganism 66
4.4 Fed Batch Addition of Copper at Peak Microbial Oxidation: Assessment of relative Ferric Ion Production and Consumption Rates 69
4.4.1 Motivation of experimental approach 69
4.4.2 Fed Batch Addition at Peak Microbial Oxidation 70
4.4.3 Mechanisms involved Ferric ion Cycling with Sequential Copper Addition 77
5 Simulation Methodology 79
5.1 Motivation for the Simulation Approach and its Goals 79
5.2 Assumptions for the Simulation 80
5.3 Assumed Reactor Set up for the Simulation 81
5.4 Equation Derivations for the Reactor Set Up 82
5.4.1 The Generic CSTR Design Equations 82
5.4.2 Mole Balance Equations of the Chemical Reactor 83
5.4.3 Mole Balance Equations for the Biooxidation Reactor 83
5.4.4 Design Equations of the Combined System 85
6 Simulation Results and Discussion 87
6.1 Comparison of System Equation with Experimental Data 87
6.1.1 Base Conditions for the Simulation Run 87
6.1.2 Results of the simulated addition of copper 87
6.2 Varying the Biooxidation Volume (Residence Times) 89

6.2.1 Base Conditions for the Simulation Run 89
6.2.2 Results of Varying the Biooxidation Volume 89
6.2.3 Discussion of the Simulation Trends on Varying the Biooxidation Volume 93
6.3 Varying the Microbial Population 95
6.3.1 Base Conditions for the Simulation Run 95
6.3.2 Discussion of the Simulation Trends on Varying the Microbial Cell Count 98
6.4 Varying Initial Copper Metal Mass 99
6.4.1 Base Conditions for the Simulation Run 99
6.4.2 Results of Varying the Initial Copper Mass in Suspension 99
6.4.3 Discussion of the Simulation Trends on Varying the Initial Copper Mass in Suspension 102
6.5 Varying the Initial Ferric to Ferrous Ion Ratio 104
6.5.1 Base Conditions for the Simulation Run 104
6.5.2 Results of Varying the Initial Ferric to Ferrous Ion Ratio 104
6.5.3 Discussion of the Simulation Trends on Varying the Ferric to Ferrous ratio 107
6.6 Mixed metal simulation 108
6.6.1 Mixed Metal Simulation at Equal Volume Reactors 109
6.6.2 Mixed Metal Simulation at 10 L Biooxidation Volume 110
7 Conclusion and Recommendations 112
7.1 Conclusion 112
7.2 Recommendation 115
8 .... References 117
APPENDICES..... 122
Appendix A Preparation of Reagents Used in the Experiments 122
Preparation of Ferric Sulphate Solution 122
Preparation of 2 M Hydrochloric Acid 122
Appendix B Analytical Methods 124
Microorganism Cell Count 124
Appendix C Experimental Calculation 125
The Printed Circuit Board Characterization Experiments Calculations 125
Appendix D Reactor Design 127
Base Design equations 127

Design equations 128
Design Equations 128
Chemical 128
Bioxidation 129
Overall 129
Numerical Method 130
Appendix E Experimental Data 131
Base Bacterial Leaching 131
Fed batch copper additions 133
Appendix F Material Safety data and Hazards 140
Appendix G Simulation Code 142
Reactions.py 142
Reactors.py 143
System.py 145
Plot.py 146

List of Figures

Figure 2–1: Part A shows the indirect mechanism as bacteria oxidize soluble ferrous ion to ferric ion and sulphur to sulphate. Part B is the indirect contact mechanism where bacterial attachment is of physiological importance with ferric ion oxidizing the sulphide minerals. The specifics of microorganism electrochemical (interaction) with the mineral surface and/or direct contact contribution to sulphide dissolution is unknown (Watling, 2006). 13
Figure 2–2. Time profile of ferrous ion and copper ions in solution at different initial ferrous ion concentrations (Choi, et al., 2004). 21
Figure 2–3. The influence of pH on the copper mobilization rate (Yang, et al., 2009). 22
Figure 2–4. The influence of time on copper mobilization rates at different quantities of stock culture addition. (Yang, et al., 2009) 25
Figure 3–1. Counting grid of Hawskley Thoma counting chamber. 35
Figure 3–2. Ferric chloride calibration curve for the determination of total iron. 37
Figure 3–3. Magnetic stirrer set up 39
Figure 3–4. Shake flask set up for the experiments. 40
Figure 3–5. Fed-batch copper addition at peak microbial population example 43
Figure 4–1. Ferric ion concentration trends for the dissolution of copper. 48
Figure 4–2. Copper conversion trends for changing initial ferric ion concentration and changing initial metal mass in suspension 48
Figure 4–3. Chemical controlled reaction model for copper to determine constants of $1-(1-X)^{1/3}=k.t$ 49
Figure 4–4. Comparison of experimental and calculated dissolution fraction of copper in ferric sulphate 51
Figure 4–5. Ferric ion concentration trends for the dissolution of tin 52
Figure 4–6. Tin conversion trends for changing initial ferric ion concentration and changing initial metal mass in suspension 53
Figure 4–7. Chemical controlled reaction model for tin to determine constants of $1-(1-X)^{1/3}=k.t$ 54
Figure 4–8. Comparison of experimental and calculated dissolution fraction of tin in ferric sulphate 55
Figure 4–9. Ferric ion concentration trends for the dissolution of zinc 56
Figure 4–10. Zinc conversion trends for changing initial ferric ion concentration and changing initial metal mass in suspension 57
Figure 4–11. Ferric ion concentration trends for the dissolution of zinc over 5 minutes 58
Figure 4–12. Zinc conversion trends for changing initial ferric ion concentration and changing initial metal mass in suspension over 5 minutes 58
Figure 4–13. Chemical controlled reaction model for zinc to determine constants of $1-(1-X)^{1/3}=k.t$ .. 59

Figure 4–14. Chemical controlled reaction model for zinc to determine constants of $(-\ln(1-X))^2=k.t$. 60
Figure 4–15. Comparison of experimental and calculated dissolution fraction of zinc in ferric sulphate 61
Figure 4–16. The trends of the ferric ion concentration in the bioleach flasks in the presence of different initial concentrations of copper metal powder 62
Figure 4–17. The trends of the total iron concentration in the bioleach flasks in the presence of different initial concentrations of copper metal powder 64
Figure 4–18. The trends of redox potential in the bioleach flasks in the presence of different initial concentrations of copper metal powder 65
Figure 4–19. PH reading for bacteria batch leaching experiments. 66
Figure 4–20. Ferric ion concentration trends for the fed-batch addition of copper metal powder to an active bioleach environment operated at a starting concentration of 9 g/l iron in solution. 71
Figure 4–21. Normalized ferric ion concentration trends for the fed-batch addition of copper metal powder to an active bioleach environment operated at a starting concentration of 9 g/l iron in solution. 72
Figure 4–22. Ferric ion to total iron concentration ratio in the ferric ion consumption phase of the fed-batch addition of copper metal powder experiment to an active bioleach environment for the 4.0 g Cu addition batch run. 73
Figure 4–23. Ferric ion to total iron concentration ratio in the ferric ion production phase of the fed-batch addition of copper metal powder experiment to an active bioleach environment for the 4.0 g Cu addition batch run. 74
Figure 4–24. Variation of pH after the fed-batch addition of copper metal powder experiment to an active bioleach environment for the 4.0 g Cu addition batch run. 76
Figure 5–1. Closed cyclic system set-up for the simulation 82
Figure 6–1. Fed batch addition simulation. 88
Figure 6–2. Ferric ion, cupric ion, biomass and base copper trends in the biooxidation and chemical reactor at varying biooxidation volume 92
Figure 6–3. Ferric ion, cupric ion, biomass and base copper trends in the biooxidation and chemical reactor at varying initial microbial cell count 97
Figure 6–4. Ferric ion, cupric ion, biomass and base copper trends in the biooxidation and chemical reactor at initial copper mass in suspension 101
Figure 6–5. Ferric ion, cupric ion, biomass and base copper trends in the biooxidation and chemical reactor at changing ferric to ferrous ion ratio 106
Figure 6–6. Metal Ion Concentration in the Metal Dissolution Reactor in a Mixed Metal System 109

Figure 6–7. Metal Ion Concentration in the Metal Dissolution Reactor in a Mixed Metal System at 10 L biooxidation volume. 110

List of tables

Table 2-1. Weight composition of metals in PCBs according to different references..... 8
Table 2-2. Microorganisms that are known to recover metals from E-waste (Pant, et al., 2011). 18
Table 2-3. Effect of initial ferrous concentration on the recovery efficiency of copper from crushed printed circuit boards (Xiang, et al., 2010) 20
Table 3-1. Composition of Lungrid 9k medium for the maintenance of bacteria 35
Table 4-1. Metal ion concentration per gram of printed circuit boards leached in ferric sulphate..... 46
Table 4-2. Comparison of the ferric ion consumption rate to ferric ion production rate 74
Table 4-3. Bacteria cell count in the fed batch addition of copper experiments. 76
Table 5-1. Shrinking particle models for the metals of focus. 83
Table 6-1. Simulation conditions to compare with experimental addition data..... 87
Table 6-2. Simulation conditions for varying biooxidation reactor volume 89
Table 6-3. Simulation conditions for varying microbial population 95
Table 6-4. Simulation conditions for varying initial copper mass in the chemical reactor..... 99
Table 6-5. Simulation conditions for varying ferric to ferrous iron ratio 104
Table 6-6. Simulation conditions for varying initial copper mass in the chemical reactor..... 109
Table 8-1. Mass of PCB samples before and after leaching in ferric sulphate solution 125
Table 8-2. Results from the ICP analysis of the metal ions in solution..... 125
Table 8-3. ICP analysis concentration in $g.l^{-1}$ 126
Table 8-4. Mass of metal ions leached into solution per mass of PCB 126

Glossary

Dioxins	Polychlorinated dibenzodioxins, environmental pollutant.
Dosage	Solid fraction in solution
Electronic waste	Discarded electrical or electronic devices
Furan	Heterocyclic organic compound, toxic and carcinogenic
Hydrometallurgy	Extraction of metals using wet methods
Inhibition	Prevention of microbial function due to external factors
Inoculum	Source of material used for an inoculation
Printed Circuit Boards	Mechanically supports and electrically connects electronic equipment
Residence time	The average time a particle remains in a system.

Nomenclature

Abbreviations

AAS	Atomic Absorption Spectrum spectroscopy
CeBER	Centre for Bioprocessing Engineering Research
CSTR	Continuous Stirred Tank Reactor
ICP	Inductively Coupled Plasma
PCB	Printed Circuit Board
WEEE	Waste Electronic and Electric Equipment

Chemical Formulae

Cu	Copper
Fe^{3+}	Ferric ion
Fe^{2+}	Ferrous ion
H^{+}	Hydrogen proton
H_2SO_4	Sulphuric acid
HCl	Hydrochloric Acid
pH	Decimal logarithm of the reciprocal of the hydrogen ion activity in a solution
Sn	Tin
Zn	Zinc

List of symbols

Symbol	Description	Units
C_X	Biomass concentration	$molC^{-1}.L^{-1}$
E_h	Redox potential	mV
E_o	Standard redox potential	mV
$[Fe^{3+}]$	Ferric ion concentration	$mol.L^{-1}$
$[Fe^{2+}]$	Ferrous ion concentration	$mol.L^{-1}$
K_m, $K_{Fe^{2+}}$	Michaelis-Menten constant for substrate utilisation	Dimensionless
μ	Microbial growth rate	h^{-1}
μ_{max}	Maximum microbial growth rate	h^{-1}
$q_{Fe^{2+}}^{max}$	Maximum specific ferrous ion utilisation rate	$mol\ .molC^{-1}.h^{-1}$
R	Universal gas constant (8.314)	$J.mol.K^{-1}$
$r_{Fe^{2+}}$	Volumetric rate of microbial ferrous ion oxidation	$mol\ Fe^{2+}.h^{-1}.\ l^{-1}$
$r_{Fe^{3+}}$	Volumetric rate of ferric ion consumption through metal dissolution	$mol\ Fe^{3+}.h^{-1}.\ l^{-1}$
$r^*_{Fe^{2+}}$	Molar rate of microbial ferrous ion oxidation	$mol\ Fe^{2+}.h^{-1}$
$r^*_{Fe^{3+}}$	Molar rate of ferric ion consumption through metal dissolution	$mol\ Fe^{3+}.h^{-1}$
τ	Residence time	Seconds
V	Reactor volume	L
X	Conversion of metals	X

1 Introduction

1.1 Background of e-waste recovery

Waste electrical and electronic equipment (WEEE) is the fastest growing waste stream in the world, with an estimated production between 20 – 50 million tonnes per annum and increasing at 4 % per annum (Reuter, et al., 2013). Printed circuit boards (PCBs) are an integral part of electronic devices and form 3 % of the total weight of WEEE (Karwowska, et al., 2014).

The composition of PCB's vary and on average PCBs consist of: 19 % plastic, 4 % bromine, 49 % glass and ceramics, with the balance made up of a complex mix of metals (Yang, et al., 2009). The average metal composition is: 20 % copper, 8 % iron, 4 % tin, 2 % nickel, 2 % lead, 1 % zinc, 0.2 % silver, 0.1 % gold and 0.005 % palladium (Huang, et al., 2009). The micro-electric components are mounted on a fiber glass and epoxy resin board, which has been designed to have high flexural strength and resistance to cracking as it serves as a structural support. The epoxy resins are produced from the combination of epoxy and phenolic resins, hardeners (dicyanamide), catalysts (2-methyl imidazole), antimony oxide, pigments, acetone, and ethylene glycol monomethyl ether (LaDou, 2006).

Although the use of PCBs have become an integral part of modern day life, it is difficult to dispose the boards as the materials are not biodegradable. It has been shown that the metal content in the PCBs are higher than the allowable toxicity threshold for disposal (Musson, et al., 2006). Recycling PCBs, a subset of the overall e-waste stream, reduces demand on resources such as ores, energy and landfill sites (Mishra, et al., 2008).

However, as PCB composition varies with manufacture and year of manufacture, coupled with decreasing concentration of precious metals in the boards (Cui & Zhang, 2008), understanding the kinetics of metal dissolution at a fundamental level will allow for good response to the changes.

1.2 Recycling Technologies for e-waste recovery

There are several technologies that exist that can be used to recycle the PCB e-waste stream. However as with all methods, each have their advantages and disadvantages.

1.2.1 Pyrometallurgy Technology for the Recovery of Metals from E-waste

Pyrometallurgical processing of e-waste is the traditional method for recovering metals from waste electronics (Cui & Zhang, 2008). However, the by-products of pyrometallurgy include high emissions of dioxins, furans, polybrominated organic pollutants and polycyclic aromatic hydrocarbons, mainly from the combustion of brominated flame retardants found in the epoxy resin and plastics of the PCBs (Huang, et al., 2009; Yang, et al., 2009). These pollutants are toxic to human health and the

environment. It has also been found that copper is a catalyst for dioxin formation when flame-retardants are incinerated (Cui & Zhang, 2008). Further, expensive state of the art smelters are required, hence pyrometallurgical processes are dependent on large capital investments (Cui & Zhang, 2008).

1.2.2 Electromechanical Separation Technology for the Recovery of Metals from E-waste

In the electromechanical processes, the boards are crushed to a 0.6 - 1 mm size fraction from which the metallic components are separated by a powerful electromagnet (Huang, et al., 2009). It is an environmentally friendly process as no liquid or gaseous contaminants are formed which can prove to be difficult to contain. However the technology is expensive due to the specialized mills needed to crush the PCBs which have a high flexural strength (Yang, et al., 2009). Due to crushing requirements, the technology consumes significant amounts of energy thus resulting in high operational cost and the environmental cost associated with producing the electrical energy.

1.2.3 Hydrometallurgy for the Recovery of Metals from E-waste

Using hydrometallurgical processes, the e-waste stream can be solubilised using strong acids for base metal recovery and cyanide (or thiosulphate) for precious metal recovery. This is only favorable if the metals occur in high concentration in the e-waste stream (Vestola, et al., 2010). It is operationally expensive due to the extensive usage of chemical leaching agents which cannot be recycled. As the there is no regeneration of the reactants, fresh reactants have to be used each time (Choi, et al., 2004). The operations also require large capital investments due to the specialised equipment required to withstand the highly corrosive environment. There is also an environmental consideration in terms of the safety measures involved in maintaining this highly toxic environment and the safe disposal of the effluent stream.

1.2.4 Bioleaching Technology for the Recovery of Metals from E-waste

The bioleaching technology offers significant advantages over other methods due to lower capital and operating costs involved, and lower environmental pollutants produced. In bioleaching, microorganisms such as bacteria and fungi (Brandl, et al., 2001) are used to extract the metals from the PCBs. Bioleaching is an economically viable process used to extract metals from low grade and complex ores (May, et al., 1997) with greater efficiency than traditional recovery technologies at lower costs and fewer industrial requirements (Mishra, et al., 2008). However, the disadvantage of bioleaching is that it has slower metal extraction rates compared with other technologies.

Bioleaching of base metals uses ferric ion and dissolved oxygen in acidic conditions as the primary oxidizing agents (Vestola, et al., 2010). The main role of the microorganisms is to regenerate the ferric ion thus reducing the cost of the reactants. This is because the ferric ion is reduced in the dissolution

and leaching of metals from the ore or waste. The resulting ferrous ion is used by the microorganisms as an energy source through its oxidation to ferric ion. This consumption and regeneration of ferric ion is an auto-catalyzed reaction.

1.3 Problem statement

Several bioleaching studies have been conducted on the recovery of metals from PCBs. However the bulk of the research focuses on the recovery of copper metal, with little work conducted towards the recovery of the other major metals occurring in printed circuit boards. The studies conducted investigated the bioleaching of printed circuit boards at; varying initial iron concentration (Ozkaya, et al., 2007; Xiang, et al., 2010), varying the particle size of PCBs (Yang, et al., 2011), varying microbial population (Brandl, et al., 2001; Yang, et al., 2009; Sadia, et al., 2012); varying the initial pH of the ferric ion solution (Anders & Colin, 1995; Yang, et al., 2009; Xiang, et al., 2010) etc.

Despite all the work that has been reported, few kinetics studies are presented (Demir, et al., 2004; Younesi, et al., 2006; Wang, et al., 2010; Yang, et al., 2014; Huang, et al., 2014; Zhao, et al., 2014). The metal leaching rates from PCBs, and their interaction with microbial ferric iron generation, has not been well understood. Metal extraction from PCBs using bioleaching depends on the relative availability of ferric ion for metal dissolution and ferrous ion for microbial growth and metabolic activity, which impacts on the ferric ion regeneration rate. The relationship between ferric ion consumption and production needs to be understood in order to determine the optimal leaching conditions necessary to ensure maximum dissolution efficiencies of metals from PCBs.

Such an understanding is vital as the leaching rates of metals from PCBS vary from the leaching rates of metals in mineral ores and thus the rate of ferric ion production and consumption will vary.

1.4 Research Objectives

The main objective of this study is to develop a model to simulate the relationship between the rates ferric ion consumption through the dissolution of simulated metals found in e-waste, and ferric ion production through microbial oxidation of ferrous ion to ferric ion. This is conducted in order to investigate the dissolution efficiency of copper which acts as a representative of the base metals in PCBs and therefore, optimize the overall process. In the study, ideal conditions were investigated, this means:

- The effect of mass transfer limitations on the leaching of PCBs was not studied as due to lack of access to specialized mills, the PCB samples could not be crushed to fine powder to achieve the desired effect. In the ideal system under investigation, fine metal powder was leached at high stirrer speeds.

- The toxicity effect of the metals, metal ions and PCB boards on the microorganisms was not investigated as the experimental system was divided into two reactor systems; separating the microbial oxidation of ferric ion from the base metal leach reactor.

The outcome of this study is targeted towards understanding the ferric ion production and consumption trends when bioleaching base metals found in PCBs. This was achieved by:

- Determining the ferric ion production and consumption trends experimentally in a system containing microorganisms and copper metal powder as the representative base metal.
- Determining the rate expression for ferric ion consumption during the dissolution of copper, tin and zinc to derive kinetic data for the model simulation.
- Using the determined rate equations to develop a model to simulate base metal dissolution from PCBs in a bioleaching system, in order to understand the operating variables that can be manipulated to maximize the ferric ion concentration in solution, and hence, maximize the dissolution efficiency of the base metals. The parameters to be investigated in the model simulation include:
    - Varying the residence time of the microbial growth reactor in order to control the ferric ion production rate.
    - Varying the initial microbial population in order to investigate the effects of microbial concentration on the ferric ion regeneration cycle.
    - Varying the initial ferric and ferrous ion concentration in order to investigate the effect of initial iron concentration on the ferric ion regeneration cycle and how it affects metal dissolution efficiency.
    - Varying the initial base metal mass in order to determine how the leaching time is affected and at high initial metal mass, how the metal dissolution rates may be increased.
    - Simulating a mixture of metals in order to understand the dissolution trends when the metals in PCBs are leached simultaneously into solution.

1.5 Scope and Limitation

As research into the recovery of metals from WEEE is still at its infancy, there is significant work that needs to be conducted. However, the scope of this study has been limited to investigating the ferric ion production and consumption trends under ideal conditions where metal powder has been substituted in place of printed circuit boards. A limitation of this study is that the simulation results are not fully validated, as this would require further experimental work to be conducted on reactor design which is outside the scope of this study.

1.6 Thesis Outline

The thesis begins with the background and literature review provided in Chapter 2. An overview of the printed circuit board industry is presented. The manufacturing steps of PCBs and current recycling technologies are reviewed. This is then followed by review of the bioleaching technology and the microorganisms and mechanisms involved in ferric ion regeneration. Previous literature focusing on factors affecting metal dissolution efficiencies in the bioleaching of WEEE (mainly PCBs) is then presented. In order to inform the model simulation and sensitivity analysis section, the kinetics of metal recovery from WEEE were reviewed from literature. The objectives, key questions and hypothesis are thereafter presented.

The research methodology section follows in Chapter 3. This contains the experimental methodology used in order to investigate the ferric ion production and consumption trends. Experiments to determine the leaching kinetics of base metal powder were also described.

Chapter 4 contains the results and discussion from the experimental section which include; identifying the key metals that were leached from PCBs, identifying the dominant rate based on experimental data, and calculating the rate constants of the base metal powder leaching kinetics.

Chapter 5 contains the simulation methodology, which highlights the assumptions and derivation of the model that was used to perform a scenario analysis on the different aspects that affect metal dissolution efficiency as a function of the ferric ion regeneration cycle. The results of the simulation are presented in Chapter 6.

In Chapter 7, the conclusions drawn from the experimental section and simulation sections, are presented and discussed. The relevance of the study is discussed and key recommendations are presented.

2 Literature Review

Waste Electrical and Electronic Equipment (WEEE) is the fastest growing waste stream, with about 50 million metric tonnes generated per annum (Petranikova, 2008) and increasing by 3-5 % annually (Drechse, 2006). It is said that by 2017 the WEEE will be in excess of 65.4 million tonnes per annum (Kandil, 2013). Designing efficient and environmentally responsible metal recovery technologies for the WEEE stream is useful both in terms of removing waste burden and providing metals essential for ongoing development. Understanding the characteristics of the WEEE stream is essential in determining the best approach to recovering metals from the secondary resource and the relevance of biohydrometallurgy as a treatment option.

Even though printed circuit boards (PCBs) form a small portion of the WEEE stream of about 3 % (Karwowska, et al., 2014), PCBs contain significant amounts of both precious and hazardous metals. Thus the majority of research that has been conducted on the recovery of metals from WEEE using bioleaching has been targeted towards PCB treatment. In order to make use of literature sources, current data on PCB research will be used as a basis to investigate the recovery of metals from a simulated WEEE environment in this study.

In order to formulate a good understanding of metal recovery from printed circuit boards, studying the background of both printed circuit board technology and bioleaching technology is required. To address the potential for bioleaching of metals from e-waste such as PCBs, it is necessary to have a comprehensive knowledge of the PCB industry (including recycling process options), the properties of the boards, the current state and application of bioleaching technology, the application of bioleaching to PCBs treatment and the kinetics of both the generation of leach agents and leaching of metals into solution. A comprehensive review of the literature in these fields is presented to provide the grounding for further experimental study and the modelling approach used in this study.

2.1 Background of Printed Circuit Boards (PCBs)

The printed circuit board manufacturing industry has been placed at a $50.8 billion valuation in 2009 (Mingjiang Zhan, 2013) and contains 20 – 250 times more gold than in gold ores (250 g/ton in PCBs vs 1-10 g/ton in ores) and 20 – 40 times more copper than in copper ores (20 % in PCBs vs 0.5 – 1 % in ore) (Tuncuk, et al., 2012).

In this dissertation, the review of PCBs has been undertaken to provide insight into the WEEE sector. This review highlights the varying composition trends of the metals in the boards, which depends on the year of manufacture and function of the PCB. The varying metal composition impacts the metal recovery efficiencies of the recycling processes. In addition, knowledge of the potential pollutants that

PCB recovery generates, will aid in designing processes that are in alignment with environmental regulations.

2.1.1 Properties of Printed Circuit Boards

Printed circuit boards form the platform onto which components, such as semiconductor chips and capacitors, are mounted. The PCBs also contain the electric interconnections (made of copper) between the components on the boards (LaDou, 2006). The creation of printed circuit boards is a complex process and can take over 50 process steps (LaDou, 2006).

The boards are made of polymer, glass or ceramic substrates with higher end boards consisting of a woven fibre glass mat impregnated with flame resistant epoxy resins (LaDou, 2006). There are three basic varieties of PCBs which are single-sided, double-sided and multi-layered boards (Sohaili, et al., 2012). This refers to the number of layers of resin, with a multi-layered board usually containing between 2 – 40 layers of fibre glass and epoxy resin. The boards have high flexural strength and are therefore resistant to fracturing and breakage. This is ideal for their function as it means the boards have a long life span, however, it makes the metal recovery process difficult where crushing of the boards into particulate form is required. Crushing is important for bio- and hydrometallurgical treatment options as it increases metal liberation, enhances surface area exposure to the leach solution and facilitates easy handling of the solid suspensions.

Printed circuit boards used for computers and communication equipment are usually higher end boards and contain glass fibre reinforced epoxy resins, referred to commercially as FR-4. Printed circuit boards for use in televisions are usually lower end boards and contain cellulose paper reinforced phenolic resin with the commercial name being FR-2. The boards are also classified according to value, with boards containing less than 100 ppm gold termed low value boards (Tuncuk, et al., 2012). The structural and metal components of the board informs selection of the best approaches to crush the boards and recover the metals.

2.1.2 Production of Printed Circuit Boards

The main processes in PCB production are drilling, image transfer and electroplating. Drilling involves forming holes to provide layer to layer interconnections. The holes are made conductive by plating copper through the hole barrels. The image transfer step follows and involves transferring an image of the circuit layer from film/glass to the PCB material. For outer layers, the image transfer includes the electroplating of copper, tin, tin-lead or nickel/gold onto the PCB surface. The image transfer method is predominantly done by a print-and-etch system. This is where the board is uniformly plated with copper foil and then selectively etched to form a conductive circuit pattern. The use of copper for the circuits in the boards explains why it has the highest overall concentration.

Due to the risk of ignition when components are soldered onto the platform and ignition from electric currents during usage of the boards, the board matrix often contains about 15 % bromine, which acts as a flame retardant (Luda, 2011). If pyro-metallurgy is used as the recycling technology this flame retardant forms dioxins and furans which are serious pollutants.

Precious metals serve as contact metals on the PCBs due to their chemical stability and conducting properties. For example, platinum group metals are used as switching contacts and sensors on the boards. However, precious metal concentrations have been on the decline due to the decreasing power consumption of modern switching circuits (Luda, 2011). In the 1980s the metal contact layer was 1-2 µm, while in the past decade it has decreased to between 300 and 600 nm in thickness (Cui & Zhang, 2008). Thus designing optimal e-waste recycling systems is difficult as an optimal process designed today may not be efficient in the future, when the concentrations of the metals may change drastically. A recovery technology, therefore, which is relatively non-capital intensive, easy to set up and to modify, does not produce a lot of pollutants, and is flexible enough to adapt to the changing metal concentrations, is necessary for the recycling of PCBs.

2.1.3 Metal Composition in Printed Circuit Boards

The high metal content in printed circuit boards makes disposing of them difficult as some of the metals are toxic to the environment (Musson, et al., 2006). There is also a significant concentration of high value metals in PCBs hence their recovery can prove to be profitable. Further, they form an important inventory of metals in the world's metal reserves, with the "grade" of electronic waste frequently being higher than the grade of virgin ores. The metal concentration in printed circuit boards varies significantly according to board functionality and year of manufacture. Typical average metal inventories of boards from a range of literature sources are given in Table 2.1.

Table 2-1. Weight composition of metals in PCBs according to different references

Metals (%)									Reference
Cu	**Pb**	**Al**	**Sn**	**Zn**	**Fe**	**Ni**	**Ag**	**Au**	
23.10	2.89	2.60	1.88	1.75	0.81	0.19	0.0217	0.0014	(Xiang, et al., 2010)
12.60	3.10	1.40	-	5.60	1.20	-	0.0033	0.0014	(Liang, et al., 2010)
18.50	2.66	1.33	4.91	-	2.05	0.43	0.0694	0.0086	(Yazici & Deveci, 2014)
19.00	0.51	1.10	0.95	0.26	-	-	-	-	(Kim, et al., 2011)

From the literature cited, copper has the highest concentration on PCBS which explains why most studies conducted on metal recovery from e-waste has been focused on copper. Removing Cu is also

an essential step to getting effective leaching of Au and precious metals by cyanide leaching. The lead content is also high and poses a hazard as lead is known to have high toxicity. However, the inclusion of lead in PCBs is decreasing (Bizzo, et al., 2014). Depending on the literature source zinc or tin has the second highest concentration to copper on PCBs, while other sources state that aluminium has the second highest concentration.

2.1.4 Recovery of Metals from Printed Circuit Boards

As the amount of WEEE and thus PCB generated worldwide is rapidly growing, 50 – 80 % of it is transported to developing countries, especially countries in the African and Asian continents, where they may be disposed in landfill sites (Pant, et al., 2011) or further processed typically through the informal sector. Disposal of PCBs in landfill sites is problematic as toxic substances can leach into the soil and water supply (Bizzo, et al., 2014). Recycling the PCBs would, therefore, prevent contamination of the soil and water supply. The recovery of metals from printed circuit boards is also useful in that it preserves the metal resources and also reduces the carbon footprint on the environment as it is less energy intensive to recover the metals from PCBs than to mine them from the ground (Tuncuk, et al., 2012).

2.1.4.1 Sourcing the Printed Circuit Boards for Recycling

The first step prior to PCB preparation is the sourcing of the PCB e-waste stream. This can come directly from companies that collect, dismantle and sort e-waste for recycling or can be collected directly from landfill sites.

2.1.4.2 Pre-treatment Step in Printed Circuit Boards Prior to Recycling

After the PCBs have been sourced, a mechanical pre-treatment step is necessary. The different devices and components are selectively dismantled into various type fractions such as metals, plastics, ceramics, capacitors, batteries etc. (Tuncuk, et al., 2012). This process serves two purposes which are (Luda, 2011):

1. To recover valuable components, such as undamaged units, from the PCBs which can be reused without treatment.
2. To remove hazardous waste prior to shredding of the printed circuit boards (Xiang, et al., 2010).

The initial dismantling phase involves the manual separation of the specific components of the PCBs to prevent the build-up of toxic chemicals further down the line (Xiang, et al., 2010; Salhofer & Tesar, 2011). This is because it may prove to be very difficult to control the toxicity levels of metals in solution which can be inhibitory to the microorganisms, if a bioleach treatment process is selected (Salhofer & Tesar, 2011).

2.1.4.3 Particle Size Reduction in Printed Circuit Boards

The next step in the e-waste preparation process is the particle size reduction step. It has been stated in literature that the initial shredding should be between 20 & 40 mesh size fraction (Yang, et al., 2011) or 0.1 - 0.5 mm (Brandl, et al., 2001; Yang, et al., 2009) depending on the recovery technology selected. In some cases, for example in the electromechanical processing of PCBs, the particle size has to be reduced further, either by more shredding (Yang, et al., 2011) or by crushing the PCBs. The size reduction first consists of a crude shearing action by rotor cutters and a hammer grinder is utilized as the second crusher (Huang, et al., 2009). The crushing is one of the most energy intensive stages in the recycling process. This is because the PCB e-waste stream is primarily comprised of reinforced resin, fibre glass and metal components, such as copper wires and joints that have high hardness and tenacity, where the shearing action is the best method to break them (Huang, et al., 2009). Depending on the recovery process, crushing serves various purposes. In electromechanical (magnetic) processes, size reduction is conducted to liberate the metals from the board to allow for current/density separation to be conducted. In hydrometallurgical and biohydrometallurgical processes, it is to increase the surface area and expose the embedded metals to the leaching reagents.

2.1.4.4 Processing Options for the Treatment of Printed Circuit Boards

Separation of the metals from the printed circuit boards is conducted using various technologies such as pyrometallurgical processes, hydrometallurgical processes and electromechanical processes.

Electromechanical processes require that the boards be crushed to smaller size fractions. This approach has been associated with significant metal losses amounting to 10 – 35 %. This is attributed to the metals being closely associated with the resins, generation of fines (75 µm) and inadequate separation processes (Tuncuk, et al., 2012). The separation process makes use of the different physical properties of the materials such as specific gravity, magnetic susceptibility, electrical conductivity etc.

In pyrometallurgical processes, since the boards are made from epoxy resins which are petroleum based, the boards can be used as a source of fuel in the recovery process. The process remains energy intensive requiring high-cost equipment. Thus the metal content of the boards must be sufficiently high for the process to be profitable. Further, various pollutants are formed due to the presence of halogenated flame retardants and volatile metals in the PCBs, including dioxins, furans and dust, hence an off gas treatment step is necessary (Tuncuk, et al., 2012). Complex metal interactions mean that an alloy of metals is formed which is difficult to separate out into pure metals.

Hydrometallurgical processes may provide better alternatives than the pyrometallurgical process in that they have a lower capital cost, reduced environmental impact, and a higher metal recovery efficiency is possible (Tuncuk, et al., 2012). Hydro- and pyro-metallurgical processes may be used in

tandem. Hydrometallurgical processes are reported to be more predictable, more easily controlled and more exact than pyrometallurgical processes (Sohaili, et al., 2012). The metal content in the boards also does not have to be high for the technology to be viable. However the technology consumes high amounts of reactants which are not regenerated. In addition, the equipment costs are significant due to the use of caustic alkalis and acids.

Biohydrometallurgical processes provide one of the more promising technologies for the recovery of metals from PCBs. This is attributed to relatively low capital cost, regeneration of reactants using microorganisms and lower levels of pollutants. There are two main disadvantages of biohydrometallurgy. The first is that it is that it is perceived to be a slow process relative to pyrometallurgy and hydrometallurgy, due to the long residence time necessary to attain high metal recoveries. The second is that the potential metal toxicity to microorganisms may result in low pulp densities being processed (Tuncuk, et al., 2012). Despite the drawbacks of biohydrometallurgy, there are significant advantages and thus the potential for metal recovery from PCBs by bioleaching as a treatment option requires further study.

2.1.4.5 Recovery of Metals after Metal Extraction

After the metals have been extracted from the boards, the solution purification and metal recovery step needs to be conducted. The recovery process depends on the technology that was used to liberate the metals from the PCBs. If the metals are in solution as ions as a result of a (bio)hydrometallurgical process, then a solvent extraction step followed by an electro-winning stage can be used. Other metal recovery techniques include adsorption onto activated carbon, ion exchange, precipitation, cementation, etc. (Tuncuk, et al., 2012).

2.1.4.6 Disposal of Printed Circuit Board Non-Metallic Fraction

The non-metallic portions of the e-waste streams can be discarded to landfills. However, new research is currently being conducted to provide further uses of the non-metallic materials. Authors suggest that the non-metallic components can be used as fillers, or as a partial replacement of inorganic aggregates in concrete, or reprocessing into kitchen utensils, adhesives etc. (Tuncuk, et al., 2012).

2.2 Bioleaching Technology for Base Metal Extraction

To assess the applicability of bioleaching to recover metals from printed circuit boards, a good understanding of the technology and its current industrial application to metal recovery from sulphidic ores and concentrates needs to be attained. Thus this section looks into the background of bioleaching technology based on its origins and how it is used in industry.

2.2.1 Overview of Bioleaching of Sulphide Minerals

Bioleaching has been largely conducted on sulfide minerals in an acidic medium with a high concentration of ferric ion as the primary oxidant in the leaching process (Watling, 2006). The ferric ion is regenerated by microorganisms through an oxidative process. The factors that contribute to the overall leach efficiency are: acidity of the solution, redox interactions between sulfide minerals, and the concentration of ferric ions in solution.

It has been found that leaching kinetics may change when two minerals are in electrical contact with each other. This has been attributed to redox interactions between the minerals (Watling, 2006). As an example, pyrite leaching is faster than chalcopyrite leaching when each mineral is leached in isolation, however, when pyrite and chalcopyrite are in contact in the same reaction environment, pyrite will appear to have a slower leaching rate than when leached in isolation. Redox interaction considerations are crucial in PCB bioleaching as the metals in the boards are in intimate contact with one another and should be taken into account during PCB bioleaching.

Microorganisms play a catalytic role in the bioleaching process as they oxidize ferrous ion to ferric ion thus regenerating the ferric ion oxidant (Watling, 2006). The ferric ion is then reduced to ferrous ion by the sulphide ion in the mineral sulphides as they leach as metal ions into solution. This mineral leaching reaction generates the ferrous ion that is oxidised by microorganisms, as an electron donor for energy requirements, whilst the carbon source comes from carbon dioxide in the air. One drawback of using high concentrations of ferric ion is that it precipitates to form jarosite, which can hinder further dissolution as the reactants have to diffuse through the precipitation layer. The jarosite formation equation is given below (Watling, 2006):

$$3Fe^{3+} + 2SO_4^{2-} + 6H_2O + M^+ \rightarrow MFe_3(SO_4)_2(OH)_6 + 6H^+ \qquad \textit{Equation 2-1}$$

The symbol M above can either be K^+, Na^+ or NH_4^+. The precipitation of ferric ions from solution can be prevented by keeping the leaching environment at low pH values. The second problem is that high ferric ion concentrations have been known to be inhibitory to microorganisms (Watling, 2006), thus using microorganisms that operate at low pH and high ferric ion concentration is desirable.

2.2.2 Bioleaching Mechanisms for Metal Sulphide Leaching

There has been a lot of discussion about the possible mechanisms of bioleaching metal sulfides into solution. There are three main leaching mechanisms which have been suggested by which microorganisms oxidizes metal sulfides, these are (Crundwell, 2003):

1. The indirect mechanism – this is where microorganisms oxidize the ferrous ion to ferric ion in the bulk solution. The ferric ion then diffuses to the mineral surface and oxidizes the metals (in mineral sulfides or e-waste).
2. The indirect contact mechanism – this is where the microorganisms are attached to the mineral surface and oxidize ferrous ion to ferric ion within a biofilm. The biofilm is made up of microorganisms and exo-polymeric material. The ferric ion generated within the biofilm oxidizes the mineral sulfide.
3. The direct contact mechanism – this is where the microorganisms attach to the surface of the mineral (or waste) and oxidize the mineral sulfide (or metal) directly by biological means. This is done in the absence of ferric or ferrous ions. However, there is no evidence that supports the direct contact mechanism, where the microorganisms directly break the metal-sulfide bond of a mineral.

The diagrams below illustrate and summarise the indirect and indirect contact mechanisms:

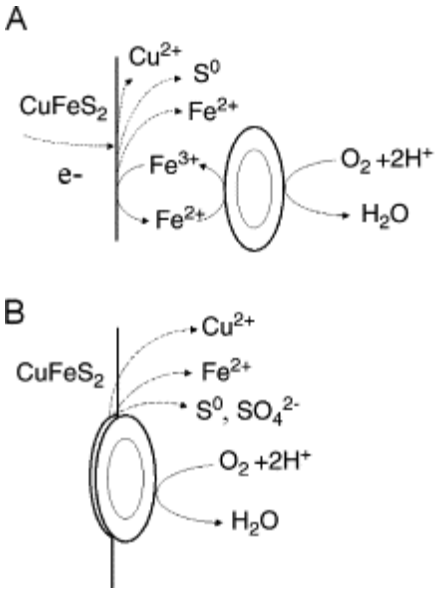

Figure 2–1: Part A shows the indirect mechanism as bacteria oxidize soluble ferrous ion to ferric ion and sulphur to sulphate. Part B is the indirect contact mechanism where bacterial attachment is of physiological importance with ferric ion oxidizing the sulphide minerals. The specifics of microorganism electrochemical (interaction) with the mineral surface and/or direct contact contribution to sulphide dissolution is unknown (Watling, 2006).

In both the indirect leaching and indirect contact leaching mechanism, ferric ion is the oxidizing agent. The role of the microorganism is to regenerate ferric ion through the oxidation of ferrous ion. In a sulfide bioleaching system, the equations can be summarised as follows (Cui & Zhang, 2008):

$$MS + 2Fe^{3+} \rightarrow M^{2+} + 2Fe^{2+} + S^0$$
$$2Fe^{2+} + 0.5O_2 + 2H^+ \rightarrow 2Fe^{3+} + H_2O \qquad \textit{Equation 2-2}$$

2.2.3 Use of Bioleaching in Extraction Metals from Mineral Sulphide Ores

Bioleaching describes the extraction of metals from primary sources (metal-containing ores and concentrates) and secondary sources (waste materials, including e-waste) using prokaryotic and/or eukaryotic microorganisms (Ehrlich, 2004; Brierley, 2008).

Bioleaching technology is used to extract metals which are complexed in sulphide minerals and also for the extraction of copper from copper ores using ferric ions regenerated by microorganisms through ferrous ion oxidation (Brierley, 2008). Despite the number of metals which have been studied that can be recovered by the technology, only copper and gold are currently recovered industrially in significant portions (Cui & Zhang, 2008). The standard applications of bioleaching in industry are through dump bioleaching, heap bioleaching and continuous stirred tank bioleaching.

Dump bioleaching is applied to low grade copper containing ore (≤ 0.5 % copper) (Brierley, 2008). The low grade ores are placed in pits which are approximately 60 m deep. Acidified water is then sprinkled at the top of the pile, and the solution percolates through the dump. This provides conditions that allow for the growth of microorganisms that oxidize ferrous ion to ferric ion, which then oxidizes copper in sulphide ores. Due to the large particle size and low grade of the ore, slow leaching rates are observed (150 – 210 days for a recovery efficiency of 75 – 80 % of copper from ore) (Watling, 2006). The cupric ion solution is collected at the bottom of the heap and transported to the metal recovery stage. Despite the low leaching rates, dump bioleaching is profitable due to the high tonnage of copper ores that can be processed at very low costs. An example of dump bioleach in industry is the BHP Billiton Escondida mine in Chile, which is expected to produce 180 000 - 200 000 tons per annum of copper over the next 40 years (Brierley, 2008).

Heap bioleaching is mainly applied to the extraction of copper from chalcocite (Cu_2S) and covellite (CuS) which are termed as "secondary copper ores". The difference between heap and dump leaching is that in heap leaching the copper ore is first crushed to particle sizes that are less than 19 mm in diameter, followed by agglomeration in rotating drums with acidified water. This is to affix fine particles onto larger ones thereby producing coarser particles, and to condition the ore for microorganism growth. The ore is stacked on special pads containing high-density polyethylene drain pipes that allow solution to be easily collected from the bottom. The pipes also allow for air to be blown into the heap from the bottom as opposed to dump bioleaching where no artificial aeration takes place. The heap is stacked to a height of 6 - 10 m and is irrigated with acidic raffinate which is recycled from the solvent extraction stage. The microorganisms then grow on the ore and can exceed 10^6 cells per gram of ore, with an extraction efficiency of 80 - 90 % after about 250 - 350 days of operation (Brierley, 2008). The advantages of heap leaching are its low capital and operating costs, which are attributed to the high recycling of reactants within the system, and low toxic emissions.

Heap leaching operations account for approximately 7 % of the world's copper production. Heap bioleaching is also applied to "pre-treat" gold ores, where the initial biooxidation of base metals from mineral sulphides facilitates greater exposure of gold particles to cyanide leaching downstream.

Continuous stirred-tank reactors (CSTRs) are only used to process high value minerals, such as gold mineral concentrates, due to the high capital and operating costs involved in the process (Brierley, 1997; Dew & Miller, 1997). The process is carried out in a series of large bioreactors which are made of acid-resistant, stainless steel. Air is introduced below the impeller, which breaks up the gas bubbles ensuring good mass transfer of oxygen and carbon dioxide to the leach solution. Agitation keeps the minerals suspended and provides good contacting between the gas, solution and solids phases. Cooling coils are inserted into the reactor to remove excess heat and maintain optimum temperature for mineral leaching and microbial growth. The combination of these factors creates an environment where fast leaching rates of 3 - 5 days can be achieved (Brierley, 2008). CSTRs allow for the monitoring and fine control of process variables such as pH, temperature, and ferric ion concentration in solution. In industry, CSTRs used for gold extraction operate at slurry densities of 15 – 20 %, with the slurry fed continuously to the primary reactor where most of the bacterial growth occurs. The slurry residence time in the primary reactor is 2 – 2.5 days after which the slurry overflows to smaller secondary reactors. The residence time of the whole process is 4 – 6 days (Cui & Zhang, 2008).

Understanding the current technology is important in determining how to apply bioleaching for the treatment of PCBs. As PCBs contain high value metals, such as gold and palladium, continuous stirred-tank reactors could be used. However, heap and dump leaching reactor systems should be considered in order to minimise the high costs involved in reducing the particle size of the boards.

2.3 Application of Bioleaching for the Treatment of Printed Circuit Boards

There are several studies which have been conducted to investigate the extraction of metals from printed circuit boards. These studies will be briefly described to provide an understanding of the various factors affecting the extraction of metals from PCBs.

2.3.1 Mechanisms of Metal Recovery from Printed Circuit Boards

One of the most important distinctions between PCB bioleaching and traditional bioleaching of mineral sulphides, is that the metals in PCBs are in their zero-valence state and/or as alloys (Tuncuk, et al., 2012). Therefore, the mechanisms by which metals from PCBs are dissolved into solution may differ from the mechanisms observed in mineral sulphide bioleaching.

Several studies have confirmed that the dissolution of metals in their zero-valence state from PCBs is via the reaction of ferric ion with the metals (through the indirect mechanism) (Demir, et al., 2004;

Younesi, et al., 2006; Wang, et al., 2010; Huang, et al., 2014; Yang, et al., 2014; Zhao, et al., 2014). Using copper as the representative metal, leaching occurs according to the following equations (Choi, et al., 2004).

$$2Fe^{2+} + 0.5O_2 + 2H^+ \xrightarrow{microorganisms} 2Fe^{3+} + H_2O \quad \textit{Equation 2-3}$$

$$2Fe^{3+} + Cu^0 \rightarrow 2Fe^{2+} + Cu^{2+} \quad \textit{Equation 2-4}$$

It has also been found that some of the copper in PCBs is leached out chemically by the action of protons in solution. A study done by Xiang et al (2010) was conducted by adding copper to a control solution without an iron source but with microorganisms, the system was maintained at a pH value of 2.0. It was observed that copper was able to dissolve into solution but at a significantly slower rate than in the presence of ferric ion. The authors concluded that the main mechanism for dissolution of copper is by the oxidative effect of ferric ion on the copper. However, the proton dissolution process does contribute to the dissolution of copper metal into solution. The reaction for the dissolution of the copper by protons is provided below (Xiang, et al., 2010).

$$Cu^0 + 2H^+ + 0.5O_2 \rightarrow Cu^{2+} + H_2O \quad \textit{Equation 2-5}$$

Contact leaching is as a result of the extracellular polymeric substances (EPS) attaching to the mineral surface via Van der Waals forces in elemental sulfur leaching or electrostatic forces in the case of semi conducting metal sulfides. This means that the microorganisms are unable to attach to PCBs as there is no sulfur on the surface hence no Van der Waals or electrostatic forces by which to attach. This means that only the indirect non-contact mechanism will be present in metal leaching from PCBs.

The indirect contact leaching mechanism is even more probable given that high concentrations of the metals are toxic to the bacteria and the highest metal ion concentration will be found on the metal/leachate interface. This may prevent microorganisms growing directly on the metal-containing PCB surface.

2.3.2 Industrial applications of Metal Extraction from PCBs using Bioleaching Technology

At present there are no examples of an industrial scale application of bioleaching to extract metals from PCBs. This may be attributed to the fact that the knowledge and understanding of the process of metal extraction from PCBs is still in its infancy.

2.3.3 The Role of Microorganisms in PCB bioleaching

In order to determine the factors that affect the recovery efficiency of metals from PCBs, it is important to know the role of microorganisms and which microorganisms are best suited to the recovery of metals from the PCBs. Due to the large number of metals in printed circuit boards, it is unlikely that a single microorganism can be used to recover all the metals found in the PCBs. Table 2-2 below lists the different microorganisms that have been studied in dissolving metals from e-waste.

The role of microorganisms in PCB bioleaching is to oxidize ferrous ion to ferric ion. The ferric ion then oxidises the base metals producing metal ions and ferrous ion. The ferrous ion is once again utilized by the microorganisms for energy and growth, thus regenerating the ferric ion. This consumption and regeneration of ferrous ion in the system is cyclic hence no fresh reactants have to be introduced in the system.

Regardless of the number of microorganisms that have been investigated previously, the microorganism that will be considered for further investigation is *Leptospirillum ferriphilum*, as it is readily available for use in this study. Bacteria belonging to the *Leptospirillum* genus are highly acid tolerant with an optimum range of pH 1.5 – 1.8, it is gram negative and chemolithoautotrophic. The microorganism is autotrophic in that it uses CO_2 as a carbon source. It is mesophilic in that it operates between 20 – 40 ^{o}C. The *Leptospirillum* genus utilises ferric ion as an electron donor for energy requirements and is unable to utilize sulphur. Studies have shown that *Leptospirillum* has a higher affinity for ferric ions (Rawlings, 2002) and therefore, is more active in a non-sulphide environment with high ferric ion concentrations. This suggests that *Leptospirillum* is appropriately suited for the e-waste/PCB bioleaching environment, where there is no sulphur.

Table 2-2. Microorganisms that are known to recover metals from E-waste (Pant, et al., 2011).

Metals to be recovered	Microorganisms involved	pH	Temperature (°C)
Cu	*Acidithiobacillus ferrooxidans*	2 - 3	45
	Acidithiobacillus thiooxidans	3 - 4	45
	Aspergillus niger	2 - 6	30
	Penicillium simplicissimum	2 - 6	32
	Gallionella sp.	3	30
	Leptospirillum sp.	2 - 3	45
Al	*Bacillus circulans and B. mucilaginosus*	4 - 5	35
	Acidithiobacillus thiooxidans	3 - 4	45
	A. ferrooxidans	2 - 3	45
	Aspergillus niger	2 - 6	30
	Penicillium simplicissimu	2 - 6	32
Pb	*Acidithiobacillus ferrooxidans*	2 - 3	45
	Acidithiobacillus thiooxidans	3 - 4	45
	Aspergillus niger	2 - 6	30
	Penicillium simplicissimu.	2 - 6	32
Zn	*Acidithiobacillus ferrooxidans*	2 - 3	45
	Acidithiobacillus thiooxidans	3 - 4	45
	Aspergillus niger	2 - 6	30
	Penicillium simplicissimum	2 - 6	32
Ni	*Acidithiobacillus thiooxidans*	3 - 4	45
	A. ferrooxidans	2 - 3	45
	Aspergillus niger	2 - 6	30
	Penicillium simplicissimu	2 - 6	32
Cd	*Aspergillus niger*	2 - 6	30

2.3.4 Inhibition of Microorganisms by High Zero-Valence Metal and Metal Ion Concentrations

As efficiency of microorganisms in regenerating ferric ion is crucial to the bioleaching of metals from PCBs, it is important to understand the toxicity effects of certain metals in solution on the microorganisms. Due to the high metal concentrations found in printed circuit boards, the maximum concentration of metal ions in solution that can be tolerated by the microorganisms is of interest. Significant literature on mineral bioleaching has been presented with a focus on metal toxicity. A second consideration is what processes and techniques can be implemented to increase the tolerance or reduce the concentration of toxic metals in solution.

In the bioleaching of mineral sulphides, a two-stage process is proposed as a strategy to prevent microbial inhibition, enhance biooxidation rates and increase the selectively of specific products (Gericke et al. 2009). Mintek has patented a two-stage process for the treatment of copper-bearing mineral sulphides, where the bacterial ferric iron generator (BFIG) was separated from the mineral

leach reactor, which allowed for variation in reactor temperatures (Gericke et al. 2009). A two-stage reactor approach was also successfully applied for the bioleaching of zinc-bearing mineral sulphides, as part of the BioMinE project (Morin et al. 2008). This indirect bioleaching process facilitated the independent optimisation of the biological reactor, thereby facilitating favourable economics (Morin et al. 2008).

Brandl et al (2001) conducted a study in-order to test for possible inhibition of microorganisms when leaching metals from PCBs. The study found that microorganisms were inhibited by high metal concentrations (observed when scrap concentration was at 100 $g.l^{-1}$). From the results, two techniques were suggested to lower the effect of the toxicity. The first was a two-stage process where the microorganisms were grown in the absence of metals, after which metals were then added to the solution. The second technique applied by Brandl et al. (2001) was for PCB leaching by fungi, where an adaptation time of 6 weeks was required to allow the microorganisms to have the same recovery efficiencies at high waste concentrations as was observed at lower concentrations. The adaptation was achieved by growing the fungi at progressively higher concentrations of metal ions.

Adaptation of bioleaching microorganisms to environments of high toxic stress has most notably been demonstrated by Das et al. (1997). The authors successfully adapted *A. ferrooxidans* cultures to 10 $g.l^{-1}$ Fe^{3+}, 25 $g.l^{-1}$ Cu^{2+} and 40 $g.l^{-1}$ Zn^{2+}, respectively, with each of the adapted cultures demonstrating comparable biooxidation rates to that of the unadapted cultures in the absence of metal ion stress. In addition, the oxidation ability of the copper adapted culture was shown to be only slightly affected in the a multi-metal solution containing 10 $g.l^{-1}$ Fe^{3+}, 25 $g.l^{-1}$ Cu^{2+} and 40 $g.l^{-1}$ Zn^{2+}. In general, however, the inhibitory effect on the oxidation ability of adapted microorganisms is cumulative for single metal ions, with toxicity increasing with increasing number of metals ions.

Studies conducted by Ilyas et al (2012) found that a consortium of *Sulfobacillus thermosulfidooxidans* with *Thermoplasma acidophilum* could be adapted to mixed metal ions of Cu, Ni, Al and Zn. The adaptation was achieved through successive step-wise growth in increasing metal ion concentrations. It was found that at 7 $g.l^{-1}$ mixed metal ion concentration, the microorganisms that were used for the experiments grew with a lag phase of 5 days. However, in the presence of 12 $g.l^{-1}$ metal ion concentration the lag phase was much longer. At 14 $g.l^{-1}$ metal concentrations all the microorganisms died which was concluded after an incubation period of 52 days. After adaptation, the microorganisms were able to grow in a mixed ion metal concentration of up to 20 $g.l^{-1}$ with an initial lag phase of only 6 days which was attributed to physiological changes within the cells (Ilyas et al. 2012).

The presence of highly toxic metals in the bioleaching process, such as lead, which occurs at high concentrations in PCBs and is highly toxic to microorganisms, can reduce dissolution efficiency as a

result of the reduced microbial activity. A possible solution is to remove these metals from PCBs before the bioleaching process. One method is to immerse the printed circuit boards for 3 hours in dilute nitric acid at 2 mol.l^{-1} and at room temperature. The nitric acid reacts with the tin/lead solder to form an insoluble stannic acid (containing the tin) and a soluble lead nitrate solution. Thereafter, the tin can be separated from lead via a filtration/decantation technique. The lead ions can then be precipitated from solution by adding sulphuric acid (Yang, et al., 2011). In the process described above, it was found that the copper in the PCBs only reacts with nitric acid when most of the tin solder had been dissolved, which suggests negligible copper losses at low nitric acid concentrations. However, as of 2006, there has been significant legal pressure to reduce the use of lead in PCBs as stated in the RoHS directive (Öko-Institut & Fraunhofer, 2003).

2.3.5 Influence of Initial Iron Concentration on the Leaching Efficiency of Metals from PCBs

Ferric ion concentration plays a primary role in bioleaching of metals from PCBs and metal sulphides, as it is the main oxidant in the system. Ferric ion is oxidized naturally from ferrous ion in the presence of oxygen, but this is a slow process which can be increased by 10^5 – 10^6 times in the presence of microorganisms (Ozkaya, et al., 2007).

Xiang et al (2010) conducted a study where leaching of crushed PCBs was conducted in 500 ml Erlenmeyer flasks containing different initial concentrations of ferrous ions and a bacterial consortium consisting mainly of genera of *Acidithiobacillus* and *Gallionella* at a pH of 2.0. Table 2-3 summarises the copper dissolution efficiency after 16 days using different initial concentrations of ferrous ions.

Table 2-3. Effect of initial ferrous concentration on the recovery efficiency of copper from crushed printed circuit boards (Xiang, et al., 2010)

Initial ferrous concentration (g.l^{-1})	**Leaching efficiency of copper**
0	12.7 %
3	60.0 %
6	75.8 %
9	93.3 %
12	87.1 %
15	81.2 %

Xiang et al (2010) found that as the initial ferrous ion concentration increased, the leaching efficiency of copper increased to a maximum value of 93.3 % at 9 g.l^{-1} initial ferrous ion concentration. However, when the initial ferrous ion concentration was increased to 12 g.l^{-1} and 15 g.l^{-1}, there was a decline in the leaching efficiency of copper. This was attributed to the formation of jarosite precipitate which

reduced the available ferric ion concentration, and was also hypothesised to form a layer on the PCB surface leading to passivation and thus mass transfer limitations (Xiang, et al., 2010).

A similar study was conducted by Choi et al (2004) where 50 $g.l^{-1}$ PCB shreds, at a size fraction of -14/+20 mesh, was bioleached in shake flasks in the presence of *Acidithiobacillus (A.) ferrooxidans*. Some of the results from this study are presented in Figure 2–2. From the study, it was found that in the absence of ferrous ion, 2.55 $g.l^{-1}$ of copper was leached into solution by *A. ferrooxidans* (this supports the direct proton leach mechanism given in Equation 2-5). The value of copper ions in solution increased to 5.19 $g.l^{-1}$ when 7 $g.l^{-1}$ ferrous ion was added to the flasks. However, when 9 $g.l^{-1}$ of ferrous ion was added, the amount of leached copper reduced to 3.85 $g.l^{-1}$. This follows the trend that was observed by Xiang et al (2010). However, the optimal ferrous ion concentration in this study was lower (at 7 $g.l^{-1}$) than was reported by Xiang et al (2010), which was at 9 $g.l^{-1}$. Several factors could be attributed to this difference, such as, a lower dosage of PCBs used in the study conducted by Xiang et al (2010), at 20 $g.l^{-1}$ as opposed to 50 $g.l^{-1}$ PCBs used by Choi et al (2004) or the use of a consortium of microorganisms instead of the pure culture used by Choi et al (2004). However, the conclusion was the same, in that significantly higher ferrous ion concentrations reduce copper dissolution efficiency.

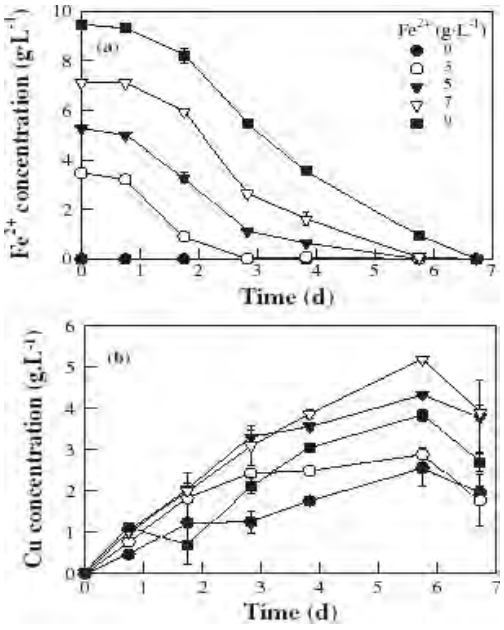

Figure 2–2. Time profile of ferrous ion and copper ions in solution at different initial ferrous ion concentrations (Choi, et al., 2004).

2.3.5.1 Effect of pH on Metal Dissolution Efficiencies from PCBs

Studies have been conducted to understand the effect of pH on dissolution efficiency of metals from PCBs. One such study was by Xiang et al (2010), where the authors found that the copper dissolution efficiency from PCBs was low at pH 1.0, this was attributed to the inhibition of *A. ferrooxidans* at low pH. It was also found that high pH values also resulted in low copper dissolution efficiencies from PCBs,

possibly due to the decrease in ferric ion concentration through iron precipitation. In this study, an optimum pH of 1.5 resulted in the highest PCB leaching rates (Xiang, et al., 2010). In order to limit the extent of ferric ion precipitation, a pH value below 1.8 has been suggested (Anders & Colin, 1995).

Yang et al (2009) also studied the effect of pH on copper dissolution from PCBs. In the study, the microorganism used was *A. ferrooxidans*, with 7 $g.l^{-1}$ initial ferrous ion concentration, a PCB particle size fraction of < 0.5 mm and 15 $g.l^{-1}$ PCB dosage. The experiments were conducted at pH values of 1.5, 1.7 and 2.0, which were maintained using sulphuric acid. The results of the experiments is shown in Figure 2–3.

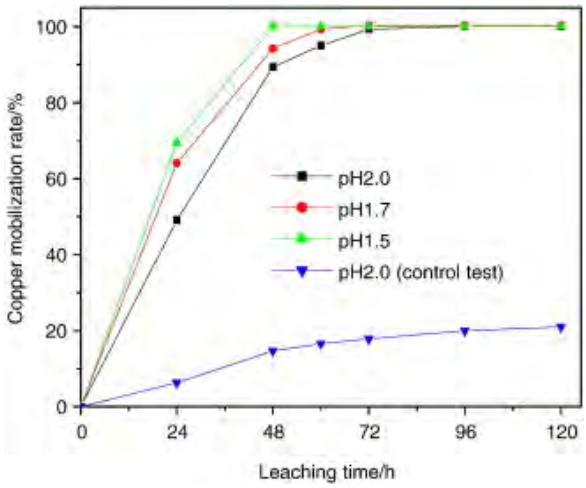

Figure 2–3. The influence of pH on the copper mobilization rate (Yang, et al., 2009).

It was found that after 48 hours, the dissolution efficiency of copper was 99 % at pH 1.5, 93 % at pH 1.7 and 88 % at pH 2.0. This shows that the lower the pH the faster the rate of leaching. Control experiments were also conducted in the absence of microorganisms and where the pH was maintained at 2.0. It was found that 21 % of copper was dissolved into solution after 120 hours. Thus it was concluded that pH alone resulted in slow dissolution rates of copper but optimum pH conditions resulted in high dissolution efficiencies of copper from PCBs (Yang, et al., 2009).

2.3.5.2 Mechanisms and Factors affecting pH Variation in Bioleaching of PCBs

As was discussed in Section 2.3.5.1, the pH of the bioleaching solution affects the dissolution efficiency of metals from PCBs. There are several factors which have been reported to affect the pH of solution in a bioleaching environment.

One of the factors which causes an initial increase in pH is the alkalinity of the non-metallic components in the PCBs (Brandl, et al., 2001). Studies were also conducted by Illyas et al (2007) to investigate what effect the alkalinity of PCBs has on the pH of the leach solution. The study was conducted using *Sulfobacillus thermosulfidooxidans* and crushed PCBs. The particle size of the PCBs

was in the range of 50 – 150 µm, at a pH of 2.0 and dosage of 10 $g.l^{-1}$ PCBs. In the study, the non-metallic component was separated from the metallic component using density separation which could be achieved due to the small particle sizes involved. It was assumed that the metals were sufficiently liberated from the plastics and thus could be separated as the metals have greater density. For the separation, 10 g of the shredded PCB mixture was added to 100 ml of saturated sodium chloride solution for 10 min. The heavier metal containing particles sank to the bottom and the lighter non-metallic portion floated to the top where it was decanted out. This bottom fraction formed the "lower/no plastic concentration" part of the study, thereby eliminating the effect of the plastic component on the pH and its associated effect on iron solubility, presented previously in Equation 2-5. An unwashed sample (i.e. not added to NaCl solution) represented the native PCBs sample. From the study it was found that for the unwashed sample, the pH reached a value of 3.4 after 3 days, even though sulphuric acid was added every 24 hours to reduce the pH to 2.0. However, for the washed sample, the maximum pH reached after 3 days was 3.0. This suggested that the non-metallic component of PCBs contributed to an increase in pH, indicating that the PCBs are alkaline and this should be taken into consideration when performing dissolution experiments.

A second factor that contributes to the increase of pH in solution is from the oxidation of ferrous ion to ferric ion (Equation 2-3), where the reaction consumes protons (Xiang, et al., 2010). This is from the natural process by which microorganisms acquire energy for growth and maintenance as they convert ferrous ion to ferric ion. Thus, in the bioleaching of PCBs, an increase in pH will always occur unless a proton source is added constantly.

A third factor that contributes to an increase in pH during bioleaching of PCBs is the consumption of protons by metals e.g. Zn, Ni, Cu etc. via direct chemical dissolution. This has been shown experimentally by Choi et al (2004) to increase the solution pH in PCB leaching. The equation for this reaction is the proton leach reaction presented previously in Equation 2-5.

The fourth factor, however, acts to reduce the solution pH through the hydrolysis and precipitation of ferric ion according to Equation 2-6.

$$Fe^{3+} + H_2O \rightarrow Fe(OH)_3 + H^+$$
$$Fe(OH)_3 + SO_4^{2-} + Fe^{3+} + H_2O + K^+ \rightarrow KFe_3(SO)_4(OH)_6 + H^+ \qquad \textit{Equation 2-6}$$

A reddish brown precipitate is formed which has been determined to be jarosite ($KFe_3(SO)_4(OH)_6$) by X-ray diffraction analysis (Xiang, et al., 2010). The authors also suggested that the amount of precipitate is closely related to the variation in pH. According to *le Chatelier's Principle,* at high pH

values, the precipitation of ferric ion as jarosite will be favoured in order decrease the pH. Hence, keeping the solution at low pH values should decrease the rate of precipitation of ferric ion from solution. This also supports the observed high solubility of ferric ion at pH values lower 1.8, when hydroxide precipitate, $Fe(OH)_3$, forms preferentially.

2.3.5.3 Strategies for maintaining the desired pH during Bioleaching of PCBs

As maintaining the optimal pH for bioleaching is crucial for maintaining high leaching efficiencies, an understanding of the different methods and techniques to maintain the pH needs to be considered. The simplest way to maintain the desired pH of the solution is by regularly adding sulphuric acid. However, this approach is expensive as the sulphuric acid has to be constantly replaced.

Studies conducted by Illyas et al (2007) using *Sulfobacillus thermosulfidooxidans* showed that when PCBs were leached in the presence of sulfur, there was no increase in pH observed. The sulphuric acid produced by the sulphur oxidising microorganisms counteracts the increase in pH due to the alkalinity of PCBs and direct proton chemical oxidation of zero-valence metals in PCBs. This scenario provides one of the cheaper options to maintain low pH values in the leach solution. However, it requires the presence of sulphur oxidizing bacteria in a consortia and is not viable when using only iron oxidising bacteria, such as, *Leptospirillum ferriphillum*.

2.3.6 Effect of Particle Size on Metal Recovery from PCBs

It has been stated that shredding PCBs is a highly energy intensive process. In practice, it is difficult to shred all the waste PCBs samples to particle sizes smaller than 0.5 mm (Yang, et al., 2011). Thus, understanding how the particle size of PCBs affects the recovery efficiencies of metals from the board is useful in informing a process where the PCB crushing can be minimized.

A study was conducted by Yang el al (2011) where different size fractions of PCBs were leached in hydrogen peroxide as an oxidant with 1 M sulphuric acid. It was found that the copper recovery varied with PCB particle size. The results showed copper recoveries after 5 hours at varied PCB particle sizes to be: 55.35 % at of 4 – 8 mm, 69.69 % at 2 – 4 mm, 87.38 % at 1 – 2 mm, and greater than 95 % at less than 1 mm particle size. This shows a strong relationship between PCB particle size and efficiency of copper recovery in a metal oxidizing environment. At PCB particle sizes below the 1 mm size fraction, no significant increase in copper recovery was observed; this suggests that it may not be economically viable to crush further.

2.3.7 Impact of Microorganism Concentration on the Leaching Rate of Metals from PCBs

Studies on PCB bioleaching are usually conducted in batch systems, where PCBs and microorganisms are added to the same reaction vessel at the same time. Initially, the microorganism inoculum

concentration in this system contributes about 20 % of the initial volume of the solution. However, the microorganism concentration may need to increase further in order for a high ferric ion production rate to be achieved and hence, higher metal dissolution efficiencies.

Low initial microbial populations may result in longer leaching times required to recover significant amounts of copper. This effect was studied by Yang et al (2009) where a known initial concentration of microorganism was used for the experiments. A result from this study is provided in Figure 2–4 below.

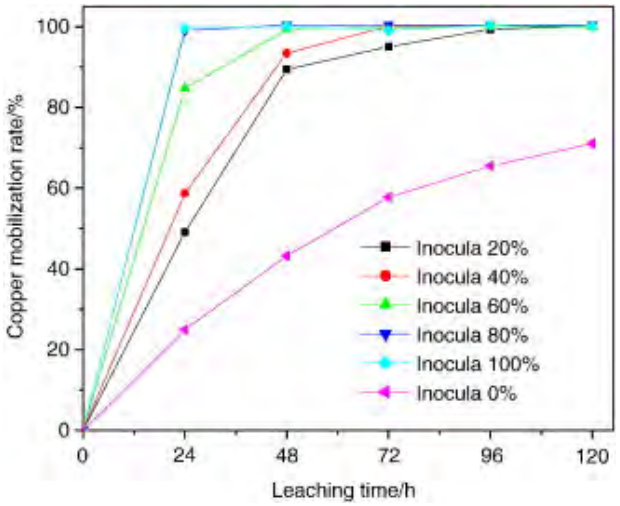

Figure 2–4. The influence of time on copper mobilization rates at different quantities of stock culture addition. (Yang, et al., 2009)

Yang et al (2009) found that when using 100 % and 80 % stock culture containing *A. ferrooxidans*, 98.6 % and 98.1 % of copper was leached after 24 hours, respectively. Over the same 24 hour time period, when 60 %, 40 % and 20 % of stock culture was used, the dissolution efficiency of copper was 84.6 %, 58.7 % and 49.1 %, respectively. The leaching of some 70% over 120 h in the control sample suggests that the control may have become contaminated with micro-organisms over the course of the study. The potential for abiotic oxidative solution leaching requires further evaluation. This result suggested that high microorganism concentrations accelerate copper dissolution efficiencies from PCBs. This is because of the increased production of ferric ion in the presence of higher microorganism concentrations (Yang, et al., 2009).

2.4 Kinetics of Metal Recovery from Printed Circuit Boards by Bioleaching

The indirect contact mechanism has been found to be the main mechanism for the dissolution of metals from PCBs and can be broken down further into the following two sub processes (Crundwell, 1994):

1. The biological oxidation of ferrous ion to ferric ion by microorganisms i.e. ferric ion production, and
2. The chemical reduction of ferric ion to ferrous ion through the dissolution of metals from metal sulphides (or zero-valence metals in PCBs) i.e. ferric ion consumption.

The kinetic analysis of the two sub-processes can be considered independently of each other (Rossi, 1990). It has been found that a two-step reactor configuration is optimal for metal recovery in that when the PCBs are kept free from microorganisms, higher waste streams can be processed than when both systems are in a single reactor (Brandl, et al., 2001).

2.4.1 Kinetics of the Reactions in the Bioleaching Process

As there are two main processes that affect the bioleaching efficiency of metals from PCBs i.e. biological oxidation vs chemical reduction, further analysis of the two processes are conducted in order to understand the rate kinetics. These will be reviewed further in Chapter 5.

2.4.1.1 Kinetics of Microorganism Growth and Oxidation of Ferrous ion

The literature reviewed this far suggests that the initial microorganism concentration and rate of microorganism oxidation of ferrous ion determines the rate of ferric ion production, which in turn governs the rate of dissolution of metals from PCBs.

2.4.1.1.1 Microorganism Ferrous Ion Oxidation Kinetics

As the microbial oxidation of ferrous ion to ferric ion plays a significant role in the bioleaching of metals, understanding the factors affecting the rate of the oxidation process is necessary. It was found by Hansford (1997) that the microbial oxidation reaction rate can be based on modified Michaelis-Menten and Monod-type kinetics and be simplified to the form:

$$-r_{Fe^{2+}} = \frac{C_X q_{Fe^{2+}}^{max}}{1 + K\frac{[Fe^{3+}]}{[Fe^{2+}]}} = r_{Fe^{3+}} \qquad \textit{Equation 2-7}$$

In Equation 2-7, $q_{Fe^{2+}}^{max}$ (mol Fe^{2+} (mol C . h)$^{-1}$) is the maximum microbial specific utilization rate, C_X (mol C . l^{-1}) is the biomass concentration and K is the apparent affinity constant to ferrous ion. The equation shows the rate of ferrous ion consumption is the negative of the rate of ferric ion production. In addition, the ferric/ferrous ion ratio in the denominator of Equation 2-7, can be related to the measured solution redox potential through the Nernst equation (Breed & Hansford, 1999):

$$E = E^0 + \frac{RT}{zF} ln \frac{[Fe^{3+}]}{[Fe^{2+}]} \qquad \textit{Equation 2-8}$$

2.4.1.1.2 Determining the Microbial Growth Rate

As was shown in Section 2.3.7, the initial microbial population in suspension impacts the dissolution rate of copper from PCBs. A high microbial population in suspension means more active sites for the oxidation of ferrous to ferric ion. The faster generation of ferric ion means more reactants in solution and, therefore, greater metal dissolution rates, which in turn regenerates the ferrous ion substrate. The microorganisms use the electron donated by ferric ion for cell maintenance and growth, thus producing more cells in the process which leads to faster regeneration of the ferric ion.

Determining the microbial growth rate is important for prediction of the increased ferric and ferrous ion regeneration cycle with time. The most commonly used expression to define microbial growth kinetics, corresponds to the basic Monod type model. It was developed for the specific growth rate based on substrate utilisation through the Michaelis-Menten type model, where the substrate utilisation was defined as a function of the ferric to ferrous iron ratio (Hansford, 1997; Ojumu, et al., 2006; Ojumu, et al., 2008):

$$\mu = \frac{r_x}{c_x} = \frac{\mu_{max}}{1 + K_m \frac{[Fe^{3+}]}{[Fe^{2+}]}}$$ *Equation 2-9*

The Monod parameter μ_{max} is the maximum specific growth rate constant and is dependent on the type of microorganism involved and K_m is the substrate saturation (or affinity constant). The Monod equation works only for balanced growth where the biomass composition remains constant. This means it is not applicable in rapidly changing growth conditions (Sundkvist, et al., 2007). In order to account for inhibition effects due to substrate, product and/or toxic species, extra terms have to be added to the Monod equation.

2.4.1.2 Kinetics of Zero-Valence Metal Dissolution from PCBs

As the ferric ion consumption rate is governed by the metal dissolution rate, the factors affecting the dissolution rates of the metals needs to be considered. The only metal which has been significantly studied in this context is copper, with little work having been done on the other metals. This section, therefore, addresses the dissolution kinetics of copper and the theoretical dissolution kinetics of the other metals found in printed circuit boards.

2.4.1.2.1 Electrochemical Effect on the Leaching of Zero-Valence Metals

In order to develop the rate equations and the rate constants required, it is important to know which metals will be leached from the PCB component of the e-waste stream. As was shown in Table 2-1, a large number of metals are found in PCBs. However, investigating the recovery of all the metals found

in PCBs is beyond the scope of the project, thus several criteria will be used to decide what metals to focus on.

The first criterion is based on the electrochemical mechanism that is the driving force in the leaching of metals into solution. These are determined by the set of half-reactions presented as Equation 2-10.

$$
\begin{aligned}
Al^{3+}_{(aq)} + 3e^- &\rightarrow Al_{(s)} && (E^0 = -1.68)\\
Zn^{2+}_{(aq)} + 2e^- &\rightarrow Zn_{(s)} && (E^0 = -0.76)\\
Ni^{2+}_{(aq)} + 2e^- &\rightarrow Ni_{(s)} && (E^0 = -0.26)\\
Pb^{2+}_{(aq)} + 2e^- &\rightarrow Pb_{(s)} && (E^0 = -0.13)\\
Cu^{2+}_{(aq)} + 2e^- &\rightarrow Cu_{(s)} && (E^0 = 0.34)\\
Fe^{3+}_{(aq)} + e^- &\rightarrow Fe^{2+}_{(aq)} && (E^0 = 0.77)\\
Ag^{+}_{(aq)} + e^- &\rightarrow Ag_{(s)} && (E^0 = 0.80)\\
O_{2(g)} + 4H^{2+}_{(aq)} + 4e^- &\rightarrow H_2O && (E^0 = 1.23)\\
Au^{3+}_{(aq)} + 3e^- &\rightarrow Au_{(s)} && (E^0 = 1.50)
\end{aligned}
$$

Equation 2-10

As the ferric/ferrous couple is the basis for the bioleaching system, it forms the reference point to determine which metals will be leached into solution. Any metals with a redox potential less than the ferric/ferrous couple is expected to be leached into solution and as such, any metals that have a redox potential greater than the ferric/ferrous couple will not be leached into solution. Therefore, silver and gold will not be leached into solution as their redox potential is higher than the ferric/ferrous redox potential.

2.4.1.2.2 Kinetics of Metal Dissolution

The rate of reaction between a solid and a fluid can be described using the heterogeneous reaction models. This includes the shrinking particle model which has been used in various studies to determine the dissolution kinetics of metal powders and metals from printed circuit boards (Demir, et al., 2004; Younesi, et al., 2006; Wang, et al., 2010; Huang, et al., 2014; Yang, et al., 2014; Zhao, et al., 2014)..

The shrinking particle model has been used to determine the conversion of particles with spherical geometry, this means that it will not work with particles with complex geometry. In the model, the reaction occurs on the surface of the particle and as dissolution occurs, the particle becomes smaller and the reaction surface moves into the solid, implying that the particle shrinks in size.

However, if the reaction produces a precipitate, this will form on the surface of the reaction surface meaning reactants will have to diffuse through the particle layer. This scenario describes the shrinking particle model. The steps involved in the shrinking particle reaction include (Younesi, et al., 2006):

1. Diffusion of the ferric ion reactant through the fluid film surrounding the metal particle to the surface of the reacted or unreacted particle.
2. If there is a precipitate layer, the ferric iron reactant will have to diffuse through the reacted layer to the surface of the unreacted core.
3. Reaction of the ferric ion with the metal particle surface and diffusion of products away from the surface.

The standard equations governing the shrinking particle model can be represented by:

$$1 - (1 - X)^{1/3} = k_c . t \qquad \textit{Equation 2-11}$$

$$1 - \frac{2}{3}X - (1 - X)^{2/3} = k_d . t \qquad \textit{Equation 2-12}$$

$$(-\ln (1 - x))^2 = k_l . t \qquad \textit{Equation 2-13}$$

The variable *X* represents the fraction of metal converted; k_c, k_d and k_l represent the rate constants and *t* is the reaction time. In the shrinking particle model, the rate of the leaching process is generally controlled either by: the rate of the chemical reaction at the surface of the core of the unreacted particle (Equation 2-11), or the diffusion of the reactants through the liquid film (Equation 2-12). However, for complex relationships where the chemical controlled leaching model or the diffusion controlled leaching model doesn't apply, the empirical model of leaching may be governed by the logarithmic relation in Equation 2-13 which assumes surface layer diffusion is limiting (Kim, et al., 2011; Levenspiel, 1999).

Determining which is the dominant controlling factor, and hence kinetic equation, depends on several parameters. The presence of precipitation on the reaction surface can cause the reaction to become diffusion controlled as reactants have to diffuse through the precipitate (Yang, et al., 2014). Using large particle sizes of PCBs at low stirring speeds can introduce mass transfer limitations, hence, the system will also be diffusion limited. These factors add significant complexity when investigating the interaction between ferric ion consumption and ferric ion production trends.

In order to determine the dependence of the shrinking particle model on the ferric ion concentration, the rate constant can be represented as (Demir, et al., 2004):

$$k = k_0 A^a \left(\frac{S}{L}\right)^b W^c [C]^d e^{-E_a/RT}$$ *Equation 2-14*

In equation 2-14, k_0 is the new rate constant, A represents the surface area available for the reaction to occur, S/L represents the solid to liquid ratio, W is the stirring speed, $[C]$ is the reactant concentration and $e^{-E_a/RT}$ represents the Arrhenius rate law and gives the dependence of the rate on temperature. At constant temperature, stirring speed, solid to liquid ratio and surface area, the term $e^{-E_a/RT}$, W, A and S/L can be lumped into k_0.

For this study the experiments have been designed so that surface kinetics will be dominant as opposed to a diffusion controlled reaction i.e. using metal powder at high stirring speeds, at constant temperature (Section 3.4.1).

2.5 Overview of Literature and Research Approach

2.5.1 Motivation for Study from Literature Review

To date, research reported on the recovery of metals from WEEE has largely focussed on PCBs. Several technologies have been suggested for the recovery of metals from WEEE, including PCBs. These include pyro- and hydrometallurgy. Both advantages and disadvantages are given. It has further been proposed that learnings from the bioleaching of base metal sulphides could be adapted to metal extraction from WEEE to overcome the high energy requirement and mixed metal products restricting efficiency of the pyrometallurgical processes and to reduce the requirement for chemical lixiviant in the abiotic hydrometallurgical processes. This dissertation is focussed on providing an understanding of the potential and limitations of biohydrometallurgy for metal recovery from WEEE, with particular interest in PCBs.

Several studies have investigated the extraction of metals from PCBs using ferric leaching with the microbial regeneration of the lixiviant in a process similar to the bioleaching of mineral sulphides. Many of these studies focused on copper as a metal of interest to determine the leaching efficiency of metals from PCBs. This was due to the suitability of ferric leaching for the solubilisation of base metals, the high concentration of copper in the PCBs, its interference in the recovery of precious metals from PCBs and its significant potential market value. It has been found that various factors affect the recovery of metals from PCBs, these include: solution pH, particle size of PCBs, initial iron concentration and initial concentration of microorganisms.

Solution pH plays one of the key roles in the recovery efficiency of metals from PCBs, as it affects the solubility of ferric ions. At low pH (i.e. less than 2.0) ferric ion is highly soluble, however, as the pH value increases ferric ion precipitates as jarosite, thus lowering its concentration in the solution. This

impacts recovery efficiency of metals from PCBs as there is less ferric ion reactant in the solution, which affects the ferric ion consumption rate.

It was also found that the initial ferrous iron concentration affects the extraction of metals from PCBs. Under bioleaching conditions, low initial ferrous ion concentrations resulted in low concentration of ferric ion in solution. However, when the initial ferrous ion concentration is too high, the recovery efficiency of metals from PCBs also decreases, this has been attributed to inhibition of microorganisms at high concentrations of ferric ion, which in turn, impacts the ferric ion production rate negatively.

In addition, high initial microbial populations were found to increase the leaching efficiency of copper from PCBs. A high population means that there are more microorganisms to oxidize ferrous ion to ferric ion, which in turn, leaches metals into solution at a faster rate.

The potential for a bioleaching process for recovery of base metals from PCBs and other WEEE was premised on the understanding of the indirect contact mechanism of mineral bioleaching in which microorganisms catalyse ferrous iron oxidation for the regeneration of the ferric lixiviant which is used to solubilise elemental base metals, such as copper, tin, zinc and nickel. In other words, the bioleaching of WEEE is expected to proceed via two inter-linked sub-processes. In a recent study, Lambert et al. (2015) studied the rate kinetics for the bioleaching of copper cable waste, using the iron and sulphur oxidising microorganism, *A. ferrooxidans*. The authors investigated the effect of initial ferric ion concentration and temperature on the leaching of copper. At optimum conditions, the bioleaching system was comparable to the chemical leaching system, however, it was limited by the rate of ferric ion regeneration.

This study set out to explore the same phenomenon in a simplified system using elemental powder of copper (as principal model component) or zinc or tin. In the study, the relative rates of biological regeneration of the ferric leach agent and chemical leaching of the metal are compared and used to inform a model simulation. The understanding generated through the study of metal powders will form the basis for further research on PCBs.

2.5.2 Objectives of Study

At the start of this study, no correlation had been presented between the rates of ferrous iron oxidation by microorganisms to the rate of ferric ion reduction by metals and the impact of the microbial population. In other words, how fast can microorganisms regenerate ferric ion at their highest activity and population? How does this compare to how fast metals consume the ferric ion when mass transfer is not limiting? This is an important consideration as it provides an indication of how best to optimize the bioleaching process. Thus, an objective of the study was to compare the rates of ferric ion production through microbial oxidation of ferrous iron, with the rate of reduction of

ferric ion through metal dissolution. Metal powder was used to minimize mass transfer effects and simplify considerations of mixed metal systems. In particular, copper was used as the representative metal for the majority of the experimental work and the simulation. Applicability of the approach was tested by extension of the experimental study to test applicability to zinc and tin. Crushed PCB powder could not be used due to lack of specialized mills to crush the PCBs and the complexity of ensuring a representative head grade across all experiments. Further, the complexity of crushed PCBs was expected to restrict the fundamental understanding necessary in the first instance to assess the potential of bioleaching in the treatment of electronic waste.

Following the determination of trends of ferric ion consumption and ferric ion production in terms of the dominant rate, a further objective of this study is to perform a sensitivity analysis in order to determine the system conditions that will maximize dissolution of metals. For the sensitivity analysis to be conducted, the metal dissolution kinetic equations of the major metals found in PCBs were determined empirically using the heterogeneous models described in Section 2.4.1.2 previously. A leaching model was compiled and used to investigate a variety of scenarios.

2.5.3 Hypothesis

The summary of literature findings presented and objectives stated above have led to the formulation of the following research hypothesis:

The relative ferric ion production and consumption rates form a key consideration for the optimisation of the bioleaching of base metals found in PCBs. In the absence of mass transfer limitations, the microbial production of ferric iron is rate limiting for bioleaching of copper metal. This limitation can be alleviated by enhancing microbial concentration and activity in the leach process.

2.5.4 Key Questions

In order to address the proposed hypothesis, the following set of key questions regarding ferric ion production and consumption trends, as well as the model simulation conditions that can potentially maximize metal dissolution, will be answered.

1. The first set of key questions consider the ferric ion production and consumption trends empirically, in the presence of microorganisms:
    a. Which will be the dominant rate between ferric ion production and consumption?
    b. How is this result affected by the microbial concentration and activity?
2. The second set of key questions focus on the simulation, in particular, the model variables that result in high ferric ion production rates and consequently, increased metal dissolution rates:

a. What are the rates of ferric iron production and consumption and what variables affect these? What are the rate constants?
b. Which variables may be optimised for increased extraction of metals from a mixture?
c. To which design considerations and operating variables is the process most sensitive?

3 Materials and Method

This section describes the materials and methods that were used for the experiments in the bioleaching of base metals, representing the PCB waste sample. It begins by discussing the microorganisms used in the bioleaching experiments, including the maintenance medium and cell count procedure. The next section describes the analytical procedures used for the measurements conducted, including: determining the concentration of iron species, monitoring the pH, recording the redox potential, and analysing the metal ions in solution. This is then followed by the experimental setup section, which describes the equipment and procedure that were used.

The experiments conducted were divided into the two categories described below:

1. Bioleaching experiments, where elemental metal powder was dissolved in the presence of microorganisms and dissolved ferrous or ferric sulphate. These experiments were conducted in order to determine the ferric ion production and consumption trends in a bioleaching environment.
2. Chemical leaching experiments, in which dissolution of elemental metal powder in the absence of microorganisms and in a solution of ferric sulphate, was studied. These experiments were performed in order to determine the rate constants of metal dissolution and ferric ion consumption, for the sensitivity analysis conducted in the simulation section.

3.1 Microorganisms used for the Bioleaching Experiments

The culture used for the experiments was a mesophilic culture where the dominant microorganism was *Leptospirillum ferriphilum,* sourced from the Centre of Bioprocess Engineering Research (CeBER) laboratories in the University of Cape Town. The stock cultures were maintained in a feed stock containing nutrients and 5 $g.l^{-1}$ ferrous ion (as ferrous sulphate) at 35^{o}C, in stirred tank reactors (STRs) with 55 hr residence times. Typically, other micro-organisms present included *Acidithiobacillus ferrooxidans*, *At.thiooxidans*, *At.caldus* and various archaea.

3.1.1 Maintenance Growth Media for the Microorganisms

The microorganisms used in the experiments were maintained in the Lungrid 9 K growth medium, with the composition provided in Table 3-1 below. The concentrations were determined experimentally by Silverman & Ehrlich (1964). All the compounds were analytical grade reagents. The Lungrid 9K medium used in the experiment was produced as follows:

Table 3-1. Composition of Lungrid 9k medium for the maintenance of bacteria

Compound	**Concentration ($g.l^{-1}$)**
$(NH_4)SO_4$	3.0
KCl	0.1
K_2HPO_4	0.5
$MgSO_4.7H_2O$	0.5
$Ca(NO_3)_2$	0.1
$FeSO_4.7H_2O$	44.22

3.1.2 Microorganism Cell Count

The purpose of determining the microbial cell concentration was to investigate the effect the addition of elemental copper powder had on the microbial population according to Section 3.5.4. The bacterial cell count was done using the Hawksley counting chamber (Figure 3–1) and phase contrast optical Olympus CX40 microscope. The counting chamber consists of 4x4 large grids where each large grid was subdivided into a further 4x4 sub-squares. Each of the sub-squares has a surface area of 1/400 mm^2 with a depth of 0.02 mm. The cell counts were done at a 100 times magnification. In order to get a representative sample, 4 large grids from the counting chamber were selected randomly and the cells were counted. When the cells exceeded 100 cells per count, an appropriate dilution was conducted to reduce the cell concentration. Equation 3-1 was used to calculate the original cell number, as shown in Appendix B:

$$Cell\ concentration = cells\ counted * 312500 * Dilution\ factor \qquad \textit{Equation 3-1}$$

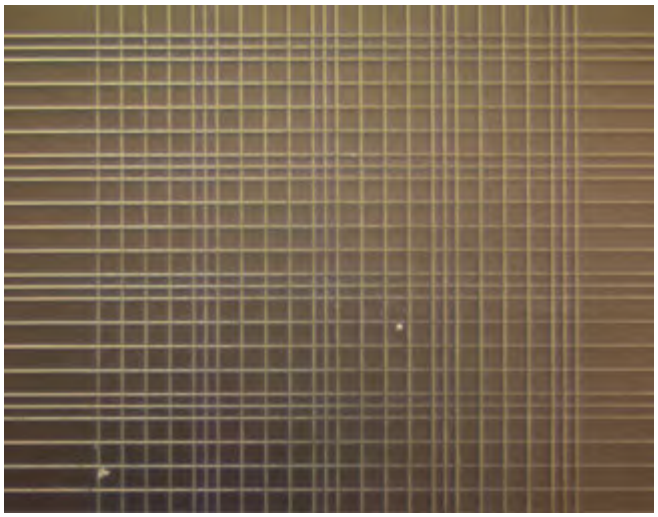

Figure 3–1. Counting grid of Hawskley Thoma counting chamber.

3.2 Analytical Techniques

This section outlines the techniques that were used to determine the concentrations of elements in solution, and also describes the measure of pH and redox readings.

3.2.1 Iron Determination

Measuring the dissolved iron concentration in solution was critical as it was used to determine: the ferric ion consumption trends and thus the leaching efficiency of the base metals, the ferric ion production trends which indicate the growth rate of the bacteria, and to determine the occurrence of precipitation of ferric ion from solution.

The ferric chloride assay was used to determine the iron concentration in solution. The basis of the ferric chloride assay is the yellow ferric chloride complex formed on the addition of 2 M hydrochloric acid to ferric ion in solution. The ferric chloride method has been found to give better results at high copper concentrations than the 1, 10 Phenanthroline system (Govender, et al., 2012).

Details for the produre are provided in Govender et al. (2012). In order for the absorbance readings to be converted to ferric ion concentration, a ferric chloride standard curve was generated using different concentrations of ferrous sulphate solution using the following procedure.

1. A 100 $mg.l^{-1}$ solution of ferrous sulphate solution was initially made up.
2. Dilutions were done using deionised water to form 10, 20, 40, 60, 80 $mg.l^{-1}$ solutions.
3. The ferric ion absorbance was then measured and recorded.
4. Potassium persulfate was added to each of the dilutions to convert all the ferrous ion to ferric ions in order to determine the total iron concentration. This gave the calibration curve for the total iron concentration at different dilutions.

A typical standard curve is shown in Figure 3.2. The gradient was found by adding a trend line through the points to give a linear relationship. It was found to be similar to the literature value of 0.015 (Govender, et al., 2012). The slope of the curve gives the conversion factor to convert the absorbance readings to ferric ion concentrations. This is according to Equation 3-2 below.

$$Ferric\ ion\ concentration\ (\frac{mg}{l}) = Dilution\ Factor * Absorbance/0.0157 \qquad \textit{Equation 3-2}$$

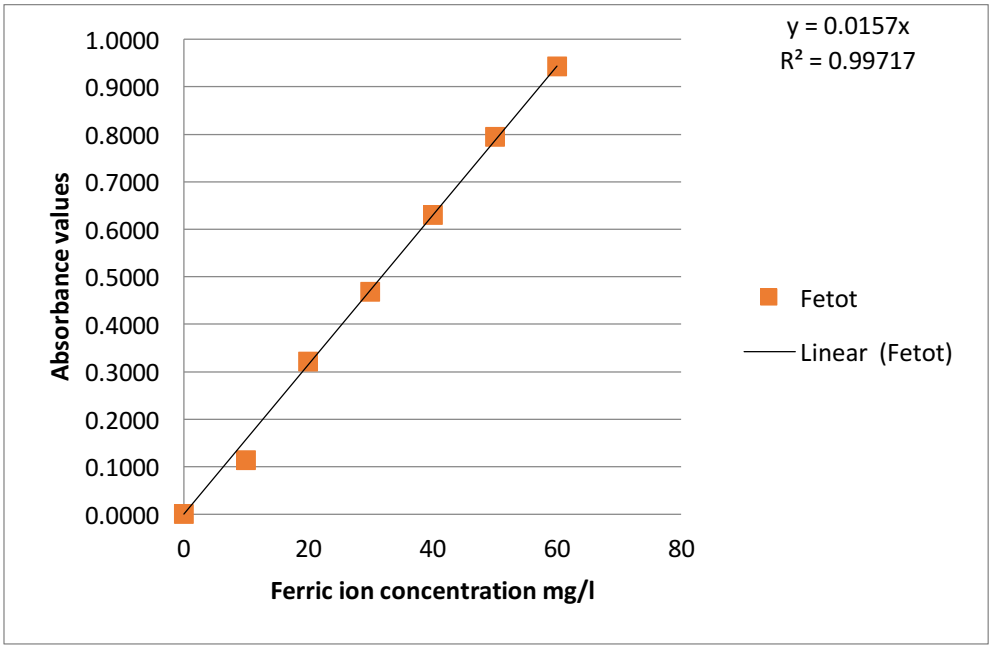

Figure 3–2. Ferric chloride calibration curve for the determination of total iron.

3.2.2 Monitoring of pH

The pH readings were conducted using a Metrohm® 713 pH meter which was calibrated daily using standards at pH 1 and pH 4 of buffer solution.

3.2.3 Monitoring of Redox

The redox readings were conducted using a Metrohm® 827 Meter containing a platinum ring electrode with a 3 M KCl & AgCl electrolyte. The redox meter was calibrated daily using a standard solution (from Crisson).

3.2.4 Metal Ion Analysis

Analysis of metal ions in the solution was conducted using the inductively coupled plasma mass spectrometry (ICP) method using a Varian ICP-730 ES equipment. The sample from the ferric chloride assay at a 10 times dilution was used for the analysis.

3.3 Chemicals and Solutions Used

There were various chemicals used in the experiments which includes: ferric sulphate and ferrous sulphate solution, 98 % sulphuric acid solution and 2 M hydrochloric solution. This section describes how the appropriate solutions were made up.

3.3.1 Hydrochloric Acid

The hydrochloric acid was used in the ferric chloride assay in order to determine the ferric ion concentration in solution. A solution of 2 M hydrochloric acid was required; the required

concentration was produced from analytical grade reagent made of 37 % hydrochloric acid (by mass) with a density of 1.19 $kg.l^{-1}$ (from Merck). This meant that the volume of HCl that was used was 371 ml and the volume of water was 789 ml, the calculations for this is given in Appendix A.

3.3.2 Ferric Sulphate Solution

Ferric sulphate was used as an oxidizing agent for the dissolution of metals in the printed circuit board characterization experiment and in the chemical leach experiment. Ferric sulphate hydrate ($Fe_2(SO_4)_3.xH_2O$) was used as the source of the ferric ion. The minimum $Fe_2(SO_4)_3$ concentration was 70 % on a mass basis. As the degree of hydration was not known, the concentration of ferric sulphate that was necessary to produce the required concentration of ferric sulphate solution (11 $g.l^{-1}$) was calculated from an initially assumed solution. The procedure to determine the required mass was:

1. A mass of 4.5 g of ferric sulphate was diluted in 100 ml deionised water in a 250 ml Erlenmeyer flask.
2. The pH was adjusted to 1.8 using 98 % concentrated sulphuric acid.
3. The ferric chloride assay was conducted on the sample and based on the absorbance and standard curve in Figure 3–2, the concentration of ferric ion was calculated.
4. The concentration of the ferric ion from the assay was divided by the required ferric ion concentration to get a fraction which was used to determine the required mass of ferric sulphate hydrate compound that was to be used. Detailed calculations can be found in Appendix A.

3.4 Experimental Equipment and Set-up

Erlenmeyer shake flasks of volume 250 ml and containing 100 ml volume of solution were used in the experiments (unless otherwise specified). The experiments were conducted in one of two modes which were:

1. Magnetic stirrer mode of operation.
2. Orbital shake flask mode of operation.

3.4.1 Magnetic Stirrer Mode of Operation

This formed the simplest mode of operation where 250 ml Erlenmeyer flasks with 100 ml solution volume were placed on top of magnetic stirrers (MRC model GMHS, 220 V magnetic stirrer) with magnets placed inside the Erlenmeyer flask. The magnetic stirrers were kept at a setting range of 700 - 800 rpm which ensured high mass transfer rates. This approach were suitable for experiments with a short run time e.g. for the chemical dissolution of metals where the duration of the run was 30

minutes. This is because for shorter experimental runs it was assumed that there will be negligible variation in environmental conditions. Figure 3–3 shows the setup of the magnetic stirrer experiment.

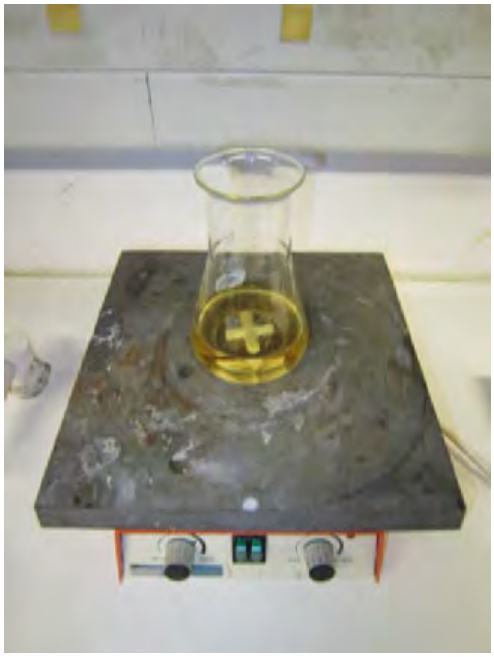

Figure 3–3. Magnetic stirrer set up

3.4.2 Shake Flasks Experiments

The shake flask system was used for experiments that lasted for a significantly longer period of time (> 1 day) and where the environmental conditions needed to be kept constant. The system was set up in a 37 ^{o}C incubator with a shake speed of 180 rpm. The lower shaker speed (180 rpm) meant that there was lower mass transfer rates than in the magnetic stirrer experiments (700 – 800 rpm). The limitation of this is that the rate of metal dissolution could be diffusion limited (Equation 2-12) on the orbital shaker as opposed to the magnetic stirrer experiments which could be chemical reaction rate limiting (Equation 2-11). However, the elevated temperature was conducive to microbial activity and the controlled environmental conditions prevented temperature fluctuations having an uncontrolled effect on the system. Figure 3–4 shows the shaker set-up used in the shake flask system.

Figure 3–4. Shake flask set up for the experiments.

3.5 Experimental Plan

3.5.1 Printed Circuit Board Characterization Experiments

The PCB waste used for metal analysis was donated by DESCO Electronic Recyclers South Africa. The waste consisted of two samples of PCBs (sample A and sample B). Within each sample, the boards were crushed to 2 different size fractions < 15 mm and < 50 mm size fractions which gave a total of four unique bags for analysis. In order to determine the metals with the highest dissolution concentration in ferric sulphate, the following procedure was followed:

1. A volume of 100 ml ferric sulphate solution (as described in Appendix A) was added into each of two 250 ml Erlenmeyer flasks.
2. A sample of 9.8 mm mesh fraction from the two samples of PCBs were weighed and added to each of the Erlenmeyer flasks (each sample in its own flask).
3. The leaching was conducted on the shake flask system (Figure 3–4).
4. The experiment was allowed to run for 3 days and the resulting solution was withdrawn and the ICP analysis was conducted. The time was chosen based on literature values where it was demonstrated approximately 80 % of the copper would be dissolved (Yang, et al., 2009).

3.5.2 Chemical Leach of Select Metal Powders

The purpose of the chemical leach experiments was to determine the rate kinetics and the rate constants of the metal leach reactions, using metal concentrations informed by the PCB leach experiments described in Section 3.5.1. Determining the rate equations was important as it

contributed to the sensitivity analysis in the simulation which was designed to investigate the factors affecting the dissolution of metals in a reactor leaching environment. The metals investigated were copper, tin and zinc, with results discussed in Section 4.1. Each metal was dissolved in 100 ml ferric sulphate solution in the absence of microorganisms to find the dissolution rate constant. The powdered form of the metal and high stirring speeds were used to reduce mass transfer limitations. The procedure for the experiments was:

1. Ferric sulfate solution was made as described in Section 3.3.2.
2. In order to calculate the rate constants using the shrinking particle method as described in Section 2.4.1.2, the following 3 experiments were conducted in triplicate:
    a. 0.2 g metal in 100 ml of approximately 11 $g.l^{-1}$ ferric sulphate solution.
    b. 0.4 g metal in 100 ml of approximately 11 $g.l^{-1}$ ferric sulphate solution.
    c. 0.2 g metal in 100 ml of approximately 5.5 $g.l^{-1}$ ferric sulphate solution.
3. The experiments were conducted in 250 ml Erlenmeyer shake flasks with 100 ml solution. Stirring was done by magnetic stirrers at a setting range of 700 - 800 rpm.
4. The experiments were conducted for 30 minutes and the pH and redox readings were recorded at the beginning and at the end of the experiment.
5. Samples were withdrawn every 5 minutes to measure the ferric ion and total iron concentrations using the ferric chloride method. The samples were then used to determine the concentration of the metal ions dissolved into solution using the ICP method.In order to prevent further reaction following sampling, sampling was done from the top of the reaction vessel such that only the supernatant solution was withdrawn. Owing to the high densities of the metal powder, the metal powder was at the bottom of the reaction vessel during sampling, leaving the supernatant metal free.

3.5.3 Bacteria Batch Leaching Experiments to Understand Ferric Ion Trends during Microorganism Growth

This section describes the experiments where 20 % inoculum (containing microorganisms) was added to shake flasks containing 80 ml growth medium after which various masses of copper powder was added. This was conducted in order to investigate the ferric ion consumption and production trends during microorganism growth, at different initial zero-valence copper metal masses in the medium. As the metal dissolution rate depends on the ferric ion concentration, understanding the conditions that affect the ferric ion production and consumption trends is necessary in order to optimize the metal dissolution efficiency.

The bacterial culture in this experiment was grown in the presence of 0, 2.0, 5.0 and 10.0 g copper powder per litre of ferrous sulphate solution. The ferrous ion substrate source for this experiment was

provided by the Lungrid 9 K medium as described in Section 3.1.1. The experimental procedure is as follows:

1. A volume of 20 ml of inoculum from a mixed mesophilic culture (containing predominantly *Leptospirillum ferriphilum*) was added to 80 ml of growth medium in four Erlenmeyer flasks to form a final volume of 100 ml in each flask (for each metal concentration).
2. Then 0 g, 0.2 g, 0.5 g and 1 g of copper, respectively, was added to the Erlenmeyer flasks to form final concentrations of 0, 2, 5 and 10 g copper powder per litre of ferrous sulphate solution. Measurements of the pH, redox potential, ferric ion and total iron concentrations were conducted and recorded for each flask.
3. The Erlenmeyer flasks were then placed in a 37 ^{o}C incubator on top of the shake flask tray (Section 3.4.2) and the shaker was set at 180 rpm.
4. The pH was adjusted daily to below 2.0 using 98 % concentrated sulphuric acid solution whenever the pH measurement was above 2.0. This was to reduce the effects of precipitation, which would become significant above pH 2.0 (Jensen & Webb, 1995). A high concentration of sulphuric acid was used to prevent significant changes in volume whenever pH adjustments were conducted.
5. Due to the elevated temperatures used, significant evaporation occurred. Hence, the solution was kept at constant volume by the addition of deionized water. The total volume was measured each day using a 100 ml measuring cylinder and deionized water was added when the volume dropped to less than 95 ml.
6. Single readings of the pH, redox ferric ion and total iron concentration were conducted daily[1].

3.5.4 Bioleaching with Fed Batch Copper Addition at Peak Microbial oxidation

A drawback of the experimental design in Section 3.5.3 was that the rate of ferric ion production (which is determined by the microbial population) was not at its peak when the initial copper mass was added. This is because in the previous experiment 20 % inoculum was added together with the copper metal. The population would increase as ferrous ion was consumed and ferric ion was produced. This continued with the regeneration of ferrous iron until the microbial concentration reached its peak. It has been found that a higher microbial population produces ferric ion at a faster rate than a lower microbial population (Yang, et al., 2009), owing to a constant specific ferrous iron oxidation rate in the absence of inhibition or limitation.

[1] Cell counts were not conducted in this experiment, in hindsight, they should have been.

Thus designing an experiment where the microbial population was at its highest concentration was important in determining if a peak rate of ferric ion production resulted in an increased rate of elemental copper dissolution (Yang, et al., 2009; Xiang, et al., 2010).

The steady state in microbial population was identified when there was no more increase in either the ferric ion concentration or the redox potential at which point copper metal powder was then added to the system. When the ferric ion concentration peaked again, another measure of copper was added. This was repeated at every peak as shown:

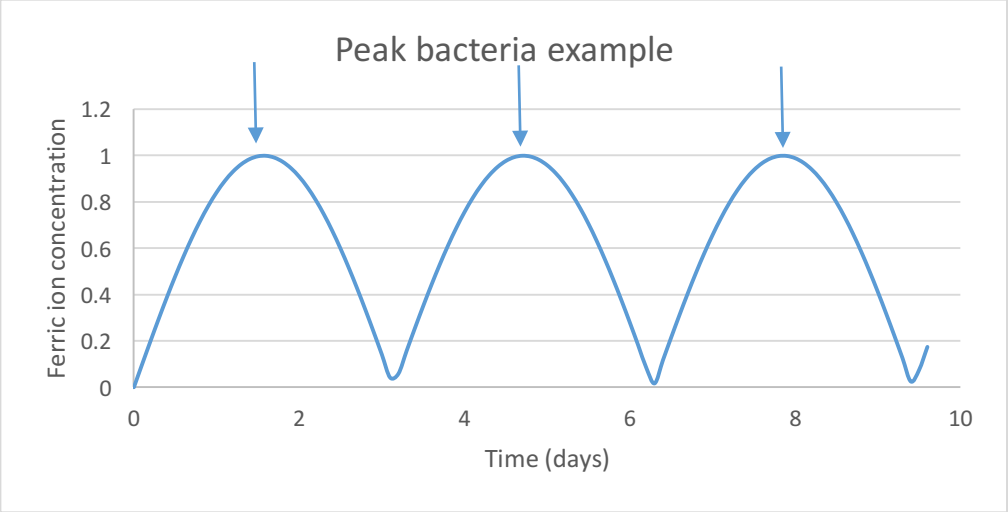

Figure 3–5. Fed-batch copper addition at peak microbial population example

Copper metal powder was added at the points indicated by the arrows which indicates the maximum concentration of ferric ion and as a consequence maximum microbial population. It is assumed that when elemental copper was added the ferric ion concentration would decrease as it was reduced to ferrous ion by oxidising copper to cupric ions. This experiment was conducted as follows:

1. A fresh volume of 500 ml microbial culture was grown in a single 1000 ml Erlenmeyer flask where 400 ml of it consisted of 9K growth medium and 100 ml of it consisted of an inoculum of mesophilic culture, containing predominantly *Leptospirillum ferriphilum*. The culture was incubated until all the ferrous ion was consumed which was indicated by both a high redox potential of around 700mV with no further increase observed and where the ratio of the ferric ion and total iron concentrations was 1.
2. The pH, redox potential, cell concentration and ferric ion and total iron concentration were recorded.
3. Two 100 ml samples of the culture were then placed in separate 250 ml Erlenmeyer flasks labelled 2 g Cu addition and 4 g Cu addition.

4. Initial masses of 0.2 g and 0.4 g copper metal powder were weighed out in separate shake flasks to result in 2 g of base metal per litre and 4 g of base metal per litre, respectively, as control flasks.
5. A mass of 0.2 g and 0.4 g copper were added to the 2 g and 4 g addition culture flasks respectively to form 2 and 4 g copper per litre cultures respectively. The additions were done simultaneously and a stop watch was started to keep track of the time.
6. The redox, pH, ferric and total iron concentrations were recorded at 0 hrs, 0.5 hrs, 1 hr, 2 hrs, 6 hrs and 12 hrs. After 24 hours the readings were recorded every 24 hours.
7. Whenever the measured pH exceeded the 1.8 threshold value, 98 % concentrated sulphuric acid was added to lower the pH below the threshold value.
8. Once the ferric ion production stopped as indicated by a ferric and total iron ratio of 1, it was assumed that all the copper metal powder had been dissolved.
9. Measurements of pH, Eh, redox ferric ion concentration, total iron concentration, cell counts and cupric ion concentrations were conducted at this point.
10. A further 0.2 g copper was added to the 2 g Cu addition flask and 0.4 g copper was added to the 4 g Cu addition Erlenmeyer flask to bring the theoretical total copper concentration in each solution to 4 $g.l^{-1}$ and 8 $g.l^{-1}$, respectively. The redox, pH, ferric and total iron concentrations were recorded at 0 hrs, 0.5 hrs, 1 hr, 2 hrs, 6 hrs and 12 hrs. After 24 hours the readings were recorded every 24 hour until the ferric to total iron ratio of 1 was reached and further additions made.

Copper measurements were not conducted in these experiments., owing to the cost of the assay and number of points required. It is well accepted that a relationship exists between copper solubilised and ferric iron reduction in this system, allowing indirect estimation of dissolution. It is recognised that confirmatory evidence of this relationship would add confidence to the data generated. Further, metal analysis is required where mixed metal systems are used. Hence, it is suggested that copper readings be conducted in future experiments.

4 Understanding the Kinetics of Metal Dissolution

In this chapter, the results and discussion of the metal bioleaching and chemical leaching experiments carried out are presented. Section 4.1 describes the results of the chemical leaching of printed circuit boards. These experiments were aimed at highlighting the metals of interest to focus on, during the bioleaching experiments and the base metal chemical leaching experiments. Section 4.3 presents and discusses the results of comparative chemical leaching experiments of copper, zinc and tin are presented.

In Section 4.3, the results of the microbial leaching of elemental copper experiments are presented. This provides an indication of ferric ion production and consumption trends in the presence of microorganisms, in response to varying initial masses of copper. In Section 4.4, the results of the copper dissolution rates as a result of fed-batch addition of copper metal powder to a well-established microbial leaching system are discussed.

The results of the leaching experiments were used to provide the reaction kinetics data for the sensitivity analysis in the model simulation developed and discussed in Chapters 5 and 6, respectively. The experimental data is then fitted to the shrinking particle model to determine the controlling factors and the rate constants as highlighted in Section 2.4.1.2.2. The shrinking particle model requires uniform particles. This is a simplification as seldom found in particulate systems. The measurement to determine particle uniformity was not conducted as the laboratory grade metals were assumed to be largely uniform. Subsequent particle size distribution measurement demonstrates the distribution e.g. for copper powder, the d_{10}, d_{50} and d_{90} were determined as 20, 63 and 154 micron respectively

4.1 Characterisation of Printed Circuit Boards

Previous studies have shown the presence of a significant number of metals in various PCB samples (Table 2-1). The objective of the characterisation experiments was to demonstrate metal recovery from shredded PCBs through ferric ion leaching. In addition, the metals with the highest concentration in solution at the termination of the experiments, were selected as metals of interest for further study of the ferric ion leach kinetics.

Two samples of PCBs, prepared differently and labelled Sample A and Sample B, were subjected to abiotic ferric ion leaching. The experiments were conducted in 100 ml Erlenmeyer flasks with agitation using the following PCB mass in solution: 36.7 g PCB sample A per litre of ferric solution and 17.1 g PCB sample B per litre of ferric solution. The mass of PCB was reduced to 89.0% and 80.7% of the initial mass over the leach period of 3 days. The detailed methodology for this experiment was shown in Section 3.5.1. The metal ion concentration in solution was determined using the ICP analysis as

described in Section 3.2.4 and the resultant mass of metal leached per mass PCB sample is given in Table 4-1. The associated calculations are given in Appendix C.

Table 4-1. Metal ion concentration per gram of printed circuit boards leached in ferric sulphate.

	mg metal ion . g^{-1} PCB sample	
	Sample A	**Sample B**
Cu	44.65	99.40
Sn	42.06	118.68
Pb	23.96	0.28
Zn	20.50	6.25
Ni	1.22	0.71
Mn	1.06	2.41

Leaching of the PCB samples under these conditions provides an estimation of the total leachable metal content under acid and ferric leach conditions. Copper, tin, lead and zinc was leached in high amounts from both PCB samples. The high tin and lead concentration in sample A is proposed to originate from the solder that is used to hold the micro electric components in place. The high copper concentrations observed in both experiments is proposed to originate from the copper used for electrical conductivity in the boards (Luda, 2011).

Assuming that most of the metals present in the PCBs initially, had leached into solution by the termination of the experiment, the weight percent of metals leached compares well to those presented in literature (Table 2-1). The results indicate the relevance of copper, tin, lead, zinc, nickel and manganese in PCB leaching experiments. Copper was selected as the metal of focus for this study, owing to the highest prevalence in PCBs. Tin was chosen as an additional metal for demonstration of applicability of the bioleaching approach owing to its presence in solder. Zinc was selected as it was present in high levels in some PCBs and has been the subject of many mineral bioleaching studies. Whilst lead is also an important metal, it was not included in the study as it is expected that additional studies on acclimatisation will be necessary and this would extend the duration of this study. Instead, the potential for and requirements of the bioleaching circuits for PCBs were sought using metals that have been well characterised in mineral bioleaching studies. Should the technology demonstrate potential, adaptation to lead is recommended to follow. Further to this, it is well recognised that the inclusion of lead in PCBs is being phased out, hence it will be of diminishing importance in the future (Bizzo, et al., 2014).

Nickel and manganese are also of interest for further study as, although extracted at lower concentrations i.e. 0.7 - 1.2 and 1.1 – 2.4 mg metal per g PCBs respectively, they are potentially high value metals.

4.2 Chemical Leach Experiments

The objective of the chemical leach experiments was to determine the rates of dissolution of copper, tin and zinc by ferric leaching in the absence of mass transfer limitations. The results are expected to provide kinetic data for the rate of metal dissolution and associated ferric consumption, which is necessary to populate the simulation model compiled and used for scenario analysis, in Chapter 5 Section 5.4.2.

4.2.1 Kinetics for Chemical Leaching of Copper

Three experiments, described in Section 3.5.4, were conducted in order to determine the rate constants for copper metal dissolution by ferric leaching. Each experimental run is described briefly below:

1. 2 g copper per litre of ferric ion solution where the ferric ion concentration was 11 $g.l^{-1}$.
2. 4 g copper per litre of ferric ion solution where the ferric ion concentration was 11 $g.l^{-1}$.
3. 2 g copper per litre of ferric ion solution where the ferric ion concentration was 5.5 $g.l^{-1}$.

The observed changes to ferric ion concentration with time for each of the experimental runs, is found in Figure 4–1. The initial ferric ion consumption rate seems to be high as indicated by the steep slopes of the graphs in the first 5 minutes of the experimental run. After 5 minutes the rate appears to slow down and then reach a steady state where minimal net change of ferric ion concentration is observed.

As observed in Figure 4–1, Run 1 and Run 2 had similar copper conversion values of 0.95 at 10 minutes. The fractional conversion for Run 3 was 0.70 increasing to a steady state value of 0.93 at 20 minutes. These preliminary results suggest that initial copper dissolution in the presence of ferric ion is rapid, occurring over the few minutes as seen by the initial steep copper conversion. This suggests that it would be useful to sample more frequently within the first 10 minutes for kinetic rate analysis. Additionally, the difference in conversion profiles between Run 1 and Run 3 confirms the importance of ferric ion availability for the initial, rapid dissolution of copper.

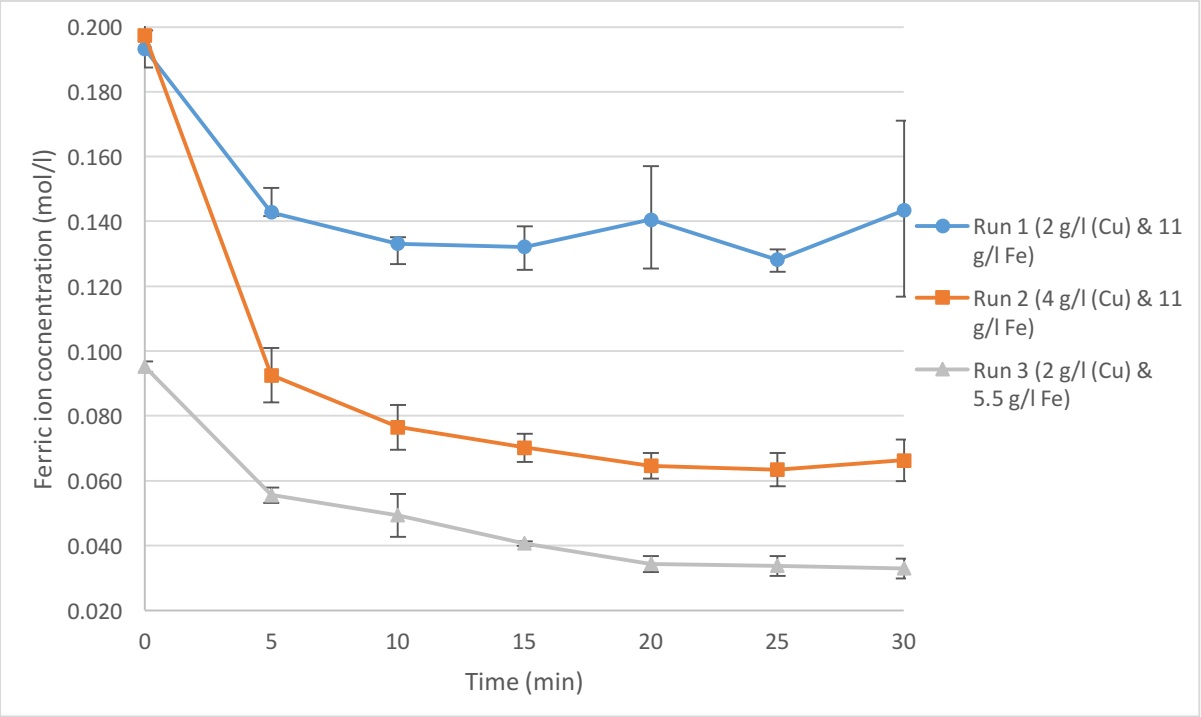

Figure 4–1. Ferric ion concentration trends for the dissolution of copper.

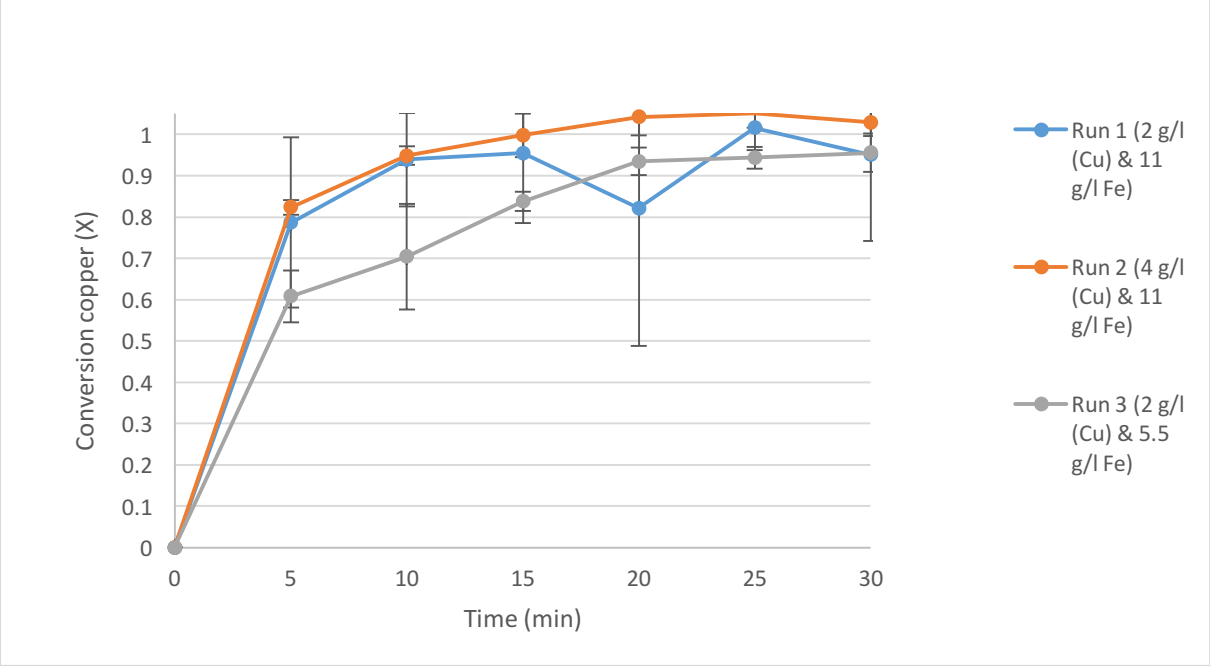

Figure 4–2. Copper conversion trends for changing initial ferric ion concentration and changing initial metal mass in suspension

The rate of reaction between a solid and fluid can be analysed according to the heterogeneous reaction model as discussed in Section 2.4.1.2.2 (Levenspiel, 1999; Demir, et al., 2004). As high stirring rates were used, it was assumed that the diffusion through the fluid film was negligible. Due to the low pH values i.e. pH 1.3 in solution, it was assumed that negligible precipitation would occur hence

diffusion through a precipitate layer would not be limiting (Anders & Colin, 1995; Xiang, et al., 2010). Thus the chemical controlled shrinking particle model, given in Equation 2-11, was used to find the rate constants. The rate constant was determined by plotting $1-(1-X)^{1/3}$ as a function of t as shown in Figure 4–2, where X was the conversion of the copper metal at time t.

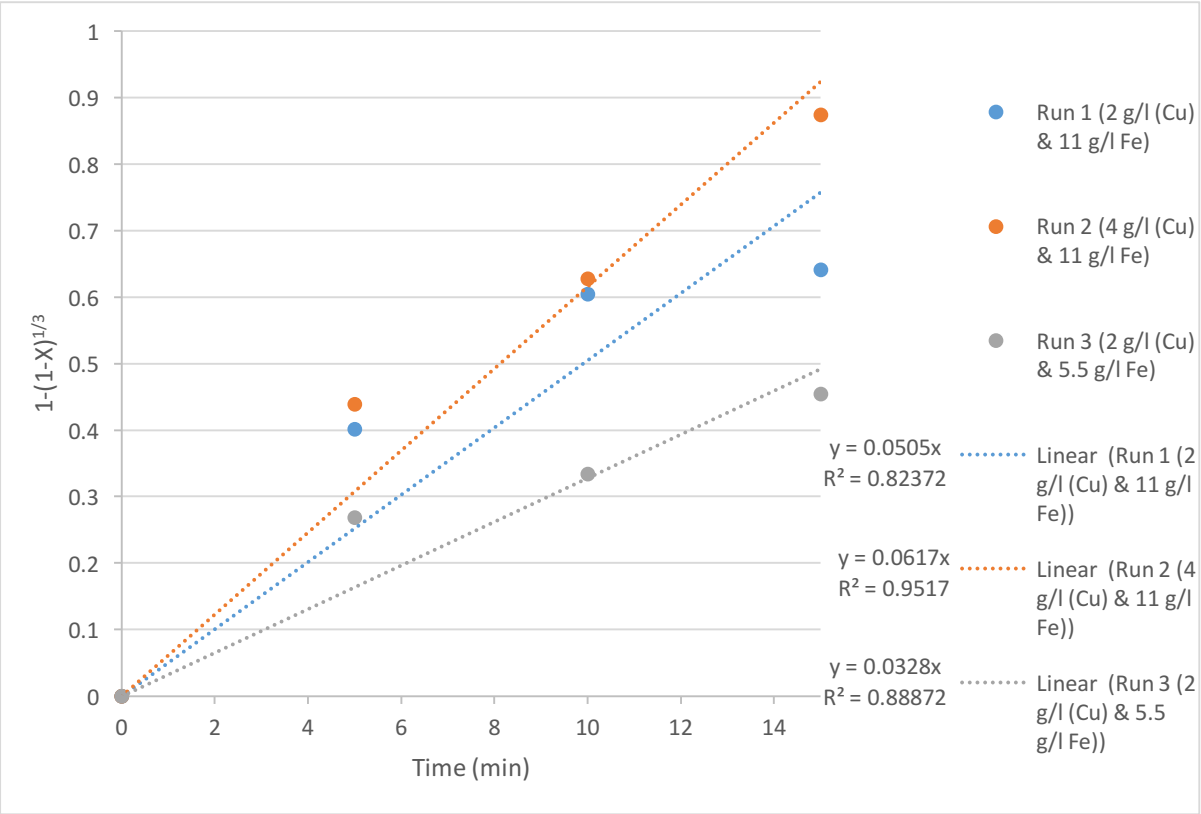

Figure 4–3. Chemical controlled reaction model for copper to determine constants of $1-(1-X)^{1/3}=k.t$

Run 2 had a high correlation coefficient (R^2) of 0.9517 for the linear relationship between the conversion function and the time. The gradient (representing the rate constant, k) was 0.0617. The high R^2 value indicates that the copper dissolution data in Run 2 can be modelled well by the chemical controlled shrinking particle model.

However, when the initial copper mass was reduced to 2 g metal per litre of solution (i.e. Run 1), the gradient was 0.0505 and the R^2 value reduced to 0.8237. This meant Run 1 was not modelled as well by the chemical controlled shrinking particle model as Run 2 (R^2 of 0.9517) and Run 3 (R^2 of 0.8887). The low R^2 in Run 1 may be attributed to several factors, as the constant k depends on the ferric ion concentration, the stirring speed and temperature according to Equation 4-1 (Demir, et al., 2004). The lack of sufficient sampling affected the data and may have also been the cause of low R^2.

$$1-(1-x)^{\frac{1}{3}}=kt=k_oW^cC_{Fe^{3+}}^n e^{-E_a/RT}t=k_cC_{Fe^{3+}}^n t$$ *Equation 4-1*

The value *W* represents the stirring speed and $e^{-E_a/RT}$ represents the dependence on temperature. For Run 3, which was conducted at half the ferric iron concentration, the correlation coefficient value was 0.8887 and the gradient was 0.0328. The gradient value was about half of the gradient in Run 1, while the correlation coefficient was higher than Run 2 but lower than Run 1. This is consistent with the dependence of the rate constant *k* on the ferric ion concentration, shown in Figure 4–2, in that reducing the ferric ion concentration reduced the rate constant.

Using regression analysis, the coefficient of the effect of ferric ion concentration (*n*) was estimated to be 0.56. Study at additional ferric concentrations should be used to validate this exponent. The value of the lumped parameter k_o representing $W^c e^{-E_a/RT}$ was calculated to be 0.00436 as the experimental runs were carried out at constant temperature and stirring speed. This means that the conversion fraction for copper (X) can be calculated by the following expression.

$$X=1-(1-0.00436.C_{Fe^{3+}}^{0.56}.t)^3$$ *Equation 4-2*

To test the agreement between the calculated conversions and the experimental conversion values, the parity plot of X experimental against X calculated was drawn. Using regression analysis, the regression coefficient was found to be 0.948 and with a standard error of 0.0674 as calculated in Excel. This shows a sufficient fit between the calculated data and the experimental data. Figure 4–4 was used in the simulation model to determine the copper dissolution rate and, as a result, the ferric ion consumption rate for copper dissolution.

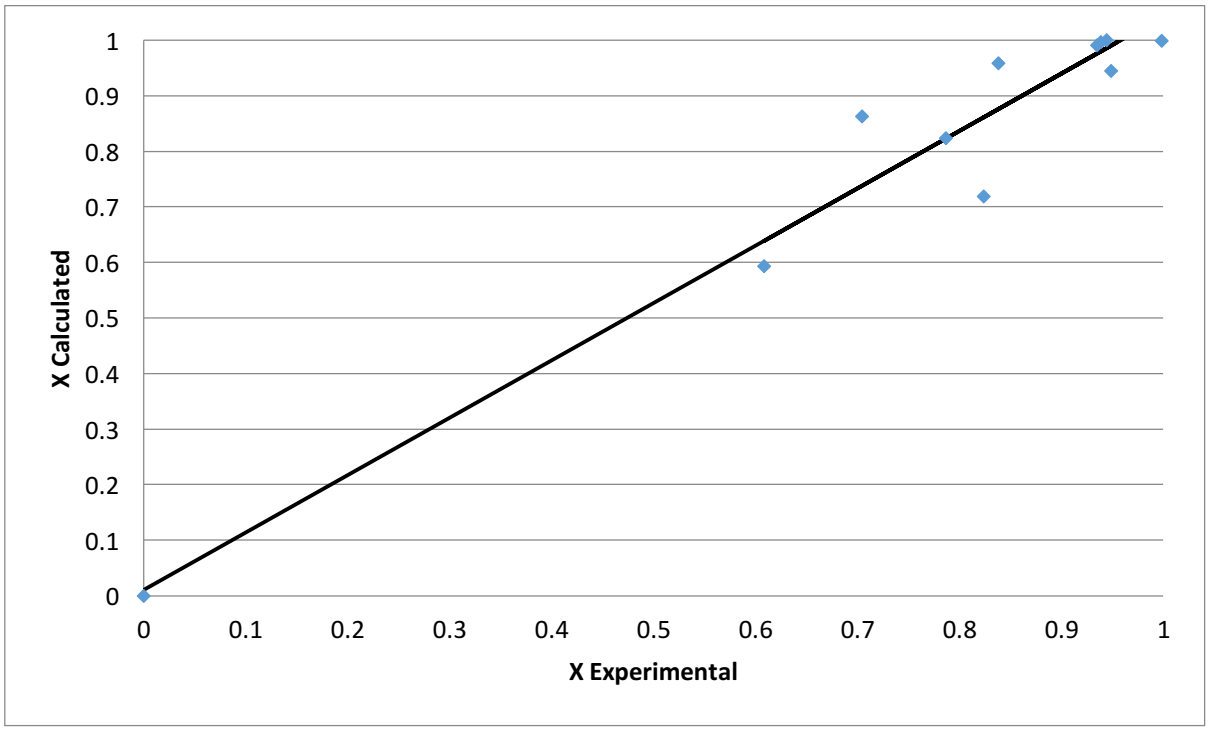

Figure 4–4. Comparison of experimental and calculated dissolution fraction of copper in ferric sulphate

4.2.2 Kinetics for Chemical Leaching of Tin

Three experiments were conducted in order to calculate the rate constants for leaching of tin metal with ferric ion. Each experimental run is listed and described briefly below:

1. 2 g tin per litre of ferric ion solution where the ferric ion concentration was 11 $g.l^{-1}$.
2. 4 g tin per litre of ferric ion solution where the ferric ion concentration was 11 $g.l^{-1}$.
3. 2 g tin per litre of ferric ion solution where the ferric ion concentration was 5.5 $g.l^{-1}$.

The observed changes to ferric ion concentration with time for each of the experimental runs, is found in Figure 4–5. The initial ferric ion consumption rate seems to be high as indicated by the steep slopes of the graphs in the first 15 minutes of the experimental run. After 15 minutes the rate appears to slow down as indicated by a decrease in the gradient of the ferric ion concentrations.

As observed from Figure 4–5, the conversion of Run 1 was the highest of the 3 experimental runs conducted, reaching a value of 0.84 after 20 minutes. Initially, Run 2 and Run 3 were found to have similar initial fractional conversion values until 10 minutes. At the 20 minute time interval, however, Run 3 had a faster rate of tin conversion reaching a value of 0.51, while Run 2 reached a value of 0.42.

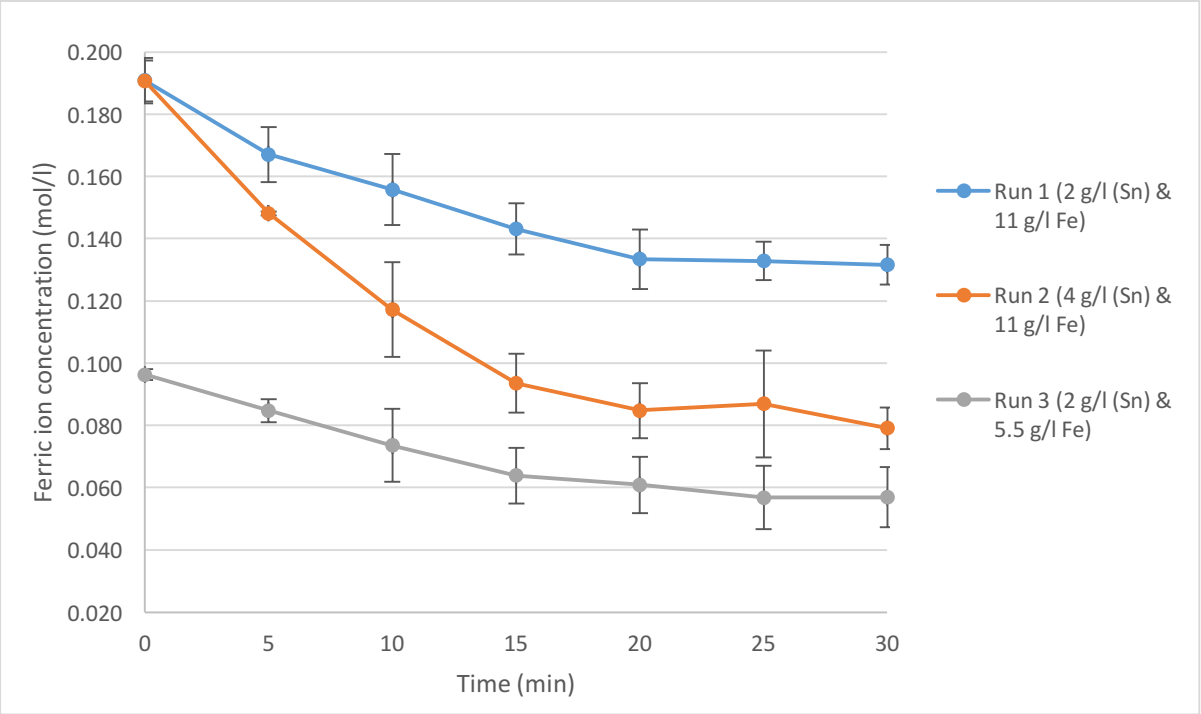

Figure 4–5. Ferric ion concentration trends for the dissolution of tin

At the termination of the experiment, a conversion of 87% was attained for 2 g Sn per litre in 11 g $Fe^{3+}.l^{-1}$. When the mass of metal was doubled i.e. to 4 g/l. there was no significant change in the final conversion which was 81 %. However reducing the ferric ion concentration to 5.5 g/l, the conversion reduced to 57 % which suggests that the dissolution of tin is dependent on the availability of ferric ion, necessary for complete dissolution to occur.

At the termination of the experiments, a comparison of the differences in copper and tin conversion for experimental runs with 2 $g.l^{-1}$ metal and 11 $g.l^{-1}$ ferric ion demonstrated over 95 % conversion for copper, with about 87 % conversion of tin. This indicated that tin had slower dissolution kinetics than copper in the presence of ferric ion.

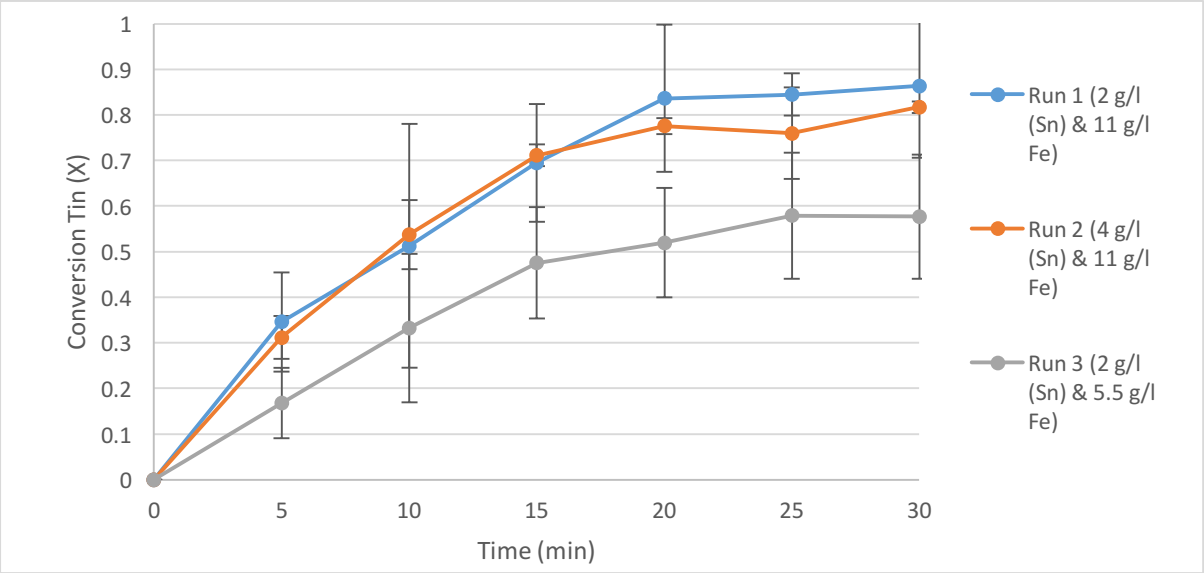

Figure 4–6. Tin conversion trends for changing initial ferric ion concentration and changing initial metal mass in suspension

Using the chemical controlled shrinking particle model, the same calculations were performed as shown in Section 4.2.1. The rate constant was determined by plotting $1-(1-X)^{1/3}$ vs t as shown in Figure 4–6. The variable X represents the conversion of the tin metal at time t.

In the runs where the initial ferric ion concentration was the same but with different metal concentrations i.e. Run 1 and Run 2, the gradients were very similar with high correlation coefficients (R^2). Run 1 had a gradient of 0.0227 with a R^2 value of 0.9998, while run 2 had a gradient of 0.0219 with a R^2 value of 0.9901. This indicates that for tin, the chemical controlled shrinking particle model should simulate the dissolution of tin well. The similar gradients also indicate that varying the initial metal mass in suspension should not change the conversion significantly, unless available ferric ion is limited.

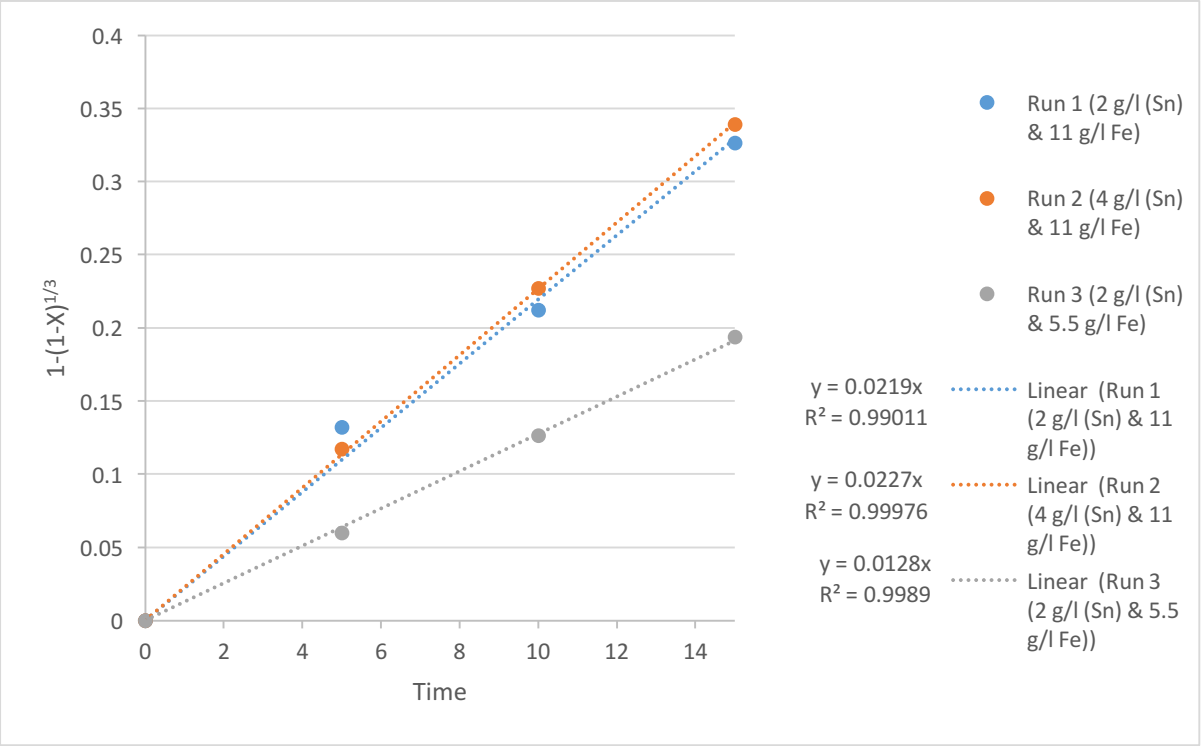

Figure 4–7. Chemical controlled reaction model for tin to determine constants of $1-(1-X)^{1/3}=k.t$

When halving the ferric ion concentration i.e. run 1 vs run 3, the gradient (which represents the coefficient *k*) also halved. This indicates that the reaction coefficient is dependent on the ferric ion concentration in solution.

Thus by using the same calculation steps that was used to determine the copper rate constants in Section 4.2.1, the coefficient constant (*n*) for ferric ion was calculated to be 0.269 and the new rate constant k_0 was calculated to be 0.000593. Thus the conversion for tin can be calculated by:

$$X = 1 - (1 - 0.000593.C_{Fe^{3+}}^{0.269}.t)^3 \qquad \textit{Equation 4-3}$$

To test the agreement between the calculated vs the experimental conversion values, the parity plot of X experimental vs X calculated was done and is presented in Figure 4–8. Using regression analysis, the regression coefficient was found to be 0.905 and with a standard error of 0.0658 as calculated in excel. This showed a good fit between the calculated data and the experimental data. Equation 4-3 used in the simulation to determine the tin dissolution rate and as a consequence the ferric ion consumption rate.

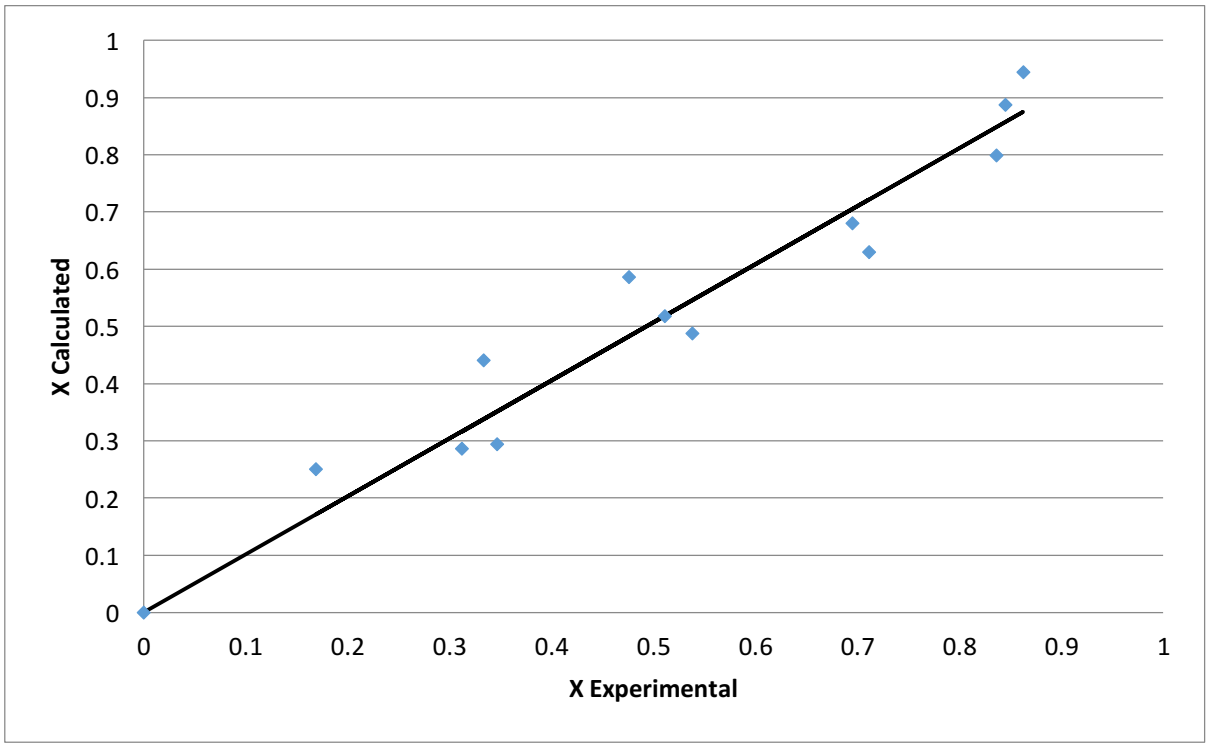

Figure 4–8. Comparison of experimental and calculated dissolution fraction of tin in ferric sulphate

4.2.3 Kinetics for Chemical Leaching of Zinc

Three further experiments were conducted in order to calculate the rate constants for the ferric leaching of zinc metal. The experimental conditions are briefly described below:

1. 2 g zinc per litre of ferric ion solution where the ferric ion concentration was 11 $g.l^{-1}$.
2. 4 g zinc per litre of ferric ion solution where the ferric ion concentration was 11 $g.l^{-1}$.
3. 2 g zinc per litre of ferric ion solution where the ferric
4. ion concentration was 5.5 $g.l^{-1}$.

As noted from Figure 4–9, the leaching of zinc metal in the presence of ferric ions resulted in the fastest rates of ferric ion consumption of all three metals considered. After a period of rapid metal dissolution over the first 5 minutes, the rate of consumption of ferric ion decreased.

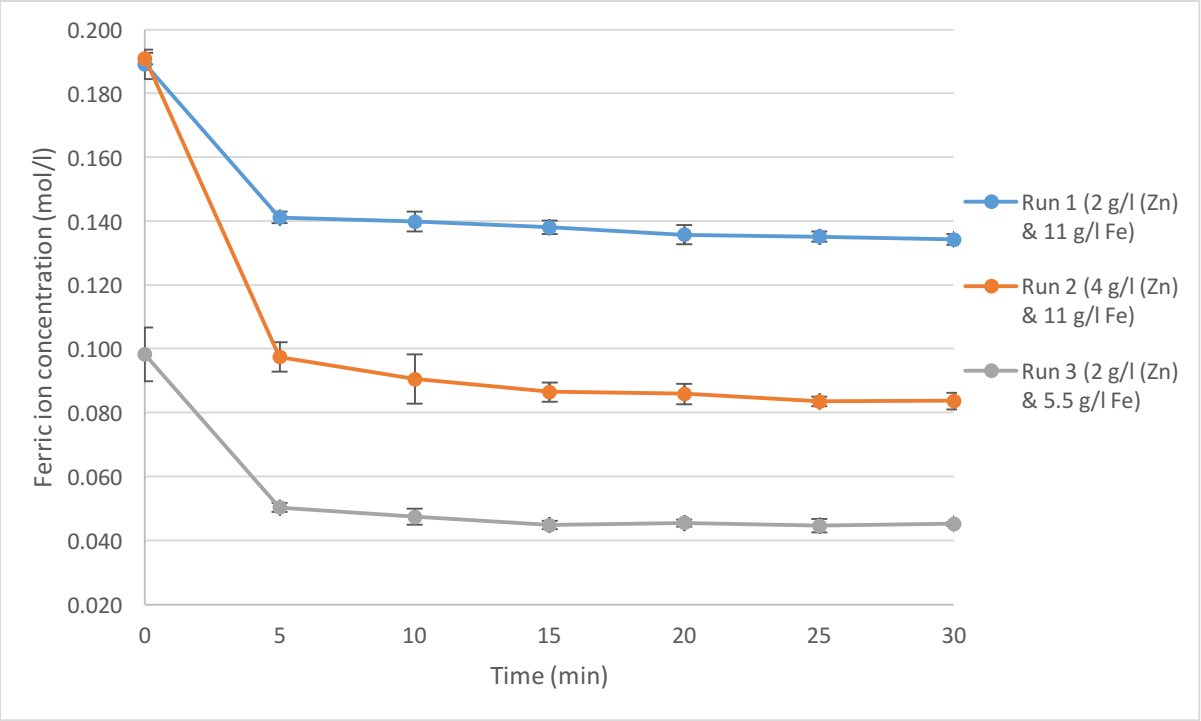

Figure 4–9. Ferric ion concentration trends for the dissolution of zinc

As observed in Figure 4–9, over 75 % conversion of zinc occurred in the first 5 minutes in all the experimental runs. Due to the high conversion after 5 minutes, these experiments were repeated over a shorter time interval. However, these initial experiments provide valuable information as to the extent of zinc metal dissolution over a time period comparable to that of copper and tin dissolution. For the experimental runs with 2 $g.l^{-1}$ metal and 11 $g.l^{-1}$ ferric ion, at the termination of the experiment, the conversion of zinc was at 85%, in comparison to a 95 % conversion for copper and 87 % conversion.

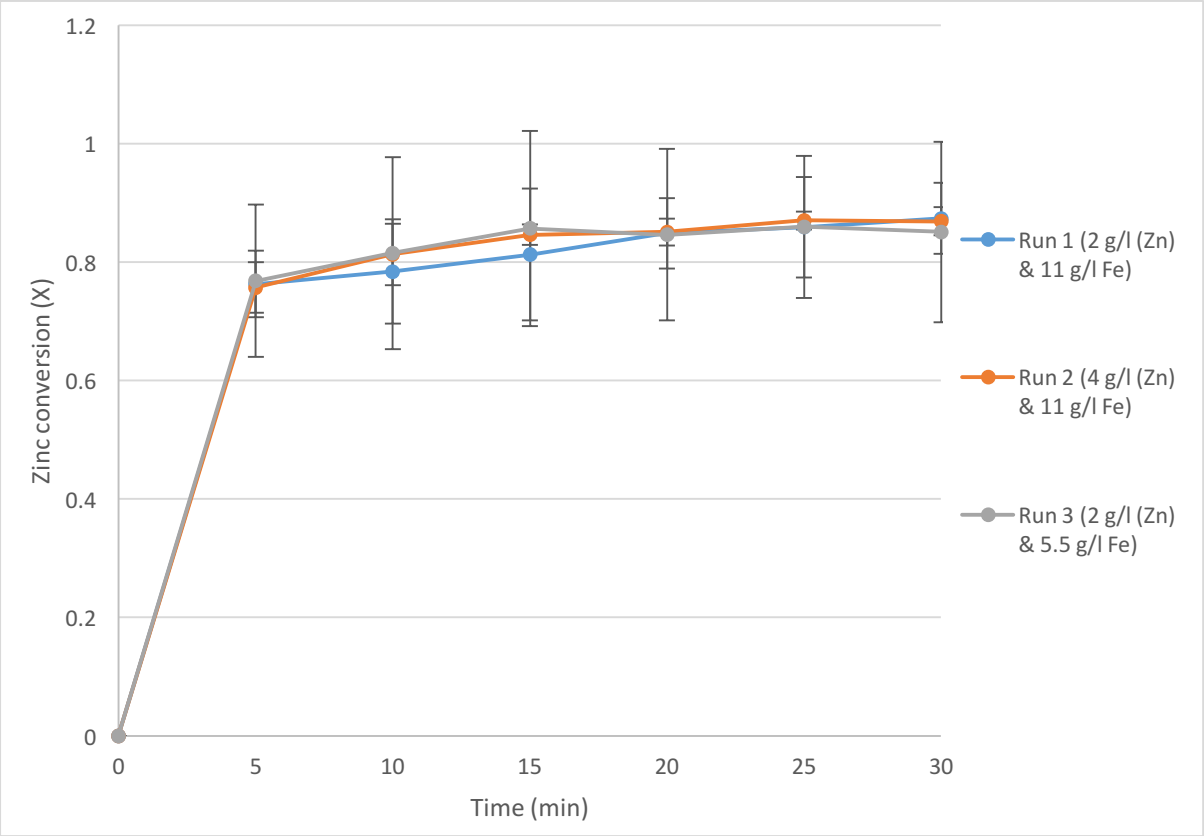

Figure 4–10. Zinc conversion trends for changing initial ferric ion concentration and changing initial metal mass in suspension

The results for zinc dissolution over the shorter experimental run of 5 minutes rather than 30 minutes are given in Figure 4–11 and Figure 4–12. It can be seen that, in Run 1, zinc conversion values reached 50 % conversion in the 1st minute. However, Run 2 and Run 3 had lower conversion values initially. In all cases, 70 to 80% conversion was achieved in 5 minutes, consistent with Figure 4–10.

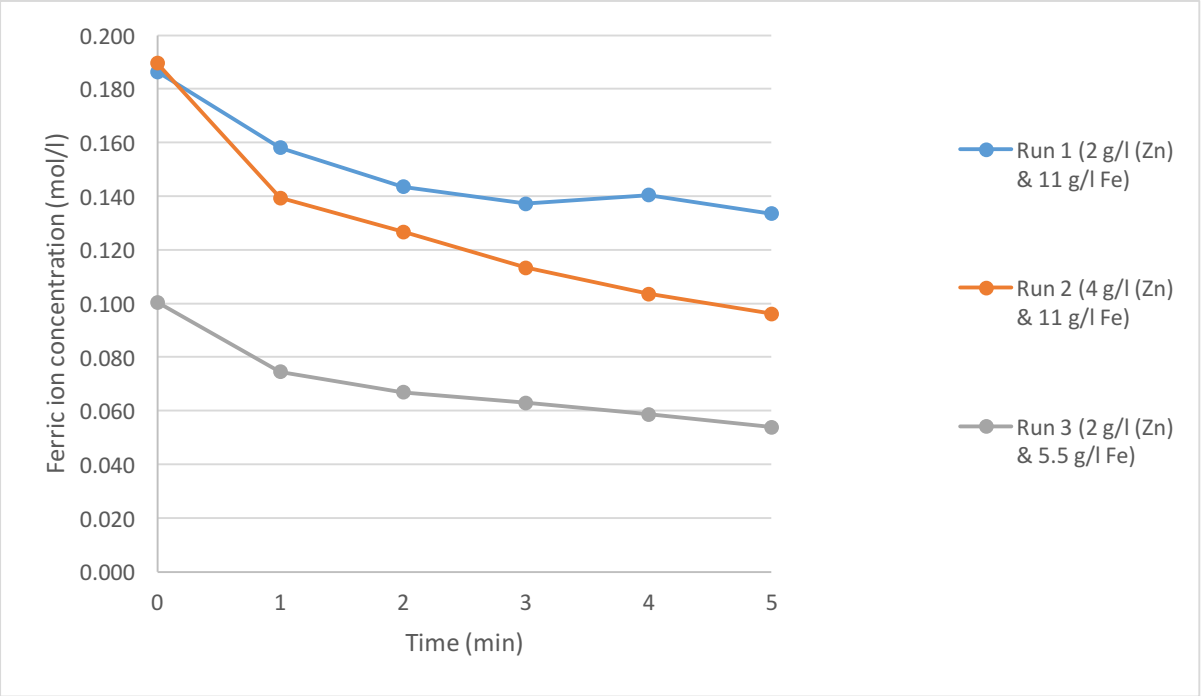

Figure 4–11. Ferric ion concentration trends for the dissolution of zinc over 5 minutes

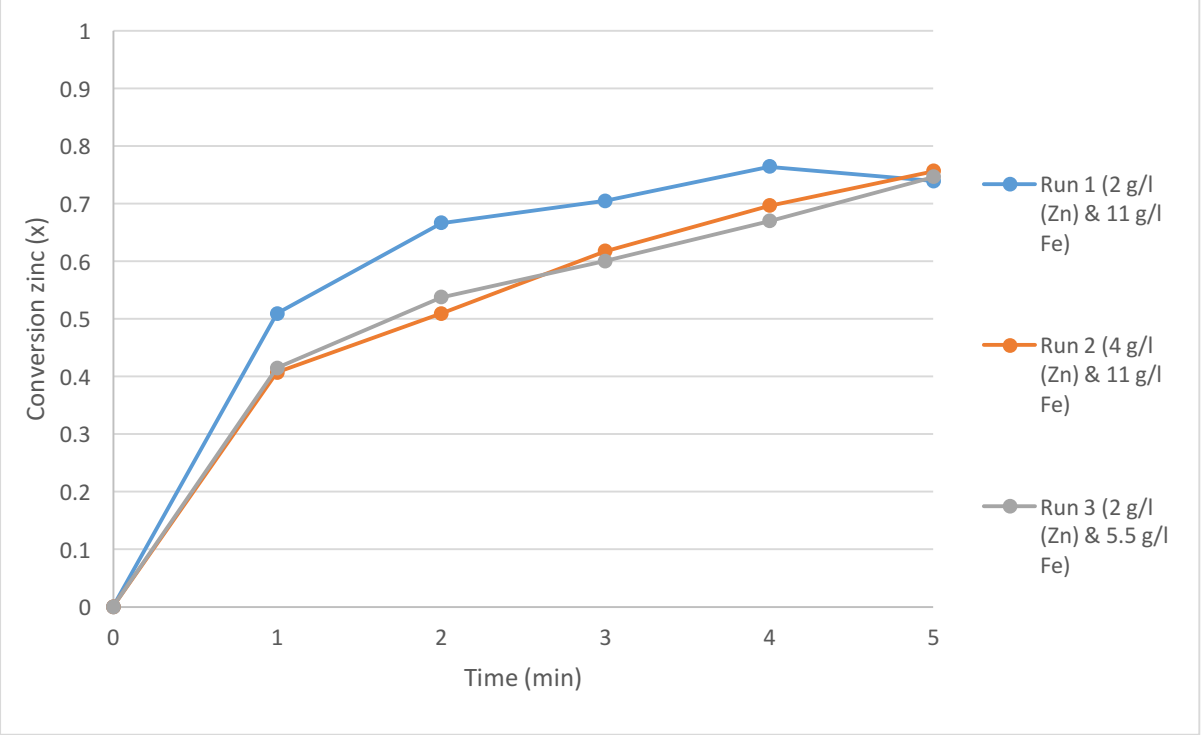

Figure 4–12. Zinc conversion trends for changing initial ferric ion concentration and changing initial metal mass in suspension over 5 minutes

Using the chemical controlled shrinking particle model, the same calculations were performed for the zinc data as for the copper data (Section 4.2.1) and tin data (Section 4.2.2). The rate constant was determined by plotting $1-(1-X)^{1/3}$ vs t as shown in Figure 4–13 where X is the conversion of the zinc metal at time t.

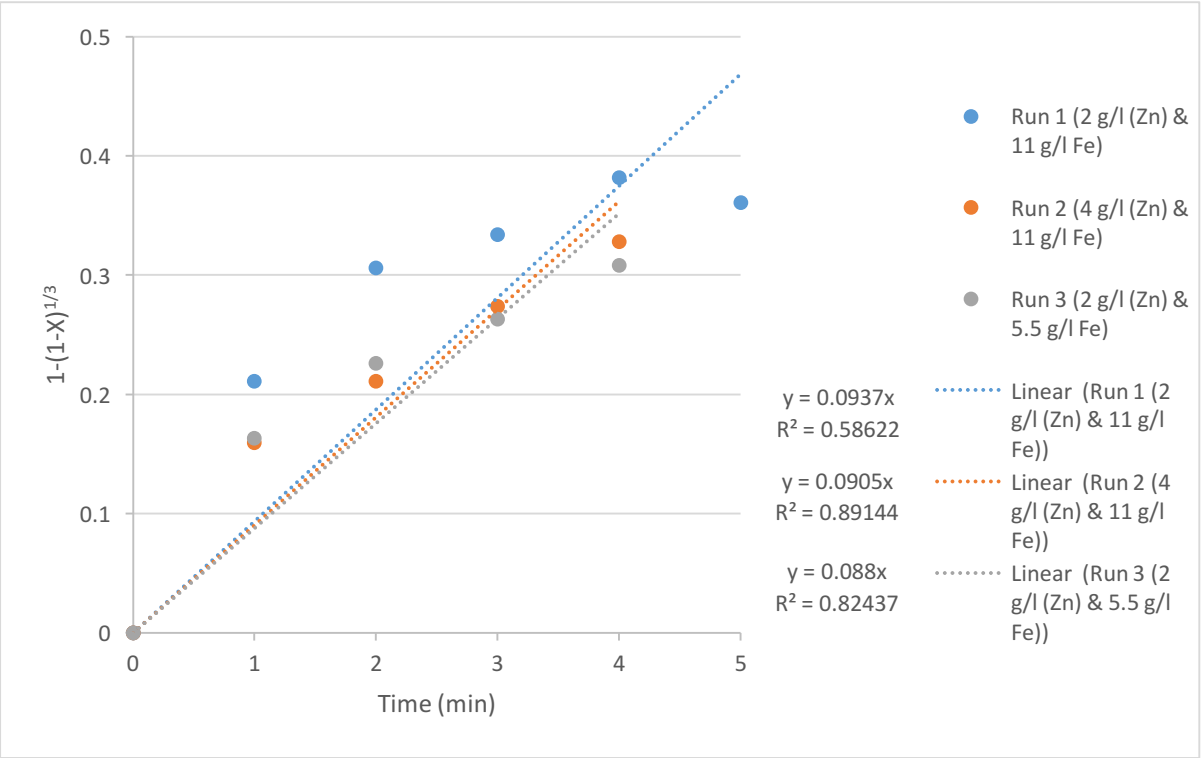

Figure 4–13. Chemical controlled shrinking particle reaction model for zinc to determine constants of $1-(1-X)^{1/3}=k.t$

Zinc dissolution kinetics demonstrated the lowest correlation coefficient among the three metals investigated, i.e. R^2 values for Run 1, Run 2; and Run 3 were 0.741, 0.8076 and 0.7915 respectively. This result suggests that the chemical controlled, shrinking particle model did not adequately describe the leach kinetics of zinc metal in the presence of ferric ion. Hence, either the diffusion limiting model or the logarithmic model could be used to describe the zinc leaching data. A particle size analysis was also conducted and it was found to be bimodal with a peak at 11 and 796 microns which could potentially affect the analysis.

The logarithmic model, which assumes surface layer diffusion is limiting (Kim, et al., 2011), was used and the results are plotted in Figure 4–14. The logarithmic model provides a better fit with the R^2 value for the run 1, run 2 and run 3 was 0.8749, 0.959 and 0.9609 respectively. The assumption that the chemical reaction was not limiting is reasonable when considering the reaction time, i.e. at 5 minutes over 70 % of the zinc had dissolved, as this is indicative of rapid reaction kinetics.

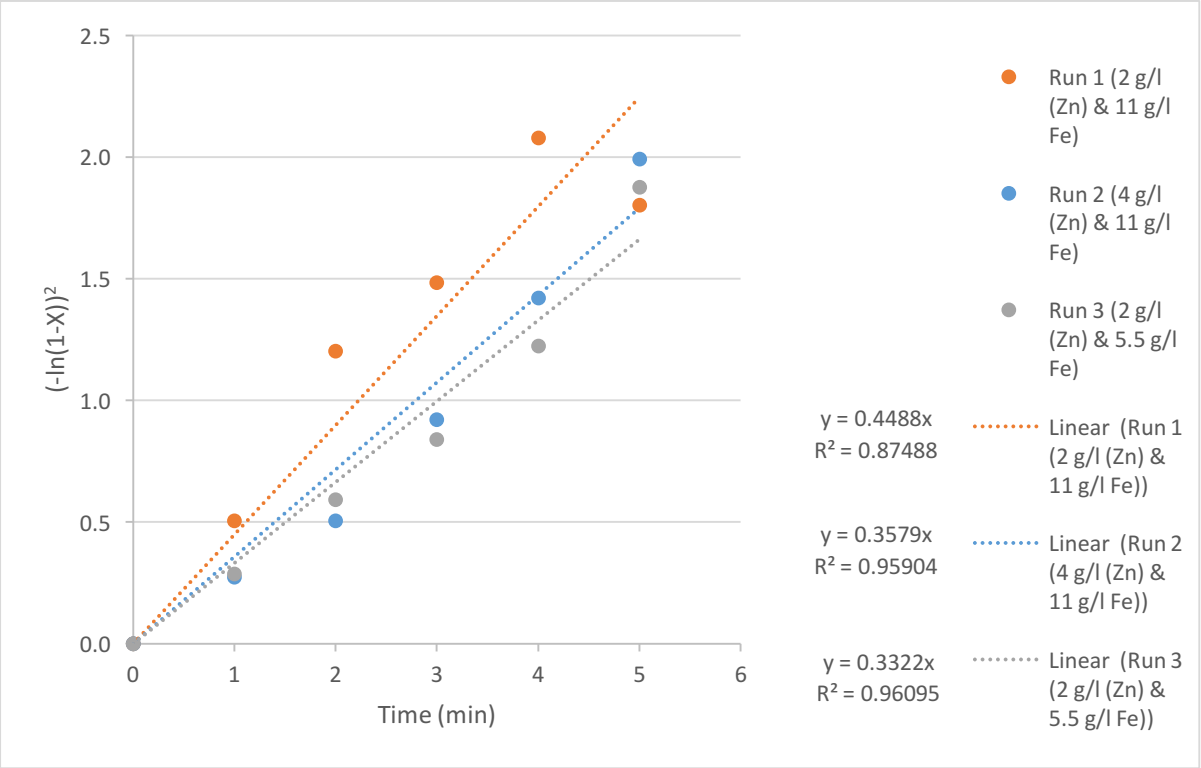

Figure 4–14. Chemical controlled reaction model for zinc to determine constants of $(-ln(1-X))^2=k.t$

The value of the rate constant (k), from the logarithmic model also depends on the temperature, stirring speed etc.

$$(-\ln(1-x))^2 = k_l.t = k_o W^c C_{Fe^{3+}}^n e^{-E_a/RT} t \qquad \textit{Equation 4-4}$$

Thus by using the same calculation steps that was used to determine the copper rate constants in Section 4.2.1, the coefficient constant, k, for zinc dissolution by ferric ion was calculated to be 0 and the new rate constant k_0 was calculated to be 0.451. This means zinc does not have a dependence on the ferric ion concentration. The conversion for zinc metal can be calculated by:

$$X = 1 - e^{-(0.00751t)^{0.5}} \qquad \textit{Equation 4-5}$$

To test the agreement between the calculated vs the experimental conversion values using the logarithmic rate law, the parity plot of X experimental vs X calculated was drawn. Using regression analysis, the regression coefficient was found to be 0.927 and with a standard error of 0.050 as calculated in excel. This shows a good fit between the calculated data and the experimental data when the logarithmic shrinking particle model is used. Equation 4-5 was used in the sensitivity analysis simulation to determine the zinc dissolution rate and thus, predict the ferric ion consumption rate.

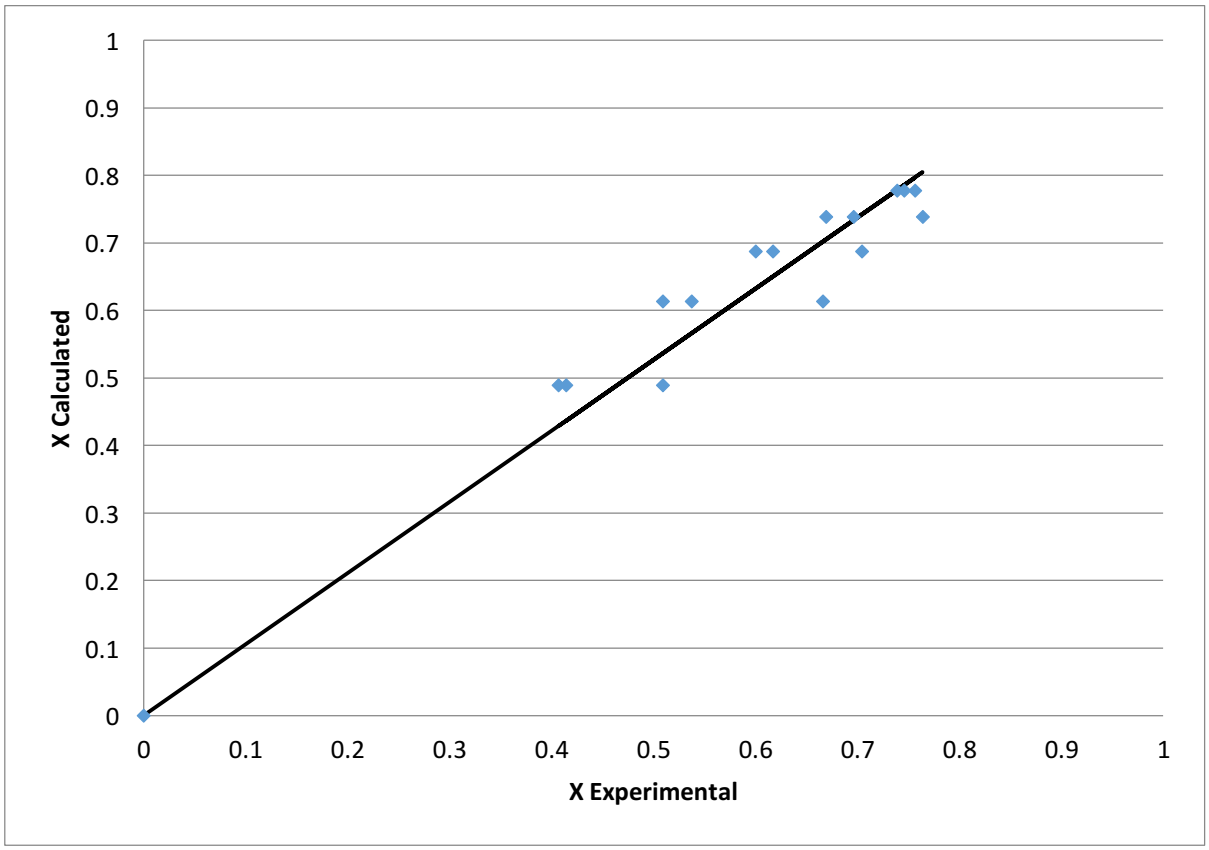

Figure 4–15. Comparison of experimental and calculated dissolution fraction of zinc in ferric sulphate using the logarithmic rate law

4.3 Batch Bioleaching Experiments

Bioleaching of base metals from electronic waste is driven by ferric ion leaching of the metals of interest and the associated microbial re-generation of this ferric ion. In this section, the preliminary bioleaching experiments are reported to provide trends in ferric ion production and consumption in the presence of microbial growth occurring at varying copper concentrations. Copper, supplied as copper powder, was used as a representative of the base metals found in PCB waste.

These preliminary batch bioleaching experiments were conducted using a 20% (by volume) inoculum of mixed mesophilic acidophilic autotrophs in Lungrid 9K medium (Table 3-1). The initial iron (ferric and ferrous ion) concentration in the shake flasks was therefore, 0.8 mol.l^{-1}. Copper metal powder was then added to separate shake flasks, at concentrations of 0, 0.2, 0.5 and 1 g initial mass per 100 ml of medium, to form solutions of 0, 2.0, 5.0 and 10.0 g Cu per litre. The pH, redox potential, ferric ion and total iron concentrations were measured and recorded. The detailed methodology was provided in Section 3.5.3.

4.3.1 Ferric ion Production in the presence of Microorganisms

The ferric ion concentration trends at the four initial concentrations of copper metal powder is presented in Figure 4–16. The time for maximum ferric ion concentration to be reached was observed to be dependent on the initial copper metal mass in solution. When the initial mass was 0 g (batch 1), the maximum ferric ion concentration of 0.127 mol.l^{-1} was reached in 6 days. However, as the initial metal mass increased, it took longer for the maximum ferric ion concentration to be reached i.e. at 1 g Cu (batch 2) it took 9 days, at 5 g Cu (Batch 3) it took 11 days and at 10.0 g Cu (batch 4) it took 18 days.

The exponential phase (ferric ion production phase) seems to be broken up into two stages, an initial stage showing a slow increase in ferric ion concentration and a second stage showing a faster increase in ferric ion concentration. Consider batch 3 for example, the initial slow stage lasted from day 1 to day 9, while the fast stage was from day 9 to about day 11.

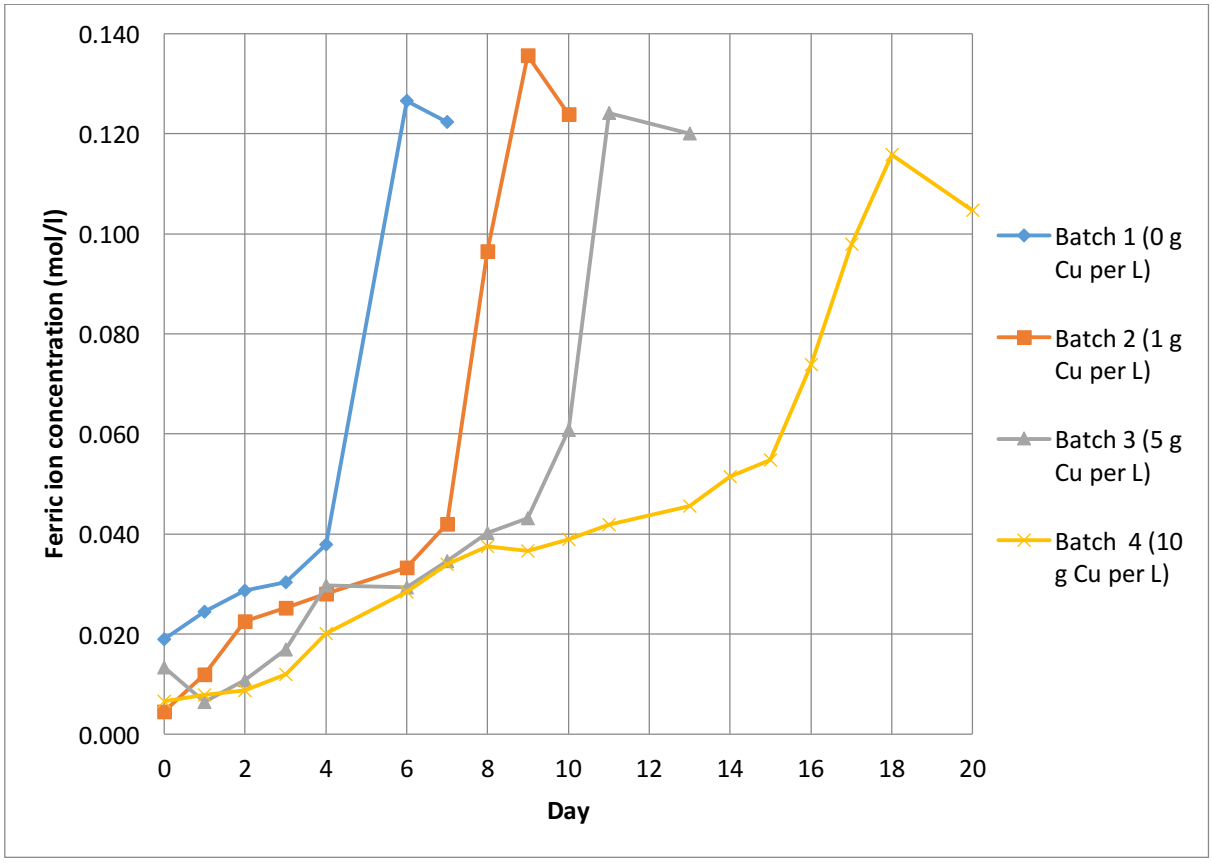

Figure 4–16. The trends of the ferric ion concentration in the bioleach flasks in the presence of different initial concentrations of copper metal powder

The duration of the initial stage of ferric ion production was proportional to the initial copper metal mass, such that, the higher the copper mass, the longer this stage lasted. Comparing the results of batch 4 (10 g Cu) to those of batch 2 (1 g Cu), the initial slow stage lasted for about 7 days for batch 2

(1 g Cu) which increased to about 15 days for the batch 4 (10 g Cu). Over this leaching stage, the observed trends in ferric ion concentration are attributed to the ongoing metal leaching by ferric ion whilst simultaneous oxidation of ferrous ion to ferric ion occurs. In the presence of a greater amount of initial elemental copper, a greater surface area is available for metal leaching, therefore, more ferric ion is consumed and is required to be regenerated over each time interval. However, the microorganisms present also require a period of adaptation to the new leaching environment, which will be affected by the amount of copper ions in solution (Das, et al., 1997).

The second stage, the exponential (ferric ion production) phase, showed a faster increase in the ferric ion concentration. For batch 1 (0 g Cu), batch 2 (1 g Cu), batch 3 (5 g Cu), this fast stage lasted about 1 day before a maximum concentration of approximately 0.125 $mol.l^{-1}$ ferric ion concentration was observed in the batches. However, in batch 4 (10 g Cu), this takes about 3 days to reach the maximum concentration of 0.116 $mol.l^{-1}$. In all 4 batches, there was a peak in ferric ion concentration that was then followed by a decrease in the ferric ion concentration. This stage of rapid ferric ion production is proposed to demonstrate the dominance of the ferrous ion oxidation reaction by microorganisms over the metal oxidation reaction, which consumes ferric ion. The difference in time interval between the maximum ferric ion concentration reached for batches 1, 2 and 3 in comparison to batch 4, may be due to the additional time required by the microorganisms to adapt to the higher copper concentrations in batch 4. This result provides an indication of the tolerance of the microorganisms to increasing copper concentrations between 1 and 10 $g.l^{-1}$. The drop in the ferric ion concentration can be attributed to precipitation of iron, which is expected to occur at pH above 1.8, as demonstrated previously by Xiang et al. (2010) and Anders and Colin (1995).

Figure 4–17 presents the results of the measured total iron concentration, as described in the methods presented in Section 3.2.1. At the beginning of the experiment, the total iron concentration was between 0.137 – 0.158 $mol.l^{-1}$ across all batches, which decreased in all the batches as the experiment progressed. A comparison of Figure 4–16 and Figure 4–17 shows that initially most of the iron present was in the form of ferrous ion. Thereafter, the total iron concentration remained relatively constant with the cycling of ferric ion, until the decrease in ferric ion in Figure 4–16 was reflected in the decrease of total iron concentration.

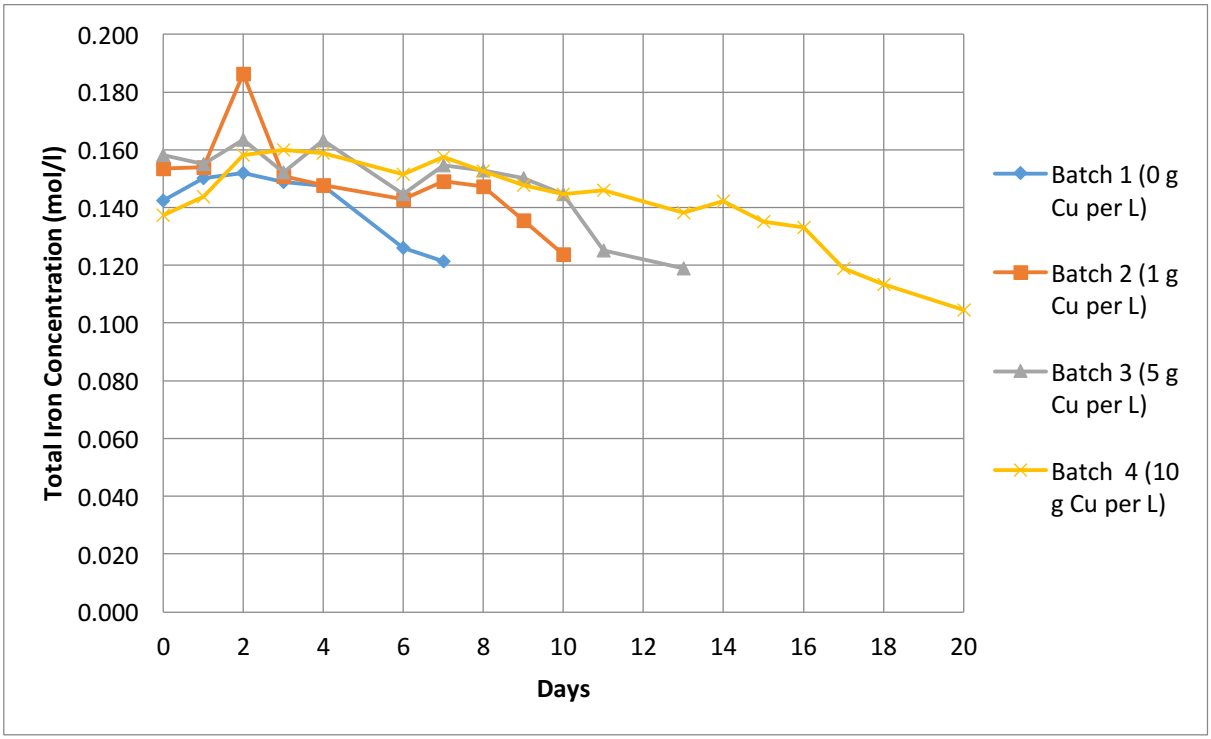

Figure 4–17. The trends of the total iron concentration in the bioleach flasks in the presence of different initial concentrations of copper metal powder

The redox potential, shown in Figure 4–18, follows the same trend as in Figure 4–16, in that the time for the maximum redox potential to be reached is proportional to the initial metal mass in solution i.e. the higher the metal mass the longer it takes for the redox potential to reach its maximum value of 710 mV. As the measured redox potential is an indication of the ferric to ferrous ion ratio, it also provides a measure of the ferrous ion oxidation activity of the microorganisms. The observed result, therefore, supports the earlier proposition that the higher metal concentrations required longer time periods for microbial adaptation and metal tolerance to occur.

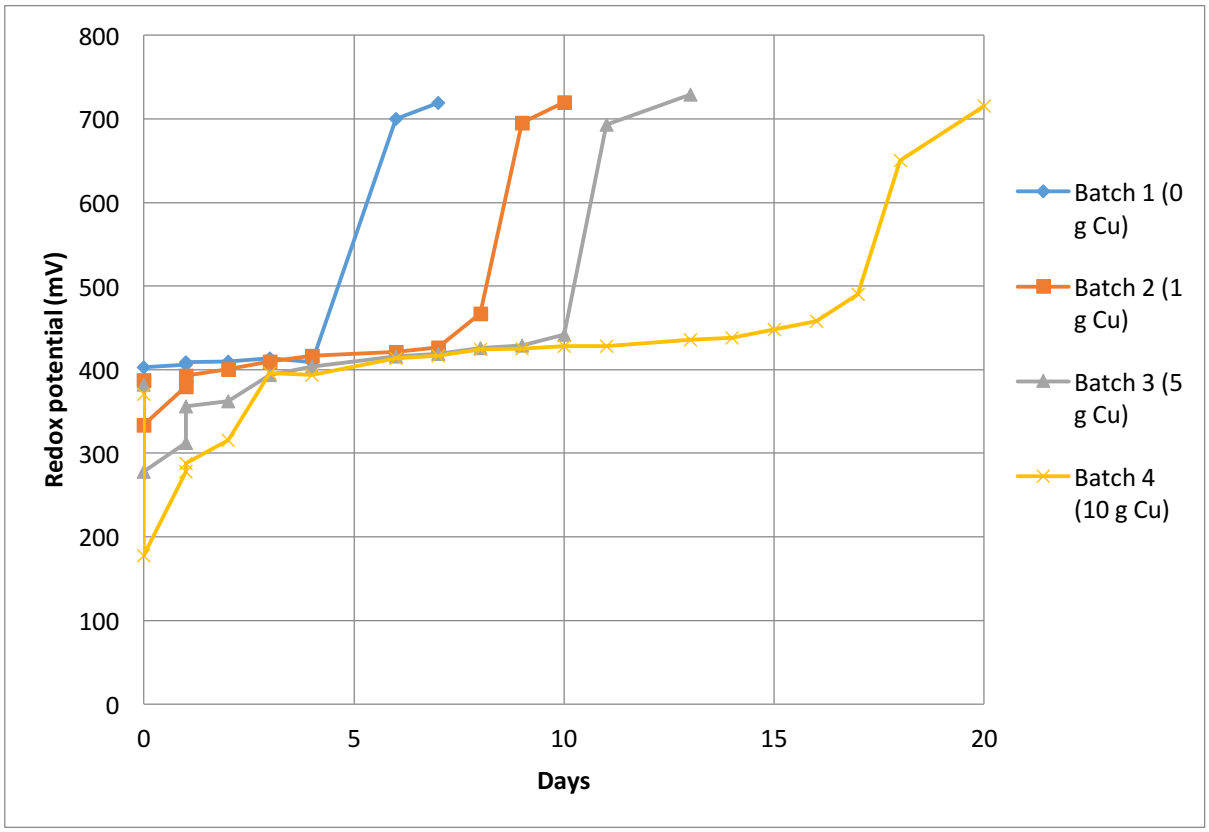

Figure 4–18. The trends of redox potential in the bioleach flasks in the presence of different initial concentrations of copper metal powder

Figure 4–19 shows that the initial pH values of batch 4 (10 g Cu) and batch 3 (5 g Cu) were high i.e. 3.80 and 3.70 respectively. There was a slight initial increase in the pH of batch 2 (1 g Cu) to about 2.30, while there was no initial increase in batch 1 (0 g Cu). There was also a slight increase in the pH for all the batches after day 3. The pH adjustments were conducted consistently when the pH exceeded the value of 2.0 (at the point marked by the arrows) in an attempt to reduce ferric ion precipitation. The adjustments were conducted using sulphuric acid.

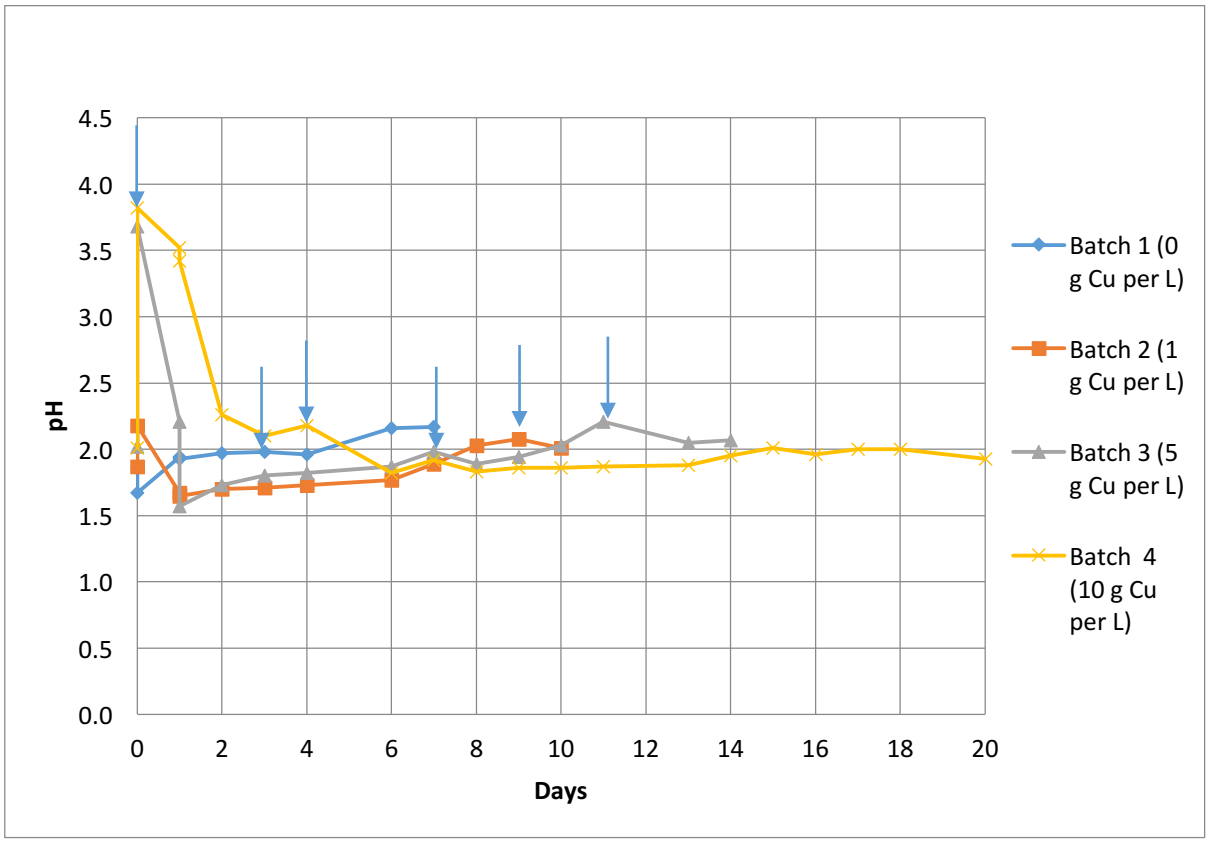

Figure 4–19. PH reading for bacteria batch leaching experiments.

4.3.2 Reaction Mechanisms involved in the Leaching of Copper in the presence of Microorganism

Based on the ferric ion results in Figure 4–16 and the redox results in Figure 4–18, there is a correlation between the initial copper mass in suspension and the length of time it takes for the maximum ferric ion concentration and redox potential to be reached. It was seen that the higher the initial copper metal mass, the longer it took for the maximum ferric ion concentration to be reached. Yang et al. (2014) has proposed the following equations that describe the leaching of copper metal by ferric in the presence of microorganisms that regenerate the ferric ion:

$$2Fe^{3+} + Cu^{0} \rightarrow 2Fe^{2+} + Cu^{2+}\ [Chemical\ ferric\ ion\ consumption] \quad \textit{Equation 4-6}$$

$$4Fe^{2+} + O_2 + 4H^{+} \rightarrow 4Fe^{3+} + 2H_2O\ [Bacteria\ ferric\ ion\ production] \quad \textit{Equation 4-7}$$

$$2SO_4^{2-} + 3Fe^{3+} + 6H_2O + K^{+} \leftrightarrow KFe_3(SO_4)_2(OH)_6 + 6H^{+}[Precipitation] \quad \textit{Equation 4-8}$$

$$\Delta Fe^{3+}_{observed} = \Delta Fe^{3+}_{production} - \Delta Fe^{3+}_{consumption} \quad \textit{Equation 4-9}$$

The observed ferric ion concentration in solution is a sum of two reactions, the ferric ion consumption via Equation 4-6 and the ferric ion production by Equation 4-7, thus the observed ferric ion concentration can be described by Equation 4-9.

As microbial growth and metabolic activity occur, the ferrous ion is converted to ferric ion as described in Equation 4-7. This ferric ion reacts with the elemental metal leading to the dissolution of base metals occurring as described in Equation 4-6. Hence, there are two competing processes: one is the ferric ion production through the oxidative action of microorganisms on ferrous ion and the second is the ferric ion consumption which occurs through its reduction on the dissolution of base metal.

An explanation for the correlation of the time it took for the maximum ferric ion and redox potential to be reached with metal in suspension (as shown in Figure 4–16 and Figure 4–18 respectively) was that the higher the metal mass in suspension, the greater the amount of ferric ion required for the complete dissolution of the initial metal. This meant that for batch 1 (0 g Cu), no ferric ion reduction occurred and so the ferric ion concentration in solution increased rapidly, along with the redox potential as there was no initial metal mass present to cause the consumption of ferric ion. As the initial metal mass increased in suspension, the ferric ion reacted with the copper metal as it was formed via Equation 4-6. The more mass of elemental copper present, the more was the ferric ion needed. This required cycling of the ferrous ion product of metal dissolution through microbial oxidation, hence the longer it took for maximum accumulation of ferric ion.

It was shown in Figure 4–16 that there was a slow and fast phase in the production of ferric ion in proportion with the initial metal mass in that the higher the metal mass added, the longer the slow phase. The slow phase could indicate the observed net ferric ion concentration (Equation 4-9), due to the combined ferric ion consumption and ferric ion production in that both processes were occurring at this point. This was then followed by a fast phase which could indicate that the ferric ion concentration in solution was due to the production of ferric ion as all the copper had been dissolved, hence there was no further or slower ferric ion consumption[2].

In this experiment it was difficult to determine which, whether ferric ion consumption or ferric ion production was the limiting rate equation. This is because ferric ion consumption in Equation 4-6 was dependent on how fast the ferric ions were produced in Equation 4-7. This meant that the ferric ion consumption rate was governed by the ferric ion production rate in that, if the ferric ion production rate was slow, the ferric ion consumption rate would appear to be slow as well. However, the ferric

[2] This is an assumption due to the lack of cupric ion data for the duration of the experiment.

ion production rate governed by Equation 4-7 was impacted by how fast the microorganisms could grow and produce the ferric ion.

Another explanation for this lengthening of time was discussed by Xiang et al (2010) where the effect of toxicity of metals on microorganisms was suggested. Thus when the initial copper loading was higher, the effect of the copper toxicity should be greater when it is in solution. This may result in lower microbial activity with associated reduced rate of ferric ion production, during the period of adaptation to the higher metal ion presence.

Figure 4–19 showed that there was an initial high increase of pH when the copper metal was introduced i.e. between day 0 and 3 for batch 2 (2 g Cu), batch 3 (5 g Cu), and batch 4 (10 g Cu).The sharp decrease of the pH which followed was the result of the manual addition of sulphuric acid to the system. As the experiment proceeded (after day 4), there was a slight increase in the pH in all the batches. There have been several factors that can be attributed to the increase in pH in the leaching experiments.

The first is the alkalinity of PCBs (Brandl, et al., 2001; Ilyas, et al., 2007), however, this was ruled out as in this experiment copper metal powder was used instead of PCBs. A second alternative was the microbial action in oxidizing ferrous ion to ferric ion which consumes protons according to Equation 4-7 (Xiang, et al., 2010). However, this is unlikely to be the dominant reason in that the initial pH in all four batches should have increased equally. However, this may explain why there was a gradual increase in the pH as the experiment progressed (after day 4 in Figure 4–19).

The initial spike in the pH was attributed to the acid leaching of the base copper metals (Choi, et al., 2004; Xiang, et al., 2010). This is supported by the absence of increase in pH in the control experiment i.e. batch 1 (0 g Cu). However, the spike became larger with increasing initial copper metal mass in solution. This suggests that the more copper there was, the more protons were consumed through the acid leaching mechanism. This was confirmed by Yang et al (2009) as was shown in Section 2.3.5.1 in the literature review. Subsequent to this, the value of pH was maintained at about 2.0 using the sulphuric acid.

From Figure 4–17, it was shown that there was an overall decrease in the total iron concentration with time. The decrease of the total iron concentration could be attributed to the precipitation of the ferric ion from solution. This was consistent with literature findings where it was shown that ferric ion precipitates as jarosite (Xiang, et al., 2010). This reaction was shown in Equation 4-8. The precipitation was closely linked with the pH in that the higher the pH the faster the precipitation of ferric ion. In

order to prevent the precipitation of ferric ion a pH value of less than 1.8 was suggested (Anders & Colin, 1995). The precipitate was observed as a yellow solid at the bottom of the Erlenmeyer flask.

4.4 Fed Batch Addition of Copper at Peak Microbial Oxidation: Assessment of relative Ferric Ion Production and Consumption Rates

4.4.1 Motivation of experimental approach

The rate of copper dissolution by ferric ion leaching is a function of the ferric ion concentration as shown in Equation 4-6. However, the ferric ion concentration in solution is controlled by the relative rate of consumption of the ferric ion (related to leach rate) and its production (related to the microbial ferrous ion oxidation rate). Under specified physiochemical conditions, a particular specific ferrous ion oxidation rate can be predicted for each microbial species (Ojumu, et al., 2006). Therefore, the volumetric ferrous ion oxidation rate is expected to be a function of the microbial concentration and microbial species present. Hence, the microbial concentration is expected to affect the dissolution efficiency of copper from e-waste (including PCBs). This is supported by Yang et al. (2009) who showed that the higher the microbial population the faster the dissolution rate of copper from PCBs.

In heap bioleaching of low grade mineral ore, typically the oxidation of ferrous ion by microorganisms is faster than the reduction of ferric ion by mineral sulfides. In tank leaching of mineral concentrates, the relative rates of these sub-processes depends on the activity of the microbial culture which is a function of the physiochemical conditions present. In the context of PCB bioleaching where metals are in their zero-valence state (or as alloys), ferric ion consumption through metal dissolution may potentially be faster than the ferric ion production through the microbial ferrous ion oxidation.

Thus the objective of this study is to develop a way to compare the rates of ferric ion consumption and the ferric ion production at maximum ferric ion production rates. This was conducted using copper powder at high stirring speeds to avoid mass transfer limitations associated with PCBs. To ensure a high microbial population at the start of the metal dissolution phase on introduction of copper metal into the system, the microorganisms were grown in the absence of copper metal powder until all the initial ferrous ions in the system were consumed (approximately 9 g/l ferrous ion). At this point copper metal powder was added to the Erlenmeyer flasks and the ferric ion concentration, pH and redox potential were recorded.

On addition of the copper metal powder, the ferric ion was reduced to ferrous ion through the dissolution of copper. Once the complete dissolution of copper by the ferric ion had occurred and microbial oxidation of the ferrous ion formed was complete, ferric ion reached its maximum concentration again. At this point, more copper metal powder was added. This cycle was repeated continuously for 6 additions.

This approach allowed comparison of the ferric ion production and consumption trends through analysing the observed ferric ion concentration in solution in the presence of a high and active microbial community. If the ferric ion consumption rate was lower than the ferric ion production rate, the observed ferric ion concentration (Equation 4-9) would be expected to remain constant with the dissolution rate being limiting. However, if the dissolution rate and associated ferric ion consumption rate was faster than the ferric ion production rate through microbial ferrous ion oxidation, then the observed ferric ion concentration would be expected to decrease rapidly (proportional to the dissolution rate) to a minimum. This would be followed by a slow increase at a rate proportional to the ferrous ion oxidation rate.

4.4.2 Fed Batch Addition at Peak Microbial Oxidation

The results of the experiments include analysing the trends of the ferric ion concentration, pH and microorganism cell count. These are presented in two groupings, related to increasing copper ions in solution.

4.4.2.1 The Effect of Six Additions of the Copper

This section investigates the trend of the ferric ion concentration during the six additions of the copper metal powder to the microbial cultures in Erlenmeyer flasks.

Figure 4–20 presents the ferric ion concentration and Figure 4–21 shows the ratio of the ferric ion to the total iron concentration (similar to conversion *X*).

Figure 4–21 shows that at time 0, the iron was present in solution as ferric ion with negligible amounts of ferrous ion i.e. the ferric ion to total iron ratio is 1. On addition of the copper metal powder, there was a rapid decrease of the ferric ion concentration (

Figure 4–20, reaching a minimum of 0.036 mol.l^{-1} in the 4.0 g Cu addition batch and 0.103 mol.l^{-1} in the 2.0 g Cu addition batch. This resulted in a ferric to total iron ratio of 0.21 and 0.61 respectively, as shown in Figure 4–21. After attaining these minima, the ferric ion concentrations increased and reached a peak of about 0.175 mol.l^{-1} in the 2.0 g Cu addition batch and 0.166 mol.l^{-1} in the 4.0 g Cu addition batch at about 120 hours after first the first addition. The ferric to total iron ratio at this point was 1.0 for both batches, implying all the iron in the system had been converted back to ferric ion.

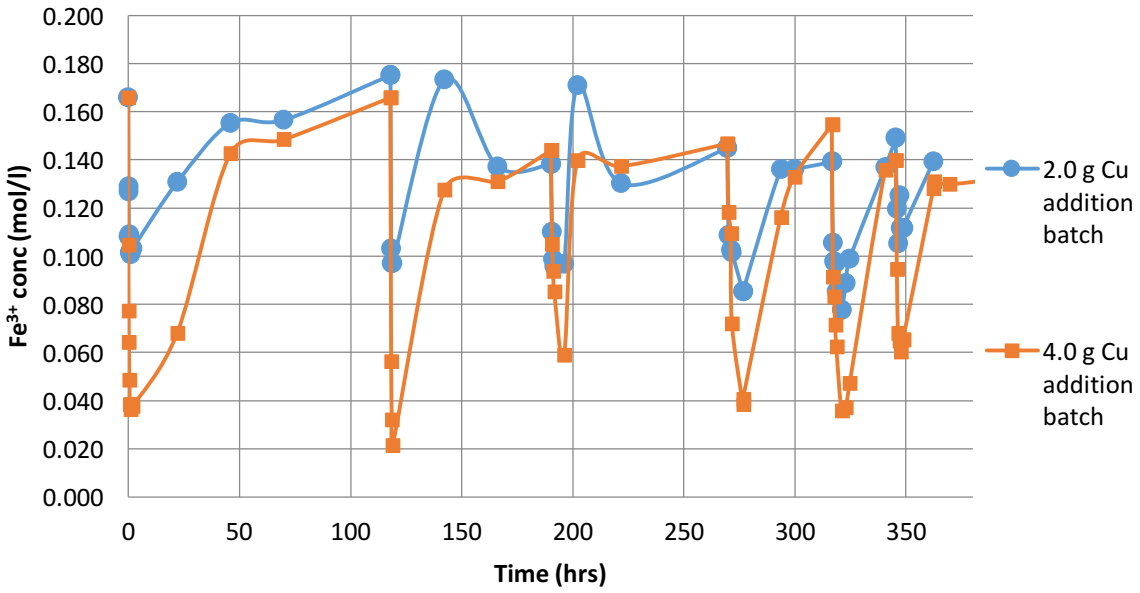

Figure 4–20. Ferric ion concentration trends for the fed-batch addition of copper metal powder to an active bioleach environment operated at a starting concentration of 9 g/l iron in solution.

At the peak ferric ion concentration, more copper metal was added to the system. A sharp decline of ferric ion in solution was again observed where the ferric ion concentration reached a minimum of approximately 0.022 mol.l^{-1} in the 4.0 g Cu addition batch and 0.056 in the 2.0 g Cu addition batch. This resulted in ferric ion to total iron ratios of 0.13 and 0.56 respectively as shown in Figure 4–21. This was followed by a faster increase of the ferric ion concentration to a maximum of about 0.144 mol.l^{-1} in both batches at approximately 190 hours at which point the ferric to total iron ratios were 1.0 for both batches.

This trend was observed multiple times with each addition of copper metal powder. From all the additions of the copper metal powder, the decrease of the ferric ion concentration was significantly faster than the increase of the ferric ion concentration. Also the first increase in the ferric ion concentration was slower than subsequent increases.

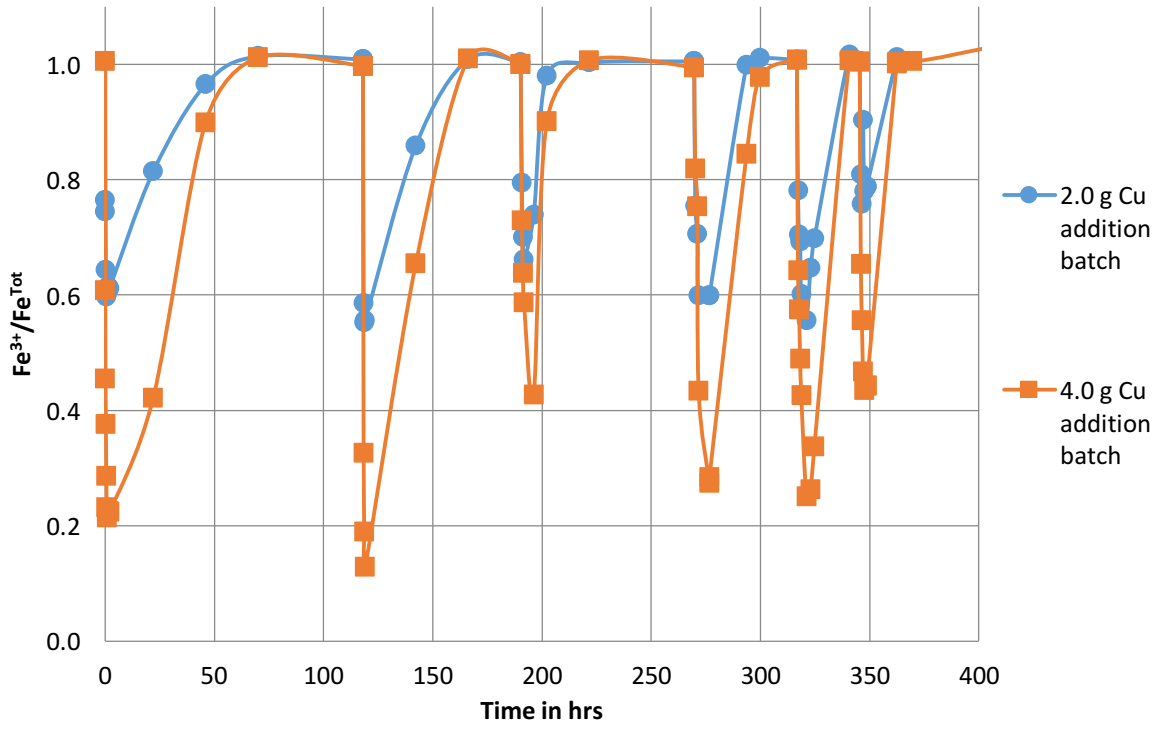

Figure 4–21. Normalized ferric ion concentration trends for the fed-batch addition of copper metal powder to an active bioleach environment operated at a starting concentration of 9 g/l iron in solution.

4.4.2.2 Ferric to Total Iron Ratio during the Ferric Ion Consumption Phase

In this section, the trend in ferric to total iron ratio for the 4.0 g Cu addition batch is shown and presented in Figure 4–22. The 4.0 g Cu addition batch experimental data is used as the consumption trends are clearer than in the 2.0 g Cu addition batch. The time scale for the observation conducted was 2 hours after each copper addition.

In Addition 1 and 2, the ferric to total iron ratio was the lowest after 1 hour i.e. 0.21 and 0.13 respectively, which means it had the lowest ferric ion concentration at this point due to its reduction to ferrous ion through the dissolution of copper (Equation 4-6). However, following Addition 3 – 6 the ferric ion and total iron ratio was above 0.40. This may indicate that with higher additions of copper powder, the observed residual ferric ion concentration increased.

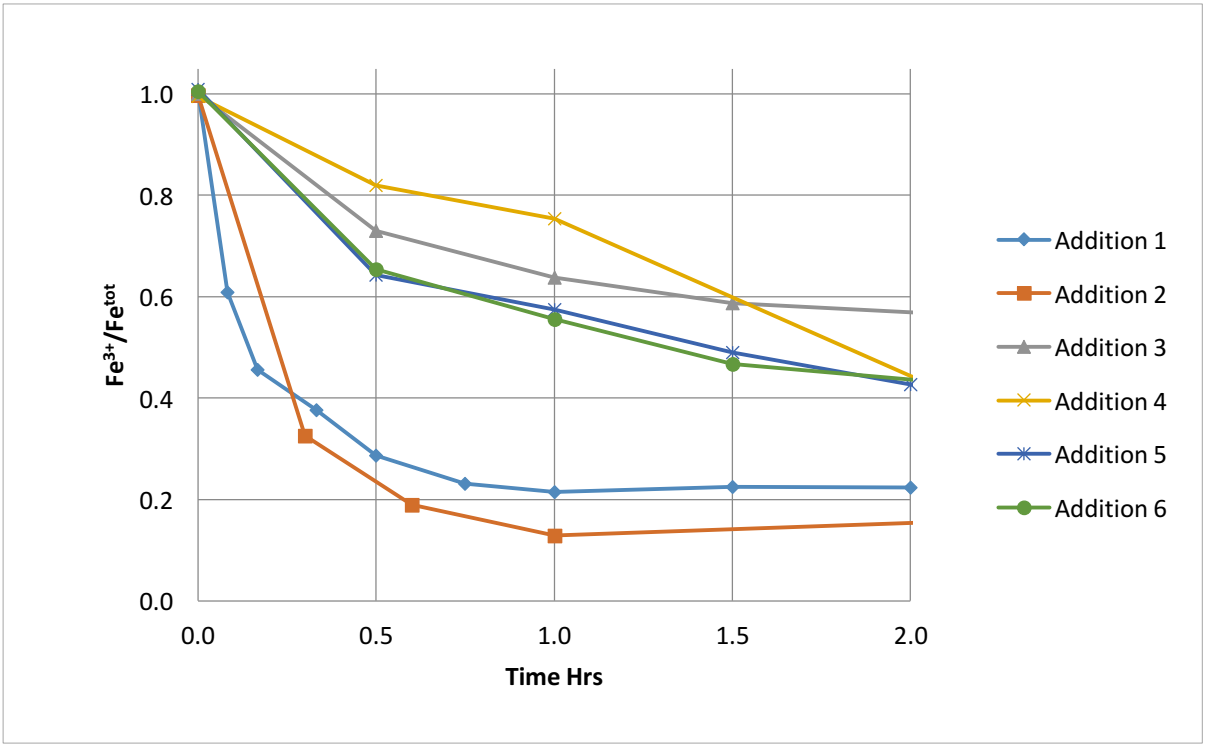

Figure 4–22. Ferric ion to total iron concentration ratio in the ferric ion consumption phase of the fed-batch addition of copper metal powder experiment to an active bioleach environment for the 4.0 g Cu addition batch run.

4.4.2.3 Ferric Ion to Total Iron Ratio during the Ferric Ion Production Phase

This section focuses on the ferric ion production phase of the six additions. The time scale for the observation was 90 hours after each copper addition.

From Figure 4–23, following Addition 1 it took 70 hours for the ferrous ion that was generated from the dissolution of copper (Equation 4-6) to be converted to ferric ion as indicated by a ferric ion to total iron ratio of 1.0 (meaning no ferrous ion in solution). This was slower than following Addition 2 when it took about 48 hours. Addition 2 was slower than Addition 3 (31 hours) after which, the time it took to get to maximum ferric ion and total iron ratio decreased to 30, 24 and 17 hours respectively for Additions 4 to 6.

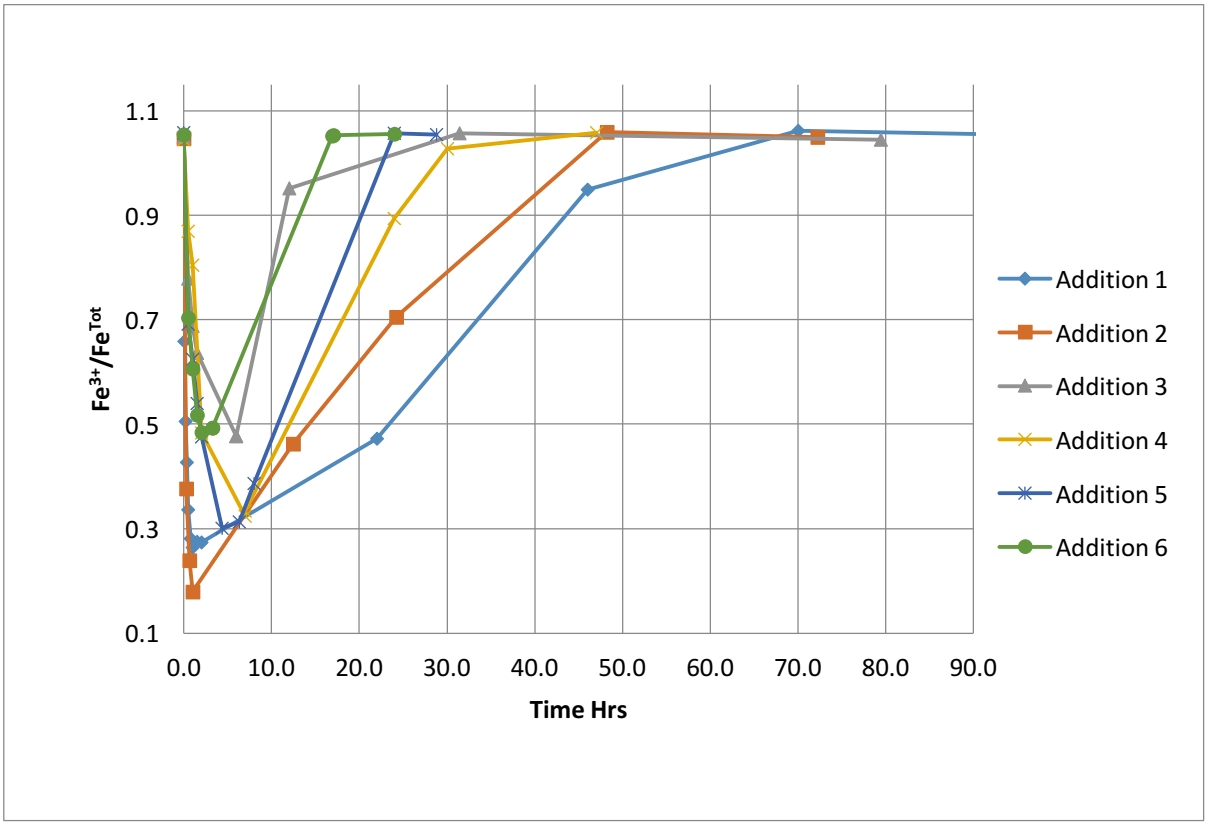

Figure 4–23. Ferric ion to total iron concentration ratio in the ferric ion production phase of the fed-batch addition of copper metal powder experiment to an active bioleach environment for the 4.0 g Cu addition batch run.

4.4.2.4 Comparison of the Ferric Ion Consumption Rate and the Ferric Ion Production Rate

A comparison of the ferric ion consumption and production rates was conducted. The duration of the ferric ion consumption phase was taken at the point of the maximum ferric ion concentration to the minimum ferric ion concentration. The duration of the ferric ion production phase was considered to be from the minimum ferric ion concentration to the maximum ferric ion concentration. The rates of the ferric ion production phase were then compared in Table 4-2.

Table 4-2. Comparison of the ferric ion consumption rate to ferric ion production rate

	Consumption rate (mol $Fe^{3+}.hr^{-1}$)	Production rate (mol $Fe^{3+}.hr^{-1}$)	rate ratio ($\left\lvert \frac{consumption}{production} \right\rvert$)
Addition 1	-0.0640	0.001627	39.3549
Addition 2	-0.0605	0.001866	32.4476
Addition 3	-0.0424	0.002663	15.9325
Addition 4	-0.0374	0.002174	17.1843
Addition 5	-0.0461	0.003331	13.8306
Addition 6	-0.0397	0.003087	12.8752

In all the additions the ferric ion consumption rate was always greater than the ferric ion production rate. However, in the first two additions the ratio of the consumption to the production phase was approximately double the ratio in Additions 4 – 6. This indicates an increase in the ferric ion production rate at increasing additions of copper metal in suspension.

It is noted that the ferric ion consumption rate decreased from additions 1 and 2 to additions 3 – 6. This may be partly attributed to the concomitant ferric regeneration but may also result from a microbial biofilm forming on the metal surface, affecting surface contacting. The possibility of this should be investigated in further studies.

The results supported that of the Yang et al. (2009) study, as it demonstrated that the rate of biooxidation increased with subsequent metal additions, which corresponded to increasing microbial populations. Further, the prolonged duration of the study together the sequential increase in copper metal loading, may have resulted in microbial adaptation to copper ions. Microbial adaptation is expected to increase metal extraction (Brandl et al. 2001) and decrease the lag in microbial growth (Ilyas et al. 2012). Therefore, it was expected that the consumption and generation rates would vary as the ferric ion availability changed with increasing microbial populations and adaptation.

4.4.2.5 Variation in pH on each Addition of Copper

Figure 4–24 shows the variation in pH in the 4.0 g Cu addition batch after each copper addition. On the addition of the elemental copper, there was a high spike in the pH to a range of approximately pH 2.2 - 2.4 for all the additions. The pH values were then corrected by adding concentrated sulphuric acid into the system. The large pH spikes at the beginning occurred within the first 15 hours of the additions, at which point pH adjustments were conducted. In general, when the pH exceeded pH 2.0, adjustments were conducted to lower the pH to approximately 1.5.

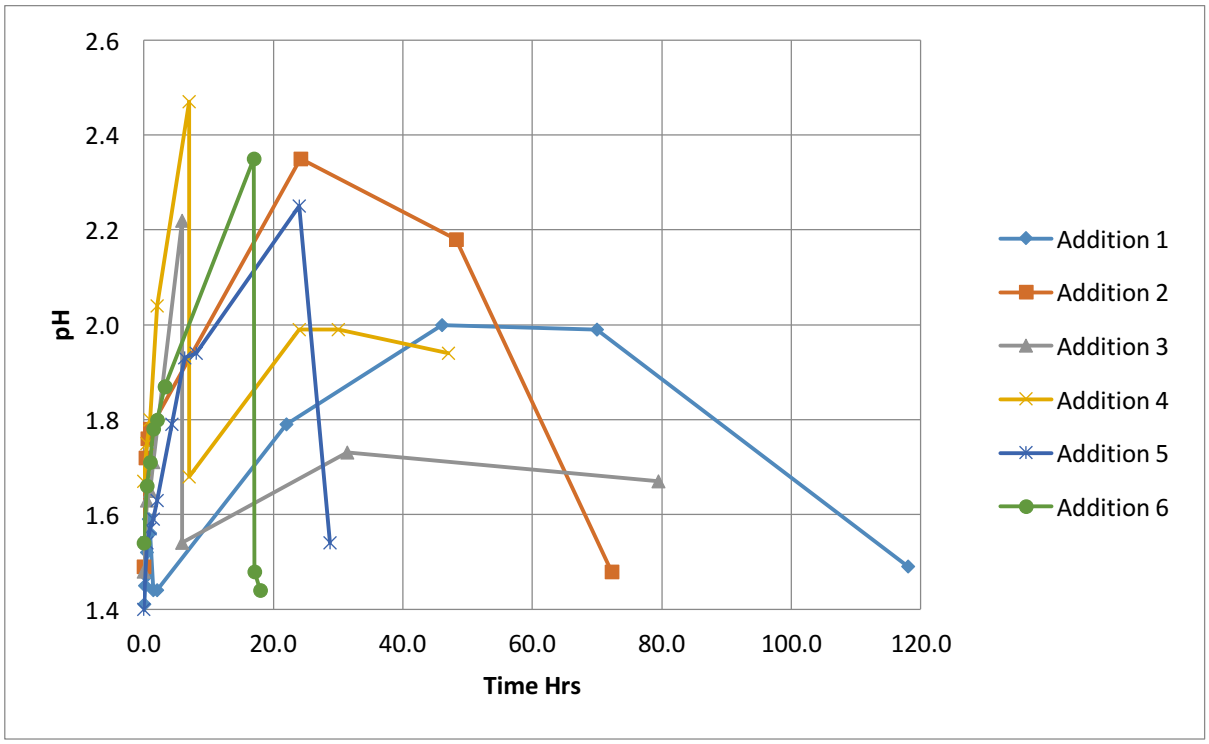

Figure 4–24. Variation of pH after the fed-batch addition of copper metal powder experiment to an active bioleach environment for the 4.0 g Cu addition batch run.

4.4.2.6 Total microorganism count

From Table 4-3, there was a steady increase in the bacterial number after each addition of copper up to Addition 4 in both batches. The bacterial population in the 4.0 g Cu addition batch was greater than in the 2.0 g Cu addition batch following all the additions.

Table 4-3. Bacteria cell count in the fed batch addition of copper experiments.

	2.0 g Cu addition batch (cells/ml)	**4.0 g Cu addition batch (cells/ml)**
Addition 0	7.250E+07	7.250E+07
Addition 1	8.375E+07	1.478E+08
Addition 2	1.275E+08	2.794E+08
Addition 3	2.625E+08	4.172E+08
Addition 4	3.688E+08	5.359E+08
Addition 5	3.25E+08	4.81E+08
Addition 6	3.75E+08	6.19E+08

4.4.3 Mechanisms involved Ferric ion Cycling with Sequential Copper Addition

In order to understand the processes that are occurring on the addition of metallic copper powder, the following equations need to be taken into account (Yang, et al., 2014).

$$2Fe^{3+} + Cu^{0} \rightarrow 2Fe^{2+} + Cu^{2+} \; [Chemical\ ferric\ ion\ consumption] \qquad \textit{Equation 4-10}$$

$$4Fe^{2+} + O_2 + 4H^{+} \rightarrow 4Fe^{3+} + 2H_2O \; [Bacteria\ ferric\ ion\ production] \qquad \textit{Equation 4-11}$$

$$\Delta Fe^{3+}_{observed} = \Delta Fe^{3+}_{production} - \Delta Fe^{3+}_{consumption} \qquad \textit{Equation 4-12}$$

The observed ferric ion concentration in solution is a sum of two reactions, the ferric ion consumption via Equation 4-10 and the ferric ion production by Equation 4-11, thus the observed ferric ion concentration can be described by Equation 4-12.

At time 0 before the initial addition of the copper powder, the iron in the system was in the form of ferric ion. This is confirmed in Figure 4–21 where the normalized ferric ion concentration was 1 i.e. the ferric ion concentration was equal to the total iron concentration, and no ferrous ion was in the system. On addition of the copper powder in each addition, the chemical reduction of ferric ion occurred (Equation 4-10) where the ferric ion was converted to ferrous ion as the oxidation of elemental copper to cupric ions occurred. This explains the initial decrease of the ferric ion concentration observed in Figure 4–22.

The consumption of ferric ion (Equation 4-10) was much faster than the production of ferric ion (Equation 4-11) in all the additions of copper, resulting in a net decrease of the observed ferric ion concentration (Equation 4-12) thus lowering the ferric to total iron ratio observed in Figure 4–22. This indicates that the biological process was the limiting rate in the system using metallic copper in powder form where negligible mass transfer limitations exist.

As the dissolution of copper occurred, freshly generated ferrous ion was available to the microorganisms as a substrate for growth and energy requirements. Hence, the microorganisms continued to grow to higher concentrations after each addition as shown in Table 4-3. The ferrous ion was converted to ferric ion as is shown in Figure 4–23. With each addition, the time to reach the peak ferric ion concentration became shorter owing to the increased microbial concentration.

The increased microbial population increased the ferric ion production rate with each addition as shown in Table 4-2. The increased ferric ion production rate led to a decrease in the ratio of the ferric ion consumption to production rate by more than a factor of 3 i.e. when comparing addition 1 (ratio of 39.3) to addition 6 (ratio of 12.8).

As the time progressed, the ferric ion regeneration cycle became faster for the first 3 additions of copper. This was attributed to the increase of the microbial population as shown in Table 4-3, and associated increase in volumetric ferrous ion oxidation rate as shown in Table 4-2.

On analysis of the pH results in Figure 4–24, the high pH spike initially was attributed to the acid leaching of the base copper metals (Choi, et al., 2004; Yang, et al., 2009). This is similar to the explanation given in Section 4.3.2. The subsequent decrease in pH was due to the addition of concentrated sulphuric acid.

As was mentioned in Section 3.5.4, copper measurements were not conducted in these experiments. The inclusion of copper analyses would enable the de-convultion of the reactions givn in Equations 4.10 and 4.11. However, valuable insight is gained from the iron analyses and omission of copper analyses does not negate the current findings from the data.

5 Simulation Methodology

5.1 Motivation for the Simulation Approach and its Goals

In a bioleaching system of metals from e-waste, the dissolution of metals is achieved by the ferric ion in solution which is converted to ferrous ion in the process. The ferric ion is then regenerated by the microbial oxidation of ferrous ion. The equations governing these two processes, using copper as the model metal, are (Yang, et al., 2014).

$$2Fe^{3+} + Cu^{0} \rightarrow 2Fe^{2+} + Cu^{2+} \; [Chemical\ ferric\ ion\ consumption] \qquad \textit{Equation 5-1}$$

$$4Fe^{2+} + O_2 + 4H^{+} \rightarrow 4Fe^{3+} + 2H_2O \; [Bacteria\ ferric\ ion\ production] \qquad \textit{Equation 5-2}$$

$$\Delta Fe^{3+}_{observed} = \Delta Fe^{3+}_{production} - \Delta Fe^{3+}_{consumption} \qquad \textit{Equation 5-3}$$

The observed ferric ion concentration in solution is a sum of the two reactions, the ferric ion consumption via Equation 5-1 and the ferric ion production by Equation 5-2, thus the observed ferric ion concentration can be described by Equation 5-3.

When both processes described in Equation 5-1 and Equation 5-2 are in direct contact with each other i.e. both exposed to the same iron source, the observed ferric ion concentration in solution (Equation 5-3) is determined by the dominant process. If the metal dissolution process is dominant (Equation 5-1), little ferric ion remains in the system as ferric ion is consumed rapidly; however, if the biooxidation process is dominant (Equation 5-2), the observed ferric ion concentration increases due to a higher ferric ion production rate.

Having a high ferric ion concentration is crucial to the dissolution of metals as the higher the concentration the faster the metals can be mobilized from the e-waste. The dissolution rate of metals such as tin and copper has a dependence on the ferric ion concentration. With this in mind, the objective of this section is to determine key system parameters to maximize the ferric ion production rate in an ideal system where mass transfer limitations are neglected and a maximum ferric ion production rate is assumed.

The metal dissolution kinetics determined in Section 4.2 was used to conduct a sensitivity analysis through a metal leaching simulation to provide an understanding of the system parameters that affect the ferric ion production and consumption rates. The results are used to make recommendations towards future experimental work and on the design of a PCB bioleaching process for optimal metal dissolution rates from e-waste. The system variables that are investigated in a sensitivity analysis were:

1. Varying the biooxidation reactor volume with respect to the e-waste leach reactor (Figure 5–1), which affects the overall cost and recovery of metals from in the process.
2. Varying the initial ferric to ferrous ion ratio, which determines the dominant reaction i.e. ferric ion consumption in the chemical reactor vs ferric ion production in the biooxidation reactor as is seen in the results.
3. Varying the initial metal concentrations i.e. copper, tin and zinc, to account for the varying metal concentrations in printed circuit boards.

5.2 Assumptions for the Simulation

There are many aspects that affect the production and consumption of ferric ion. These include:

- Ferric ion consumption rate is affected by mass transfer limitations posed by the metals in e-waste, effect of e-waste dosage etc.
- Ferric ion production rates are affected by the toxicity of metals to microorganisms, microbial concentration in suspension etc.

In order to investigate the conditions that lead to high metal dissolution efficiencies, several assumptions have been made. This means that the proposed model does not seek to predict the leaching efficiencies of metals accurately, but can be used to investigate and identify key system variables that can increase metal dissolution efficiencies, allowing scenario analysis to propose a preferred operating regime. These assumptions include:

- No inhibition of the microorganisms by the metals in PCBs (or e-waste) and metal ions in solution was taken into account. This assumption is necessary as, although bioleaching of e-waste was demonstrated at high metal concentrations (Section 4.3), the inhibitory effects of the base metals, metal ions and the printed circuit board resin on microorganism are not yet well understood in literature. Thus a series of inhibition experiments will need to be conducted as part of the ongoing research. This was outside the scope of this thesis owing to the complexity of adaptation to metals and the mobility of metal resistance mechanisms, making it a study in its own right.
- There are negligible mass transfer limitations on the system. However as metals are embedded on the PCBs, the mass transfer effects may be significant. It is important to model an ideal system initially in order to understand the ferric ion consumption and production rates prior to modeling a non-ideal system that accounts for these limitations.
- The reactors in the model are assumed to be ideal, perfectly mixed systems. This means the outlet streams from the reactors have the same ion concentrations as in the reactors.

- There is no flow of components around the system i.e. the microorganisms remain in the biooxidation reactor and are not found in the chemical reactor and the base metals remain in the chemical reactor and are not found in the biooxidation reactor. There are, however, flow of metal ions in solution around the system.
- The proton (acid) leaching reaction of metals, described in Equation 2-5, can be neglected as it has been found to have lower contribution to metal dissolution rate as compared with the ferric ion leaching reaction (Yang, et al., 2009).
- The flow rate through the system is constant and the residence time in the biooxidation reactor (τ_{biox}) is managed by modifying the volume of the biooxidation reactor.
- The simulation completes when the dissolution of 95 % of the initial metal has occurred.

5.3 Assumed Reactor Set up for the Simulation

The simulation was used to investigate the system parameters that affect the dissolution behaviour of metals and the ferric ion consumption and production trends. This was accomplished through a sensitivity analysis where the effect of the volume of the biooxidation reactor, initial ferric to ferrous iron ratio, initial copper concentration and presence of mixed metals were simulated. The model developed assumed a two-step biooxidation process which was proposed by Brandl et al (2001),

In the first step, which occurred in the first reactor, the ferric ion oxidized the metal with its concomitant reduction to form ferrous and metal ions, as shown in Equation 5-1. Hence ferric ion was consumed in the process. The reactor in which this reaction took place was called the ***chemical reactor*** and contained the base metal in solid form to be recovered. The particulate base metals were assumed not to flow out of this reactor, but the metal ions in solution did.

The second step was represented by Equation 5-2 and was the ferric ion production step. Here, the ferrous ion formed from Equation 5-1 were converted by microorganisms to ferric iron, as part of their energy generation pathway. The reactor where this process took place was called the ***biooxidation reactor*** and contained the microorganisms. The microorganisms were retained in this reactor, not flowing elsewhere in the process; however, there was a flow of metal ions, including Fe^{2+}, Fe^{3+} and Cu^{2+}, through the reactor.

There was flow of ions between the two reactors, which meant that observed ferric ion concentration in Equation 5-3 was the difference between the ferric ion consumption and production rates in the chemical leaching and biooxidation reactors, respectively. The reactor set-up assumed a closed cyclic system as shown in Figure 5–1.

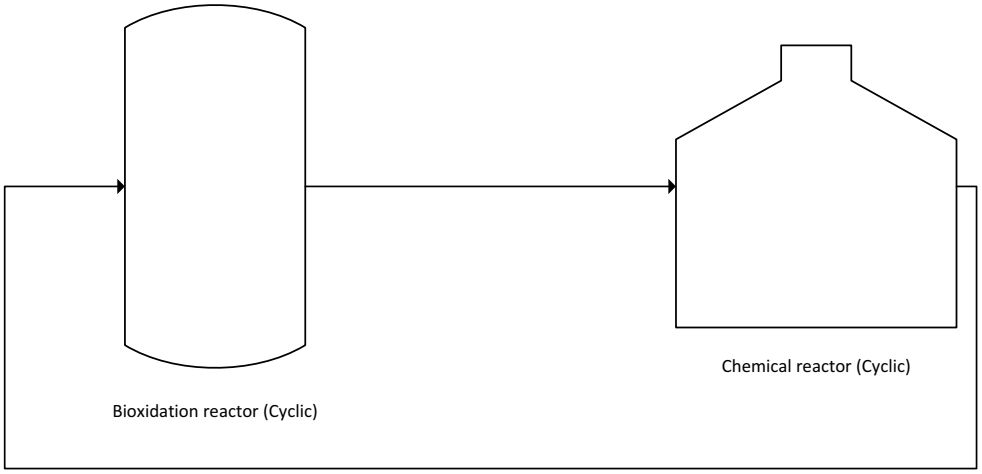

Figure 5–1. Closed cyclic system set-up for the simulation

The closed cyclic system implied that the overall system was a batch process as there was no flow in and out of the system. However, there was flow of ions internally around the reactors. The purpose of the above configuration was to investigate the response of the system on the rate of ferric ion consumption against ferric ion production. The results could be used in future work to determine the most relevant experiments to conduct in understanding a PCB bioleaching system. Further, the simulation can be extended in future work to provide a continuous system with the ongoing recovery of the dissolved copper from solution.

5.4 Equation Derivations for the Reactor Set Up

5.4.1 The Generic CSTR Design Equations

The reaction vessels are assumed to be ideal stirred tank reactors with the following mole balance equation:

$$\frac{VdC_j}{dt} = vC_{j0} - vC_j + Vr_j \qquad \textit{Equation 5-4}$$

Where vC_{j0} represents the flow rate (mol/s) of components j into the system e.g. ferric ion, ferrous ion and metal ions; vC_j represents the flow rates of the same components out of the system. Vr_j represents the rate at which the components are either formed (positive rate) or consumed (negative rate) over the volume of the reactor. This consists of the ferric ion consumption ($-r_{Fe^{3+}}$), ferric ion production ($+r_{Fe^{3+}}$) and metal ion formation through metal dissolution ($+r_{Cu^{2+}}$) in the system. The variable $\frac{VdC_j}{dt}$ in the left hand side of the equation represents the accumulation of components in the reactor. The generic concentration balance equations over the reactors in the system is given by:

$$\frac{V_{chem}dC_{i^{n+}\_chem}}{dt} = v_{chem}C_{i^{n+}in\_chem} - v_{chem}C_{i^{n+}out\_chem} - V_{chem}r_{i^{n+}\_chem} \quad \text{Equation 5-5}$$

$$\frac{V_{biox}dC_{i^{n+}\_biox}}{dt} = v_{biox}C_{i^{n+}in\_biox} - v_{biox}C_{i^{n+}out\_biox} + V_{biox}r_{i^{n+}\_biox} \quad \text{Equation 5-6}$$

5.4.2 Mole Balance Equations of the Chemical Reactor

The dominant reaction that took place in the chemical reactor is the dissolution of the base metals and concomitant consumption of ferric ion through the dissolution of the base metals. The equation governing the dissolution of metals was determined experimentally in Section 4.2 where the following rate laws were found for the three different metals and were shown to have a good data fit.

Table 5-1. Shrinking particle models for the metals of focus.

	Shrinking particle model rate law	Correlation	Standard Error	
Copper	$X = 1 - (1 - 0.00436.C_{Fe^{3+}}^{0.56}.t)^3$	0.948	0.0674	*Equation 5-7*
Tin	$X = 1 - (1 - 0.000593.C_{Fe^{3+}}^{0.269}.t)^3$	0.905	0.0658	*Equation 5-8*
Zinc	$X = 1 - e^{-0.00751t^{0.5}}$	0.927	0.050	*Equation 5-9*

The overall accumulation of metal ions in the reactor is a function of the metal ions coming into the reactor, the metal ions leaving the reactor and the metal ions formed through reaction over the reactor volume. The ferric ions consumed over the reactor volume are linked to the metal dissolution by:

$$2Fe^{3+} + Cu^0 \rightarrow 2Fe^{2+} + Cu^{2+}$$

$$r_{Fe^{3+}} = -\frac{r_{Cu^{2+}}}{2} \quad \text{Equation 5-10}$$

5.4.3 Mole Balance Equations for the Biooxidation Reactor

The dominant reaction that took place in the biooxidation reactor is the production of ferric ion by the oxidative effect of microorganisms on ferrous ions for microbial growth and metabolic activity. There is no metal dissolution in the reactor hence the formation of metal ions ($V_{biox}r_{i^{n+}\_biox}$) in the generic balance Equation 5-6 is zero.

The rate of ferric ion produced in the reactor was taken to be the negative of the rate of ferrous ion consumed. The ferrous ion consumed was determined by the simplified Hansford model (Hansford, 1997):

$$-r_{Fe^{2+}} = \frac{C_x q_{Fe^{2+}}^{max}}{1 + K_{Fe^{2+}} \frac{C_{Fe^{3+}}}{C_{Fe^{2+}}}} = r_{Fe^{3+}}$$ *Equation 5-11*

The microbial rate constant $q_{Fe^{2+}}^{max}$ is the maximum specific ferrous-iron oxidation rate and was assumed to be 23.55 (mol.Fe^{2+}.molC^{-1}.h^{-1}) (Ojumu, et al., 2008). $K_{Fe^{2+}}$ is the apparent affinity constant was assumed to be 0.0024 (Ojumu, et al., 2008). C_x (molC.l^{-1}) represents the biomass concentration. It was calculated using the initial cell count data in Table 4-3 (7.25×10^7 cells/ml). Moon (1996) calculated the number of moles of carbon in each cell to be 4.8×10^{-15} (molC.$cell^{-1}$) for a mixed mesophilic culture dominated by *At. ferroxidans*, *L.ferriphilum* and *At.thiooxidans* or *At.caldus*. Thus the initial biomass concentration was found to be:

$$7.250 \times 10^7 \frac{cells}{ml} * 4.8 * 10^{-15} \frac{mol\ C}{cell} * 1000 \frac{ml}{l} = 0.00348 \frac{mol\ C}{l}$$ *Equation 5-12*

The change in biomass concentration produced over the volume of the reactor was calculated by substituting the rate of microbial growth in Equation 5-13 to the accumulation of microorganisms as represented in Equation 5-4.

$$\mu = \frac{r_x}{c_x} = \frac{\mu_{max}}{1 + K_{Fe^{2+}} \frac{[Fe^{3+}]}{[Fe^{2+}]}}$$ *Equation 5-13*

The value μ_{max} is the maximum specific growth rate and was assumed to be 0.13 h^{-1} (Ojumu, et al., 2008), S is the substrate concentration (mol.l^{-1}) where the substrate was ferrous ion and $K_{Fe^{2+}}$ is the apparent affinity constant and was assumed to be 0.0024 (Ojumu, et al., 2008).

Equation 5-11 was substituted into Equation 5-6 in order determine rate of ferric ion production in the biooxidation reactor.

The ferric ion production and consumption rates are given as volumetric rates, where the rate depends on the volume of the reactor. To convert to molar rate of reaction which takes into account the volume of the reactor, the calculation in Equation 5-14 was conducted.

$$r^*_{Fe^{3+}}(molar) = r_{Fe^{3+}}(volumetric) * V\ (reactor\ volume)$$ *Equation 5-14*

5.4.4 Design Equations of the Combined System

Due to the tightly coupled nature of the cyclic system, the following relationships exist. The first relationship is that between the flow of ions in the chemical reactor and the biooxidation reactor. The flow of ions out of the chemical reactor is equal to the flow of ions into the biooxidation reactor. The flow of ions out of the biooxidation reactor is equal to the flow of ions into the chemical reactor. This is because the overall system is closed and there is no ions entering or leaving the system.

$$v_{chem}C_{i^{n+}in\_chem} = v_{biox}C_{i^{n+}out\_biox}$$
$$v_{chem}C_{i^{n+}out\_chem} = v_{biox}C_{i^{n+}in\_biox}$$ *Equation 5-15*

The second relationship is that the overall accumulation of ions in the system is a sum of the accumulation of ions in each reactor adjusted by the reactor volume as shown in Equation 5-16.

$$\frac{V_{biox}dC_{i^{n+}\_biox}}{dt} + \frac{V_{chem}dC_{i^{n+}\_chem}}{dt} = \frac{V_{tot}dC_{i^{n+}\_tot}}{dt}$$
$$V_{biox} + V_{chem} = V_{tot}$$ *Equation 5-16*

In order to determine the accumulation of metal ions in the system, Equation 5-5 and Equation 5-6 were solved as algebraic simultaneous equations using the relationship given in Equation 5-16, the result is shown in Equation 5-17.

$$\frac{V_{chem}dC_{Cu^{2+}\_chem}}{dt} + \frac{V_{biox}dC_{Cu^{2+}_{biox}}}{dt} = V_{chem}r_{Cu^{2+}\_chem} = \frac{V_{tot}dC_{Cu^{2+}\_tot}}{dt}$$ *Equation 5-17*

This means that the accumulation of cupric (or other base metal) ions in the system is a sum of the accumulation of cupric ions in the biooxidation reactor and chemical reactor which is controlled by the rate of ferric ion formation in the biooxidation reactor.

Applying Equation 5-5 and Equation 5-6 to ferric ion and using the relationship given in Equation 5-16, the ferric ion concentration balance can be written as Equation 5-18.

$$\frac{V_{tot}dC_{Fe^{3+}\_tot}}{dt} = \frac{V_{chem}dC_{Fe^{3+}\_chem}}{dt} + \frac{V_{biox}dC_{Fe^{3+}_{biox}}}{dt}$$
$$= V_{chem}r_{Fe^{3+}_{chem}} + V_{biox}r_{Fe^{3+}\_biox}$$ *Equation 5-18*

This provides a way to compare the ferric ion production rate against the ferric ion consumption rate. Making a division by the volume of the chemical reactor helps to show how changing the reactor volume affects the accumulation of ferric ions in the system.

$$\frac{V_{tot} dC_{Fe^{3+}\_tot}}{V_{chem} dt} = -r_{Fe^{3+}_{chem}} + \frac{V_{biox}}{V_{chem}} r_{Fe^{3+}\_biox} \qquad \textit{Equation 5-19}$$

As was shown in Section 4.4, the production of ferric ions ($r_{Fe^{3+}\_biox}$) is the slow reaction. Equation 5-19 shows that one way to increase the overall concentration of ferric ion produced in the biooxidation reactor is by having a large biooxidation volume. This means that ratio of volumes (V_{biox}/V_{chem}) or alternatively residence times (τ_{biox}/τ_{chem}) acts as a rate multiplier for ferric ion production in the biooxidation process. It is worth noting that the observed ferric ion concentration as described in Equation 5-3 was a simplification of Equation 5-19.

If the rates of reaction are known, the model can be used to compare the ferric ion production and consumption trends in a bioleaching process at varying reactor volumes to optimize the slow process. The model however does not take into account ideal reactor performance such as mass transfer effects of the oxygen and carbon dioxide affecting microbial growth and mass transfer limitations of metal dissolution. Thus it cannot be applied to a real system where these effects will be significant.

The numerical method algorithm and detailed equation derivation is shown in Appendix D.

6 Simulation Results and Discussion

In the chapter, the results of the simulation sensitivity analysis are presented, addressing: varying initial volume of the biooxidation reactor; varying the initial microbial population; varying initial concentration of base metals; varying initial ferric ion and ferrous ion concentrations.

6.1 Comparison of System Equation with Experimental Data

6.1.1 Base Conditions for the Simulation Run

In order to check that the model predicts the trend shown in the fed-batch addition experiment (Section 4.4), a simulation was conducted where virtual copper metal additions were added to the chemical reactor at system conditions shown in Table 6-1. The fed-batch addition leaching experiments, presented in Section 4.4, can be used to approximate an equal volume set up (chemical and biological reactors of equal volume) in the reactor simulation (Equation 5-19).

Table 6-1. Simulation conditions to compare with experimental addition data

Cu concentration	10	g
Total iron concentration	9	$g.l^{-1}$
Fe^{3+}/Fe^{2+}	1000	
Ferric ion	0.161	$moles.l^{-1}$
Ferrous ion	0.000161	$moles.l^{-1}$
Biooxidation reactor Volume	1	litre
Chemical reactor Volume	1	litre
Volumetric flow rate	0.0167	$l.s^{-1}$
Microbial cell count	7.25×10^{7}	cells/ml

6.1.2 Results of the simulated addition of copper

From Figure 6–1, on the virtual addition of copper metal powder there was an initial decrease in the ferric ion concentration, this was then followed by a slower increase of the ferric ion concentration. On the second addition, there was also a fast decrease in the ferric ion concentration, followed by a gradual increase. However the increase of the second addition was faster than the increase in the first addition. This cycle was repeated for all 6 additions with increasingly fast increase in ferric concentration. The time for the consumption and production cycle decreased with each copper addition. The trends of the ferric ion concentration were similar to the fed-batch addition trends shown in

Figure 4–20. These predicted that the consumption rate of ferric ion was faster than the production rate of ferric ion, as shown in

Figure 4–20.

There was an exponential increase in the biomass concentration, shown in Figure 6–1 subplot E. This was similar to the trends seen in Table 4-3. There was a steady accumulation of cupric ions in both reactors due to the addition of the copper metal.

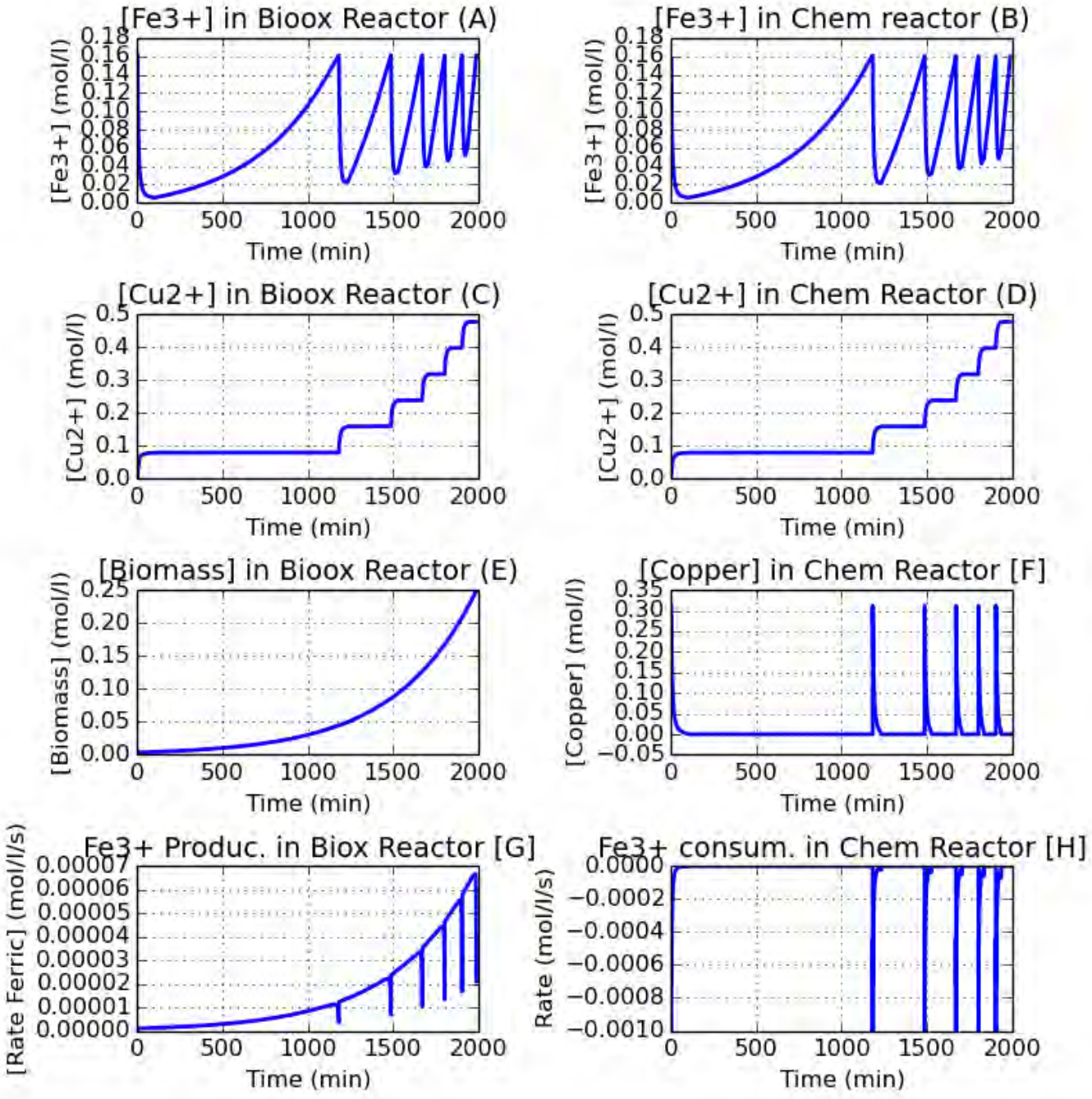

Figure 6–1. Fed batch addition simulation.

However there were notable differences between the simulation run and experimental run. The increase of the microbial population in the simulation was exponential while in the experiment the increase was not exponential. This could be attributed to the fact that the simulation assumed no inhibition of microorganisms. In the experiments, inhibition would occur at high concentration of cupric ion and hence the microbial growth would be affected. A second reason for the deviation was that literature data were used for the maximum microbial growth rate (μ_{max}) and the maximum specific ferrous ion utilisation rate ($q_{Fe^{2+}}^{max}$) rate constants. The experimental constants may have been significantly different from the literature values in that the literature values were assumed for CSTR reactors, while the experiments were conducted in a batch reactor. There may have been mass transfer limitations that affected the rate of oxygen and carbon dioxide uptake. The maximum volumetric concentration of cells supported in a microbial culture was not included in the simulation.

The higher microbial concentration could explain the reason why the cycling of ferric ion increased faster in the simulation as opposed to the experimental run.

6.2 Varying the Biooxidation Volume (Residence Times)

6.2.1 Base Conditions for the Simulation Run

The ferric ion consumption and production trends were investigated at varying biooxidation reactor volume and, as a result, varying residence time. In this simulation run, copper was used as the representative base metal for PCBs. The conditions used during the simulation are shown in Table 6-2.

Table 6-2. Simulation conditions for varying biooxidation reactor volume

Cu concentration	10	g
Total iron concentration	9	$g.l^{-1}$
Fe^{3+}/Fe^{2+}	1000	
Ferric ion	0.161	$moles.l^{-1}$
Ferrous ion	0.000161	$moles.l^{-1}$
Biooxidation reactor Volume	1 – 1000 L	litre
Chemical reactor Volume	1	litre
Volumetric flow rate	0.0167	$l.s^{-1}$
Microbial cell count	7.25×10^{7}	cells/ml

6.2.2 Results of Varying the Biooxidation Volume

From Figure 6–2 subplot A (in which the ferric ion concentration in the biooxidation reactor is predicted over a short time period), the ferric ion concentration in the 1 L biooxidation reactor decreased with time. The initial rate of ferric ion consumption was fast but slowed down as the simulation progressed. It took 33 minutes for the simulation to complete and the final ferric ion concentration was 0.025 $mol.l^{-1}$. The time for the simulation to complete decreased as the

biooxidation reactor volume increased with a higher final ferric ion concentration. At 1000 L biooxidation volume, the final ferric ion concentration was the highest at 0.16 mol.l-1 with no net observed change of the ferric ion concentration for the duration of the simulation. The simulation completed in 15 minutes which was the shortest amount of time in the simulation run.

From Figure 6–2 subplot B (ferric ion concentration in the chemical reactor), at a biooxidation reactor volume of 1 L, the ferric ion concentration in the chemical reactor showed the same trends as the biooxidation reactor with the same final ferric ion concentration of 0.02 $mol.l^{-1}$ at the end of the simulation run. On increasing the volume of the biooxidation reactor, the initial rate of decrease of the ferric ion remained similar to the 1 L volume for the first 2 minutes, however the ferric ion concentration reached a minimum, then increased. The increase in the ferric ion concentration after the minimum was more noticeable as the reactor volume increased, with the 1000 L volume having a final concentration of 0.158 $mol.l^{-1}$.

From Figure 6–2 subplot C (cupric ion concentration in the biooxidation reactor), at biooxidation reactor volumes of 1 L to 12 L, the overall cupric ion concentration in solution accumulated in the biooxidation reactor. However the overall cupric concentration at the end of the simulation decreased as volume increased. The final cupric ion concentration showed no visible net change at a 1000 L biooxidation volume. This may be expected as the cupric ions entering solution are diluted into a much larger volume.

From Figure 6–2 subplot D (cupric ion concentration in the chemical reactor), at a biooxidation reactor volume of 1 L and 3 L, the overall cupric ion concentration in solution accumulated in the chemical reactor. However, at 6 L – 1000 L biooxidation volume, the cupric ion concentration in solution reached a maximum value and then decreased. The greater the volume of the biooxidation reactor, the lower was the overall cupric ion concentration at the end of the simulation i.e. at 1000 L biooxidation reactor volume the final cupric ion concentration was approximately 0.005 $mol.l^{-1}$.

From Figure 6–2 subplot E (biomass concentration in the biooxidation reactor), the biomass concentration increased in the biooxidation reactor. The increase seems to be linear in all the volumes except the 1000 L simulation which does not seem to increase.

From Figure 6–2 subplot E (copper metal concentration in the chemical reactor), the copper mass decreased with time as the simulation progressed The rate of decrease of copper in the 1 L biooxidation volume run was the slowest.

From Figure 6–2 subplot G (ferric ion production rate in the biooxidation reactor), when the volume in the biooxidation reactor was 1 L - 12 L, there was a fast increase of the ferric ion production rate

after which it remained constant at approximately 0.000020 mol $Fe^{3+}.l^{-1}.s^{-1}$. At a volume of 1000 L, there was a fast initial decrease in the ferric ion production rate followed by a slower decrease to a final value of 0 mol $Fe^{3+}.l^{-1}.s^{-1}$.

From Figure 6–2 subplot G (ferric ion production rate in the biooxidation reactor), there was an overall decrease in the ferric ion consumption rate as the simulation progressed reaching a value of 0 mol $Fe^{3+}.l^{-1}.s^{-1}$at the end of the simulation.

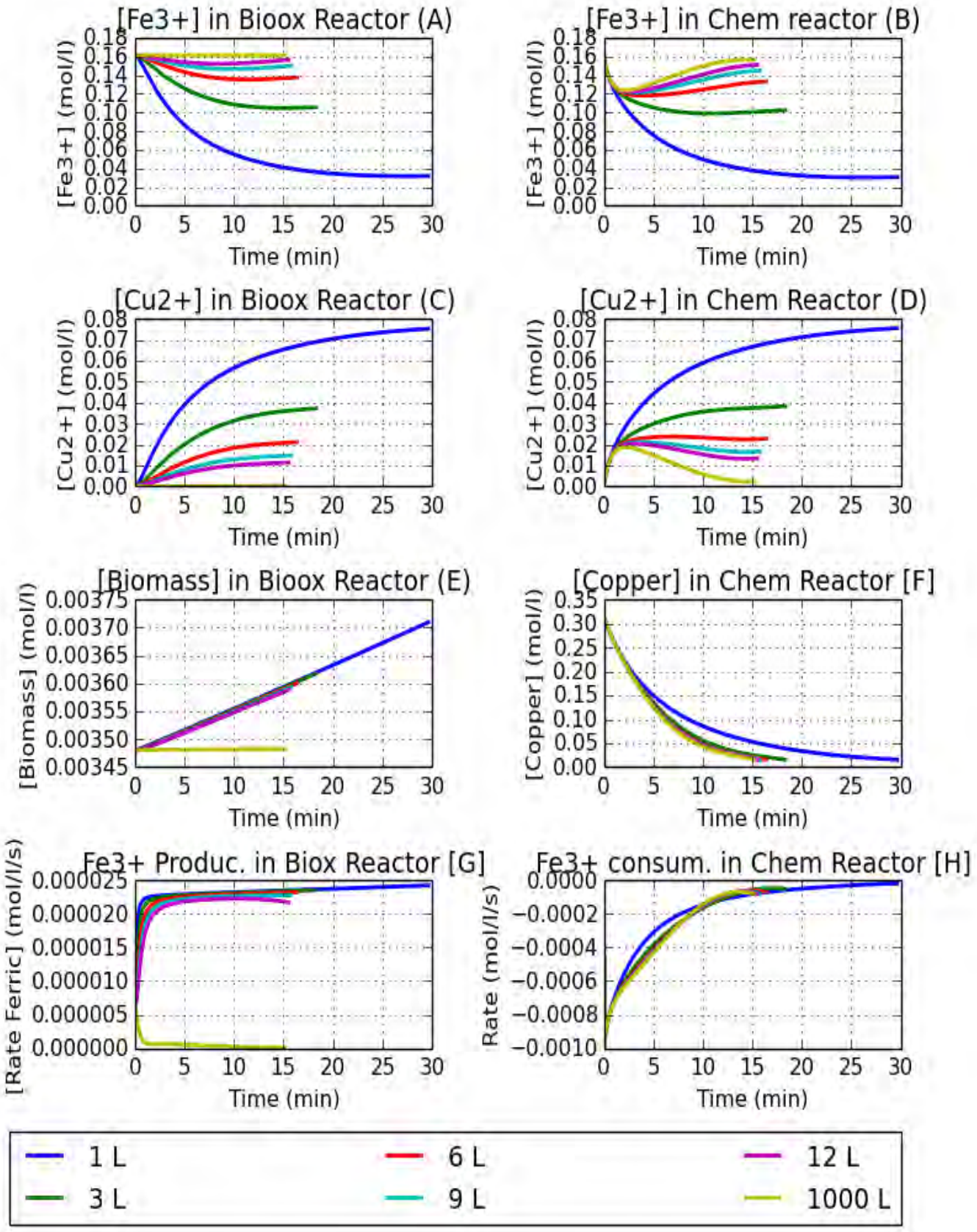

Figure 6–2. Ferric ion, cupric ion, biomass and base copper trends in the biooxidation and chemical reactor at varying biooxidation volume

6.2.3 Discussion of the Simulation Trends on Varying the Biooxidation Volume

The volumetric rate of the ferric ion consumption reaction (Equation 5-1) was shown to be faster (Section 4.4) than the volumetric rate of ferric ion production reaction (Equation 5-2). It was expected that when the volumes of both reactors were equal, the net observed ferric ion concentration would decrease in the reactor because the total ferric ion concentration was a function of the volumetric ferric ion production and consumption rates as presented in Equation 5-19. This trend was similar to the results found in Section 4.4.2.2. This is confirmed by subplots G where the volumetric ferric ion production rate was a lower than the ferric ion consumption rate subplot H i.e. initially the volumetric rates were 0.00001 mol $Fe^{3+}.s^{-1}$ vs -0.0008 mol $Fe^{3+}.s^{-1}$ respectively.

When increasing the volume of the biooxidation reactor, the ratio of volumes V_{biox}/V_{chem} (or residence time (τ_{biox}/τ_{chem}) from Equation 5-19 increased by factors of 1 at 1 L, 3 at 3 L, 6 at 6 L, 9 at 9L, 12 at 12 L and 1000 at 1000 L. Even though the volumetric ferric ion production rate was slower, the larger volumes resulted in a greater molar ferric ion production rate as described in Equation 5-14. This explains a higher net observed ferric ion concentration at the end of the run as described in Equation 5-3 and Equation 5-19.

At high biooxidation volumes (e.g. 1000 L and residence time of 60 000 seconds), the system approached a steady state where there was no change in the ferric ion concentration. When considering the volumetric ferric ion production rate in subplot G, there was an overall decrease in the rate. It is proposed that when considering the volume of the reactor, the molar ferric ion production rate will be higher than the molar ferric ion consumption rate (Equation 5-14) i.e. initially 0.005 mol $Fe^{3+}.s^{-1}$ vs -0.0008 mol $Fe^{3+}.s^{-1}$ respectively. This higher rate means a fast utilisation rate of ferrous ion and as a result a fast production rate of ferric ion. This explained why the observed ferric ion concentration in the biooxidation reactor (Figure 6–2 subplot A) appeared as a zero gradient indicating no net observed change of the concentration. As the ferric ion production rate depends on the ferrous ion utilisation rate Equation 5-11, the high molar ferric ion utilisation rate meant the fast depletion of ferrous ions which caused the ferric ion production rate to decrease due to lack of reactants.

It is proposed that the reason the simulation took shorter periods of time in the higher biooxidation volumes was due to the increased molar ferric ion production rate. This was indicated by the increasing concentrations of the final ferric ion concentration in both reactors as the biooxidation volume increased. This higher ferric ion concentration accelerated metal dissolution.

Initially in the chemical reactor, the sum of the rate at which ferric ion was consumed over the volume of the reactor (Equation 5-1) and was leaving the chemical reactor was greater than the rate at which

ferric ion was entering the reactor. Hence a net decrease in the ferric ion concentration in the chemical reactor was observed from 0 to 2 minutes. As there was less copper metal for dissolution as the simulation progressed, the ferric ion consumption rate slowed down with time as shown in subplot H. The molar rate of generation of ferric iron in the bioreactor and hence its rate of entry remained lower than the molar ferric ion consumption rate, the ferric iron concentration continued to decrease over the time interval considered, as shown in the 1 L and 3 L simulation runs.

However, 2 minutes into the simulation in the 3 L – 1000 L runs, the decreased molar ferric ion consumption rate and increased molar ferric ion production rate resulted in the rate at which ferric ion was entering the chemical reactor was equal to the rate at which ferric ion was consumed over the reactor volume and the rate it was leaving the reactor. This resulted in no net change in the observed ferric ion concentration as indicated by the minima observed (Figure 6–2 subplot B). As the simulation time progressed, the rate of ferric ion consumption decreased further, which meant the rate at which ferric ion was entering the chemical reactor was greater than the rate of ferric ion consumption in the reactor and the rate it was leaving the reactor, resulting in a net observed increase in the ferric ion concentration.

The high initial increase of the cupric ion concentration in the chemical reactor (0 – 2 minutes in Figure 6–2 subplot D) was due to the high initial rates of copper metal dissolution (Figure 6–2 subplot F and G). In the 1 L and 3 L simulation, the overall cupric ion concentration continued to increase. However, when the biooxidation volume was greater or equal to 6 L, the overall cupric ion concentration reached a maxima and decreased. This is explained by the cupric ion formed in the chemical reactor flowing out into the biooxidation reactor (Figure 6–2 subplot C). The residence time of the biooxidation reactor at 1 L and 3 L was 59 and 180 seconds respectively, while the residence time of the 6 L and 1000 L biooxidation volume was 360 and 60 000 seconds respectively. This meant at 1 L and 3 L biooxidation volumes, the cupric ion remained in the biooxidation reactor for a shorter time interval before going back into the chemical reactor. Here the rate of cupric ion production in the reactor from metal dissolution and entering from the biooxidation reactor was greater than the rate it was leaving the chemical reactor. This explained the overall accumulation of cupric ion in the reactor at low volume simulations. However, as the time progressed the copper metal dissolution rate decreased and finally stopped (subplot F), this was because the maximum specified conversion (95 %) of the copper metal had been reached hence the simulation ended.

However at larger biooxidation volumes τ_{biox} was longer e.g. 360 seconds for 6 L and 60 000 seconds for 1000 L. At high cupric ion dissolution rates (0 - 2 minutes), the rate at which cupric ion was accumulating in the chemical reactor (from dissolution of copper metal and re-entering from the

biooxidation reactor) was faster than the rate at which it was leaving the chemical reactor into the biooxidation reactor. However as the ferric ion consumption rate (subplot H) hence the metal dissolution rate slowed down, the rate the cupric ion exited the chemical reactor into the biooxidation reactor matched the rate at which the cupric ion was entering the reactor (from dissolution and flow in), hence no net change in the cupric ion concentration and the maxima were observed at 2 minutes in the chemical reactor. However as the time progressed, the rate at which cupric ion entered the chemical reactor from copper dissolution and flow in was slower than the rate it was transferred into the biooxidation reactor, which explained the net decrease in cupric ion concentration.

It was shown that there was a relationship between the biooxidation volume and final cupric ion concentration, in that the higher the biooxidation volume hence τ_{biox} the lower the final cupric ion concentration. This is because as τ_{biox} increased, the greater the dilution of the cupric ions as indicated by the decreasing concentration of the cupric ions in the biooxidation reactor. Due to the ideal reactor assumption, the concentration of ions flowing out of the biooxidation reactor was equal to the concentration in the reactor, this affected the cupric ion concentration entering the chemical reactor.

6.3 Varying the Microbial Population

6.3.1 Base Conditions for the Simulation Run

This section uses copper as a representative metal and investigates ferric ion production and consumption trends by varying the initial microbial population in the biological reactor, affecting effective microbial population. Table 6-3 contains the base conditions for 4 simulations runs.

Table 6-3. Simulation conditions for varying microbial population

Cu concentration	10	g
Total iron concentration	9	$g.l^{-1}$
Fe^{3+}/Fe^{2+}	1000	
Ferric ion	0.161	$moles.l^{-1}$
Ferrous ion	0.000161	$moles.l^{-1}$
Biooxidation reactor Volume	1	litre
Chemical reactor Volume	1	litre
Volumetric flow rate	0.0167	$l.s^{-1}$
Microbial cell count	$1\times10^{4} – 1\times10^{9}$	$cells.ml^{-1}$

From Figure 6–3, as the microbial population increased, the simulation time decreased proportionally. When the cell number was between 1×10^{4} to 1×10^{7} the ferric ion concentration trends in both reactors and the ferric ion production trends were similar. On increasing the cell number to 1×10^{8} and 1×10^{9}, the rate of decrease of the ferric ion was lower than at the low cell count simulations while the rate of ferric ion production increased. Also the final ferric ion concentration in the system was increased.

However when the cell count was 1×10^{9}, the ferric ion concentration decreased, then reached a minima and then increased. The minima in the biooxidation reactor formed at a higher point (0.12 $mol.l^{-1}$) than the minima in the chemical reactor (0.10 $mol.l^{-1}$). The ferric ion production rate rapidly increased to a maxima then decreased when the cell count was 1×10^{9}. There was an overall accumulation of cupric ions in both reactors. As different orders of magnitude were used in the cell number, the biomass concentration trends (in subplot E) was not informative. The ferric ion consumption trend (subplot H) was the same in all the simulation runs.

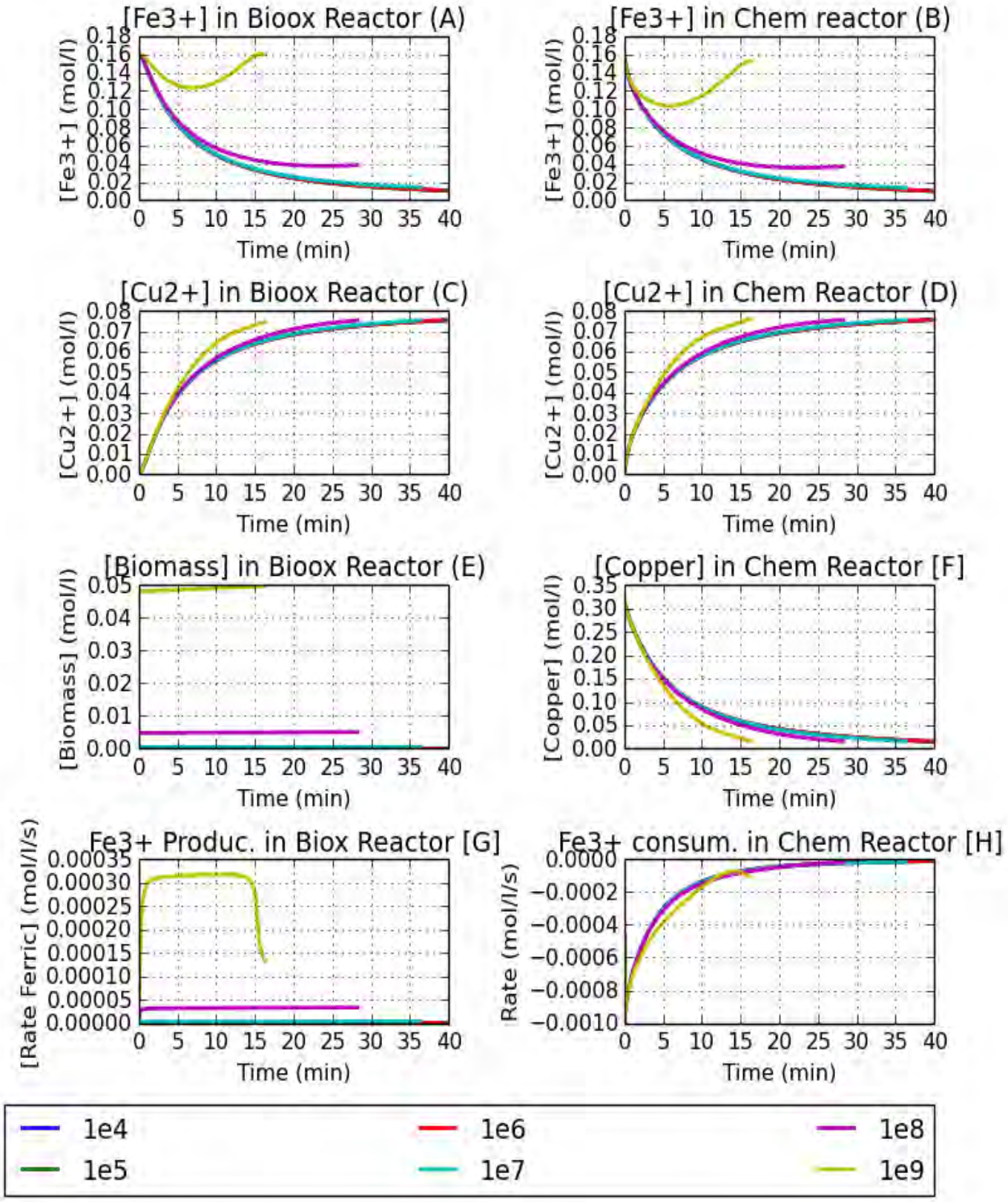

Figure 6–3. Ferric ion, cupric ion, biomass and base copper trends in the biooxidation and chemical reactor at varying initial microbial cell count

6.3.2 Discussion of the Simulation Trends on Varying the Microbial Cell Count

At all microbial concentrations used, there was an initial net decrease of the ferric ion concentration in both reactors. This was because of faster ferric ion consumption rates when compared to ferric ion production rates. When the cell counts were between 1×10^{4} cells.ml^{-1} and 1×10^{7} cells.ml^{-1}, the final concentration remained similar. However on increasing the cell number to 1×10^{8} cells.ml^{-1} and 1×10^{9} cells.ml^{-1}, the final ferric ion concentration was higher. The increase in the ferric ion concentration was attributed to the larger concentration of cells, this resulted in a greater volumetric microbial ferrous iron oxidation rate as this is the product of the specific rate q_{Fe2+} and the biomass concentration. This was indicated by the higher volumetric ferric ion production rate in subplot G. If the microbial population was sufficiently high (1×10^{9} cells.ml^{-1}), the ferric ion production rate became greater and began to dominate the ferric ion consumption rate. This is shown by the minima formed at 7 minutes in both reactors where the volumetric ferric ion production rate of 0.00030 mol $Fe^{3+}.l^{-1}.s^{-1}$ vs consumption rate of -0.00030 mol $Fe^{3+}.l^{-1}.s^{-1}$. At this point both rates were equal hence no net change in the ferric ion concentration occurred. However, as the metal concentration in the chemical reactor decreased (subplot F), the rate of copper dissolution slowed down, hence the ferric ion consumption rate also slowed down. This meant that the ferric ion production rate dominated the ferric ion consumption rate leading to a net increase in ferric ion concentration. However as the metal dissolution process slowed down, there would be less ferrous ion in solution, as a result the ferric ion production rate would also decrease, this explains the decrease in the production rate at 15 minutes in subplot G.

When the cell counts were in the range of 1×10^{4} – 1×10^{7} cells.ml^{-1}, the ferric trends were the same with the final ferric ion concentration of 0.018 mol.l^{-1}. When the cell counts increased further, the final ferric ion concentration increased significantly with a final ferric ion concentration of 0.04 mol.l^{-1} at 1×10^{8} cells.ml^{-1} and 0.16 mol.l^{-1} (in the biooxidation reactor) at 1×10^{9} cells.ml^{-1}. This significant change indicates a transition point in cell number where at which point the ferric ion production rate becomes noticeable. This could explain the fed batch addition results, where in addition 1 and 2, the time to reach maximum rate of production was high (48 and 70 hours). As the microbial population increased, the reach maximum ferric ion concentration decreased significantly and remained constant (< 30 hours).

6.4 Varying Initial Copper Metal Mass

6.4.1 Base Conditions for the Simulation Run

This section used copper as a representative metal and investigated ferric ion consumption and production trends by varying the initial copper mass in the chemical reactor. Table 6-4 contains the base conditions for 4 simulations runs.

Table 6-4. Simulation conditions for varying initial copper mass in the chemical reactor

Cu concentration	2 - 20	g
Total iron concentration	9	$g.l^{-1}$
Fe^{3+}/Fe^{2+}	1000	
Ferric ion	0.161	$moles.l^{-1}$
Ferrous ion	0.000161	$moles.l^{-1}$
Biooxidation reactor Volume	1	litre
Chemical reactor Volume	1	litre
Volumetric flow rate	0.0167	$l.s^{-1}$
Microbial cell count	7.25×10^{7}	$cells.ml^{-1}$

For the 5th simulation run, the volume and as a consequence the residence time of the biooxidation reactor was changed to 10 L (600 seconds residence time). For the 6th simulation run the microbial population was increased by a factor to 7.25×10^{8} $cells.ml^{-1}$ at a biooxidation volume of 1 L. For the 5th and 6th simulation an initial copper mass of 20 g was used.

6.4.2 Results of Varying the Initial Copper Mass in Suspension

Figure 6–4 contains the result of the ferric and cupric ion concentration trends at different initial masses of copper in the chemical reactor with the base conditions given in Table 6-4 as well as super-imposing increased copper (20 g) with increased residence time or increased microbial population.

As the initial copper mass in the system increased, the time it took for the simulation to complete also increased proportionally i.e. at initial mass of 2 g, 10 g and 20 g, the time for completion was 16 minutes, 18 minutes and 33 minutes respectively. Subplot H showed that at high initial metal mass, the rate of consumption of ferric ion was higher than at low masses.

On increasing the biooxidation volume to 10 L and 20 g Cu initial mass in suspension, the time for the simulation to complete decreased from 33 minutes to 16 minutes when compared with the 1 L and 20 g initial Cu. On increasing the microbial population to 7.25×10^{8} $cells.ml^{-1}$, the simulation time decreased from 33 minutes to 18 minutes.

At 1 L biooxidation reactor volume and a microbial population 7.25×10^{7} $cells.ml^{-1}$ simulations, the ferric and cupric ion concentration trends in both reactors were the same. At low initial copper mass,

the final ferric ion concentration in the reactors were higher than at high initial copper mass. At 2 g initial Cu, the final ferric ion concentration was 0.15 mol.l^{-1}, when the initial copper mass was 20 g, the final ferric ion concentration was 0.018 mol.l^{-1} in both reactors. The decrease in the ferric ion concentration was proportional to the initial copper mass. The ferric ion production trends (Subplot G) were the same for the runs, showing a fast increase to a constant of 0.000023 mol $Fe^{3+}.l^{-1}.s^{-1}$.

There was an overall accumulation of cupric ion in both reactors at 1 L biooxidation reactor volume simulations. The final cupric ion concentration was proportional to the initial copper mass in suspension, in that the higher the initial mass, the higher the final cupric ion concentration.

The trends in the ferric and cupric ion concentration were different when the volume of the biooxidation reactor increased to 10 L (600 seconds τ_{biox}) and 20 g initial copper mass in suspension. There was an overall decrease in the ferric ion concentration in the biooxidation reactor to a final concentration of 0.148 mol.l^{-1}. In the chemical reactor, the initial ferric ion concentration rapidly decreased, reached a minimum of 0.12 mol.l^{-1} after 2 minutes and then increased to a final value of 0.14 mol.l^{-1}. For both reactors the final ferric ion concentration was higher than the 5 g and 1 L run which was at 0.138 mol.l^{-1}. There was an overall accumulation of the cupric ion concentration in the biooxidation reactor to a final concentration of 0.014 mol.l^{-1}. However in the chemical reactor, there was an initial accumulation of cupric ion to a maxima of 0.02 mol.l^{-1}, which was followed by a decrease to 0.017 mol.l^{-1}.

On increasing the cell count by a factor of 10 to 7.25×10^{8} cells.ml^{-1}, there was an overall accumulation of cupric ions in both reactors. However, there was an initial decrease of the ferric ion concentration in both reactors which reached a minimum and then increased. The minimum formed in the chemical reactor (0.12 mol.ml-1) was lower than in the biooxidation reactor (0.15 mol.ml^{-1}). The volumetric ferric ion production rate had a steady state which was 10 times higher i.e. 0.00023 mol $Fe^{3+}.l^{-1}.s^{-1}$ when the population was 7.25×10^{8} cells.ml^{-1} vs 0.000023 mol $Fe^{3+}.l^{-1}.s^{-1}$ when it was at 7.25×10^{7} cells.ml^{-1}.

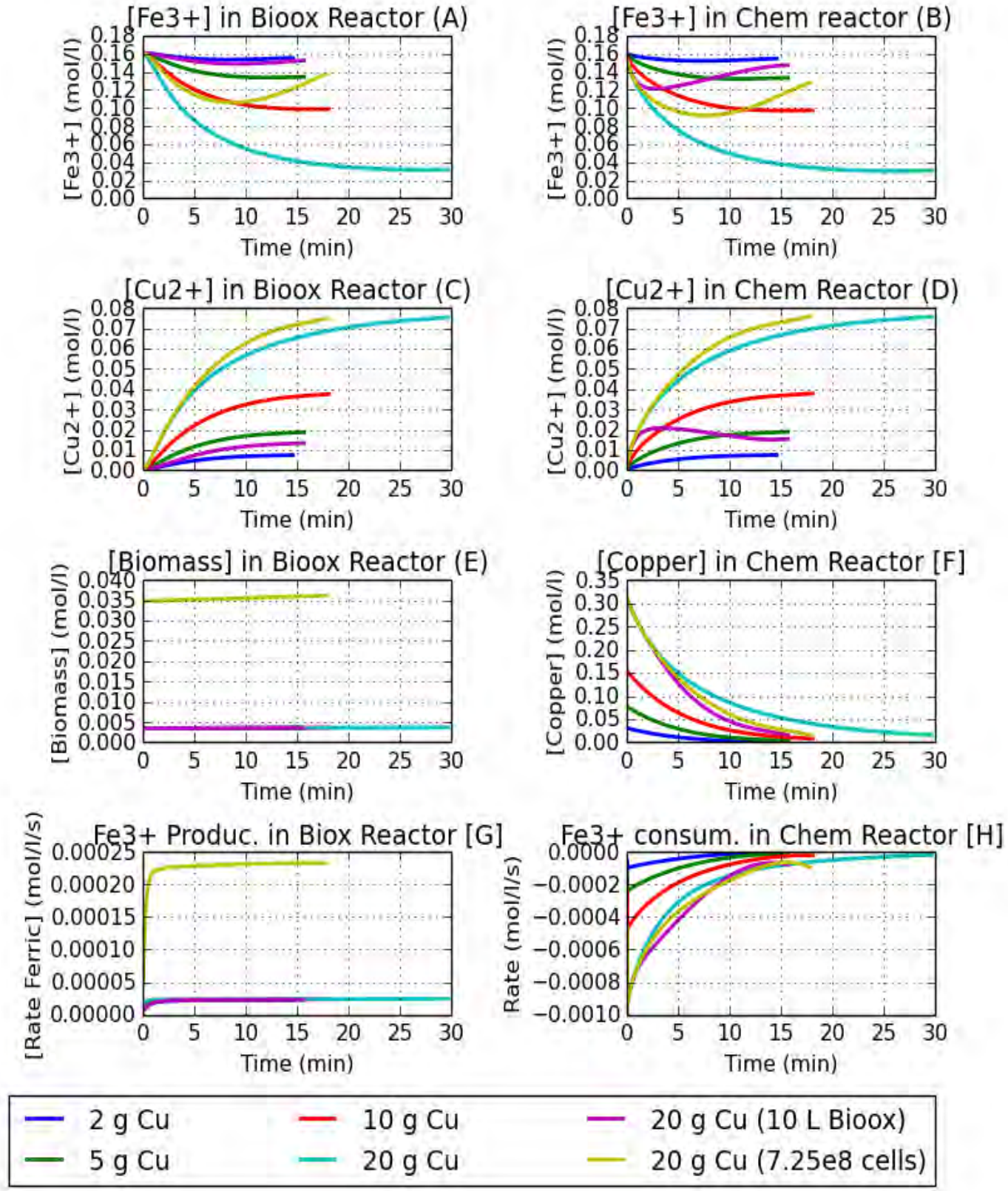

Figure 6–4. Ferric ion, cupric ion, biomass and base copper trends in the biooxidation and chemical reactor at initial copper mass in suspension

6.4.3 Discussion of the Simulation Trends on Varying the Initial Copper Mass in Suspension

The decrease in the ferric ion concentration was due to the consumption of ferric ion in the overall system as governed by Equation 5-1. It was shown empirically in Table 4-2, that ferric ion consumption rate was faster than the ferric ion production rate causing a net decrease of the observed ferric ion concentration.

At a biooxidation volume of 1 L and a cell concentration of 7.25×10^{7} cells.ml^{-1}, as the initial copper mass increased, the final ferric ion concentration became lower. The higher the initial metal mass, the more ferric ion was necessary for the required conversion of the initial copper. The increase of initial copper also led to an increase in time for the required conversion to be achieved as a higher mass required more time for dissolution. The kinetics governing the observed ferric ion concentration is described in Equation 5-19 where the ratio of volumes V_{biox}/V_{chem} at 1 L biooxidation volume was 1.

When the initial copper mass increased, the final cupric ion concentration also increased. This was expected as the higher the initial copper mass, the more copper was available for dissolution hence the higher the cupric ion concentration as described in Equation 5-1. This explains why the ferric ion consumption rate increased with copper mass in Subplot H.

When increasing the volume of the biooxidation reactor to 10 L, the ratio of volumes V_{biox}/V_{chem} (or residence time (τ_{biox}/τ_{chem}) from Equation 5-19 increased by a factor of 10. The volumetric rate of ferric ion production described in Equation 5-19 was adjusted by a factor of 10 to form a molar rate of 0.00023 mol $Fe^{3+}.l^{-1}.s^{-1}$ at steady state. Even though the volumetric ferric ion production rate was lower than the volumetric ferric ion consumption rate 0.000023 mol $Fe^{3+}.l^{-1}.s^{-1}$ vs -0.0004 mol $Fe^{3+}.l^{-1}.s^{-1}$, the higher molar ferric ion production rate 0.00023 mol $Fe^{3+}.l^{-1}.s^{-1}$ counteracted the ferric ion consumption rate resulted in a higher overall ferric ion concentration in the 10 L reactor as opposed to the 1 L simulation.

At 10 L biooxidation volume, the ferric ion concentration in the chemical reactor (Figure 6–4 subplot B) initially decreased (from 0 – 2 minutes). This is because the rate of ferric ion consumption in the chemical reactor (Equation 5-1) and the rate it was leaving the chemical reactor was greater than the rate at which ferric ion was entering the reactor. However, the ferric ion consumption rate slowed down with time (subplot H) as there was less copper metal for dissolution as shown in subplot F. The decreased ferric ion consumption rate resulted in the rate at which ferric ion was entering the chemical reactor matched to the rate at which ferric ion was consumed over the reactor volume and the rate it was leaving the reactor. As such there was no net change in the observed ferric ion concentration as indicated by the minima observed in the ferric ion concentration. As the simulation progressed there was an increase in the ferric ion concentration, which was because as the rate of

ferric ion consumption decreased, the rate at which ferric ion was entering the chemical reactor became greater than the rate at which ferric ion was consumed in the reactor and the rate it was leaving the reactor.

The shorter simulation time at the increased biooxidation volume (10 L) was attributed to the increased ferric ion concentration due to the higher molar ferric ion production rate. This is because the conversion of copper metal is dependent on the ferric ion concentration as indicated in Table 5-1, as the ferric ion concentration increased, the rate of copper conversion should increase.

The increased τ_{biox} (600 seconds) in the 10 L simulation run meant that a greater dilution rate of the cupric ion was observed at 10 L than at the 1 L simulation (60 seconds τ_{biox}). This was confirmed by the decreased concentration of cupric ion in the biooxidation reactor in Figure 6–4 subplot C. As a result, a lower concentration of cupric ion flowed out of the biooxidation reactor at 10 L than at 1 L. At 0 – 2 minutes, the rate at which cupric ion was accumulating in the chemical reactor through production and flow was faster than the rate at which it was leaving the chemical reactor. This was observed as a net increase of the cupric ion concentration in the chemical reactor (Figure 6–4 subplot D). However as the copper dissolution rate slowed down (subplot F and H), the rate the cupric ion was leaving the chemical reactor matched the rate it was produced in the chemical reactor and entered from the biooxidation reactor. As such no net change of the cupric ion concentration was observed explaining the maxima seen at 2 minutes. However as the time progressed, the rate at which cupric ion flowed out of the chemical reactor was faster than the rate at which cupric ion flowed from the biooxidation reactor and was produced in the chemical reactor. Which explained the net decrease in cupric ion concentration was observed.

When the microbial population increased by a factor of 10 to 7.25×10^{8} cells.ml^{-1}, there was an overall accumulation of cupric ion in both reactors. However the ferric ion concentration decreased to a minima then increased. The greater the cell number, the greater the ferrous ion utilization rate (which depends on cell number) as shown in Equation 5-11. The increased ferrous ion utilization rate results in a greater rate of ferric production as shown in subplot G. Initially the ferric ion consumption rate was higher than the ferric ion production rate (-0.0008 mol $Fe^{3+}.l^{-1}.s^{-1}$ vs 0.000023 mol $Fe^{3+}.l^{-1}.s^{-1}$ respectively) which led to a net decrease in the ferric ion concentration. However as the metal dissolution rate slowed down (subplot F), the ferric ion consumption rate also slowed down. This meant the ferric ion production rate matched the consumption rate leading to no net change in the ferric ion concentration which occurred at 7 minutes. The ferric ion concentration increased as the ferric ion production rate began to dominate the ferric ion consumption rate because the metal

dissolution rate slowed down further (at 10 minutes the rates were 0.00023 mol $Fe^{3+}.l^{-1}.s^{-1}$ vs -0.00020 mol $Fe^{3+}.l^{-1}.s^{-1}$ respectively).

The simulation completed at a shorter time (16 minutes) when the biooxidation volume was increased by a factor of 10 than when the initial cell concentration was increased by a factor 10 (18 minutes). This means that at high metal concentrations, changing the volume which affects the molar ferric ion consumption rate has a greater impact on conversion than changing the microbial cell count which affects the volumetric ferric ion consumption rate.

6.5 Varying the Initial Ferric to Ferrous Ion Ratio

6.5.1 Base Conditions for the Simulation Run

This section uses copper as a representative metal and investigated the ferric ion production and consumption trends by varying the initial ferric to ferrous iron ratio. This means that the initial ferric ion and ferrous ion concentration will change. Table 6-5 contains the base conditions for 4 simulations runs.

Table 6-5. Simulation conditions for varying ferric to ferrous iron ratio

Cu concentration	20	g
Total iron concentration	9	$g.l^{-1}$
Fe^{3+}/Fe^{2+}	Changing	
Ferric ion	Changing	$moles.l^{-1}$
Ferrous ion	Changing	$Moles.l^{-1}$
Biooxidation reactor Volume	1	litre
Chemical reactor Volume	1	litre
Volumetric flow rate	0.0167	$l.s^{-1}$
Microbial cell count	7.25×10^{7}	cells/ml

For the 5th simulation run, the volume and as a consequence the residence time of the biooxidation reactor was changed to 10 L (600 seconds residence time). For the 6th simulation run the microbial population was increased by a factor to 7.25×10^{8} $cells.ml^{-1}$.

6.5.2 Results of Varying the Initial Ferric to Ferrous Ion Ratio

Figure 6–5 contains the result of the ferric ion and ion cupric concentration trends at varying initial ferric to ferrous iron ratios at the base conditions given in Table 6-5.

At 1 L biooxidation reactor volume simulations, the ferric and cupric ion concentration trends in both reactors were the same. At lower ratios, the final ferric ion concentration in the reactors were lower than at higher ratios. At 1000, the final ferric ion concentration was 0.03 $mol.l^{-1}$, when the ratio was 0.1, the final ferric ion concentration was < 0.01 $mol.l^{-1}$ in both reactors. The decrease in the ferric ion

concentration was proportional to the initial ratio. The ferric ion concentration in both reactors completely depleted and the ferric ion consumption rate was 0 for the 1 and 0.1 ratios for a portion of the simulation e.g. 10 – 120 minutes at 0.1 ratio and 30 – 80 minutes at a ratio 1. As the initial ferric to ferrous ratio in the system decreased the time it took for the simulation to complete also increased proportionally i.e. at 1000, 10, 1 and 0.1 initial ratio, the time for completion was 30, 35, 100 and 170 minutes respectively.

The accumulation of cupric ion in the reactors at 1 L biooxidation volume occurred in two stages at the simulation run ratio of 1 and 0.1. There was an initial fast rate of accumulation of the cupric ion in solution followed by a slower accumulation. The transition between the fast rate of accumulation and the slower rate was dependent on the initial ferric ion and ferrous ion ratio value i.e. at a ratio of 1, the accumulation occurred at 0.04 $mol.l^{-1}$ cupric ion concentration, while at a ratio of 0.1 the transition occurs at a cupric ion concentration of 0.006 $mol.l^{-1}$.

When the ratio was kept at 0.1 and the volume of the biooxidation reactor is increased to 10 L (600 s τ_{biox}), the simulation completed at a shorter time than when the biooxidation volume was 1 L (60 s τ_{biox}) i.e. 40 minutes vs 170 minutes. The ferric ion concentration in both reactors increased as opposed to an initial decrease in the concentration. However, the final ferric ion concentration in the biooxidation reactor was higher (at 0.042 $mol.l^{-1}$) than in the chemical reactor (at 0.038 $mol.l^{-1}$). The cupric ion at the increased volume was similar in both reactors that there was an overall accumulation of cupric ions.

When the ratio was kept at 0.1 and the initial microbial population was increased by a factor of 10 to 7.25×10^{8} $cells.ml^{-1}$. There was a net increase in the ferric ion concentration. The concentration in the biooxidation reactor was higher (0.0842 $mol.l^{-1}$) than in the chemical reactor 0.07 $mol.l^{-1}$. Both concentrations were higher than when increasing the biooxidation volume. There was a net accumulation of cupric ions in both reactors and the time for the simulation decreased from 170 minutes to 30 minutes. There was a net increase in the ferric ion production rate and it was higher than in the other simulation runs.

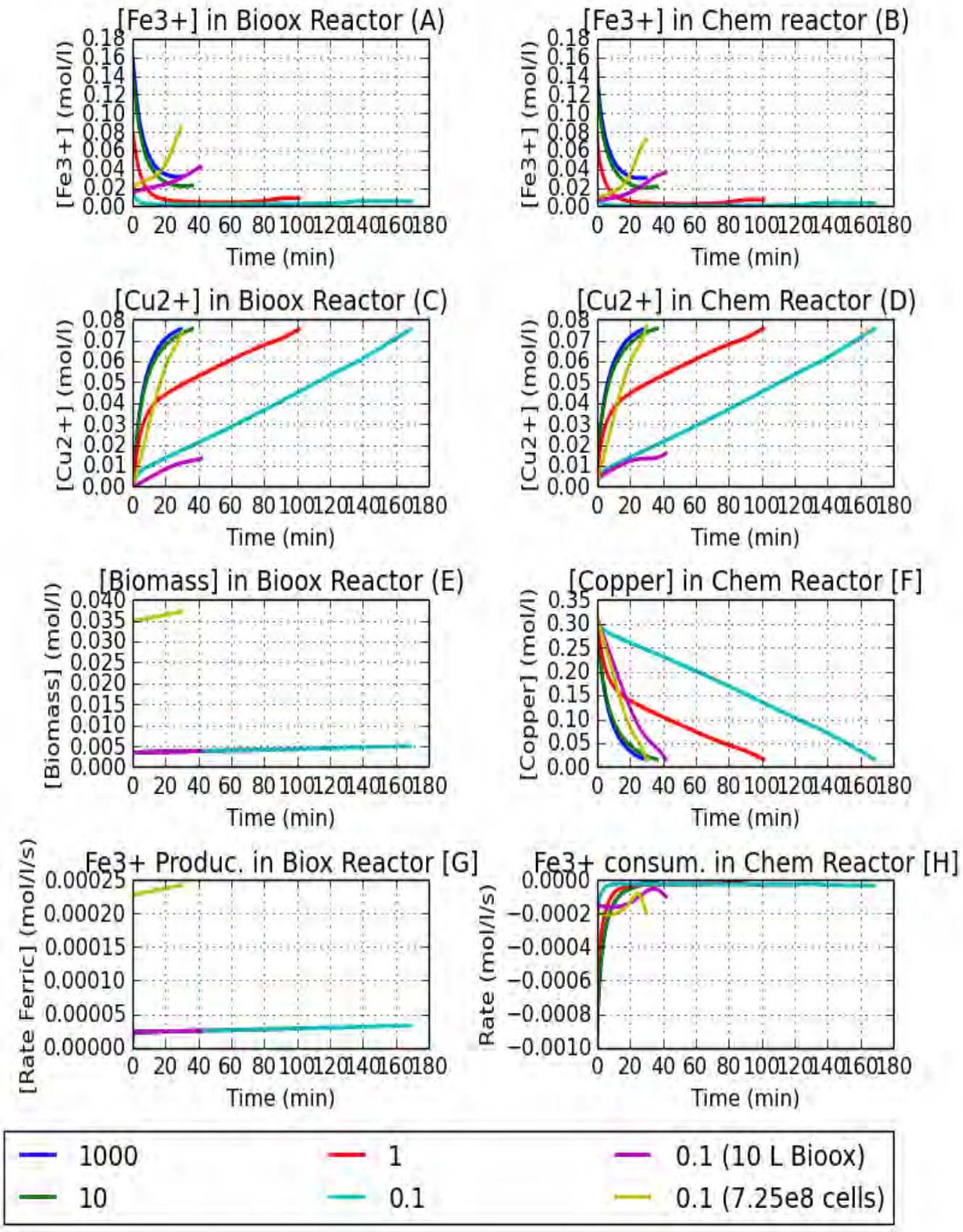

Figure 6–5. Ferric ion, cupric ion, biomass and base copper trends in the biooxidation and chemical reactor at changing ferric to ferrous ion ratio

6.5.3 Discussion of the Simulation Trends on Varying the Ferric to Ferrous ratio

At high ferric to ferrous iron ratios (1000 and 10) and a biooxidation volume of 1 L, there was an overall decrease in the ferric ion concentration in solution. This was because the ferric ion consumption rate was faster than the ferric ion production rate as was shown in Table 4-2.

On lowering the ferric to ferrous iron ratio to 1 and 0.1, there was an initial decrease of the ferric ion concentration, where it was depleted after 10 minutes at a ratio 0.1 and 30 minutes at ratio of 1, the ferric ion consumption rate was 0 at the points where ferric ion was depleted. The initial decrease of the ferric ion concentration was through copper dissolution (Equation 5-1). The ferrous ion was then oxidized by microorganism to ferric ion which continued the dissolution process (Equation 5-2). The ferric ion was consumed faster than it was produced which explains the prolonged depletion of ferric ion in the system. The low ferric ion consumption rates was determined by ferric ion limitations at this point as opposed to copper metal limitation. The low ferric ion concentrations explains the slow accumulation of cupric ion observed in both reactors. The transition stage from fast to slow accumulation of cupric ion can be explained by observing the ferric ion concentration trends. The transition from the fast to slow accumulation phase occurred at the time when the ferric ion concentration had been depleted from the reactor. As such the copper dissolution process was dependent on the biooxidation process for the production of ferric ion. In that in order for the process to continue, more ferric ion needed to be oxidized from ferrous ion through microbial activity.

As the metal dissolution process progressed, the rate of conversion of copper metal decreased (subplot F and H) which meant that the rate of ferric ion production became greater than the rate of ferric ion consumption due to copper metal limitation as opposed to ferric ion concentration limitations. This lead to a net increase in the ferric ion concentration after 80 minutes at a ratio of 1 and 120 minutes at a ratio of 0.1. The difference in time was attributed to that the lower the initial ferric ion in solution, the less reactant there was hence the longer the time needed to generate the required concentration of ferric ion.

On increasing the volume of the biooxidation reactor to 10 L for the 0.1 ratio, the ratio of volumes V_{biox}/V_{chem} (or residence time (τ_{biox}/τ_{chem}) increased by a factor of 10. The volumetric rate of ferric ion production described in Equation 5-11 resulted in a molar rate of ferric ion production according to Equation 5-14. This meant that the molar ferric ion production rate was greater than the molar ferric ion consumption rate, hence a net increase in the observed ferric ion concentration. As the copper dissolution rate was dependent on the ferric ion concentration (Table 5-1), increasing ferric ion concentration meant faster dissolution kinetics, this explains why the simulation lasts 60 minutes at 10 L vs 280 minutes for 1 L.

The ferric ion concentration in Figure 6–5 subplot B showed a small minima at the start of the simulation run i.e. at 2 minutes. Initially the rate of consumption of ferric ion in the chemical reactor was greater than the rate of production of ferric ion and transport to the chemical reactor. This was similar to the trends in Figure 6–2 subplot B, where there was an initial drop in the ferric ion concentration followed by an increase. However, at low ratios the minima forms earlier and lasts for a shorter time as microorganisms had a larger supply of the ferrous ion substrate for biooxidation over a larger τ_{biox}, as such the rate of ferric ion production was faster.

The cupric ion concentration trend at the higher biooxidation reactor volume was different as compared to the other simulation runs where there was an initial increase of the cupric ion concentration followed by a maxima then a decrease. In this simulation the cupric ion concentration slowly accumulated in the reactors without decreasing. This because, due to the lower initial ferric ion concentrations, the initial rate of copper dissolution was low. As the simulation progressed the ferric ion concentration increased which would lead to faster copper dissolution kinetics hence faster accumulation of the cupric ion towards the end of the simulation. This is different from the other simulation runs in that the initial ferric ion concentration was high which resulted in faster copper dissolution kinetics hence faster accumulation of cupric ion at the initial stages of the simulation which slowed down with time.

On increasing the microbial population by a factor of 10 to 7.25×10^{8} cells.ml^{-1}, the time for the simulation to complete decreased from 170 minutes to 30 minutes. As there was more microorganisms in solution the ferrous ion utilization rate increased which increased the ferric ion production rate (subplot G).

As the simulation time was shorter when the microbial population increased (30 minutes) than when the biooxidation volume increased (40 minutes). The impact of increasing the microbial population was greater at low ratios than the impact of increasing the biooxidation reactor volume. This is because there was a large supply of ferrous ions which the microbes could utilize for growth and metabolic activity.

6.6 Mixed metal simulation

For the mixed metal simulation, the metals investigated are copper, zinc and tin. The conditions of the first simulation are given in Table 6-6. For the second simulation the volume of the biooxidation reactor was increased to a volume of 10 L. The simulation ended when 95 % of the metals were converted.

Table 6-6. Simulation conditions for varying initial copper mass in the chemical reactor

Cu mass	5	g
Zn mass	5	g
Sn mass	5	g
Total iron concentration	9	$g.l^{-1}$
Fe^{3+}/Fe^{2+}	1000	
Ferric ion	0.161	$moles.l^{-1}$
Ferrous ion	0.000161	$moles.l^{-1}$
Biooxidation reactor Volume	1	litre
Chemical reactor Volume	1	litre
Volumetric flow rate	0.0167	$l.s^{-1}$

6.6.1 Mixed Metal Simulation at Equal Volume Reactors

6.6.1.1 Metal Ion Concentration in the Chemical Reactor

From Figure 6–6, it is shown that zinc has the highest dissolution rate in that it takes about 10 minutes until no further increase in zinc ions are observed. This is closely followed by copper, tin showing the slowest rate. The final concentration of tin was about half of zinc and copper. Copper finished with an overall higher concentration than zinc. There was an overall accumulation of metal ions in the chemical reactor.

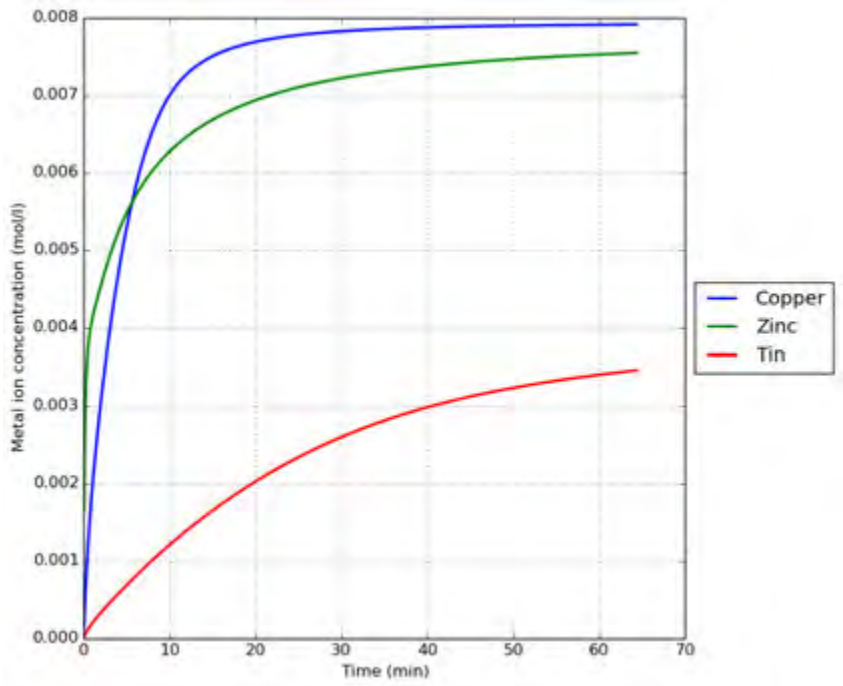

Figure 6–6. Metal Ion Concentration in the Metal Dissolution Reactor in a Mixed Metal System

6.6.1.2 *Discussion of the Metal Ions Concentration Trends at 1 L Biooxidation Volume*

The differences in the final concentration was attributed to the fact that the initial mass of the metals was used instead of moles. Tin has the highest molecular weight followed by zinc then copper has the lowest molecular weight. This is shown in that tin (MR of 188.71) has the lowest final concentration, then followed by zinc (MR 65.38) and then copper (MR 63.55).

The overall accumulation of metal ions in the chemical reactor can be explained by the low residence time (60 seconds) in the biooxidation volume as was discussed in Section 6.2.3.

6.6.2 Mixed Metal Simulation at 10 L Biooxidation Volume

This section gives a brief snapshot at the effect of increasing the biooxidation reactor volume on metal recovery in the mixed metal simulation. The base conditions given in Table 6-2 were used with the exception that the biooxidation reactor volume reactor will be increased to 10 L.

6.6.2.1 *Metal Ion Concentration in the Metal Dissolution Reactor*

Figure 6–7 below contains the results of the metal ion concentration in solution in the metal dissolution reactor. The same initial trends are observed to those in the "equal volume" reactors. However as the simulation progresses the metal ion concentrations in solution reach a maxima then decreased. The maxima reached is highest for the zinc metal, followed by copper and with tin having the lowest maxima.

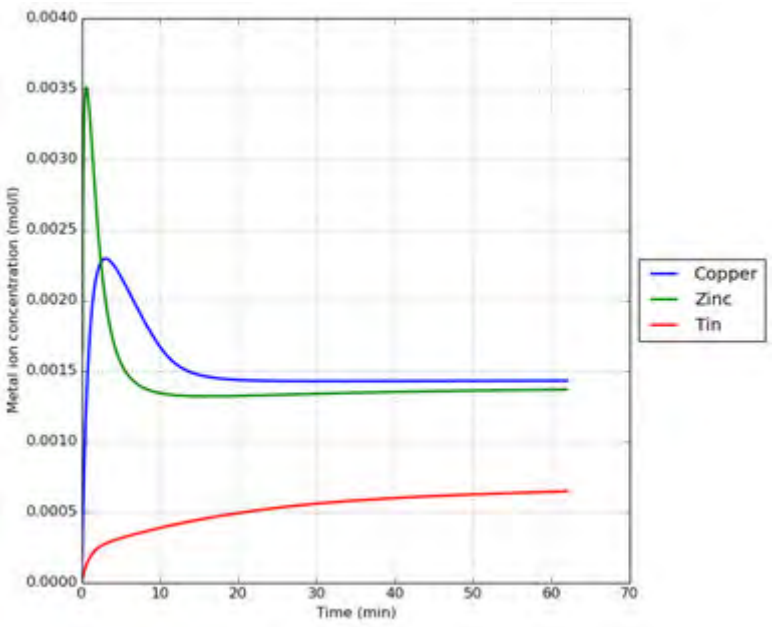

Figure 6–7. Metal Ion Concentration in the Metal Dissolution Reactor in a Mixed Metal System at 10 L biooxidation volume.

6.6.2.2 Discussion of the Metal Ions Concentration Trends at 10 L Biooxidation Volume

On increasing the volume of the biooxidation reactor to 10 L, the ratio of residence time (τ_{biox}/τ_{chem}) increased by a factor of 10 which meant that the overall rate of ferric ion production described in Equation 5-19 was adjusted by a factor of 10. The higher residence time in the biooxidation reactor (600 seconds residence time) meant the metal ions remained in the reactor for a longer time than in the 1 L (60 seconds residence time) simulation. As metal dissolution occurred, the metals with the highest dissolution rates i.e. zinc and copper accumulated faster in the reactor. This high concentration meant that the metal ion concentration flowing out of the reactor was high. As the simulation progressed the metal dissolution rate decreased for zinc and copper to a point where the metal entering the reactor i.e. from dissolution and flow in, was equal to the rate the metal ions were leaving the reactor so no net change in metal ion concentration. This explained the observed maxima in copper and zinc concentrations.

As the simulation progressed further, the dissolution rates of copper and zinc decreased. However due to the high concentration of metal ion still in the chemical reactor, and the ideal reactor assumption where the concentration of the flow out of the reactor is equal to the reactor concentration, there was still a high flow rate of metal ions out of the reactor. This meant the rate of metal ions leaving the reactor was greater than the rates the metal ions were entering the reactor through dissolution and flow. This explained the decrease in the cupric and zinc ion concentration observed.

The overall accumulation of tin in the chemical reactor can be explained by the fact that tin had slow dissolution rates. This meant that initially tin had a lower concentration in solution due to the lower dissolution rates, thus the concentration of tin in the out flow stream was low. Hence the tin ion that was entering the reactor through dissolution and flow from the biooxidation reactor was always higher than the rate it was leaving the reactor, this explains the net accumulation.

7 Conclusion and Recommendations

7.1 Conclusion

WEEE is one of the fastest growing waste streams worldwide containing high concentrations of both toxic and valuable metals. Finding ways to avoid release of the toxic metals into the environment and to recover the valuable metals will help alleviate environmental impact and enhance resource productivity, offering safe disposal and an incentive to recycle.

The purpose of this study was to develop a sound understanding of the application of bioleaching of base metals from their element form in WEEE using a ferric:ferrous iron system with microbial regeneration of the ferric leach agent. Of particular importance for both system design and optimisation of its operational performance is the need to compare the ferric ion production and consumption trends in order to determine the rate-limiting stage within the two sub-processes. This understanding was sought through a combination of experimental studies and simulation through mathematical modelling to address the following hypothesis:

The relative ferric ion production and consumption rates form a key consideration for the optimisation of the bioleaching of base metals found in PCBs. In the absence of mass transfer limitations, the microbial production of ferric iron is rate limiting for bioleaching of copper metal. This limitation can be alleviated by enhancing microbial concentration and activity in the leach process.

Several simplifying assumptions were made. These include:

- Finely divided metal powder was used to reduce mass transfer effects as it was not possible to carry out the fine crushing of PCBs.;
- Microbial inhibition by metals and metal ions in solution was not taken into account.

The first set of key questions considered the relative ferric ion production and consumption rates empirically and the dissolution of metals that occurred through ferric-mediated bioleaching. These focussed on determining key metals leached and the rate of ferric consumption and regeneration. This was followed by determining the leach rates of three metals: copper, zinc and tin. These rate data were used to populate model equations. The latter were used in the sensitivity analysis to determine the system parameters that would result in greater dissolution efficiency of metal, thus addressing the second set of key questions.

The metals that were leached from PCBs by ferric leaching to give the highest mass in solution per mass PCB were copper, tin, lead and zinc where the mass fraction leached was in the range of 20 – 45 mg of each metal per g PCB in Sample A and 6 – 120 mg of each metal per g PCB in Sample B. However

as lead is toxic and is being discontinued as a key component of PCBs, it was not considered for this study. It is recognised that its presence may impact the efficiency of the microbial system; however, a decision was taken to characterise the system in the absence of this inhibition in this study, allowing potential of the approach to be assessed. Copper formed the metal of focus for the microbial leaching experiment as it is most abundant in PCBs, had a high leaching efficiency and has been a source of focus in literature. Further removal of copper (through recovery) is of importance for the subsequent recovery of gold.

When copper leaching was conducted during inoculation and at concentrations 0, 0.2, 0.5 and 1.0 g Cu per 100 ml solution, the initial concentration of ferric ion was low, thus the ferric ion consumption process was limited and dependent on the ferric ion production process. The rate of ferric ion production however depended on the microbial population, which was also low. As a result it was difficult to determine the dominant rate between the ferric ion consumption rate and the ferric ion production rate due to the dependency observed.

In order to determine the dominant rate between the ferric ion production rate and the ferric ion consumption rate at optimal conditions, copper leaching was conducted by the fed batch addition of the copper metal to a solution of ferrous sulphate at peak microbial population. It was found that, for all sequential additions, the ferric ion consumption rate was faster than the ferric ion production rate where the ratio of the ferric ion production rate to consumption was greater than 10. However as more additions were made, the ferric ion production rate increased from 0.0016 mol $Fe^{3+}.hr^{-1}$ in addition 1 to 0.0031 mol $Fe^{3+}.hr^{-1}$ in addition 6. The increased rate of ferric ion production meant that the ratio of ferric ion consumption to production rate decreased from 39 to 13 respectively. The increase in the ferric ion production rate was attributed to an increase in the microbial population from 7.366×10^{7} in addition 1 to 6.29×10^{8} cells.ml^{-1} in addition 6. As such a possible way to increase the ferric ion production rate which impacts the iron cycle is to increase the microbial population. In this experiment, the microbial population was increased by the indirect supply of ferrous ion which was achieved through the addition of copper metal powder. This is because the copper metal powder reacted with ferric ion to form ferrous ion, the ferrous ion was then used for microbial growth and metabolic activity thus producing ferric ion in the process. However in a practical leaching environment, a potential way to increase the microbial population present could be increasing mass transfer rates by having high stirring speeds, increasing the ferrous ion production reaction by having higher metal mass in solution etc. As metal powder was used, mass transfer limitations were kept at a minimum. However, when PCBs are considered, mass transfer limitations may be significant resulting in lower ferric ion consumption rates. If the ferric ion consumption rate becomes slower than

the ferric ion production rate, an important consideration is that at what conditions will the rates be equal i.e. at what particle size or stirring speeds will mass transfer effects be significant.

In the final experiment, the relative dissolution rates of copper, zinc and tin were measured and kinetic data collected. It was found that zinc had the fastest dissolution kinetics, followed by copper, then tin. The shrinking particle model could be used to simulate the dissolution of copper and tin adequately with correlation coefficients of 0.948 and 0.905 respectively. The following model equations resulted:

	Shrinking particle model rate law	Correlation	Standard Error
Copper	$X = 1 - (1 - 0.00436.C_{Fe^{3+}}^{0.56}.t)^3$	0.948	0.0674
Tin	$X = 1 - (1 - 0.000593.C_{Fe^{3+}}^{0.269}.t)^3$	0.905	0.0658

However, the shrinking particle model did not describe zinc dissolution. A logarithmic model showed a good fit for the zinc data with a correlation coefficient of 0.927.

	Logarithmic model rate law	Correlation	Standard Error
Zinc	$X = 1 - e^{-0.00751t^{0.5}}$	0.927	0.050

While dissolution of copper and tin depend on the ferric ion concentration, zinc dissolution did not. Thus it was concluded for high rate of dissolution of copper and tin to be achieved, a high ferric ion concentration was necessary.

The simulation approach was conducted by modelling the ferric ion production and consumption reactions in two reactors where the contact between the two processes was through the flow of ions in solution. The model provided a reasonable representation of the experimental data. This simulation model was used to explore scenarios to determine the impact of a range of design considerations and operating variables. Through this analysis, it was proposed that the factors that increased the dissolution rate of copper include the relative volume of the biooxidation reactor and, as a result, residence time in the biooxidation reactor, and the microbial cell population. These two components had a direct impact on the ferric ion production rate which was found to be the rate limiting sub-process. Increasing the volume of the biooxidation reactor and hence the residence time, increased the molar rate ($mol.s^{-1}$) of ferric ion production as the molar rate is a function of the volume of the reactor. Increasing the microbial population affected the rate of ferrous ion utilisation and associated

ferric iron production as it was catalysed by a larger biomass concentration. The volumetric ferrous iron oxidation rate (mol.L^{-1}.s^{-1}) is the product of specific rate and biomass concentration.

The study has shown that for ideal conditions, the ferric ion consumption rate is greater than the ferric ion production rate at equal volumes of the biooxidation and chemical process and high ferric ion concentrations. The sensitivity analysis has shown that the ferric ion production rate can be increased by adjusting the volume of the biooxidation reactor and the microbial population available. This knowledge is useful as provides a guideline for future work towards the recovery of metals through bioleaching, suggesting key system parameters on which to focus for maximum metal dissolution.

7.2 Recommendations

The study conducted has provided key insights into the bioleaching of base metals from PCBs using a ferric:ferrous iron system. In furthering this work, it is recommended that the simplifying assumptions made in this study are investigated to identify which simplifying assumptions point toward the requirement for additional research. This will provide a more accurate simulation of the metal recovery process from printed circuit boards.

For the duration of the experiments and simulation, the system was designed to ensure that mass transfer effects were low and so could be neglected. However, in practice, mass transfer effects cannot be neglected. It is recommended that future work studying the effects of mass transfer on the rate of ferric ion consumption and production be conducted. This will determine the conditions under which the ferric ion consumption remains the dominant rate. If ferric ion consumption remains the dominant rate, an implication is that crushing may not be required to reduce the particle size of the e-waste. The impact of this on the extent of metal recovery would require investigation.

It was assumed that inhibition of microorganisms by metal ions would not be significant. However it is well known from the literature on mineral bioleaching that inhibition of microorganisms varies with the metals in solution and that adaptation to metal concentrations can take place. The nature of the PCBs, their plastic components as well as prior exposure to metals is thus expected to influence inhibition of the microbial phase. However metal tolerance in microbial species can be both developed through adaptation and lost as typically plasmid borne. The intercalation of experimental understanding of metal inhibition and resistance with kinetics for inhibition should form a topic of further study. It is recommended that future work should focus on these for metal ions released from PCBs into solution (including minor metals), metal on PCBs and compounds released from the resin on the PCB boards.

As the simulation needs to be validated rigorously, it is recommended that reactor experiments should be conducted where the initial conditions as described in the simulation can be varied based on ideal conditions and practical conditions in order to give a good understanding of recovery rate and efficiency of metals. This includes repeating the fed batch experiments to calibrate the model and validating the model predictions at optimum reactor conditions. In addition, the assumption of spherical geometry used to model metal powder leaching should be varied to account for more planar geometries that better describe metals on PCBs. The experiments should include both the leaching of finely divided metal powders and the leaching of metals from PCBs. The effect of redox interactions should also be considered when metals of different redox potentials are in intimate contact with each other as suggested by Watling (2006).

8 References

Öko-Institut & Fraunhofer, I., 2003. *DIRECTIVE 2002/95/EC OF THE EUROPEAN PARLIAMENT AND OF THE COUNCIL,* Not Specified: Official Journal of the European Union.

Anders, B. & Colin, W., 1995. Ferric sulphate oxidation using Thiobacillus ferrooxidans: a review. *Process Biochem,* Volume 30, pp. 225 - 236.

Brandl, H., Bosshard, R. & Wegmann, M., 2001. Computer-munching microbes: metal leaching from electronic scrap by bacteria and fungi. *Hydrometallurgy,* 59(2), pp. 319-326.

Breed, A. & Hansford, G., 1999. Modelling Continous Bioleach Reactors. *Biotechnology and Bioengineering,* 64(6), pp. 671 - 677.

Brierley, C., 2008. How will biomining be applied in future?. *Transactions of nonferrous metals society of China,* 18(6), pp. 1302-1310.

Brierley, C. L., 1997. Mining biotechnology: research to commercial development and beyond. In: *Biomining.* s.l.:Springer, pp. 3-17.

Choi, M.-S., Cho, K.-S., Kim, D.-S. & Kim, D.-J., 2004. Microbial recovery of copper from printed circuit boards of waste computer by Acidithiobacillus ferrooxidans. *Journal of Environmental Science and Health, Part A,* 39(11-12), pp. 2973-2982.

Crundwell, F., 1994. Mathematical modelling of batch and continuous bacterial leaching. *The Chemical Engineering Journal and the Biochemical Engineering Journal,* 54(3), pp. 207-220.

Crundwell, F., 2003. How do bacteria interact with minerals?. *Hydrometallurgy,* 71(1), pp. 75 - 81.

Cui, J. & Zhang, L., 2008. Metallurgical recovery of metals from electronic waste: A review. *Journal of hazardous materials,* 158(2), pp. 228-256.

Das, A., Modak, J. & Natarajan, K., 1997. Studies on multi-metal ion tolerance of Thiobacillus ferrooxidans.. *Minerals Engineering,* July, 10(7), pp. 743-749.

Demir, H. et al., 2004. Determination of a semi empirical kinetic model for dissolution of metallic copper particles in HNO3 solutions. *Chemical Engineering and Processing: Process Intensification,* 43(8), pp. 1095-1100.

Dew, D. & Miller, D., 1997. *The BioNIC process, bioleaching of mineral sulphide concentrates for the recovery of nickel.* s.l., s.n., pp. 1-1.

Drechse, C., 2006. Mechanical Processes for Recycling Waste Electric and Electronic Equipment with the Roter shredder and Rotor Impact Mill. *Aufbereitungsn Technik,* p. 47.

Ehrlich, H., 2004. Beginnings of rational bioleaching and highlights in the development of biohydrometallurgy: A brief history. *European Journal of Mineral Processing and Environmental Protection,* 4(2), pp. 102-112.

Govender, E., Harrison, S. & Bryan, C., 2012. Modification of the ferric chloride assay for the spectrophotometric determination of ferric and total iron in acidic solutions containing high concentrations of copper. *Minerals Engineering,* Volume 35, pp. 46-48.

Hansford, G. S., 1997. Recent developments in modelling the kinetics of bioleaching. *Biomining: Theory, Microbes and Industrial Processes,* pp. 153-176.

Huang, J. et al., 2014. Leaching behavior of copper from waste printed circuit boards with Brønsted acidic ionic liquid.. *Waste management,* 34(2), pp. 483-488.

Huang, J. et al., 2014. Leaching behaviour of copper from waste printed circuit boards with Bronsted acidic ionic liquid. *Waste Management,* Volume 34, pp. 483-488.

Huang, K., Guo, J. & Xu, Z., 2009. Recycling of waste printed circuit boards: A review of current technologies and treatment status in China. *Journal of Hazardous Materials,* 164(2), pp. 399-408.

Ilyas, S., Anwar, M. A., Niaza, S. B. & Ghauri, M. A., 2007. Bioleaching of metals from electronic scrap by moderately thermophilic acidophilic bacteria. *Hydrometallurgy,* Volume 88, pp. 180 - 188.

Jensen, A. B. & Webb, C., 1995. Ferrous sulphate oxidation using Thiobacillus ferrooxidans: a review. *Process Biochemistry,* 30(3), pp. 225-236.

Kandil, S., 2013. *World E-Waste Map Reveals National Volumes, International Flows..* [Online] Available at: https://www.ehs.unu.edu/palm/file/get/11505 [Accessed 5 11 2014].

Karwowska, E. et al., 2014. Bioleaching of metals from printed circuit boards supported with surfactant-producing bacteria. *Journal of hazardous materials,* Volume 264, pp. 2013-2101.

Kim, E.-y.et al., 2011. Leaching kinetics of copper from waste printed circuit boards by electro-generated chlorine in HCl solution.. *Hydrometallurgy,* 107(3), pp. 124-132.

LaDou, J., 2006. Printed circuit board industry. *International journal of hygiene and environmental health,* 209(3), pp. 211-219.

Levenspiel, O., 1999. Chemical reaction engineering. In: J. W. &. Sons, ed. *Chemical reaction engineering.* New York: John Wiley & Sons, pp. 566 - 585.

Liang, G., Mo, Y. & Zhou, Q., 2010. Novel strategies of bioleaching metals from printed circuit boards (PCBs) in mixed cultivation of two acidophiles.. *Enzyme and Microbial Technology,* 47(7), pp. 322-326.

Luda, M. P., 2011. Recycling of Printed Circuit Boards. *Integrated Waste Management,* 2(3), pp. 285-298.

May, N., Ralph, D. & Hansford, G., 1997. Dynamic redox potential measurement for determining the ferric leach kinetics of pyrite. *Minerals engineering,* 10(11), pp. 1279-1290.

Mingjiang Zhan, R. P., 2013. Design and evaluation of bio-based composites for printed circuit board application. *Composites,* pp. 22-30.

Mishra, D. et al., 2008. Bioleaching of metals from spent lithium ion secondary batteries using< i> Acidithiobacillus ferrooxidans</i>. *Waste management,* 28(2), pp. 333-338.

Morin, D. et al., 2008. Progress after three years of BioMinE - Research and technological development project for a global assessment of biohydrometallurgical prospects applied to European non-ferrous metal resources. *Hydrometallurgy,* 94(1-4), pp. 58-68.

Musson, S. E. et al., 2006. RCRA toxicity characterization of discarded electronic devices. *Environmental science & technology,* 40(8), pp. 2721-2726.

Ojumu, T., Petersen, J., Searby, G. & Hansford, G., 2006. A review of rate equations proposed for microbial ferrous-iron oxidation with a view to application to heap bioleaching. *Hydrometallurgy,* 1(83), pp. 21 - 28.

Ojumu, T. V., Petersen, J. & Hansford, G. S., 2008. The effect of dissolved cations on microbial ferrous-iron oxidation by Leptospirillum ferriphilum in continuous culture. *Hydrometallurgy,* 94(1-4), pp. 69-76.

Ozkaya, B. et al., 2007. Iron oxidation and precipitation in a simulated heap leaching solution in a Leptospirillum ferriphilum dominated biofilm reactor. *Hydrometallurgy,* 88(1), pp. 67-74.

Pant, D., Deepika, J., Manoj K, U. & Kotnala, R. K., 2011. Chemical and biological extraction of metals present in E waste: A hybrid technology. *Waste Management.*

Petranikova, M., 2008. *Treatment of End of Life computers, Diploma Work.,* Kosice, Slovakia: Technical Univeristy of Kosice.

Rawlings, D. E., 2002. Heavy metal mining using microbes 1. *Annual Reviews in Microbiology,* 56(1), pp. 65-91.

Reuter, M. et al., 2013. *Metal Recycling: Opportunities, Limits, Infrastructure, a Report of the Working Group on Global Metals Flows to the International Resource Panel,* Paris: International Resources Panel.

Rossi, G., 1990. *Biohydrometallurgy.* s.l.:McGraw-Hill.

Sadia, I., Jae-chun, L. & Ru-an, C., 2012. Bioleaching of metals from electronic scrap and its potential for commercial exploitation. *Hydrometallurgy.*

Salhofer, S. & Tesar, M., 2011. Assessment of removal of components containing hazardous substances from small WEEE in Austria. *Journal of hazardous materials,* 186(2), pp. 1481-1488.

Silverman, M. P. & Ehrlich, H. L., 1964. Microbial formation and degradation of minerals. *Adv. Appl. Microbiol,* Volume 6, pp. 153-206.

Sohaili, J., Muniyandi, S. K. & Mohamad, S. S., 2012. A Review on Printed Circuit Boards Waste Recycling Technologies and Reuse of Recovered Nonmetallic Materials. *International Journal of Scientific & Engineering Research, Volume 3, Issue 2,* pp. 1-5.

Sundkvist, J.-E., Gahan, C. S. & Sandstrom, A., 2007. Modelling of ferrous iron oxidation by a leptospirillum ferrooxidans - Dominated Chemsostat Culture. *Biotechnology and Bioengineering,* 99(2).

Tuncuk, A. et al., 2012. Aqueous metal recovery techniques from e-scrap: Hydrometallurgy in recycling. *Minerals Engineering,* pp. 28-37.

Vestola, E. A. et al., 2010. Acid bioleaching of solid waste materials from copper, steel and recycling industries. *Hydrometallurgy,* 103(1), pp. 74-79.

Wang, Z., Che, J. & Ye, C., 2010. Application of ferric chloride both as oxidant and complexant to enhance the dissolution of metallic copper.. *Hydrometallurgy,* 105(1), pp. 69-74.

Watling, H., 2006. The bioleaching of sulphide minerals with emphasis on copper sulphides - A review. *Hydrometallurgy,* pp. 81-108.

Xiang, Y. et al., 2010. Bioleaching of copper from waste printed circuit boards by bacterial consortium enriched from acid mine drainage. *Journal of hazardous materials,* 184(1), pp. 812-818.

Yang, H., Liu, J. & Yang, J., 2011. Leaching copper from shredded particles of waste printed circuit boards. *Journal of hazardous materials,* 187(1), pp. 393-400.

Yang, T., Xu, Z., Wen, J. & Yang, L., 2009. Factors influencing bioleaching copper from waste printed circuit boards by Acidithiobacillus ferrooxidans. *Hydrometallurgy,* 97(1), pp. 29-32.

Yang, Y. et al., 2014. Bioleaching waste printed circuit boards by Acidithiobacillys ferrooxidans and its kinetic aspects. *Journal of Biotechnology,* pp. 24-30.

Yazici, E. & Deveci, H., 2014. Ferric sulphate leaching of metals from waste printed circuit boards. *International Journal of Mineral Processing,* Volume 133, pp. 39 - 45.

Younesi, S. R., Alimadadi, H., Alamdari, E. K. & Marashi, S. P. H., 2006. Kinetic mechanisms of cementation of cadmium ions by zinc powder from sulphate solutions.. *Hydrometallurgy ,* 84(3), pp. 155-164.

Zhao, G.-h., Luo, X.-z., Chen, G. & Zhao, Y.-j., 2014. A long-term static immersion experiment on the leaching behavior of heavy metals from waste printed circuit boards.. *Environmental Science: Processes & Impacts,* 16(8), pp. 1967-1974.

APPENDICES

Appendix A Preparation of Reagents Used in the Experiments

Preparation of Ferric Sulphate Solution

To get initial ferric ion in solution, crystals of yellow ferric sulfate ($Fe_2(SO_4)_3.xH_2O$ where the min $Fe_2(SO_4)_3$ is 70 %) was used. As the degree of hydration (hence the moles of water) is not known, a trial and error method was used as follows:

1. An initial mass of ferric sulphate was chosen e.g. 3.5 g.
2. This was then dissolved in 100 ml deionised water in an Erlenmeyer flask and the pH was adjusted to 1.8 with concentrated sulphuric acid.
3. Once the ferric sulfate had dissolved (as indicated by no solids in the solution), the ferric ion analysis was conducted using the ferric chloride method.
4. The ferric ion concentration that was calculated was then divided by the required ferric ion concentration to give the adjustment ratio.
5. The adjustment ratio was then multiplied by the initial ferric sulphate concentration to give the mass required to form a 9 $g.l^{-1}$ solution using 100 ml of deionised water. This was then multiplied by 10 to give the mass required to make a 1 litre solution.
6. Once the mass required for to make a 1 litre solution was calculated, the mass of ferric sulfate was then weighed out and added to 1 litre of deionised water.
7. The pH was then adjusted to 1.5 using concentrated sulphuric acid.

Preparation of 2 M Hydrochloric Acid

1. For the preparation of 2 M solution of hydrochloric acid 32 % w/w hydrochloric acid solution with a density of 1 160 $g.l^{-1}$ was used.
2. The mass of HCl in the solution was :

$$0.32 * 1160 = 371.2\ g\ of\ HCl$$

3. The moles of HCl in a 1.0 solution was 10.19 $mol.l^{-1}$.

$$371.2\ g * 36.46 \frac{g}{mol} = 10.18 mol.l^{-1}$$

4. In order to make a 2 M HCl solution the following relationship was used.

$$M1.V1 = M2.V2$$

5. This meant that the volume of the HCl solution used was:

$$M1.V1 = M2.V2 = 2.0 * 1000 = 10.18 * V2$$

$$V2 = \frac{2.0 * 1000}{10.18} = 196.12\ ml$$

6. The volume of water was calculated by subtracting the volume of HCl solution needed from the final volume of the required solution i.e. 1000 ml – 196 ml = 803.88 ml.

Appendix B Microbial Quantification

This section will go into detail as to how the analytical methods were conducted including how the Ferric Chloride solution was made and the graphs involved in analysis.

Microorganism Cell Count

The equation to calculate the microorganism cell counts was derived as follows:

1. The area of the smallest square that was printed on the Hawskley counting chamber was used. The area was 0.0025 mm^2.
2. The depth of the smallest square that was printed on the Hawskley counting chamber was used. The depth was 0.02 mm.
3. Based on the area and the depth, the volume of the smallest square was calculated. According to:

$$Volume = 0.0025\ mm^2 * 0.02\ mm = 0.0005\ mm^3 = 0.00000005\ ml$$

4. Considering that in the experiments 4 large squares were sampled and each square contained 16 squares this means that the total small squares that were counted were 64 i.e. 16 * 4.
5. The total volume occupied by the 64 squares were:

$$Total\ Volume = 64 * 0.00000005\ ml = 0.0000032\ ml$$

6. To calculate cell per ml, the following calculation was made.

$$\frac{1\ cell}{0.0000032\ ml} = 312500\ cells/ml$$

This means the equation for calculation the cell concentration is:

$$Cell\ concentration = cells\ counted * 312500 * Dilution\ factor$$

Equation 8-1

Appendix C Experimental Calculation

This section will contain the calculations and equations that were used in the experiments.

The Printed Circuit Board Characterization Experiments Calculations

This section contains the calculations from Section 4.1 where the ICP analysis technique was used to determine the mass of metals ions that was leached in solution per mass of PCBS. The volume of solution used was 100 ml. The following table shows the PCB sample data that was used in calculating the mass of metal ions per mass of PCBs.

Table 8-1. Mass of PCB samples before and after leaching in ferric sulphate solution

	High grade sample			Low grade sample		
	Initial	Final	Diff	Initial	Final	Diff
Mass (g)	3.669	3.267	0.403	1.708	1.378	0.330
PCB concentration in solution ($g.l^{-1}$)	36.69	32.67	4.03	17.08	13.78	3.30

The initial mass of the high grade sample was calculated using an electronic balance and it was found to be 3.669 g. In order to get a concentration of the PCB solid in the solution the following calculation was performed.

$$Concentration\ \left(\frac{g}{l}\right) = \frac{Initial\ sample\ mass\ (g)}{volume\ of\ solution\ (l)} = \frac{3.668\ (g)}{0.1\ (l)} = 36.69\ g/l$$

Equation 8-2

Once the metals in the PCBs was leached into solution, a 10 times dilution was conducted on the sample. The metals in solution was analysed using the ICP technique. The following table gives the result of the ICP analysis.

Table 8-2. Results from the ICP analysis of the metal ions in solution

SAMPLE LABEL	**Cu213.598**	**Fe239.563**	**Mn259.372**	**Ni216.555**	**Pb217.000**	**Zn202.548**	**Sn189.925**
	ppm	ppm	ppm	ppm	ppm	ppm	ppm
Std 2ppm	2.04	2.08	-	2	1.99	2.02	-
001*101	16.22	59.82	-	-	-	2.02	15.28
002 *101	16.81	59.88	-	-	-	-	20.07
001 *10	-	-	3.9	4.46	87.92	75.22	-
002 * 10	-	-	4.11	1.22	0.48	10.67	-

The results of the ICP analysis was given in parts per million. The sample label 001 indicates the high grade sample, while 002 indicates the low grade sample. The value besides the sample label i.e. 101

and 10 indicates the dilution factor which is necessary to convert to a concentration of parts per million. Thus in order to convert the sample to a concentration of $g.l^{-1}$, the following equation was used (using copper as an example):

$$Concenration\ \left(\frac{g}{l}\right) = Metal\ conc.(ppm) * dilution\ factor * conversion\ factor\ to\ g/l$$

$$Concentration\ \left(\frac{g}{l}\right) = 16.22 * 101 * \frac{1}{1000} = 1.6382\ (\frac{g}{l})$$

Equation 8-3

The concentration of the metal ions in solution as a mass in $g.l^{-1}$ is given in the table below:

Table 8-3. ICP analysis concentration in $g.l^{-1}$

SAMPLE LABEL	Cu213.598	Fe239.563	Mn259.372	Ni216.555	Pb217.000	Zn202.548	Sn189.925
	$g.l^{-1}$	$g.l^{-1}$	$g.l^{-1}$	$g.l^{-1}$	$g.l^{-1}$	$g.l^{-1}$	$g.l^{-1}$
Std 2ppm	2.04	2.08	-	2	1.99	2.02	-
HG	1.63822	6.04182	-	-	-	0.20402	1.54328
LG	1.69781	6.04788	-	-	-	-	2.02707
001 *10	-	-	0.039	0.0446	0.8792	0.7522	-
002 * 10	-	-	0.0411	0.0122	0.0048	0.1067	-

However in order to relate the metal ion concentrations with the PCB sample used, the metal ion concentration was divided by the PCB concentration in solution according to the equation below (using copper as an example).

$$Conc.\left(\frac{mg\ metal\ ion}{g\ PCB}\right) = \frac{metal\ ion\ conc.\ (g/l)}{intial\ pcb\ conc.\ (g/l)} * \frac{1000\ (mg)}{1\ (g)} = \frac{1.63822 * 1000}{36.69}$$

$$= 44.65\ (\frac{mg\ metal\ ion}{g\ PCB})$$

Equation 8-4

The following table thus gives the results of the conversion.

Table 8-4. Mass of metal ions leached into solution per mass of PCB

	Conc (mg metal ion /g PCB)	
	HG PCB	LG PCB
Fe	164.67	354.09
Cu	44.65	99.40
Sn	42.06	118.68
Pb	23.96	0.28
Zn	20.50	6.25
Ni	1.22	0.71
Mn	1.06	2.41

Appendix D Reactor Design

Base Design equations

The initial assumptions of the reactors is that they are ideal stirred tank reactors with the following design equations.

$$V\frac{dM^{n+}}{dt} = F_{M^{n+}0} - F_{M^{n+}t} + \int_0^V Vr_{M^{n+}}$$

Assuming that in the initial phase the CSTR is applied at steady state we have:

$$V\frac{dM^{n+}}{dt} = 0$$

Assuming that there is no spatial variations in the rate of reaction (i.e. perfect mixing):

$$\int_0^V Vr_{M^{n+}} = Vr_{M^{n+}}$$

Thus the design equations for the model becomes:

$$0 = F_{M^{n+}0} - F_{M^{n+}t} + Vr_{M^{n+}}$$

If these assumptions are not used the system becomes complex and ends up with the need to account for the residence time distribution in the reactors (page 867 Fogler).

Other equations of interest include.

$$F_j = C_j * v \Rightarrow {moles}/{time} = {moles}/{volume} * {volume}/{time}$$

This implies that the reactor equation becomes:

$$0 = vC_0^{n+} - vC_t^{n+} + Vr_{M^{n+}}$$

The dilution rate equation is given by:

$$D = {v(flow\ rate)}/{V\ (reactor\ volume)}$$

The residence time is given by:

$$\tau = {V\ (reactor\ volume}/{v(flow\ rate)}$$

Bioxidation Design Equations

$$0 = vC_{Fe^{2+}0\_biox} - vC_{Fe^{2+}t\_biox} + Vr_{Fe^{2+}\_biox}$$

Chemical Design Equations

$$0 = vC_{Fe^{2+}0\_chem} - vC_{Fe^{2+}t\_chem} + Vr_{Fe^{2+}\_chem}$$

Design equations

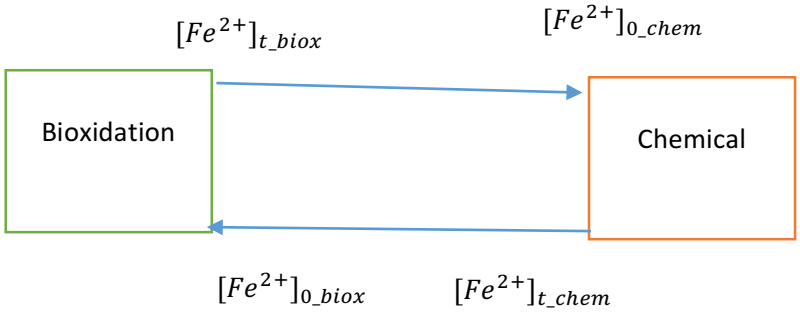

From the above diagram it can be seen the basic system equations for a closed system assumes

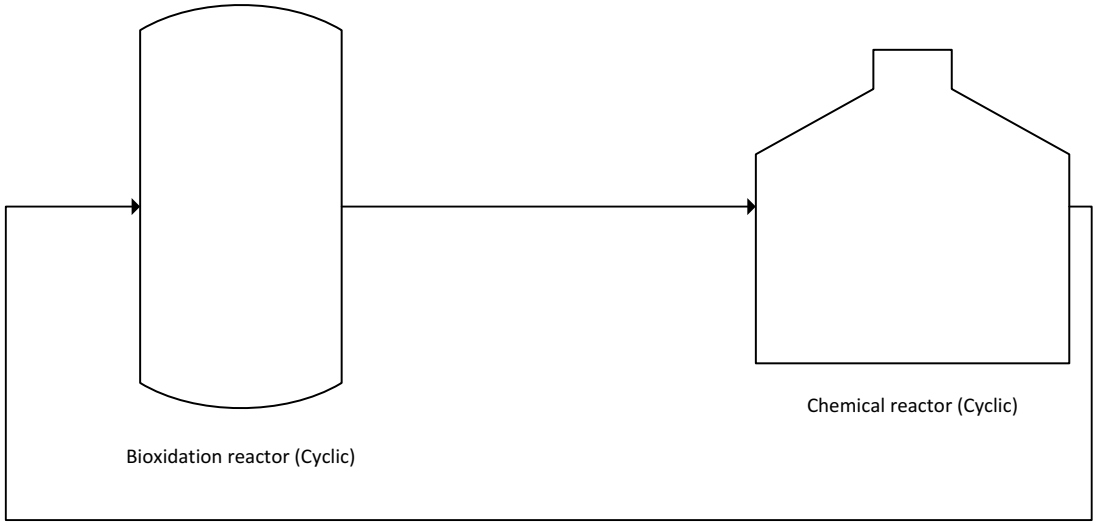

Design Equations

In this system one cannot make the assumption of no accumulation within the reactor as it is also a batch system.

Chemical

$$\frac{V_{chem}dC_{Fe^{2+}\_chem}}{dt} = v_{chem}C_{Fe^{2+}0\_chem} - v_{chem}C_{Fe^{2+}t\_chem} + V_{chem}r_{Fe^{2+}\_chem}$$

$$\frac{V_{chem}dC_{Cu^{2+}\_chem}}{dt} = v_{chem}C_{Cu^{2+}0\_chem} - v_{chem}C_{Cu^{2+}t\_chem} + V_{chem}r_{Cu^{2+}\_chem}$$

Assuming a perfectly mixed reactor and numerical methods:

Bioxidation

$$V_{biox} r_{Cu^{2+}\_biox} = 0$$

$$\frac{V_{biox} dC_{Cu^{2+}\_biox}}{dt} = v_{biox} C_{Cu^{2+}0\_biox} - v_{biox} C_{Cu^{2+}t\_biox}$$

$$\frac{V_{biox} dC_{Fe^{2+}\_biox}}{dt} = v_{biox} C_{Fe^{2+}0\_biox} - v_{biox} C_{Fe^{2+}t\_biox} + V_{biox} r_{Fe^{2+}\_biox}$$

Overall

Rate balance

$$\frac{V_{biox} dC_{Cu^{2+}\_biox}}{dt} + \frac{V_{chem} dC_{Cu^{2+}\_chem}}{dt} = \frac{V_{tot} dC_{Cu^{2+}\_tot}}{dt}$$

$$\frac{V_{biox} dC_{Fe^{2+}\_biox}}{dt} + \frac{V_{chem} dC_{Fe^{2+}\_chem}}{dt} = \frac{V_{tot} dC_{Fe^{2+}\_tot}}{dt}$$

$$v_{chem} = v_{biox}$$

Ferric balance

$$v_{chem} C_{Fe^{2+}0\_chem} = v_{biox} C_{Fe^{2+}t\_biox}$$

$$v_{chem} C_{Fe^{2+}t\_chem} = v_{biox} C_{Fe^{2+}0\_biox}$$

Copper Balance

$$v_{chem} C_{Cu^{2+}0\_chem} = v_{biox} C_{Cu^{2+}t\_biox}$$

$$v_{chem} C_{Cu^{2+}t\_chem} = v_{biox} C_{Cu^{2+}0\_biox}$$

$$V_{biox} + V_{chem} = V_{tot}$$

Combined

$$\frac{V_{biox} dC_{Cu^{2+}\_biox}}{dt} + v_{biox} C_{Cu^{2+}t\_biox} = v_{biox} C_{Cu^{2+}0\_biox}$$

$$\frac{V_{chem} dC_{Cu^{2+}\_chem}}{dt} = v_{chem} C_{Cu^{2+}0\_chem} - \frac{V_{biox} dC_{Cu^{2+}_{biox}}}{dt} - v_{biox} C_{Cu^{2+}t\_biox} + V_{chem} r_{Cu^{2+}\_chem}$$

$$\frac{V_{chem} dC_{Cu^{2+}\_chem}}{dt} = V_{chem} r_{Cu^{2+}\_chem} - \frac{V_{biox} dC_{Cu^{2+}_{biox}}}{dt}$$

Numerical Method

Chemical

$$V_{chem}C_{Fe^{2+}}(t+1) = V_{chem}C_{Fe^{2+}}(t) + h(v_{chem}C_{Fe^{2+}0} - v_{chem}C_{Fe^{2+}}(t) + V_{chem} * (k * C_{Fe^{2+}}(t) * C_{Cu^0_{chem}}(t))$$

$$C_{Fe^{2+}}(t+1) = C_{Fe^{2+}}(t) + h(D_{chem}(C_{Fe^{2+}0} - C_{Fe^{2+}}(t)) + (k * C_{Fe^{2+}}(t) * C_{Cu^0_{chem}}(t))$$

$$V_{chem}C_{Cu^{2+}}(t+1) = V_{chem}C_{Cu^{2+}}(t) + h\left(v_{chem}C_{Cu^{2+}0} - v_{chem}C_{Cu^{2+}}(t) + V_{chem} * (k * C_{Fe^{2+}}(t) * C_{Cu^0_{chem}}(t))\right)$$

$$C_{Cu^{2+}}(t+1) = C_{Cu^{2+}}(t) + h\left(D_{chem}(C_{Cu^{2+}0} - C_{Cu^{2+}}(t)) + (k * C_{Fe^{2+}}(t) * C_{Cu^0_{chem}}(t))\right)$$

$$\left(k * C_{Fe^{2+}}(t) * C_{Cu^0_{chem}}(t)\right) = C_{Cu^{2+}_{chem}}(t+1)$$

Bioxidation

$$C_{Fe^{2+}}(t+1) = C_{Fe^{2+}}(t) + h(v_{chem}C_{Fe^{2+}0} - v_{chem}C_{Fe^{2+}}(t) - V_{chem} * (C_x q_{Fe^{2+}} \Big/ 1 + \frac{Fe^{3+}(t)}{Fe^{2+}(t)})$$

$$C_{Cu^{2+}}(t+1) = C_{Cu^{2+}}$$

Appendix E Experimental Data

Base Bacterial Leaching

		Absorbance			
Date	**Day**	**Batch 1 (0 g Cu per L)**	**Batch 2 (1 g Cu per L)**	**Batch 3 (5 g Cu per L)**	**Batch 4 (10 g Cu per L)**
9-Oct	**0**	0.158	0.037	0.111	0.055
10-Oct	**1**	0.204	0.100	0.054	0.065
11-Oct	**2**	0.239	0.188	0.09	0.073
12-Oct	**3**	0.253	0.211	0.141	0.099
13-Oct	**4**	0.316	0.234	0.248	0.168
15-Oct	**6**	1.057	0.278	0.245	0.237
16-Oct	**7**	1.021	0.351	0.289	0.283
17-Oct	**8**	-	0.805	0.336	0.313
18-Oct	**9**	-	1.132	0.36	0.306
19-Oct	**10**	-	1.034	0.508	0.325
20-Oct	**11**	-	-	1.036	0.349
22-Oct	**13**	-	-	1.002	0.38
23-Oct	**14**	-	-	-	0.43
24-Oct	**15**	-	-	-	0.457
25-Oct	**16**	-	-	-	0.616
26-Oct	**17**	-	-	-	0.817
27-Oct	**18**	-	-	-	0.967
29-Oct	**20**	-	-	-	0.874
		Actual Iron Concentration (g/L)			
Date	**Day**	**Batch 1 (0 g Cu per L)**	**Batch 2 (1 g Cu per L)**	**Batch 3 (5 g Cu per L)**	**Batch 4 (10 g Cu per L)**
9-Oct	**0**	0.019	0.004	0.013	0.007
10-Oct	**1**	0.024	0.012	0.006	0.008
11-Oct	**2**	0.029	0.023	0.011	0.009
12-Oct	**3**	0.030	0.025	0.017	0.012
13-Oct	**4**	0.038	0.028	0.030	0.020
15-Oct	**6**	0.127	0.033	0.029	0.028
16-Oct	**7**	0.122	0.042	0.035	0.034
17-Oct	**8**	-	0.096	0.040	0.037
18-Oct	**9**	-	0.136	0.043	0.037
19-Oct	**10**	-	0.124	0.061	0.039
20-Oct	**11**	-	-	0.124	0.042
22-Oct	**13**	-	-	0.120	0.046
23-Oct	**14**	-	-	-	0.052
24-Oct	**15**	-	-	-	0.055
25-Oct	**16**	-	-	-	0.074
26-Oct	**17**	-	-	-	0.098
27-Oct	**18**	-	-	-	0.116

		Eh				pH			
Date	Day	Batch 1 (0 g Cu per L)	Batch 2 (1 g Cu per L)	Batch 3 (5 g Cu per L)	Batch 4 (10 g Cu per L)	Batch 1 (0 g Cu per L)	Batch 2 (1 g Cu per L)	Batch 3 (5 g Cu per L)	Batch 4 (10 g Cu per L)
9-Oct	**0**	387.00	388.00	382.00	371.00	1.86	1.87	2.02	2.01
9-Oct	**0**	403.00	334.00	278.00	178.00	1.67	2.18	3.68	3.82
10-Oct	**1**	406.00	380.00	313.00	278.00	1.94	1.67	2.21	3.52
10-Oct	**1**	409.00	393.00	356.00	288.00	1.93	1.65	1.57	3.42
11-Oct	**2**	410.00	401.00	362.00	316.00	1.97	1.70	1.73	2.26
12-Oct	**3**	414.00	410.00	394.00	396.00	1.98	1.71	1.80	2.10
13-Oct	**4**	409.00	417.00	404.00	394.00	1.96	1.73	1.82	2.18
15-Oct	**6**	700.00	421.00	416.00	414.00	2.16	1.77	1.87	1.82
16-Oct	**7**	719.00	427.00	419.00	417.00	2.17	1.89	1.98	1.92
17-Oct	**8**	-	467.00	426.00	424.00	-	2.03	1.89	1.83
18-Oct	**9**	-	695.00	429.00	425.00	-	2.08	1.94	1.86
19-Oct	**10**	-	720.00	442.00	428.00	-	2.01	2.03	1.86
20-Oct	**11**	-	-	693.00	428.00	-	-	2.21	1.87
22-Oct	**13**	-	-	729.00	436.00	-	-	2.05	1.88
23-Oct	**14**	-	-	-	438.00	-	-	-	1.95
24-Oct	**15**	-	-	-	448.00	-	-	-	2.01
25-Oct	**16**	-	-	-	458.00	-	-	-	1.96
26-Oct	**17**	-	-	-	490.00	-	-	-	2.00
27-Oct	**18**	-	-	-	650.00	-	-	-	2.00
29-Oct	**20**	-	-	-	715.00	-	-	-	1.93

Fed batch copper additions

		Addition 1													
		2 g/l							4 g/l						
		Initial copper				0.2077			Initial Copper						
		Absorbance				Concentration			Absorbance				Concentration		
Min	Hrs	Eh	pH	Fe3+	FeTot	Fe3+	FeTot	Fe3+/Fetot	Eh	pH	Fe3+	FeTot	Fe3+	FeTot	Fe3+/Fetot
0.00	0.0	723	1.330	1.390	1.382	0.166	0.165	1.006	723	1.330	1.390	1.382	0.166	0.165	1.006
5.00	0.1	493	1.340	1.081	1.414	0.129	0.169	0.764	457	1.410	0.878	1.443	0.105	0.172	0.608
10.00	0.2	471	1.360	1.063	1.428	0.127	0.170	0.744	443	1.450	0.647	1.421	0.077	0.170	0.455
20.00	0.3	466	1.420	0.907	1.409	0.108	0.168	0.644	433	1.470	0.539	1.432	0.064	0.171	0.376
30.00	0.5	461	1.420	0.913	1.492	0.109	0.178	0.612	422	1.520	0.407	1.422	0.049	0.170	0.286
45.00	0.8	461	1.430	0.851	1.424	0.102	0.170	0.598	413	1.590	0.324	1.399	0.039	0.167	0.232
60.00	1.0	461	1.430	0.844	1.405	0.101	0.168	0.601	410	1.560	0.305	1.424	0.036	0.170	0.214
90.00	1.5	460	1.450	0.863	1.403	0.103	0.167	0.615	408	1.440	0.322	1.433	0.038	0.171	0.225
120.00	2.0	459	1.430	0.865	1.413	0.103	0.169	0.612	409	1.440	0.317	1.418	0.038	0.169	0.224
1320.00	22.0	486	1.610	1.095	1.344	0.131	0.160	0.815	440	1.790	0.570	1.351	0.068	0.161	0.422
2760.00	46.0	533	1.630	1.301	1.347	0.155	0.161	0.966	494	2.000	1.195	1.328	0.143	0.159	0.900
4200.00	70.0	720	1.670	1.312	1.293	0.157	0.154	1.015	619	1.990	1.244	1.229	0.148	0.147	1.012
7080.00	118.0	685	1.550	1.468	1.455	0.175	0.174	1.009	681	1.490	1.390	1.394	0.166	0.166	0.997

		Addition 2													
		2 g/l							4 g/l						
		Initial copper				0.2054			Initial Copper				0.4086		
		Absorbance				Concentration			Absorbance				Concentration		
Min	Hrs	Eh	pH	Fe3+	FeTot	Fe3+	FeTot	Fe3+/Fetot	Eh	pH	Fe3+	FeTot	Fe3+	FeTot	Fe3+/Fetot
0.00	0.0	685	1.550	1.468	1.455	0.175	0.174	1.009	681	1.490	1.390	1.394	0.166	0.166	0.997
18.00	0.3	453	1.840	0.864	1.475	0.103	0.176	0.586	426	1.720	0.473	1.449	0.056	0.173	0.326

36.00	0.6	448	1.880	0.813	1.470	0.097	0.175	0.553	399	1.760	0.270	1.428	0.032	0.170	0.189
60.00	1.0	448	1.850	0.813	1.463	0.097	0.175	0.556	394	1.780	0.181	1.406	0.022	0.168	0.129
1453.00	12.43	476	1.480	0.903	1.374	0.108	0.164	0.657	448	1.740	0.570	1.383	0.068	0.165	0.412
2893.00	24.2	491	1.950	1.452	1.689	0.173	0.202	0.860	537	2.350	**1.068**	**1.631**	0.127	0.195	0.655
4333.00	48.2	695	1.890	1.150	1.139	0.137	0.136	1.010	647	2.180	1.098	1.087	0.131	0.130	1.010
	72.2	705	1.750	1.159	1.155	0.138	0.138	1.003	650	1.480	1.206	1.206	0.144	0.144	1.000

		Addition 3													
		2 g/l							**4 g/l**						
		Initial copper				**0.2088**			**Initial Copper**				**0.4072**		
		Absorbance				**Concentration**			**Absorbance**				**Concentration**		
Min	Hrs	**Eh**	**pH**	**Fe3+**	**FeTot**	**Fe3+**	**FeTot**	**Fe3+/Fetot**	**Eh**	**pH**	**Fe3+**	**FeTot**	**Fe3+**	**FeTot**	**Fe3+/Fetot**
0.00	0	705	1.750	1.159	1.155	0.138	0.138	1.003	650	1.480	1.206	1.206	0.144	0.144	1.000
30.00	0.5	475	1.910	0.921	1.158	0.110	0.138	0.795	470	1.630	0.879	1.205	0.105	0.144	0.729
60.00	1	461	2.000	0.826	1.179	0.099	0.141	0.701	458	1.650	0.787	1.234	0.094	0.147	0.638
90.00	1.5	455	2.040	0.802	1.213	0.096	0.145	0.661	451	1.710	0.714	1.217	0.085	0.145	0.587
357.00	5.95	462	2.200	0.802	1.213	0.096	0.145	0.661	428	2.220	0.495	1.159	0.059	0.138	0.427
357.00	5.95	478	1.530	0.810	1.096	0.097	0.131	0.739	442	1.540	0.495	1.159	0.059	0.138	0.427
720.00	12	553	1.750	1.431	1.460	0.171	0.174	0.980	484	2.090	1.172	1.300	0.140	0.155	0.902
1884.00	31.4	689	1.600	1.091	1.087	0.130	0.130	1.004	652	1.730	1.151	1.143	0.137	0.136	1.007
4764.00	79.4	738	1.510	1.214	1.207	0.145	0.144	1.006	713	1.670	1.230	1.236	0.147	0.148	0.995

		Addition 4													
		2 g/l							**4 g/l**						
		Initial copper				**0.2081**			**Initial Copper**				**0.4083**		
		Absorbance				**Concentration**			**Absorbance**				**Concentration**		
Min	Hrs	**Eh**	**pH**	**Fe3+**	**FeTot**	**Fe3+**	**FeTot**	**Fe3+/Fetot**	**Eh**	**pH**	**Fe3+**	**FeTot**	**Fe3+**	**FeTot**	**Fe3+/Fetot**

0.00	0.0	738	1.510	1.214	1.207	0.145	0.144	1.006	713	1.670	1.230	1.236	0.147	0.148	0.995
30.00	0.5	476	1.590	0.911	1.207	0.109	0.144	0.755	478	1.750	0.992	1.211	0.118	0.145	0.819
60.00	1.0	466	1.630	0.859	1.217	0.103	0.145	0.706	468	1.800	0.918	1.217	0.110	0.145	0.754
122.00	2.0	450	1.660	0.851	1.420	0.102	0.170	0.599	418	2.040	0.604	1.393	0.072	0.166	0.434
420.00	7.0	455	1.760	0.715	1.192	0.085	0.142	0.600	401	2.470	0.323	1.177	0.039	0.140	0.274
420.00	7.0	455	1.760	0.715	1.192	0.085	0.142	0.600	**418**	**1.680**	**0.341**	**1.200**	0.041	0.143	0.284
1440.00	24.0	551	1.920	1.139	1.140	0.136	0.136	0.999	481	1.990	0.974	1.153	0.116	0.138	0.845
1800.00	30.0	706	1.880	1.141	1.128	0.136	0.135	1.012	526	1.990	1.114	1.139	0.133	0.136	0.978
2820.00	47.0	721	1.820	1.166	1.156	0.139	0.138	1.009	701	1.940	1.295	1.284	0.155	0.153	1.009

		Addition 5													
		2 g/l							**4 g/l**						
		Initial copper				**0.2100**			**Initial Copper**				**0.4109**		
		Absorbance				**Concentration**			**Absorbance**				**Concentration**		
Min	Hrs	**Eh**	**pH**	**Fe3+**	**FeTot**	**Fe3+**	**FeTot**	**Fe3+/Fetot**	**Eh**	**pH**	**Fe3+**	**FeTot**	**Fe3+**	**FeTot**	**Fe3+/Fetot**
0.00	0.0	746	1.400	1.166	1.156	0.139	0.138	1.009	701	1.400	1.295	1.284	0.155	0.153	1.009
30.00	0.5	476	1.490	0.885	1.132	0.106	0.135	0.782	457	1.540	0.767	1.194	0.092	0.143	0.642
60.00	1.0	467	1.510	0.820	1.163	0.098	0.139	0.705	448	1.570	0.696	1.211	0.083	0.145	0.575
90.00	1.5	463	1.540	0.813	1.173	0.097	0.140	0.693	440	1.590	0.600	1.226	0.072	0.146	0.489
120.00	2.0	455	1.560	0.714	1.187	0.085	0.142	0.602	434	1.630	0.523	1.226	0.062	0.146	0.427
260.00	4.3	450	1.670	0.651	1.170	0.078	0.140	0.556	413	1.790	0.300	1.198	0.036	0.143	0.250
378.00	6.3	460	1.720	0.744	1.150	0.089	0.137	0.647	413	1.930	0.312	1.186	0.037	0.142	0.263
482.00	8.0	468	1.740	0.828	1.186	0.099	0.142	0.698	420	1.940	0.396	1.175	0.047	0.140	0.337
1440.00	24.0	712	1.820	1.146	1.127	0.137	0.135	1.017	652	2.250	1.137	1.129	0.136	0.135	1.007
1726.00	28.8	722	1.810	1.249	1.242	0.149	0.148	1.006	704	1.540	1.171	1.165	0.140	0.139	1.005

Addition 6	
2 g/l	**4 g/l**

		Initial copper				0.2043			Initial Copper				0.4110		
		Absorbance				Concentration			Absorbance				Concentration		
Min	Hrs	Eh	pH	Fe3+	FeTot	Fe3+	FeTot	Fe3+/Fetot	Eh	pH	Fe3+	FeTot	Fe3+	FeTot	Fe3+/Fetot
0.00	0.0	722	1.810	1.249	1.242	0.149	0.148	1.006	704	1.540	1.171	1.165	0.140	0.139	1.005
30.00	0.5	474	1.920	1.003	1.240	0.120	0.148	0.809	455	1.660	0.793	1.213	0.095	0.145	0.654
60.00	1.0	467	1.980	0.882	1.164	0.105	0.139	0.758	445	1.710	0.570	1.025	0.068	0.122	0.556
90.00	1.5	466	2.000	1.049	1.161	0.125	0.139	0.904	435	1.780	0.543	1.161	0.065	0.139	0.468
122.00	2.0	465	2.020	0.936	1.199	0.112	0.143	0.781	432	1.800	0.505	1.162	0.060	0.139	0.435
194.00	3.2	467	2.040	0.936	1.187	0.112	0.142	0.789	429	1.870	0.547	1.235	0.065	0.147	0.443
194.00	3.2	477	1.660	0.936	1.187	0.112	0.142	0.789	429	1.870	0.547	1.235	0.065	0.147	0.443
1016.00	16.9	729	1.890	1.167	1.153	0.139	0.138	1.012	566	2.350	1.074	1.072	0.128	0.128	1.002
1022.00	17.0	-	-	-	-	-	-	-	600	1.480	1.097	1.093	0.131	0.130	1.004
1078.00	24.0	-	-	-	-	-	-	-	710	1.440	1.089	1.083	0.130	0.129	1.006

	Run 1 (2 g/l (Cu) & 11 g/l Fe)								
	Cu added	0.2034	g	Cu / 100ml	0.003201154	moles/100ml	Moles Cu per l	0.032012	moles / l
Time			Absorbance			Actual Conc (moles/dm3)			
	Eh	pH	Fe3+	FeTot	Fe3+/Fetot	Fe3+	FeTot	Fe3+/Fetot	X
0	676.33	1.13	1.618	1.553	1.042	0.193	0.185	1.042	0
5			1.197	1.565	0.765	0.143	0.187	0.765	0.786746
10			1.115	1.601	0.697	0.133	0.191	0.697	0.938768
15			1.107	1.605	0.690	0.132	0.192	0.690	0.954616
20			1.178	1.703	0.690	0.141	0.203	0.690	0.821327
25			1.074	1.588	0.676	0.128	0.190	0.676	1.015504
30	471.00	1.21	1.201	1.691	0.707	0.132	0.202	0.659	0.950557

	Run 2 (4 g/l (Cu) & 11 g/l Fe)								
	Cu added	0.4045	g	Cu / 100ml	0.006365067	moles/100ml	Moles Cu per l	0.063651	moles / l
Time			Absorbance			Actual Conc (moles/dm3)			
	Eh	pH	Fe3+	FeTot	Fe3+/Fetot	Fe3+	FeTot	Fe3+/Fetot	X
0	672.33	1.14	1.653	1.612	1.025	0.197	0.192	1.025	0
5			0.775	1.557	0.498	0.093	0.186	0.498	0.823328
10			0.641	1.586	0.404	0.077	0.189	0.404	0.948615
15			0.589	1.571	0.375	0.070	0.188	0.375	0.997882
20			0.541	1.594	0.340	0.065	0.190	0.340	1.042342
25			0.532	1.556	0.342	0.063	0.186	0.342	1.051416
30	434.00	1.28	0.556	1.566	0.355	0.066	0.187	0.355	1.028851

	Run 3 (2 g/l (Cu) & 5.5 g/l Fe)								
	Cu added	0.2068	g	Cu / 100ml	0.003254131	moles/100ml	Moles Cu per l	0.032541	moles / l
Time			Absorbance			Actual Conc (moles/dm3)			
	Eh	pH	Fe3+	FeTot	Fe3+/Fetot	Fe3+	FeTot	Fe3+/Fetot	X
0	676.00	1.17	0.798	0.763	1.046	0.095	0.091	1.046	0
5			0.466	0.798	0.584	0.056	0.095	0.584	0.608306
10			0.414	0.822	0.502	0.049	0.098	0.502	0.70429
15			0.341	0.778	0.438	0.041	0.093	0.438	0.837561
20			0.288	0.776	0.371	0.034	0.093	0.371	0.934791
25			0.283	0.794	0.357	0.034	0.095	0.357	0.943957
30	445.00	1.25	0.277	0.772	0.359	0.033	0.092	0.359	0.955584

	Run 1 (2 g/l (Sn) & 11 g/l Fe)								
	Sn	0.2037	g	Cu / 100ml	0.003205	moles/100ml	Moles Cu per l	0.032048	
Time			Absorbance			Actual Conc (moles/dm3)			
	Eh	pH	Fe3+	FeTot	Fe3+/Fetot	Fe3+	FeTot	Fe3+/Fetot	X

0	668.00	1.24	1.598	1.556	1.027	0.191	0.186	1.027	0
5			1.399	1.576	0.888	0.167	0.188	0.888	0.34601
10			1.305	1.617	0.807	0.156	0.193	0.807	0.512832
15			1.199	1.571	0.763	0.143	0.187	0.763	0.694787
20			1.118	1.562	0.715	0.133	0.186	0.715	0.836339
25			1.113	1.546	0.719	0.133	0.185	0.719	0.844913
30	491.50	1.26	1.102	1.550	0.711	0.132	0.185	0.711	0.863573

	Run 2 (4 g/l (Sn) & 11 g/l Fe)								
	Sn 0.4050	g	Cu / 100ml	0.006372	moles/100ml	Moles Cu per l	0.063724		
Time			Absorbance			Actual Conc (moles/dm3)			
	Eh	pH	Fe3+	FeTot	Fe3+/Fetot	Fe3+	FeTot	Fe3+/Fetot	X
0	667.00	1.26	1.597	1.581	1.011	0.191	0.189	1.011	0
5			1.241	1.585	0.783	0.148	0.189	0.783	0.210651
10			0.982	1.589	0.618	0.117	0.190	0.618	0.409539
15			0.784	1.580	0.496	0.094	0.189	0.496	0.4992
20			0.710	1.567	0.453	0.085	0.187	0.453	0.540555
25			0.728	1.654	0.438	0.087	0.197	0.438	0.51047
30	465.50	1.33	0.663	1.582	0.418	0.079	0.189	0.418	0.552471

	Run 3 (2 g/l (Sn) & 5.5 g/l Fe)								
	Sn 0.2022	g	Cu / 100ml	0.003182	moles/100ml	Moles Cu per l	0.031823		
Time			Absorbance			Actual Conc (moles/dm3)			
	Eh	pH	Fe3+	FeTot	Fe3+/Fetot	Fe3+	FeTot	Fe3+/Fetot	X
0	652.50	1.22	0.807	0.805	1.004	0.096	0.096	1.004	0
5			0.711	0.830	0.856	0.085	0.099	0.856	0.168165
10			0.617	0.810	0.758	0.074	0.097	0.758	0.333156
15			0.535	0.787	0.679	0.064	0.094	0.679	0.475712
20			0.510	0.810	0.629	0.061	0.097	0.629	0.519618
25			0.476	0.799	0.594	0.057	0.095	0.594	0.579171
30	482.00	1.27	0.477	0.791	0.601	0.057	0.094	0.601	0.577066

	Run 1 (2 g/l (Zn) & 11 g/l Fe)								
	Zn 0.2056	g	0.003143	moles/100ml	Moles Zn per l	0.031427	mol/l		
Time			Absorbance			Actual Conc (moles/dm3)			
	Eh	pH	Fe3+	FeTot	Fe3+/Fetot	Fe3+	FeTot	Fe3+/Fetot	X
0	679.50	1.20	1.584	1.579	1.003	0.189	0.189	1.003	0
5			1.183	1.569	0.754	0.141	0.187	0.754	0.763324
10			1.172	1.567	0.748	0.140	0.187	0.748	0.784619
15			1.157	1.570	0.737	0.138	0.187	0.737	0.813276

20			1.137	1.577	0.721	0.136	0.188	0.721	0.849147
25			1.132	1.551	0.730	0.135	0.185	0.730	0.8596
30	487.00	1.26	1.124	1.558	0.722	0.134	0.186	0.722	0.874164

	Run 2 (4 g/l (Zn) & 11 g/l Fe)								
	Zn 0.4034 g 0.006168 moles/100ml					Moles Zn per l 0.061678 mol/l			
Time			Absorbance			Actual Conc (moles/dm3)			
	Eh	pH	Fe3+	FeTot	Fe3+/Fetot	Fe3+	FeTot	Fe3+/Fetot	X
0	680.50	1.23	1.599	1.587	1.008	0.191	0.189	1.008	0
5			0.816	1.587	0.515	0.097	0.189	0.515	0.757583
10			0.759	1.611	0.471	0.091	0.192	0.471	0.813423
15			0.724	1.565	0.463	0.086	0.187	0.463	0.846675
20			0.719	1.558	0.462	0.086	0.186	0.462	0.851494
25			0.699	1.537	0.455	0.083	0.183	0.455	0.87087
30	456.00	1.50	0.701	1.553	0.452	0.084	0.185	0.452	0.869234

	Run 3 (2 g/l (Zn) & 5.5 g/l Fe)								
	Zn 0.2039 g 0.003118 moles/100ml					Moles Zn per l 0.031178 mol/l			
Time			Absorbance			Actual Conc (moles/dm3)			
	Eh	pH	Fe3+	FeTot	Fe3+/Fetot	Fe3+	FeTot	Fe3+/Fetot	X
0	672.50	1.23	0.823	0.819	1.004	0.098	0.098	1.004	0
5			0.422	0.789	0.534	0.050	0.094	0.534	0.768709
10			0.397	0.802	0.495	0.047	0.096	0.495	0.815827
15			0.376	0.778	0.484	0.045	0.093	0.484	0.857112
20			0.381	0.805	0.474	0.045	0.096	0.474	0.846689
25			0.374	0.793	0.473	0.045	0.095	0.473	0.859857
30	457.50	1.36	0.379	0.794	0.478	0.045	0.095	0.478	0.851362

Appendix F Material Safety data and Hazards

This section contains the safety data for the chemicals used and their potential effects. The personnel protective equipment for handling the chemicals was largely the same in that protective clothing i.e. a lab coat, closed shoes and safety gloves were necessary.

Sulphuric Acid

Information source: http://www.sciencelab.com/msds.php?msdsId=9925146 (02-Feb-2015)

Hazards Identification: Very hazardous in case of skin contact (corrosive, irritant, permeator), of eye contact (irritant, corrosive), of ingestion, of inhalation. Liquid or spray mist may produce tissue damage particularly on mucous membranes of eyes, mouth and respiratory tract. Skin contact may produce burns. Inhalation of the spray mist may produce severe irritation of respiratory tract, characterized by coughing, choking, or shortness of breath. Severe over-exposure can result in death. Inflammation of the eye is characterized by redness, watering, and itching. Skin inflammation is characterized by itching, scaling, reddening, or, occasionally, blistering.

Hydrochloric Acid

Information source: http://www.sciencelab.com/msds.php?msdsId=9924285 (02-Feb-2015)

Hazards Identification: Very hazardous in case of skin contact (corrosive, irritant, permeator), of eye contact (irritant, corrosive), of ingestion. Slightly hazardous in case of inhalation (lung sensitizer). Non-corrosive for lungs. Liquid or spray mist may produce tissue damage particularly on mucous membranes of eyes, mouth and respiratory tract. Skin contact may produce burns. Inhalation of the spray mist may produce severe irritation of respiratory tract, characterized by coughing, choking, or shortness of breath. Severe over-exposure can result in death. Inflammation of the eye is characterized by redness, watering, and itching. Skin inflammation is characterized by itching, scaling, reddening, or, occasionally, blistering

Ferrous sulphate

Information source: http://www.sciencelab.com/msds.php?msdsId=9924056 (02-Feb-2015)

Hazards Identification: Hazardous in case of skin contact (irritant), of eye contact (irritant), of ingestion, of inhalation.

Ferric sulphate

Information source: http://www.kendon.com.au/catalogue/MSDS/Industrial/FerricSulphate.htm (02-Feb-2015)

Hazards Identification: May cause moderate to severe irritation and inflammation to the eyes. May cause abdominal pain, nausea, vomiting, bleeding stomach, incoordination, and muscle spasm and kidney injury. Ferric Sulphate can cause stingy irritation to open cuts and wounds. Prolonged contact can cause dermatitis.

Potassium Persulfate

Information source: http://www.sciencelab.com/msds.php?msdsId=9927234 (02-Feb-2015)

Hazards Identification: Very hazardous in case of skin contact (irritant), of eye contact (irritant), of ingestion, of inhalation. Slightly hazardous in case of skin contact (corrosive, permeator). Prolonged exposure may result in skin burns and ulcerations. Over-exposure by inhalation may cause respiratory irritation. Inflammation of the eye is characterized by redness, watering, and itching. Skin inflammation is characterized by itching, scaling, reddening, or, occasionally, blistering.

Appendix G Simulation Code

Reactions.py

```
from masters.calculations import constants
import numpy as np

# Raise all numpy exceptions
np.seterr(all='raise')

class BioxidationRate(object):
    """
    The initial rate assumes a CSTR
    """
    def __init__(self, ferric_initial=None, ferrous_initial=None,
initial_cells=7.25e7):
        self.ferric = ferric_initial or 0.
        self.ferrous = ferrous_initial or 0.
        self.reactant_name = "Biomass"
        self.component_conc = initial_cells * 4.8 * 10e-15 * 1000
        self.reaction_step = 0.0

    def __unicode__(self):
        return u"BIOX"

    def inhibited(self):
        pass

    def calculate_biomass_conc(self):
        return self.cell_number * 4.8 * 10e-15 * 1000

    def update_biomass_concentration(self):
        self.component_conc
        k_d = 0
        K = 0.0024 # Tunde
        u_max = (0.13 / 3600.0)

        if self.ferrous == 0:
            rate_biomass = 0.0
        else:
            try:
                rate_biomass = self.component_conc * (u_max  - k_d)
/ (1 + (K * np.divide(self.ferric, self.ferrous)))
            except Exception, e:
                raise e

        self.component_conc = self.component_conc + (1.0 *
rate_biomass)

    def simplified_hansford(self):
        q_spec_growth_rate = 23.55 / 3600

        K = 0.0024 # Tunde
        if self.ferrous == 0:
            rate_ferrous = 0.
        else:
            rate_ferrous = - (self.component_conc *
q_spec_growth_rate) / (1 + (K * np.divide(self.ferric,
self.ferrous)))
        return rate_ferrous

    def update_global_reactant_concentrations(self, ferric,
ferrous):
        self.ferric = ferric
        self.ferrous = ferrous

    def ferric_to_ferrous(self, rate_ferric_or_ferrous):
        """
        Converts the ferric rate to ferrous rate
        """
        return rate_ferric_or_ferrous * (-1)

    def update_step(self, step):
        self.reaction_step = step
        self.step = step

    def run(self):
        rate_ferrous = self.simplified_hansford()
        rate_ferric = self.ferric_to_ferrous(rate_ferrous)

        # This equation changes the biomass concentration
        self.update_biomass_concentration()
        data = {
            "rate_ferrous": rate_ferrous,
            "rate_ferric": rate_ferric,
            "component_moles": self.component_conc,
        }
        return data


class MetalDissolutionRate(object):
    def __init__(self, metal_name, metal_initial,
initial_ferric=None, system=None):
        self.reactant_name = metal_name
        self.metal_initial = metal_initial
        self.component_conc = metal_initial
        self.ferric = initial_ferric or 0.
        self.system = system or constants.BATCH
        self.metal_ion = 0
        self.step = 0
        self.system_step = 0.0
        self.reaction_step = 0.0
        self.metal_ion_previous = 0

    def metal_powder_rate(self):
        # Return 0 rate when the initial metal decreases to
negative
        if self.component_conc < 0:
            return 0

        if self.ferric == 0:
            rate_ferric = 0
        else:
            rate_ferric = self.calculate_based_on_conversion()

        self.update_metal_reactant_concentration(rate_ferric)
        self.update_metal_ion_concentration()
        return rate_ferric

    def update_step(self, step):
        self.reaction_step += 1
        self.step = step

    def shrinking_particle model(self):
        K = constants.DATA[self.reactant_name]["equation"]["K"]
        n = constants.DATA[self.reactant_name]["equation"]["n"]
        conc = np.power(self.ferric, n)

        a =  3 * K * conc
        b = - 6 * np.power(K, 2) * np.power(conc, 2) *
self.reaction_step
        c =  3 * np.power(K, 3) * np.power(conc, 3) *
np.power(self.reaction_step, 2)
        return - (a + b + c) * self.metal_initial

    def calculate_based_on_conversion(self):
        K = constants.DATA[self.reactant_name]["equation"]["K"]
        n = constants.DATA[self.reactant_name]["equation"]["n"]
```

```
        if self.reactant_name == "Zn":
            X = 1 - np.exp(- np.power(K * (self.reaction_step + 1),
0.5))
        else:
            X = 1 - (1 - K*np.power(self.ferric, n) * (self.reaction_step
+ 1))**3

        rate_ferric = - 2 * (X * self.metal_initial -
self.metal_ion)/(self.reaction_step+1)
        return rate_ferric

    def update_metal_reactant_concentration(self, rate_ferric):
        # Problem here is thar for a multi COMPONENT SYSTEM
NEED TO UPDATE
        # CONCENTRATIONS FROM OUTSIDE THE SYSTEM
        self.component_conc = self.component_conc + (rate_ferric
/ float(constants.DATA[self.reactant_name]["stoichiometry"]))

    def update_metal_ion_concentration(self):
        self.metal_ion = self.metal_initial - self.component_conc

    def update_global_reactant_concentrations(self, ferric,
ferrous):
        """
        As the ferric concentration is governed by
        [Fe2+]_out = -rate_ferrous / Dilution rate + [Fe2+]_in
        """
        self.ferric = ferric
        self.ferrous = ferrous

    def stoichiometry(self):
        """
        equation returns the stoichiometry of the metal vs ferrous,
it will
        be used in working out the summation of the sates in the
system.
        """
        pass

    def rate_component_reaction(self, rate_ferrous):
        """
        Assuming a stoichiometric ratio of r_Cu2+ = r_Fe2+ / n
        """
        return rate_ferrous /
float(constants.DATA[self.reactant_name]["stoichiometry"])


    def ferric_to_ferrous(self, rate_ferric):
        """
        Converts the ferric rate to ferrous rate
        """
        return rate_ferric * (-1)

    def run(self):
        # if self.reactant_name == constants.COPPER["symbol"]:
        rate_ferric = self.metal_powder_rate()

        # This should not be updated here but by the actual
reactor
        self.update_metal_reactant_concentration(rate_ferric)
        rate_ferrous = self.ferric_to_ferrous(rate_ferric)

        data = {
            "rate_ferrous": rate_ferrous,
            "rate_ferric": rate_ferric,
            "component_moles": self.component_conc,
            "ion_moles": self.metal_initial - self.component_conc,
            "rate_component":
self.rate_component_reaction(rate_ferrous)
        }
        return data
```

Reactors.py

```
# Third Party
import numpy as np

class BaseUpStream(object):
    """
    This class contains the default upstream component, this is
so that
    downstream.flow_in = upstream.flow_out
    """
    def __init__(self, ferric=None, ferrous=None, ratio=None,
flow_out=None):
        RATIO = ratio or 1000
        ferric = ferric or 9 / 55.85
        ferrous = ferrous or ferric / RATIO
        self.flow_out = flow_out or {"flowrate": 1. / (1 * 60),
                                     "components": {"ferrous": ferrous , "ferric":
ferric}}
    def set_flow_out(self, flow_out):
        self.flow_out = flow_out

class CSTR(object):
    """
    This class simulates the cases that occur in all reactors.
    This system uses Fe2+ as the base for all components
reactions,
    hence all reactions should be set in the basis of it.
    """
    TYPE = "CSTR"
    def __init__(self, volume, upstream):
        self.volume = volume
        self.upstream = upstream
        self.update_flow_in()
        self.set_flow_out_initial()
        self.ferric = self.flow_in["components"]["ferric"]
        self.ferrous = self.flow_in["components"]["ferrous"]
        self.components = []
        self.cstr_data = {}
        self.ions = {}
        self.step = 0

    def create_components(self, component):
        """
        Function that updates the components rate objects in the
reactor
        """

component.update_global_reactant_concentrations(self.ferric,
self.ferrous)
        self.components.append(component)

    def create_ions_in_reactor(self, system_components):
        for component_name in system_components:
            self.ions[component_name] = 0

    def reaction(self):
        cummulative_rate_ferrous = 0  # Rate is dependent on
prevoius concentrations and not
        cummulative_rate_ferric = 0
        _cstr_data = {"components": {}}  # specific rates of the
individual op

        # previous rates
        for component in self.components:
            output = component.run()
            rate_ferrous = output.get("rate_ferrous", 0.)
            rate_ferric = output.get("rate_ferric", 0.)
            rate_component = output.get("rate_component", 0.)
```

```
        component_moles = output.get("component_moles", 0.)
        ion_moles = output.get("ion_moles", 0.)
        cummulative_rate_ferrous = cummulative_rate_ferrous
+ rate_ferrous
        cummulative_rate_ferric = cummulative_rate_ferric +
rate_ferric
        _cstr_data["components"][component.reactant_name]
= {
                    "rate_ferrous": rate_ferrous,
                    "rate_ferric": rate_ferric,
                    "component_moles": component_moles,
                    "ion_moles": ion_moles,
                    "rate_component": rate_component
                }
    _cstr_data["total_rate_ferrous"] =
cummulative_rate_ferrous
    _cstr_data["total_rate_ferric"] = cummulative_rate_ferric

    return _cstr_data

  def
calculate_reactor_ferric_and_ferrous_concentration(self):
    """
    Calculating f(x, y) in the reactor, before applying the (y(t) +
h * (f(x, y)))
    (v_chem*C_Fe2+_in - v_chem*C_Fe2+_out  + Vol_chem *
total_rate_ferrous)
    """
    flow_diff_ferrous = (self.flow_in["components"]["ferrous"]
- self.flow_out["components"]["ferrous"]) *
self.get_dilution_rate()
    ferrous_conc = flow_diff_ferrous +
self.cstr_data["total_rate_ferrous"]
    flow_diff_ferric = (self.flow_in["components"]["ferric"] -
self.flow_out["components"]["ferric"]) *
self.get_dilution_rate()
    ferric_conc = flow_diff_ferric +
self.cstr_data["total_rate_ferric"]
    return ferrous_conc, ferric_conc

  def calculate_metal_ion_concentrations(self, key):
    """
    calculate y(t+1) by adding y(t) + h * ( f(x, y) )
    """
    if self.flow_in["components"].get(key) == None:
      self.flow_in["components"][key] = 0.0

    if self.flow_out["components"].get(key) == None:
      self.flow_out["components"][key] = 0.0

    flow_diff = (self.flow_in["components"][key] -
self.flow_out["components"][key]) * self.get_dilution_rate()

    # If the system component is part of original reactor
components work out rate else work out the flow rate
    if self.cstr_data["components"].get(key):
      ion_conc = flow_diff +
self.cstr_data["components"][key]["rate_component"]
    else:
      ion_conc = flow_diff
    ion_name = key
    return ion_conc, ion_name

  def perform_euler_calculation(self):
    """
    This updates the total concentrations of ferric and ferrous
in system after reaction based on the Euler method
    """
    ferrous_conc, ferric_conc =
self.calculate_reactor_ferric_and_ferrous_concentration()
    self.ferrous = self.ferrous + (1 * ferrous_conc) # Assuming
step = 1
    self.ferric = self.ferric + (1 * ferric_conc) # Assuming step =
1

    if self.ferric < 0:
      self.ferric = 0.

    if self.ferrous < 0:
      self.ferrous = 0

    self.ions["ferric"] = self.ferric
    self.ions["ferrous"] = self.ferrous

    ions = {
      "ferric": self.ferric,
      "ferrous": self.ferrous,
    }

    for key in self.ions.keys():
      if key in ions.keys():  # Do not calculate what has already
been calculated
        continue
      ion_conc, ion_name =
self.calculate_metal_ion_concentrations(key)
      ion_update = self.ions[ion_name] + (1 * ion_conc)
      ions[ion_name] = ion_update

    # Adding the system components to the new output adue
to python holding its dict reference
    for k, v in self.ions.iteritems():
      if k not in ions:
        ions[k] = v
    self.ions = ions


  def update_flow_out_stream(self):
    """
    Updating the outflow stream
    """
    self.flow_out = {"flowrate": self.flow_in["flowrate"],
            "components": self.ions}

  def update_ferric_concentrations_in_components(self):
    for component in self.components:

component.update_global_reactant_concentrations(self.ferric,
self.ferrous)

  def update_step_count_in_component(self):
    for component in self.components:
      component.update_step(self.step)

  def update_flow_in(self):
    """
    Function to set the inward flow rate according to the
upstream
    """
    self.flow_in = self.upstream.flow_out

  def set_flow_out_initial(self):
    """
    Function to set the outward flow rate according to the
upstream
    """
    self.flow_out = self.flow_in

  def get_dilution_rate(self):
    return self.flow_in["flowrate"] / self.volume

  def run(self):
```

```
        self.update_flow_in()
        self.cstr_data = self.reaction()
        self.perform_euler_calculation()
        self.update_ferric_concentrations_in_components()
        self.update_step_count_in_component()
        self.update_flow_out_stream()
        return {"cstr_data": self.cstr_data,
                "flow_out": self.flow_out,
                "flow_in": self.flow_in,
                "ions": self.ions}
```

System.py

```
import time
from masters.calculations import reactors
from masters.calculations import reactions
from masters.calculations import constants

class System(object):
    def __init__(self, biox_volume, chem_volume, ferric_ferrous,
total_iron, initial_metals={}, initial_cells=7.25e7,
additions=False):
        self.units = []
        self.biox_volume = biox_volume or 1.0
        self.chem_volume = chem_volume or 1.0
        self.initial_cells = initial_cells
        self.ferric_ferrous = ferric_ferrous or 1000.0
        self.total_iron = (9.0 or total_iron) # Converting to g/m^3
        self.ferrous = self.calculate_initial_ferrous_conc() / 55.85
        self.ferric = self.calculate_initial_ferric_conc() / 55.85
        self.initial_metals =
self.convert_initial_metals_to_moles(initial_metals)
        self.img = None
        self.system_type = None
        self.system_components = []
        self.FINAL_CONVERSION = 0.95
        self.additions = additions
        self.additions_index = 1
        self.MAX_TIME = 90 if self.additions else 10

    def convert_initial_metals_to_moles(self, initial_metals):
        for k, v in initial_metals.iteritems():
            initial_metals[k] = v / constants.DATA[k]["Mr"]
        return initial_metals

    def calculate_initial_ferric_conc(self):
        return (self.total_iron * self.ferric_ferrous) /
(self.ferric_ferrous + 1.0)

    def calculate_initial_ferrous_conc(self):
        return self.total_iron / (self.ferric_ferrous + 1.0)

    def create_reactor(self, reactor, volume, upstream):
        reactor = reactor(volume, upstream)
        self.update_units(reactor)
        return reactor

    def update_units(self, unit):
        self.units.append(unit)

    def add_reactants_to_chem_cstr(self):
        for k, v in self.initial_metals.iteritems():
            metal = reactions.MetalDissolutionRate(
                    k,
                    v,
                    system=constants.CONTINUOUS
                )
            self.chem_cstr.create_components(metal)
            self.system_components.append(metal.reactant_name)

    def build_tanks_in_series(self):
        self.upstream = reactors.BaseUpStream(ferric=self.ferric,
                                              ferrous=self.ferrous,
                                              ratio=self.ferric_ferrous)
        self.biox_rate =
reactions.BioxidationRate(initial_cells=self.initial_cells)
        self.biox_cstr = self.create_reactor(reactors.CSTR,
self.biox_volume, self.upstream)
        self.biox_cstr.create_components(self.biox_rate)

self.system_components.append(self.biox_rate.reactant_name
)

        self.chem_cstr = self.create_reactor(reactors.CSTR,
self.chem_volume, self.biox_cstr)
        self.add_reactants_to_chem_cstr()
        self.add_system_ions_to_reactors()
        self.img = "/static/img/system/tanks_in_series.png"
        self.system_type = "Tanks in Series"

    def build_cyclic_tanks(self):
        upstream = reactors.BaseUpStream(ferric=self.ferric,
                                         ferrous=self.ferrous,
                                         ratio=self.ferric_ferrous)

        self.biox_rate =
reactions.BioxidationRate(initial_cells=self.initial_cells)
        self.biox_cstr = self.create_reactor(reactors.CSTR,
self.biox_volume, upstream)
        self.biox_cstr.create_components(self.biox_rate)

self.system_components.append(self.biox_rate.reactant_name
)
        self.chem_cstr = self.create_reactor(reactors.CSTR,
self.chem_volume, self.biox_cstr)
        self.add_reactants_to_chem_cstr()
        self.biox_cstr.upstream = self.chem_cstr
        self.biox_cstr.update_flow_in()
        self.add_system_ions_to_reactors()
        self.img = "/static/img/system/closed_loop.png"
        self.system_type = "Closed Cyclic Tanks"

    def add_system_ions_to_reactors(self):
        for unit in self.units:
            unit.create_ions_in_reactor(self.system_components)

    def step(self):
        """
        output is in the form of [{"reactor": ["", [""]]}]
        Assuming an ordered list where the reactors in the list is in
the order it was created
        """
        output = [unit.run() for unit in self.units]
        return output

    def convert_to_minutes(self, i):
        return i / 60.0

    def check_conversion_above_threshhold(self):
        """
        Checks if the cummulative conversion is over the specified
threshold
        """
        total_initial_conc = sum([v for k,v in
self.initial_metals.iteritems()])
        total_current_conc = sum([ component.component_conc
for component in self.chem_cstr.components])
        return total_current_conc < ((1 - self.FINAL_CONVERSION)
* total_initial_conc)

    def update_step_in_units(self, step):
        for unit in self.units:
            unit.step = step
```

```
    def additions_update(self):
        self.chem_cstr.components[0].component_conc = 20.0 /
63.55
        self.initial_metals["Cu"] = 20.0 / 63.55
        self.chem_cstr.components[0].metal_ion = 0.0
        self.chem_cstr.components[0].reaction_step = 0
        self.additions_index += 1

    def check_ferrous_ion_above_threshold(self):
        return self.biox_cstr.ions["ferric"] >= self.ferric

    def run(self):
        biox_list = []
        chem_list = []
        summary_list = []
        t0 = time.clock()
        i = 0
        while True:
            self.update_step_in_units(i)
            sys_data = self.step()

            metal_converted =
self.check_conversion_above_threshhold()
            if self.additions:
                if metal_converted and
self.check_ferrous_ion_above_threshold():
                    if self.additions_index < 6:
                        self.additions_update()
                    else:
                        status = {"success": True, "message": "Simulation
completed succesfully"}
                        break
            else:
                if metal_converted:
                    status = {"success": True, "message": "Simulation
completed succesfully"}
                    break


            if time.clock() - t0 > self.MAX_TIME:
                status = {"success": False, "message": "Simulation
reached max time of %s" % self.MAX_TIME}
                break

            final_component_conc = {component.reactant_name:
component.component_conc for component in
self.chem_cstr.components}
            sys_data[0].update({"step": self.convert_to_minutes(i)})
            sys_data[1].update({"step": self.convert_to_minutes(i)})
            biox_list.append(sys_data[0])
            chem_list.append(sys_data[1])
            try:
                summary_list.append({"step":
self.convert_to_minutes(i),
                                     "rate_ratio":
abs(sys_data[1]["cstr_data"]["total_rate_ferric"] /
sys_data[0]["cstr_data"]["total_rate_ferric"])})
            except Exception, e:
                raise e
            i = i + 1
        _data = {"bioxidation": biox_list,
                 "chemical": chem_list,
                 "summary": {"bioxidation": {"ferric_in":
self.biox_cstr.flow_in["components"]["ferric"],
                                             "ferrous_in":
self.biox_cstr.flow_in["components"]["ferrous"],
                                             "volume": self.biox_volume,
                                             "equation": "",
                                             "dilution":
self.biox_cstr.get_dilution_rate()},
                             "chemical": {"initial_component_conc":
self.initial_metals,
                                          "final_component_conc":
final_component_conc,
                                          "volume": self.chem_volume,
                                          "equation": "",
                                          "dilution":
self.chem_cstr.get_dilution_rate()},
                             "combined": {"VChem_VBiox":
self.chem_volume/self.biox_volume,
                                          "System Type": self.system_type},
                             "system": {"img": self.img},
                             "status": status,
                             "data": summary_list
                             }
                }
        return _data
```

Plot.py

```
from optparse import make_option
from django.core.management.base import BaseCommand
from masters.calculations import system
import matplotlib.pyplot as plt

CU = 20
FERRIC_FERROUS = 1000
CHEM = 1
BIOX = 1
IRON = 9

class Command(BaseCommand):
    args = "volume"
    help = "Which simulation do you want to run: usage is --
simulate volume or --simulate metal or --simulate ferric_ratio"
    option_list = BaseCommand.option_list + (
                make_option('-s',
                            '--simulate',
                            dest='simulate',
                            default="volume",
                            type="str",
                            help=help),)

    def handle(self, *args, **kwargs):
        if kwargs["simulate"] == "volume":
            self.simulate = "volume"
            self.volume_sensitivity_analysis()

        elif kwargs["simulate"] == "metal":
            self.simulate = "initial_metal"
            self.metal_sensitivity_analysis()

        elif kwargs["simulate"] == "ferric_ratio":
            self.simulate = "ferric_ratio"
            self.ferric_ferrous_sensitivity_analysis()

        elif kwargs["simulate"] == "mixed_metals":
            self.simulate = "mixed_metals"
            self.mixed_metals_sensitivity_analysis()

        elif kwargs["simulate"] == "cells":
            self.simulate = "cells"
            self.microorganism_sensitivity_analysis()

        elif kwargs["simulate"] == "experiments":
            self.simulate = "experiments"
            self.experimental_sensitivity_analysis()

        elif kwargs["simulate"] == "additions":
            self.simulate = "additions"
            self.additions_sensitivity_analysis()
```

```
    def experimental_sensitivity_analysis(self):
        analysis_list = [(1, "1 L")]
        output = {}

        for row in analysis_list:
            BIOX = row[0]
            sys = system.System(BIOX, CHEM, FERRIC_FERROUS,
IRON, initial_metals={"Cu": CU})
            sys.build_cyclic_tanks()
            output[row[1]] = sys.run()

        self.plot_sensitivity_analysis(output, analysis_list)

    def additions_sensitivity_analysis(self):
        analysis_list = [(6, "6 additions")]
        output = {}

        for row in analysis_list:
            sys = system.System(BIOX, CHEM, FERRIC_FERROUS,
IRON, initial_metals={"Cu": 20}, additions=True)
            sys.build_cyclic_tanks()
            output[row[1]] = sys.run()

        self.plot_sensitivity_analysis(output, analysis_list)


    def volume_sensitivity_analysis(self):
        analysis_list = [(1, "1 L"),
                         (3, "3 L"),
                         (6, "6 L"),
                         (9, "9 L"),
                         (12, "12 L"),
                         (1000, "1000 L")]
        output = {}

        for row in analysis_list:
            BIOX = row[0]
            sys = system.System(BIOX, CHEM, FERRIC_FERROUS,
IRON, initial_metals={"Cu": CU})
            sys.build_cyclic_tanks()
            output[row[1]] = sys.run()

        self.plot_sensitivity_analysis(output, analysis_list)

    def metal_sensitivity_analysis(self):
        analysis_list = [(2, "2 g Cu"),
                         (5, "5 g Cu"),
                         (10, "10 g Cu"),
                         (20, "20 g Cu")]
        output = {}
        for row in analysis_list:
            CU = row[0]
            sys = system.System(BIOX, CHEM, FERRIC_FERROUS,
IRON, initial_metals={"Cu": CU})
            sys.build_cyclic_tanks()
            output[row[1]] = sys.run()

        sys = system.System(10, 1, FERRIC_FERROUS, IRON,
initial_metals={"Cu": 20})
        sys.build_cyclic_tanks()
        output["20 g Cu (10 L Bioox)"] = sys.run()
        analysis_list.append((20, "20 g Cu (10 L Bioox)"))

        sys = system.System(BIOX, CHEM, FERRIC_FERROUS, IRON,
initial_metals={"Cu": 20}, initial_cells=7.25e8)
        sys.build_cyclic_tanks()
        output["20 g Cu (7.25e8 cells)"] = sys.run()
        analysis_list.append((7.25e8, "20 g Cu (7.25e8 cells)"))

        self.plot_sensitivity_analysis(output, analysis_list)

    def mixed_metals_sensitivity_analysis(self):
        analysis_list = [(0, "Mixed Metal")]
        ZN = SN = CU = 2
        BIOX = 10

        output = {}
        sys = system.System(BIOX, CHEM, FERRIC_FERROUS, IRON,
initial_metals={"Cu": CU, "Sn": SN, "Zn": ZN})
        sys.build_cyclic_tanks()
        output["Mixed Metal"] = sys.run()
        self.plot_sensitivity_analysis(output, analysis_list)

    def ferric_ferrous_sensitivity_analysis(self):
        analysis_list = [(1000, "1000"),
                         (10, "10"),
                         (1, "1"),
                         (0.1, "0.1")]
        output = {}

        for row in analysis_list:
            FERRIC_FERROUS = row[0]
            sys = system.System(BIOX, CHEM, FERRIC_FERROUS,
IRON, initial_metals={"Cu": CU})
            sys.build_cyclic_tanks()
            output[row[1]] = sys.run()

        sys = system.System(10, 1, 0.1, 9, initial_metals={"Cu": CU})
        sys.build_cyclic_tanks()
        output["0.1 (10 L Bioox)"] = sys.run()
        analysis_list.append((20, "0.1 (10 L Bioox)"))

        sys = system.System(1, 1, 0.1, 9, initial_metals={"Cu": CU},
initial_cells=7.25e8)
        sys.build_cyclic_tanks()
        output["0.1 (7.25e8 cells)"] = sys.run()
        analysis_list.append((7.25e8, "0.1 (7.25e8 cells)"))

        self.plot_sensitivity_analysis(output, analysis_list)

    def microorganism_sensitivity_analysis(self):
        analysis_list = [(1e4, "1e4"),
                         (1e5, "1e5"),
                         (1e6, "1e6"),
                         (1e7, "1e7"),
                         (1e8, "1e8"),
                         (1e9, "1e9")]
        output = {}
        CU = 20
        for row in analysis_list:
            BIOMASS = row[0]
            sys = system.System(BIOX, CHEM, FERRIC_FERROUS,
IRON, initial_metals={"Cu": CU}, initial_cells=BIOMASS)
            sys.build_cyclic_tanks()
            output[row[1]] = sys.run()

        sys = system.System(10, 1, 0.1, 9, initial_metals={"Cu": CU})
        sys.build_cyclic_tanks()
        self.plot_sensitivity_analysis(output, analysis_list)

    def plot_sensitivity_analysis(self, sys_data, analysis_list):
        ferric_biox = {}
        ferric_chem = {}
        metals_chem = {}

        for k, data in sys_data.iteritems():
            ferric_biox[k] = {"ferric": [], "time": [], "biomass": [],
"Cu2+": [], "rate_ferric": []}
            for row in data["bioxidation"]:
```

```
            ferric_biox[k]["ferric"].append(row["ions"]["ferric"])
            ferric_biox[k]["time"].append(row["step"])

ferric_biox[k]["biomass"].append(row["cstr_data"]["components"]["Biomass"]["component_moles"])

ferric_biox[k]["Cu2+"].append(row["flow_out"]["components"]["Cu"])

ferric_biox[k]["rate_ferric"].append(row["cstr_data"]["total_rate_ferric"])

        ferric_chem[k] = {"ferric": [], "time": [], "rate_ferric": []}
        metals_chem[k] = {"Cu2+": [], "time": [], "Zn2+": [], "Sn2+": [], "copper": [], "rate_ferric": []}
        for row in data["chemical"]:
            ferric_chem[k]["ferric"].append(row["ions"]["ferric"])
            ferric_chem[k]["time"].append(row["step"])

ferric_chem[k]["rate_ferric"].append(row["cstr_data"]["total_rate_ferric"])

        for row in data["chemical"]:

metals_chem[k]["copper"].append(row["cstr_data"]["components"]["Cu"]["component_moles"])
            metals_chem[k]["Cu2+"].append(row["ions"]["Cu"])
            metals_chem[k]["time"].append(row["step"])


            if self.simulate == "mixed_metals":
                metals_chem[k]["Zn2+"].append(row["ions"]["Zn"])
                metals_chem[k]["Sn2+"].append(row["ions"]["Sn"])

    fig = plt.figure(1, figsize=(8, 8))
    fig_subplot = fig.add_subplot(421)
    fig_subplot.set_xlabel("Time (min)")
    fig_subplot.set_ylabel("[Fe3+] (mol/l)")
    fig_subplot.set_ylim(0, 0.18)
    fig_subplot.set_title("[Fe3+] in Bioox Reactor (A)")
    fig_subplot.grid('on')

    for i, item in enumerate(analysis_list):
        line, = fig_subplot.plot(ferric_biox[item[1]]["time"], ferric_biox[item[1]]["ferric"], label=item[1])
        line.set_linewidth(2)

    fig_subplot = fig.add_subplot(422)
    fig_subplot.set_xlabel("Time (min)")
    fig_subplot.set_ylabel("[Fe3+] (mol/l)")
    fig_subplot.set_ylim(0, 0.18)
    fig_subplot.set_title("[Fe3+] in Chem reactor (B)")
    fig_subplot.grid('on')

    for i, item in enumerate(analysis_list):
        line, = fig_subplot.plot(ferric_chem[item[1]]["time"], ferric_chem[item[1]]["ferric"], label=item[1])
        line.set_linewidth(2)

    fig_subplot = fig.add_subplot(423)
    fig_subplot.set_xlabel("Time (min)")
    fig_subplot.set_ylabel("[Cu2+] (mol/l)")
    fig_subplot.set_title("[Cu2+] in Bioox Reactor (C)")
    fig_subplot.grid('on')

    for i, item in enumerate(analysis_list):
        line, = fig_subplot.plot(ferric_biox[item[1]]["time"], ferric_biox[item[1]]["Cu2+"], label=item[1])
        line.set_linewidth(2)

    fig_subplot = fig.add_subplot(424)
    fig_subplot.set_xlabel("Time (min)")
    fig_subplot.set_ylabel("[Cu2+] (mol/l)")
    fig_subplot.set_title("[Cu2+] in Chem Reactor (D)")
    fig_subplot.grid('on')

    for i, item in enumerate(analysis_list):
        label = item[1] if self.simulate != "mixed_metals" else "Copper"
        line, = fig_subplot.plot(metals_chem[item[1]]["time"], metals_chem[item[1]]["Cu2+"], label=label)
        line.set_linewidth(2)

        if self.simulate == "mixed_metals":
            line, = fig_subplot.plot(metals_chem[item[1]]["time"], metals_chem[item[1]]["Zn2+"], label="Zinc")
            line.set_linewidth(2)
            line, = fig_subplot.plot(metals_chem[item[1]]["time"], metals_chem[item[1]]["Sn2+"], label="Tin")
            line.set_linewidth(2)

    fig_subplot = fig.add_subplot(425)
    fig_subplot.set_xlabel("Time (min)")
    fig_subplot.set_ylabel("[Biomass] (mol/l)")
    fig_subplot.set_title("[Biomass] in Bioox Reactor (E)")
    fig_subplot.grid('on')

    for i, item in enumerate(analysis_list):
        line, = fig_subplot.plot(ferric_biox[item[1]]["time"], ferric_biox[item[1]]["biomass"], label=item[1])
        line.set_linewidth(2)


    fig_subplot = fig.add_subplot(426)
    fig_subplot.set_xlabel("Time (min)")
    fig_subplot.set_ylabel("[Copper] (mol/l)")
    fig_subplot.set_title("[Copper] in Chem Reactor [F]")
    fig_subplot.grid('on')

    for i, item in enumerate(analysis_list):
        line, = fig_subplot.plot(metals_chem[item[1]]["time"], metals_chem[item[1]]["copper"], label=item[1])
        line.set_linewidth(2)

    fig_subplot = fig.add_subplot(427)
    fig_subplot.set_xlabel("Time (min)")
    fig_subplot.set_ylabel("[Rate Ferric] (mol/l/s)")
    fig_subplot.set_title("Fe3+ Produc. in Biox Reactor [G]")
    fig_subplot.grid('on')

    for i, item in enumerate(analysis_list):
        line, = fig_subplot.plot(ferric_biox[item[1]]["time"], ferric_biox[item[1]]["rate_ferric"], label=item[1])
        line.set_linewidth(2)

    fig_subplot = fig.add_subplot(428)
    fig_subplot.set_xlabel("Time (min)")
    fig_subplot.set_ylabel("Rate (mol/l/s)")
    fig_subplot.set_title("Fe3+ consum. in Chem Reactor [H]")
    fig_subplot.set_ylim(-0.001, 0.)
    fig_subplot.grid('on')

    for i, item in enumerate(analysis_list):
        line, = fig_subplot.plot(ferric_chem[item[1]]["time"], ferric_chem[item[1]]["rate_ferric"], label=item[1])
        line.set_linewidth(2)


    if not self.simulate == "additions":
        plt.legend(ncol=3, mode="expand", borderaxespad=0., bbox_to_anchor=(-2, -0.6, 1.*3, .102))
```

```
plt.tight_layout(h_pad=0.5)
fig.savefig('simulation_figures/' + self.simulate +'.png',
        bbox_inches='tight', pad_inches=0.5)
plt.show()
```